

**Function, mechanism and structure of
vanillyl-alcohol oxidase**

Promotor: dr. N.C.M. Laane
hoogleraar in de Biochemie

Co-promotor: dr. W.J.H. van Berkel
universitair docent, departement Biomoleculaire Wetenschappen,
laboratorium voor Biochemie

UNL 08201, 2416

Function, mechanism and structure of vanillyl-alcohol oxidase

Marco Wilhelmus Fraaije

Proefschrift

ter verkrijging van de graad van doctor
op gezag van de rector magnificus
van de Landbouwniversiteit Wageningen,
dr. C. M. Karssen,
in het openbaar te verdedigen
op maandag 6 april 1998
des namiddags te half twee in de Aula

UNL 08201, 2416

M.W. Fraaije - Function, mechanism and structure of vanillyl-alcohol oxidase - 1998

Dutch: 'Functie, mechanisme en structuur van vanillyl-alcohol oxidase'

Thesis Wageningen Agricultural University - With summary in Dutch

Cover: vanillyl-alcohol oxidase substrates (front)
 aromatic growth substrates for *P. simplicissimum* (back)

Key words: *Penicillium simplicissimum* / vanillyl-alcohol oxidase / flavin /
 kinetic mechanism / immunolocalization / phenolic compounds

ISBN 90-5485-828-1

Copyright © 1998 by M.W. Fraaije

All rights reserved

**BIBLIOTHEEK
LANDBOUWUNIVERSITEIT
WAGENINGEN**

Stellingen

1. De cellulaire locatie van covalente flavoproteïnen in eukaryoten beperkt zich niet alleen tot specifieke organellen.

Otto, A. et al., *J. Biol. Chem.* 271, 9823-9829, 1996.
Dit proefschrift, hoofdstuk 4.

2. De vorming van een flavine-adduct tijdens flavine gekatalyseerde oxidatiereacties hoeft geen bewijs te zijn voor een carbanionmechanisme.

Porter et al., *J. Biol. Chem.* 248, 4400-4416, 1973.
Dit proefschrift, hoofdstuk 8.

3. De topologie van het FAD-bindend domein van vanillyl-alcohol oxidase is typerend voor een nieuwe familie van flavine-afhankelijke oxidoreductases.

Dit proefschrift, hoofdstuk 11.

4. De afkorting VAO (vanillyl-alcohol oxidase) zou ook kunnen staan voor Various Aromats Oxidase.

Dit proefschrift, hoofdstuk 5 en 7.

5. *Penicillium simplicissimum* is noch een antibioticum noch een bacterie doch simpelweg een schimmel.

Otto, A. et al., *J. Biol. Chem.* 271, 9823-9829, 1996.
Johnsson, K. et al., *J. Biol. Chem.* 272, 2834-2840, 1997.

6. De aanname van Mayfield en Duvall dat catalase-peroxidases enkel in prokaryoten voorkomen, gaat voorbij aan bestaande literatuur en derhalve is de door hen voorgestelde evolutionaire stamboom van deze enzymen incorrect.

Mayfield, J.E. & Duvall, M.R., *J. Mol. Evolution* 42, 469-471, 1996.

7. Het ontbreken van fossiele paddestoelen in palaeontologische collecties is naast een geringe belangstelling voor deze 'lagere' organismen ook te wijten aan de samenstelling van de vruchtlichamen.

Fraaije, M.W. & Fraaije, R.H.B., *Contr. Tert. Quatern. Geol.* 32, 27-33, 1995.

8. Door het toenemende misbruik van e-mail adressen voor reclamedoeleinden zou ook op e-mail adressen een ja/nee-sticker optie moeten zitten.

Intermediair, 11 december 1997

9. Collegialiteit en een oneindige drang naar een gevoel van eigenwaarde gaan moeilijk samen.
10. Zinloos geweld is een loze kreet.
11. Tijdelijke aanstellingen zijn slecht voor het milieu.

Stellingen behorende bij het proefschrift
'Function, mechanism and structure of vanillyl-alcohol oxidase'

Marco W. Fraaije
Wageningen, 6 april 1998

Contents

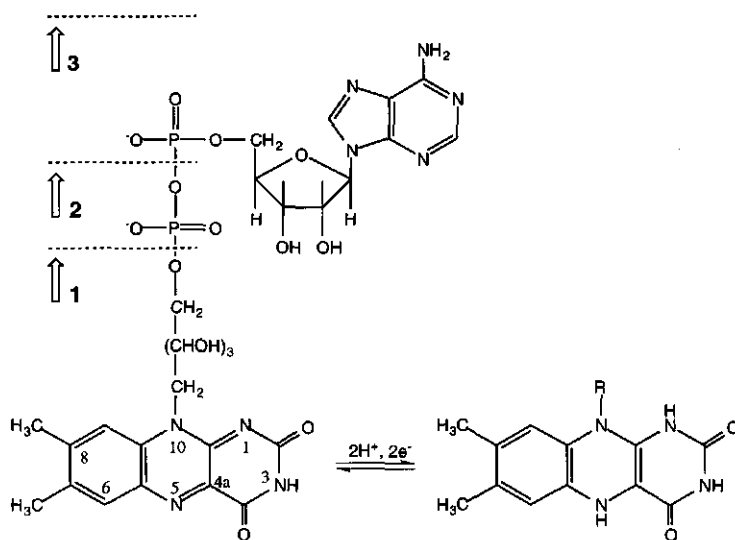
Chapter 1	General introduction	1
Chapter 2	Enigmatic gratuitous induction of the covalent flavoprotein vanillyl-alcohol oxidase in <i>Penicillium simplicissimum</i>	15
Chapter 3	Purification and characterization of an intracellular catalase-peroxidase from <i>Penicillium simplicissimum</i>	29
Chapter 4	Subcellular localization of vanillyl-alcohol oxidase in <i>Penicillium simplicissimum</i>	45
Chapter 5	Substrate specificity of flavin-dependent vanillyl-alcohol oxidase from <i>Penicillium simplicissimum</i>	57
Chapter 6	Catalytic mechanism of the oxidative demethylation of 4-(methoxymethyl)phenol by vanillyl-alcohol oxidase	73
Chapter 7	Enantioselective hydroxylation of 4-alkylphenols by vanillyl-alcohol oxidase	91
Chapter 8	Kinetic mechanism of vanillyl-alcohol oxidase with short-chain 4-alkylphenols	105
Chapter 9	Mercuration of vanillyl-alcohol oxidase from <i>Penicillium simplicissimum</i> generates inactive dimers	121
Chapter 10	Crystal structures and inhibitor binding in the octameric flavoenzyme vanillyl-alcohol oxidase	129
Chapter 11	A novel oxidoreductase family sharing a conserved FAD binding domain	153
	Abbreviations and nomenclature	161
	Summary	163
	Samenvatting	171
	Curriculum vitae	177
	List of publications	179
	Dankwoord	181

1

General introduction

1.1. Flavoenzymes

Riboflavin (vitamin B₂) is an essential vitamin for many life forms. Only plants and bacteria are able to produce this yellow (*lat.*: flavus = yellow) pigment *de novo*. Mammals, on the other hand, have to take up riboflavin in their food. In humans, riboflavin is absorbed by the gut and is transported, partially bound to serum albumin, via the bloodstream (Decker, 1994). By the subsequent action of flavokinase and FAD synthase, riboflavin is converted into the cofactors: flavin mononucleotide (FMN) and flavin adenine dinucleotide (FAD), respectively (Scheme 1). These cofactors are incorporated into the so-called flavoenzymes that need these cofactors for their activity. A striking feature of this group of enzymes is the diversity of reactions that are catalyzed which ranges from redox catalysis and DNA repair to light emission (Ghisla and Massey, 1989).

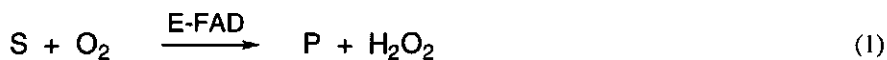


Scheme 1. Structure of riboflavin (1), FMN (2) and FAD (3) in oxidized and fully reduced state.

1.2. Flavoprotein oxidases

1.2.1. Reaction mechanism

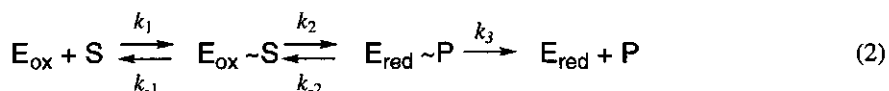
Biological oxidation reactions mostly involve the rupture of a C-H bond with a concomitant transfer of two electrons to an electron acceptor like NAD(P)⁺, cytochromes, or FAD. Flavin-mediated oxidation reactions vary from relatively simple oxidation reactions, like alcohol oxidations, to more complex reactions, e.g. stereoselective oxidative cyclization of plant alkaloids (Kutchan and Dittrich, 1995).



Reactions catalyzed by flavoprotein oxidases generally include two substrates (Equation 1): an electron donor (substrate) and molecular oxygen. Therefore, these enzymatic reactions can be characterized as two-substrate two-product reactions. As a consequence, most flavoprotein oxidases obey a ping-pong mechanism or a ternary complex mechanism. The type of kinetic mechanism varies between different flavoprotein oxidases and can depend on the type of substrate (Ramsay, 1991; Fraaije and van Berkel, 1997). Kinetic analysis of the different enzymes has revealed that the rate-limiting step in catalysis is often represented by either the rate of flavin reduction or the rate of product release. As for the type of mechanism, the rate-limiting step may vary depending on the type of substrate. Furthermore, in the case of D-amino acid oxidase, it has been found that with the yeast enzyme the rate of flavin reduction is rate-limiting while with the mammalian enzyme product release limits turnover (Pollegioni et al., 1993; Vanoni et al., 1997). Taken together, flavoprotein oxidases are quite variable with respect to their kinetic properties.

Flavoprotein oxidase catalysis involves two half-reactions in which first the flavin is reduced by the electron donor (substrate) (reductive half-reaction) and subsequently the reduced flavin is reoxidized by molecular oxygen (oxidative half-reaction). Using the stopped-flow technique, these two half-reactions can be analyzed separately.

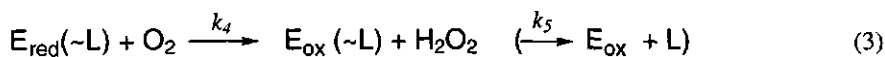
- reductive half-reaction



By anaerobically mixing the oxidized enzyme with substrate, the reductive half-reaction can be studied. The reaction includes the first step in the catalytic cycle: binding of substrate to form the Michaelis-Menten complex ($E_{\text{ox}} \sim S$) (Equation 1). In the succeeding

step the flavin cofactor is reduced by the transfer of two electrons from the substrate. The mechanism by which these electrons are transferred to the N5 atom of the flavin isoalloxazine ring is still a matter of discussion. Three types of mechanisms have been proposed. A carbanion mechanism is thought to be operative when the C-H bond to be oxidized is activated. In that case, the reaction proceeds by abstraction of a hydrogen as a proton to form a carbanion. Subsequently, a N5 flavin adduct is transiently formed by which the electrons are transferred to the flavin (Porter et al., 1973). A radical mechanism involving the transfer of a proton and two single electrons from the 'non-activated' substrate to the oxidized flavin has been proposed for e.g. monoamine oxidase and methanol oxidase (Silverman, 1995; Sherry and Abeles, 1985). Another alternative mechanism is the direct transfer of a hydride to the flavin ring system similar to the well-established reduction of pyridine nucleotides (Mattevi et al., 1996; Pollegioni et al., 1997). Depending on the enzyme, the formed product or product intermediate may be released from the active-site before the reduced flavin is reoxidized (k_3) by molecular oxygen. In case of a ternary complex mechanism, this step will be of no significance.

- oxidative half-reaction



(L represents substrate, product or other bound ligand)

The oxidative half-reaction can be examined by mixing the reduced enzyme with molecular oxygen. Reduced flavoprotein oxidases generally react rapidly with molecular oxygen yielding oxidized enzyme and hydrogen peroxide (k_4). Contrary to flavin-dependent monooxygenases, no oxygenated flavin intermediates have ever been detected during this relatively fast process (Massey, 1994). In flavoprotein dehydrogenases, reoxidation of reduced flavin by molecular oxygen is extremely slow indicating that this reaction can be highly modulated by the protein environment or the presence of active-site ligands. The rate of reoxidation of reduced flavoprotein oxidases can significantly be influenced by the binding of product, substrate or other ligands (Ramsay, 1991).

As oxidized and reduced flavins differ in their spectroscopic features (absorbance, fluorescence), the transition from the oxidized to the reduced state and vice versa can be monitored. These features have permitted detailed kinetic studies on several flavin-dependent oxidases. Examples of some flavoprotein oxidases of which the kinetic mechanism has been extensively studied are: D-amino acid oxidase (Pollegioni et al., 1997), glucose oxidase (Gibson et al., 1964), L-lactate oxidase (Maeda-Yorita et al., 1995) and monoamine oxidase (Ramsay, 1991).

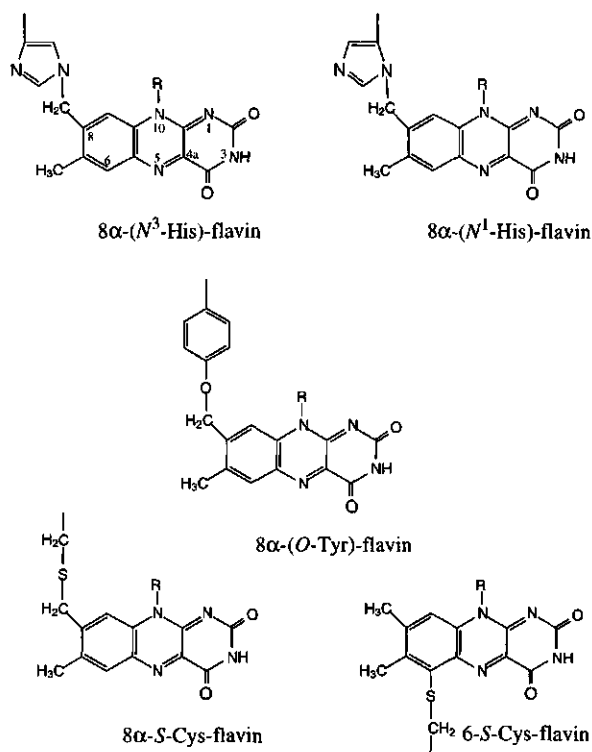
1.2.2. Crystal structures

At present, the crystal structures of six flavoprotein oxidases are known: glycolate oxidase (Lindqvist and Branden, 1985; Lindqvist, 1989), cholesterol oxidase (Vrielink et al., 1991; Li et al., 1993), glucose oxidase (Hecht et al., 1993), NADH oxidase (Hecht et al., 1995), D-amino acid oxidase (Mattevi et al., 1996) and vanillyl-alcohol oxidase (Mattevi et al., 1997, this thesis). Of these enzymes, glycolate oxidase and NADH oxidase are FMN-dependent, whereas the other oxidases contain a FAD molecule. Glucose oxidase belongs to the so-called GMC oxidoreductase family (Cavener, 1992), whose members all contain the well-characterized ADP-binding $\beta\alpha\beta$ -fold (Wierenga et al., 1983) and show significant sequence identity. Other members of the GMC family include methanol oxidase and glucose dehydrogenase. The recent determination of the crystal structures of cholesterol oxidase and D-amino acid oxidase revealed that despite a weak sequence homology both enzymes show structural homology with glucose oxidase. This suggests that these enzymes also belong to the GMC family (Li et al., 1993; Mattevi et al., 1996) or may be ranked in a larger group of FAD-dependent enzymes (Mathews, 1991). Vanillyl-alcohol oxidase shows no structural or sequence homology with the above mentioned oxidases. Crystal structure comparison has revealed that this covalent flavoprotein is structurally related to two bacterial flavoenzymes (Mattevi et al., 1997), *p*-cresol methylhydroxylase (PCMH) (Mathews et al., 1991) and UDP-*N*-acetylenolpyruvylglucosamine reductase (MurB) (Benson et al., 1995). Furthermore, it was found that both PCMH and VAO are members of a flavin-dependent oxidoreductase family which is characterized by a novel conserved FAD binding domain (Fraaije et al., 1997). Based on the known crystal structures it can be concluded that the flavin-dependent oxidase family is composed of several structurally (un)related subfamilies (Cavener, 1992; Scrutton, 1994; Fraaije et al., 1997).

1.3. Covalent flavoproteins

1.3.1. Occurrence of covalent flavoproteins

Until now, several hundred flavin-containing enzymes have been described. Most of these enzymes contain a dissociable FAD or FMN cofactor. However, it has been shown that in some cases the flavin is covalently linked to an amino acid of the polypeptide chain. In fact, in humans 10% of the cellular FAD is covalently bound to enzymes like e.g. succinate dehydrogenase and monoamine oxidase (Decker, 1994).



Scheme 2. Structural formulas of the known aminoacyl-flavin linkages.

So far, 5 different types of covalent flavin binding have been identified (Scheme 2) (Singer and McIntire, 1985; Decker, 1991). In all these cases a histidine, cysteine or tyrosine is involved. Linkage to a histidine is by far the most favored binding mode. Until now, about 20 examples of this type of linkage have been identified. A representative of a His-FAD containing enzyme is succinate dehydrogenase, which is a key enzyme in the Krebs cycle. Cysteine-bound flavins have been detected in five enzymes while only one tyrosine-linked flavin-containing enzyme is presently known. A well-known example of a Cys-FAD containing flavoprotein is monoamine oxidase, which is involved in the inactivation of various neurotransmitters, hormones and drugs in humans. The bacterial flavocytochrome *p*-cresol methylhydroxylase is the only known enzyme that contains a tyrosyl linked FAD. Unfortunately, in case of several described covalent flavoproteins, the nature of the covalent bond was not identified (Table 1). These enzymes await a more detailed characterization which might even lead to the discovery of novel types of flavin-protein interactions. Furthermore, it is to be expected that in the near future many more covalent flavoproteins will be uncovered by the current large-scale whole-genome sequencing efforts.

Table 1. Covalent flavoproteins and some of their characteristics.

Enzyme	Mass (kDa) Composition	Cofactor(s)	Source	Gene [Structure]	Cellular location	Ref.
<i>Histidyl-FAD</i>						
Succinate dehydrogenase	70,30,7-17 $\alpha\beta\gamma\delta$	8α -(N^3 -His)-FAD Fe-S clusters	A, B, F	+	mitoch.	a
Fumarate reductase	70,30,7-17 $\alpha\beta\gamma\delta$	8α -(N^3 -His)-FAD Fe-S clusters	B	+	cytopl. membr.	b
6-Hydroxy-D-nicotine oxidase	49 monomer	8α -(N^3 -His)-FAD	B	+	cytosol	b
Choline oxidase	71,59,? $\alpha\beta\gamma$	8α -(N^3 -His)-FAD	B, F	-	—	b
Dimethylglycine dehydr.	90 monomer	8α -(N^3 -His)-FAD <i>t</i> -hydrofolate	A	-	mitoch.	b
Sarcosine dehydrogenase	105 monomer	8α -(N^3 -His)-FAD <i>t</i> -hydrofolate	A	-	mitoch.	b
Sarcosine oxidase	100,42,21,7 $\alpha\beta\gamma\delta$	8α -(N^3 -His)-FMN NAD ⁺ , FAD	A	+	—	c
Sarcosine oxidase	42-45 monomer	8α -(N^3 -His)-FAD	A, B	+	peroxis.	d
D-Gluconolactone oxidase	150	8α -(N^3 -His)-FAD	F	-	intracel.	b
Vanillyl-alcohol oxidase	65 octamer	8α -(N^3 -His)-FAD	F	+ [2.5 Å]	peroxis. cytosol	e
Sugar dehydrogenases	65,50,20 $\alpha\beta\gamma$	8α -(N^3 -His)-FAD	B	-	cytopl. membr.	f
Thiamine oxidase	50 monomer	8α -(N^1 -His)-FAD	B	-	—	b
Cyclopiazone oxidocyclase	—	8α -(N^1 -His)-FAD	F	-	—	b
Cholesterol oxidase	53	8α -(N^1 -His)-FAD	B, F	-	—	b,g
L-Galactonolactone oxidase	—	8α -(N^1 -His)-FAD	F	+	peroxis.	b
L-Gulonolactone oxidase	51	8α -(N^1 -His)-FAD	A	+	e.r.	h
(S)-Reticuline oxidase (Berberine bridge enzyme)	52	His-FAD	P	+	vesicles	i,j
Hexose oxidase	63 dimer	His-FAD	P	+	—	k,l

Table 1. continued

<i>CysteinyI-FAD/FMN</i>						
Monoamine oxidase	59-60 monomer	8 α -S-Cys-FAD	A	+	mitoch.	m
Flavocytochrome C552/C553	46/47,21/10 $\alpha\beta$	8 α -S-Cys-FAD 1 or 2 hemes	B	+ [2.5 Å]	peripl.	n,o
Trimethylamine dehydr.	83 dimer	6-S-Cys-FMN 4Fe-4S	B	+ [2.4 Å]	cytosol	p
Dimethylamine dehydr.	69 dimer	6-S-Cys-FMN 4Fe-4S	B	+	—	q
<i>Tyrosyl-FAD</i>						
p-Cresol methyldehydr.	49,9 $\alpha_2\beta_2$	8 α -(O-Tyr)-FAD heme	B	+ [3.0 Å]	peripl.	r
<i>unknown covalent FAD binding</i>						
L-Pipecolic acid oxidase	46 monomer	covalent FAD	A	-	peroxis.	s
Fructosyl amino acid oxidase (amadorinase)	43 monomer	covalent FAD	F	+	peroxis.	t,u
Pyranose oxidase	76 tetramer	covalent FAD	F	-	—	v
Alcohol oxidase	73 kDa octamer	covalent FAD	F	-	—	w

Abbreviations: A: animal; P: plant; F: fungi; B: bacteria; mitoch.: mitochondria; peripl.: periplasmic; cytopl.: cytoplasmic; peroxis.: peroxisomes; intracel.: intracellular; e.r.: endoplasmic reticulum.

References: a: (Robinson et al., 1994); b: (Decker, 1991); c: (Willie and Jorns, 1995); d: (Reuber et al., 1997); e: (Mattevi et al., 1997); f: (McIntire et al., 1985); g: (Croteau and Vrielink, 1996); h: (Nishikimi et al., 1994); i: (Kutchan and Dittrich, 1995); j: (Facchini et al., 1996); k: (Hansen and Stougaard, 1997); l: (Groen et al., 1997); m: (Zhou et al., 1995); n: (Chen et al., 1994); o: (Van Driessche et al., 1996); p: (Mewies et al., 1997); q: (Yang et al., 1995); r: (Kim et al., 1995); s: (Mihalik and McGuinness, 1991); t: (Yoshida et al., 1996); u: (Takahashi et al., 1997); v: (Danneel et al., 1993); w: (Danneel et al., 1994).

1.3.2. Mechanism of covalent flavinylation

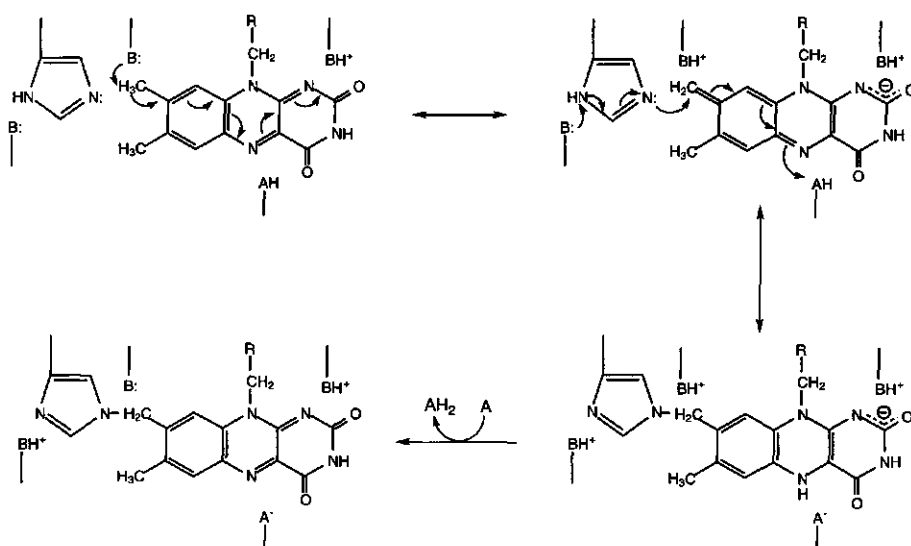
The rationale for covalent binding of flavins in flavoenzymes is still a matter of discussion as is the mechanism for this process. Recent studies have indicated that the covalent bond may prevent inactivation of the cofactor (Mewies et al., 1997) or can facilitate electron transport from the reduced flavin to an electron acceptor (Kim et al., 1995). Other relevant factors in relation to the rationale of covalent binding are:

- improved resistance against proteolysis
- altered chemical reactivity of the cofactor
- advantage of retaining activity in a flavin deficient environment
- improved protein stability

Interestingly, the efficiency of two commercially used flavoenzymes, D-amino acid oxidase and glucose oxidase, is hampered by the fact that these enzymes can lose the flavin cofactor under stress conditions (Nakajima et al., 1990; Cioci and Lavecchia, 1994). Evidently, covalent flavoenzymes are attractive for biotechnological purposes. Insight into the mechanism of covalent flavinylation may lead to the design of stable covalent flavoproteins from flavoenzymes which normally contain a dissociable flavin (Stocker et al., 1996).

The molecular mechanism of covalent attachment of FAD or FMN is, as yet, unresolved. Early reports dealing with this issue proposed that covalent bond formation involved an enzymatic activation of the cofactor (hydroxylation and subsequent phosphorylation) or modification of the receiving amino acid (Decker, 1991). Specific enzymes would be required for this process and energy would need to be provided by ATP. However, results from recent investigations indicate that for all studied covalent flavoproteins, covalent bond formation seems to be an autocatalytic process. This sets the process of covalent flavinylation apart from other covalent cofactor attachment mechanisms which generally are catalyzed by specific enzymes.

Sofar, the best studied covalent flavoprotein with respect to its cofactor binding is 6-hydroxy-D-nicotine oxidase (6-HDNO), a bacterial enzyme involved in the degradation of nicotine (Decker, 1994). The apoform of 6-HDNO has been obtained by expression of the gene in *Escherichia coli* (Brandsch and Bichler, 1991). Using apo-6-HDNO it could be shown that formation of the 8α -(N^3 -histidyl)-FAD bond is *in vitro* an autocatalytic process. Millimolar amounts of three-carbon compounds can act as allosteric effectors in this flavinylation process. Site-directed mutagenesis revealed that replacement of the FAD binding histidine prevents covalent binding of the cofactor while the enzyme remains active (Mauch et al., 1989). Similar results were reported for fumarate reductase (Ackrell et al., 1992). Changing the FAD-binding histidine in the closely related succinate dehydrogenase resulted in non-covalent binding of FAD and loss of fumarate reductase activity, but succinate dehydrogenase activity was retained (Robinson et al., 1994). Likewise, mutating the cysteine, which normally forms a 6-S-cysteiny-FMN bond in trimethylamine dehydrogenase, also resulted in an active enzyme unable to covalently bind FMN (Scrutton et al., 1994). Recent studies on the latter bacterial enzyme have indicated that covalent bond formation may play a major role in preventing inactivation of the enzyme by flavin modification (Mewies et al., 1997). It was proposed that this protective effect might also be the rationale for the occurrence of 8α -methyl flavinylated enzymes. However, some covalent flavoproteins have highly homologous flavin-dissociable counterparts that display similar enzyme activities (Schilling and Lerch, 1995; Fraaije et al., 1997). This indicates that the above-mentioned rationale is not generally valid.



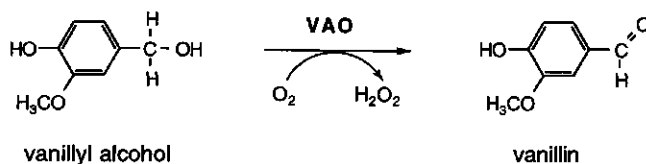
Scheme 3. Proposed mechanism of covalent flavinylation to form 8 α -(N³-histidyl)-flavin (A: e⁻ acceptor).

For *p*-cresol methylhydroxylase (Kim et al., 1995), monoamine oxidase (Weyler et al., 1990; Hiro et al., 1996) and dimethylglycine dehydrogenase (Otto et al., 1996), it has also been reported that covalent flavinylation is an autocatalytic process. From these data, a general applicable mechanism for covalent flavinylation is emerging which involves activation/deprotonation of the C8 α -methyl group leading to a reactive flavin iminoquinone methide (Scheme 3) (Decker, 1993; Kim et al., 1995; Mewies et al., 1997). Nucleophilic attack of the target amino acid at the 8 α -methyl (or the C6 position for 6-*S*-cysteinyl-FMN) results in the formation of the covalent aminoacyl-flavin bond. A prerequisite for covalent flavin attachment appears to be the formation of an apoprotein conformation capable of binding the cofactor and creating a favorable approach between the isoalloxazine ring and the reactive residue of the polypeptide chain (Brandsch and Bichler, 1991; Zhou et al. 1995).

1.4. Vanillyl-alcohol oxidase

In 1990, the fungus *Penicillium simplicissimum* was isolated from paper mill waste water (De Jong et al., 1990). The ascomycete was selected for its ability to use veratryl alcohol, a key compound in lignin biodegradation, as sole source of carbon and energy. During study on the metabolic pathway of veratryl alcohol it was found that *P. simplicissimum* can produce relatively large amounts of a flavin containing enzyme.

Subsequent purification and characterization revealed that this enzyme was able to oxidize vanillyl alcohol to form vanillin with a concomitant reduction of molecular oxygen to hydrogen peroxide. Therefore, the enzyme was named vanillyl-alcohol oxidase (De Jong et al., 1992). Recent studies have shown that the substrate specificity of vanillyl-alcohol oxidase is very broad (Fraaije et al., 1995; Drijfhout et al., 1997; Van den Heuvel et al., 1997).



Scheme 4. Conversion of vanillyl alcohol by VAO.

Vanillyl-alcohol oxidase is a homo-octamer of about 0.5 MDa with each subunit harboring a FAD cofactor. By limited proteolysis and using spectroscopic techniques the flavin cofactor was identified as FAD, which is covalently bound to a histidine residue of the polypeptide chain (8α -(N^3 -histidyl)-FAD, see Scheme 2) (De Jong et al., 1992).

Although vanillyl-alcohol oxidase production is induced when the fungus is grown on veratryl alcohol, the degradation pathway for veratryl alcohol does not involve any step which can be catalyzed by the enzyme (De Jong et al., 1990). Therefore, the physiological function of the enzyme remained obscure for some time. Furthermore, vanillyl-alcohol oxidase differs strikingly from other known flavin-dependent aryl alcohol oxidases. Aside from a more basic pH optimum for activity, vanillyl-alcohol oxidase displays a totally different substrate specificity when compared with the aryl alcohol oxidases excreted by several white-rot fungi (Farmer et al., 1960; Bourbonnais and Paice, 1988; Muheim et al., 1990; Sannia et al., 1991; Guillén et al., 1992; Asada et al., 1995). In summary, vanillyl-alcohol oxidase represents a unique flavoprotein with several intriguing properties, particularly with respect to its substrate specificity and FAD binding.

1.5. Outline of this thesis

To obtain a better insight in the catalytic mechanism of vanillyl-alcohol oxidase, a PhD project was started in 1993. The results from this study are presented in this thesis.

In the first part of this thesis (Chapter 2, 3 and 4), results are presented which are associated with the biological function of vanillyl-alcohol oxidase. In chapter 2, the induction of vanillyl-alcohol oxidase in *Penicillium simplicissimum* has been investigated.

For this, a wide range of growth substrates were tested for their ability to induce vanillyl-alcohol oxidase activity. Subsequently, the degradation pathways of the inducing growth substrates were determined. Coincident with induction of VAO, an elevated production of an intracellular catalase-peroxidase was observed. The latter enzyme was purified and characterized (Chapter 3). In chapter 4, the intracellular location of both enzymes, vanillyl-alcohol oxidase and catalase-peroxidase, has been determined.

Chapter 5-8 report on the substrate specificity and kinetic mechanism of vanillyl-alcohol oxidase. After screening the substrate specificity (Chapter 5), the kinetic mechanism of VAO with the physiological substrate 4-(methoxymethyl)phenol was studied using the stopped-flow technique (Chapter 6). The finding that VAO is active with short-chain 4-alkylphenols prompted us to investigate the stereochemistry (Chapter 7) and kinetic mechanism (Chapter 8) of these reactions.

In the final chapters (Chapter 9-11), results are presented which are related to the structural properties of VAO. Chapter 9 describes the effect of mercuration on VAO oligomerization. Chapter 10 reports on the crystal structure of native VAO and in complex with several inhibitors. In Chapter 11, a sequence homology search was performed using the VAO primary structure. From this search, a novel flavoprotein family was revealed, which contains many oxidases harbouring a covalently bound FAD. By structure comparison, it was found that members of this oxidoreductase family contain a novel FAD binding domain.

1.6. References

- Ackrell, B.A., Johnson, M.K., Gunsalus, R.P. and Cecchini, G. (1992) in *Chemistry and Biochemistry of flavoenzymes*, (Müller, F., ed.) Vol. III, pp. 229-297, CRC Press, Boca Raton.
- Asada, Y., Watanabe, A., Ohtsu, Y. and Kuwahara, M. (1995) Purification and characterization of an aryl-alcohol oxidase from the lignin-degrading basidiomycete *Phanerochaete chrysosporium*, *Biotech. Biochem.* **59**, 1339-1341.
- Benson, T.E., Filman, D.J., Walsh, C.T. and Hogle, J.M. (1995) An enzyme-substrate complex involved in bacterial cell wall biosynthesis, *Nature Struct. Biol.* **2**, 644-653.
- Bourbonnais, R. and Paice, M.G. (1988) Veratryl alcohol oxidases from the lignin degrading basidiomycete *Pleurotus sajor-caju*, *Biochem. J.* **255**, 445-450.
- Brandsch, R. and Bichler, V. (1991) Autoflavinylation of apo 6-hydroxy-D-nicotine oxidase, *J. Biol. Chem.* **266**, 19056-19062.
- Cavener, D.R. (1992) GMC oxidoreductases: a newly defined family of homologous proteins with diverse catalytic activities, *J. Mol. Biol.* **223**, 811-814.
- Chen, Z., Koh, M., van Driessche, G., van Beeumen, J.J., Bartsch, R.G., Meyer, T.E., Cusanovich, M.A. and Mathews, F.S. (1994) The structure of flavocytochrome c sulfide dehydrogenase from a purple phototrophic bacterium, *Science* **266**, 430-432.
- Cioci, F. and Lavecchia, R. (1994) Effects of polyols and sugars on heat-induced flavin dissociation in glucose oxidase, *Biochem. Mol. Biol. Int.* **34**, 705-712.
- Croteau, N. and Vrielink, A. (1996) Crystallization and preliminary X-ray analysis of cholesterol oxidase from *Brevibacterium sterolicum* containing covalently bound FAD, *J. Struct. Biol.* **116**, 317-319.

- Danneel, H.J., Roessner, E., Zeeck, A. and Giffhorn, F. (1993) Purification and characterization of a pyranose oxidase from basidiomycete *Peniophora gigantea* and chemical analyses of its reaction products, *Eur. J. Biochem.* **214**, 795-802.
- Danneel, H.J., Reichert, A. and Giffhorn, F. (1994) Production, purification and characterization of an alcohol oxidase of the ligninolytic fungus *Peniophora gigantea*, *J. Biotechn.* **33**, 33-41.
- Decker, K.F. (1991) Covalent flavoproteins, in: *Chemistry and biochemistry of flavoenzymes vol. II* (Müller, F. ed.) 343-375, CRC Press, Boca Raton, Florida.
- Decker, K.F. (1993) Biosynthesis and function of enzymes with covalently bound flavin, *Annu. Rev. Nutr.* **13**, 17-41.
- Decker, K.F. (1994) Vitamins, in: *Nutritional biochemistry* (Brody, T., ed.) pp. 443-447, Academic Press, San Diego.
- De Jong, E., Beuling, E.E., van der Zwan, R.P. and de Bont, J.A.M. (1990) Degradation of veratryl alcohol by *Penicillium simplicissimum*, *Appl. Microbiol. Biotechnol.* **34**, 420-425.
- De Jong, E., van Berkel, W.J.H., van der Zwan, R.P. and de Bont, J.A.M. (1992) Purification and characterization of vanillyl-alcohol oxidase from *Penicillium simplicissimum*, *Eur. J. Biochem.* **208**, 651-657.
- Drijfhout, F.P., Fraaije, M.W., Jongejan, H., van Berkel, W.J.H. and Franssen, M.C.R. (1997) Enantioselective hydroxylation of 4-alkylphenols by vanillyl-alcohol oxidase, *Biotech. Bioeng.* in press.
- Facchini, P.J., Penzes, C., Johnson, A.G. and Bull, D. (1996) Molecular characterization of berberine bridge enzyme genes from *Opium poppy*, *Plant Physiol.* **112**, 1669-1677.
- Farmer, V.C., Henderson, M.E.K. and Russell J.D. (1960) Aromatic-alcohol-oxidase activity in the growth medium of *Polystictus ostreiformis*, *J. Ferment. Biochem.* **74**, 257-262.
- Fraaije, M.W., Veeger, C. and van Berkel, W.J.H. (1995) Substrate specificity of flavin-dependent vanillyl-alcohol oxidase from *Penicillium simplicissimum*, *Eur. J. Biochem.* **234**, 271-277.
- Fraaije, M.W. and van Berkel, W.J.H. (1997) Catalytic mechanism of the oxidative demethylation of 4-(methoxymethyl)phenol, *J. Biol. Chem.* **272**, 18111-18116.
- Fraaije, M.W., Mattevi, A., Benen, J.A.E., Visser, J. and van Berkel, W.J.H. (1997) A novel oxidoreductase family sharing a conserved FAD binding domain, *Nature Struct. Biol.* submitted.
- Gibson, Q.H., Swoboda, B.E.P. and Massey, V. (1964) Kinetics and mechanism of action of glucose oxidase, *J. Biol. Chem.* **239**, 3927-3934.
- Ghisla, S. and Massey, V. (1989) Mechanisms of flavoprotein-catalyzed reactions, *Eur. J. Biochem.* **181**, 1-17.
- Groen, B.W., de Vries, S and Duine, J.A. (1997) Characterization of hexose oxidase from the red seaweed *Chondrus crispus*, *Eur. J. Biochem.* **244**, 858-861.
- Guillén, F., Martínez, A.T. and Martínez, M.J. (1992) Substrate specificity and properties of the aryl-alcohol oxidase from the ligninolytic fungus *Pleurotus eryngii*, *Eur. J. Biochem.* **209**, 603-611.
- Hansen, O.C. and Stougaard, P. (1997) Hexose oxidase from the red alga *Chondrus crispus*: purification, molecular cloning, and expression in *Pichia pastoris*, *J. Biol. Chem.* **272**, 11581-11587.
- Hecht, H.J., Kalisz, H.M., Hendle, J., Schmid, R.D. and Schomburg, D. (1993) Crystal structure of glucose oxidase from *Aspergillus niger* refined at 2.3 Å resolution, *J. Mol. Biol.* **229**, 153-172.
- Hecht, H.J., Erdmann, H., Park, H.J., Sprinzl, M. and Schmid, R.D. (1995) Crystal structure of NADH oxidase from *Thermus thermophilus*, *Nature Struct. Biol.* **2**, 1109-1114.
- Hiro, I., Tsugenno, Y., Hirashiki, I., Ogata, F. and Ito, A. (1996) Characterization of rat monoamine oxidase A with noncovalently bound FAD expressed in yeast cells, *J. Biochem.* **120**, 759-765.
- Kim, J., Fuller, J.H., Kuusk, V., Cunane, L., Chen, Z.-W., Mathews, F.S. and McIntire, W.S. (1995) The cytochrome subunit is necessary for covalent FAD attachment to the flavoprotein subunit of *p*-cresol methylhydroxylase, *J. Biol. Chem.* **270**, 31202-31209.
- Kutchan, T.M. and Dittich, H. (1995) Characterization and mechanism of the berberine bridge enzyme, a covalently flavinylated oxidase of benzophenanthridine alkaloid biosynthesis in plants, *J. Biol. Chem.* **270**, 24475-24481.
- Li, J., Vrieling, A., Brick, P. and Blow, D.M. (1993) Crystal structure of cholesterol oxidase complexed with a steroid substrate: implications for flavin adenine dinucleotide dependent alcohol oxidases, *Biochemistry* **32**, 11507-11515.
- Lindqvist, Y. and Branden, C.-I. (1985) Structure of glycolate oxidase from spinach, *Proc. Natl. Acad. Sci. USA* **82**, 6855-6859.

- Lindqvist, Y. (1989) Refined structure of spinach glycolate oxidase at 2 Å resolution, *J. Mol. Biol.* **209**, 151-166.
- Maeda-Yorita, K., Aki, K., Sagai, H., Misaki, H. and Massey, V. (1995) L-Lactate oxidase and L-lactate monooxygenase: mechanistic variations on a common structural theme, *Biochimie* **77**, 631-642.
- Massey, V. (1994) Activation of molecular oxygen by flavins and flavoproteins, *J. Biol. Chem.* **269**, 22459-22462.
- Mathews, F.S. (1991) New flavoenzymes, *Curr. Op. Struct. Biol.* **1**, 954-967.
- Mathews, F.S., Chen, Z., Bellamy, H.D. and McIntire, W.S. (1991) Three-dimensional structure of *p*-cresol methylhydroxylase (flavocytochrome *c*) from *Pseudomonas putida* at 3.0-Å resolution, *Biochemistry* **30**, 238-247.
- Mattevi, A., Vanoni, M.A., Todone, F., Rizzi, M., Teplyakov, A., Coda, A., Bolognesi, M. and Curti, B. (1996) Crystal structure of D-amino acid oxidase: a case of active site mirror-image convergent evolution with flavocytochrome b2, *Proc. Natl. Acad. Sc. USA* **93**, 7496-7501.
- Mattevi, A., Fraaije, M.W., Mozzarelli, A., Olivi, L., Coda, A. and van Berkel, W.J.H. (1997) Crystal structures and inhibitor binding in the octameric flavoenzyme vanillyl-alcohol oxidase: the shape of the active-site cavity controls substrate specificity, *Structure* **5**, 907-920.
- McIntire, W., Singer, T.P., Ameyama, M., Adami, O., Matsushita, K. and Shinagawa, E. (1985) Identification of the covalently bound flavins of D-gluconate dehydrogenases from *Pseudomonas aeruginosa* and *Pseudomonas fluorescens* and of 2-keto-D-gluconate dehydrogenase from *Gluconobacter melanogenus*, *Biochem. J.* **231**, 651-654.
- Mewies, M., Basran, J., Packman, L.C., Hille, R. and Scrutton, N.S. (1997) Involvement of a flavin iminoquinone methide in the formation of 6-hydroxyflavin mononucleotide in trimethylamine dehydrogenase: a rationale for the existence of 8 α -methyl and C6-linked covalent flavoproteins, *Biochemistry* **36**, 7162-7168.
- Mihalic, S.J. and McGuinness, M.C. (1991) Covalently-bound flavin in peroxisomal L-pipecolic acid oxidase from primates, in: *Flavins and Flavoproteins 1990* (Curti, B., Ronchi, S. and Zanetti, G. eds.) pp. 881-884, W. de Gruyter, Berlin.
- Muheim, A., Waldner, R., Leisola, M.S.A. and Fiechter, A. (1990) An extracellular aryl-alcohol oxidase from the white-rot fungus *Bjerkandera adusta*, *Enzyme Microb. Technol.* **12**, 204-209.
- Nakajima, N., Conrad, D., Sumi, H., Suzuki, K., Wandrey, C. and Soda, K. (1990) Continuous conversion to optically pure L-methionine from D-enantiomer contaminated preparations by an immobilized enzyme membrane reactor, *J. Ferment. Biotech.* **70**, 322-325.
- Nishikimi, M., Kobayashi, J. and Yagi, K. (1994) Production by a baculovirus expression system of the apoprotein of L-gulonolactone oxidase, a flavoenzyme possessing a covalently-bound FAD, *Biochem. Mol. Biol. Int.* **33**, 313-320.
- Otto, A., Stolz, M., Sailer, H. and Brandsch, R. (1996) Biogenesis of the covalently flavinylated mitochondrial enzyme dimethylglycine dehydrogenase, *J. Biol. Chem.* **271**, 9823-9829.
- Pollegioni, L., Langkau, B., Tischer, W., Ghisla, S. and Pilone, M.S. (1993) Kinetic mechanism of D-amino acid oxidases from *Rhodotorula gracilis* and *Trigonopsis variabilis*, *J. Biol. Chem.* **268**, 13850-13857.
- Pollegioni, L., Blodig, W. and Ghisla, S. (1997) On the mechanism of D-amino acid oxidase, *J. Biol. Chem.* **272**, 4924-4934.
- Porter, D.J.T., Voet, J.G. and Bright, H.J. (1973) Direct evidence for carbanions and covalent N⁵-flavin-carbanion adducts as catalytic intermediates in the oxidation of nitroethane by D-amino acid oxidase, *J. Biol. Chem.* **248**, 4400-4416.
- Ramsay, R.R. (1991) Kinetic mechanism of monoamine oxidase A, *Biochemistry* **30**, 4624-4629.
- Reuber, B.E., Karl, C., Reimann, S.A., Mihalik, S.J. and Dodt, G. (1997) Cloning and functional expression of a mammalian gene for a peroxisomal sarcosine oxidase, *J. Biol. Chem.* **272**, 6766-6776.
- Robinson, K.M., Rothery, R.A., Weiner, J.H. and Lemire, B.D. (1994) The covalent attachment of FAD to the flavoprotein of *Saccharomyces cerevisiae* succinate dehydrogenase is not necessary for import and assembly into mitochondria, *Eur. J. Biochem.* **222**, 983-990.
- Sannia, G., Limongi, P., Cocca, E., Buonocore, F., Nitti, G. and Giardina, P. (1991) Purification and characterization of a veratryl alcohol oxidase enzyme from the lignin degrading basidiomycete *Pleurotus ostreatus*, *Biochim. Biophys. Acta.* **1073**, 114-119.
- Schilling, B. and Lerch, K. (1995) Cloning, sequencing and heterologous expression of the monoamine oxidase gene from *Asperillus niger*, *Mol. Gen. Genet.* **247**, 430-438.

- Scrutton, N.S. (1994) $\alpha\beta$ Barrel evolution and the modular assembly of enzymes: emerging trends in the flavin oxidase/dehydrogenase family, *BioEssays* **16**, 115-122.
- Sherry, B. and Abeles, R.H. (1985) Mechanism of action of methanol oxidase, reconstitution of methanol oxidase with 5-deazaflavin, and inactivation of methanol oxidase by cyclopropanol, *Biochemistry* **24**, 2594-2605.
- Silverman, R.B. (1995) Radical ideas about monoamine oxidase, *Acc. Chem. Res.* **28**, 335-342.
- Singer, T.P. and McIntire, W.S. (1984) Covalent attachment of flavin to flavoproteins: occurrence, assay, and synthesis, in: *Methods Enzymol.* **106**, 369-378.
- Scrutton, N.S., Packman, L.C., Mathews, F.S., Rohlf, R.J. and Hille, R. (1994) Assembly of redox centers in the trimethylamine dehydrogenase of bacterium W3A1: Properties of the wild-type and a C30A mutant expressed from a cloned gene in *Escherichia coli*, *J. Biol. Chem.* **269**, 13942-13950.
- Stocker, A., Hecht, H. and Bückmann, A.F. (1996) Synthesis, characterization and preliminary crystallographic data of N^6 -(6-carbamoylhexyl)-FAD-D-amino-acid oxidase from pig kidney, a semi-synthetic oxidase, *Eur. J. Biochem.* **238**, 519-528.
- Takahashi, M., Pischetsrieder, M. and Monnier, M. (1997) Isolation, purification, and characterization of amadoriase isoenzymes (fructosyl amine-oxygen oxidoreductase EC 1.5.3) from *Aspergillus* sp., *J. Biol. Chem.* **272**, 3437-3443.
- Van Driessche, G., Koh, M., Chen, Z., Mathews, F.S., Meyer, T.E., Bartsch, R.G., Cusanovich, M.A. and van Beeumen, J.J. (1996) Covalent structure of the flavoprotein subunit of the flavocytochrome *c*: sulfide dehydrogenase from the purple phototrophic bacterium *Chromatium vinosum*, *Protein Science* **5**, 1753-1764.
- Van den Heuvel, R.H.H., Fraaije, M.W. and van Berkel, W.J.H. (1997) Reactivity of vanillyl-alcohol oxidase with medium-chain 4-alkylphenols, bicyclic phenols and 4-hydroxyphenyl alcohols, *in preparation*.
- Vanoni, M.A., Cosma, A., Mazzeo, D., Mattevi, A., Todone, F. and Curti, B. (1997) Limited proteolysis and X-ray crystallography reveal the origin of substrate specificity and of the rate-limiting product release during oxidation of D-amino acids catalyzed by mammalian D-amino acid oxidase, *Biochemistry* **36**, 5624-5632.
- Vrielink, A., Lloyd, L.F. and Blow, D.M. (1991) Crystal structure of cholesterol oxidase from *Brevibacterium sterolicum* refined at 1.8Å resolution, *J. Mol. Biol.* **219**, 533-554.
- Weyler, W., Titlow, C.C. and Salach, J.I. (1990) Catalytically active monoamine oxidase type A from human liver expressed in *Saccharomyces cerevisiae* contains covalent FAD, *Biochem. Biophys. Res. Commun.* **173**, 1205-1211.
- Wierenga, R.K., Drenth, J. and Schulz, G.E. (1983) Comparison of the three-dimensional protein and nucleotide structure of the FAD-binding domain of *p*-hydroxybenzoate hydroxylase with the FAD as well as NADPH-binding domains of glutathione reductase, *J. Mol. Biol.* **167**, 725-739.
- Willie, A. and Jorns, M.S. (1995) Discovery of a third coenzyme in sarcosine oxidase, *Biochemistry* **34**, 16703-16707.
- Yang, C.C., Packman, L.C. and Scrutton, N.S. (1995) The primary structure of *Hyphomicrobium* X dimethylamine dehydrogenase: relationship to trimethylamine dehydrogenase and implications for substrate recognition, *Eur. J. Biochem.* **232**, 264-271.
- Yoshida, N., Sakai, Y., Isogai, A., Fukuya, H., Yagi, M., Tani, Y. and Kato, N. (1996) Primary structures of fungal fructosyl amino acid oxidases and their application to the measurement of glycosylated proteins, *Eur. J. Biochem.* **242**, 499-505.
- Zhou, B.P., Lewis, D.A., Kwan, S.W. and Abell, C.W. (1995) Flavinylation of monoamine oxidase B, *J. Biol. Chem.* **270**, 23653-23660.

2

Enigmatic gratuitous induction of the covalent flavoprotein vanillyl-alcohol oxidase in *Penicillium simplicissimum*

Marco W. Fraaije, Mariël G. Pikkemaat and Willem J. H. van Berkel

Applied and Environmental Microbiology **63**, 435-439 (1997)

Abstract

When *Penicillium simplicissimum* is grown on veratryl alcohol, anisyl alcohol, or 4-(methoxymethyl)phenol, an intracellular covalent flavin-containing vanillyl-alcohol oxidase is induced. The induction is highest (up to 5 % of total protein) during the growth phase. In addition to vanillyl-alcohol oxidase, an intracellular catalase-peroxidase is induced. Induction of vanillyl-alcohol oxidase in *P. simplicissimum* is prevented by the addition of isoeugenol to veratryl alcohol-containing media, but growth is unaffected. The inhibitory effect of isoeugenol on induction is not observed when anisyl alcohol or 4-(methoxymethyl)phenol is used as growth substrate. Based on the induction experiments and the degradation pathways for veratryl and anisyl alcohol, we propose that induction of vanillyl-alcohol oxidase is superfluous when *P. simplicissimum* is grown on these aromatic alcohols. However, the enzyme plays an essential role in the degradation of the methyl ether of *p*-cresol, 4-(methoxymethyl)phenol.

2.1. Introduction

Since the existence of plants, microorganisms must have evolved which are able to degrade plant material to complete the Earth's carbon cycle. The only organisms capable of completely degrading wood, including the aromatic polymer lignin, are wood rot fungi. That these basidiomycetes have existed for a very long period of time is confirmed by the findings of their fossilized remains (8, 10). Since degradation of lignin leads to formation of a broad spectrum of aromatic compounds, other microorganisms have developed ways to use these compounds. Several penicillia, normally soil inhabitants, degrade lignin-related aromatic compounds (2, 12, 16, 20) or even lignin to some extent (18).

Penicillium simplicissimum CBS 170.90 originally was isolated on veratryl alcohol, a central metabolite in lignin degradation (2). This fungus is able to grow on a variety of aromatic compounds as sole carbon and energy source. Further study revealed that during growth on veratryl alcohol, a flavin-dependent aromatic alcohol oxidase is induced. This enzyme catalyzes the conversion of vanillyl alcohol to vanillin with the simultaneous production of hydrogen peroxide (3). Parallel with the induction of vanillyl-alcohol oxidase, a catalase-peroxidase is induced; this enzyme has been purified and characterized (6). Vanillyl-alcohol oxidase is a homo-octamer with each subunit containing a covalently bound flavin adenine dinucleotide (22). The enzyme is most active at basic pH and consequently shows little resemblance to known fungal aryl-alcohol oxidases (22). Recently, we reported that vanillyl-alcohol oxidase is also active with aromatic amines, 4-allylphenols, 4-alkylphenols, and 4-(methoxymethyl)-phenols (5, 7). The enzymatic oxidation products can be of use in the food industry because alkylphenol derivatives and aromatic aldehydes like vanillin are known flavors (4, 21). However, since the enzyme is induced in relatively large quantities and is apparently not involved in the degradation of veratryl alcohol (2), its physiological role remains obscure.

In this work, we report on the specific induction of vanillyl-alcohol oxidase by growth of *P. simplicissimum* on veratryl alcohol, anisyl alcohol, and 4-(methoxymethyl)-phenol. The degradation pathways of these aromatic compounds were studied and are discussed in relation to the physiological function of vanillyl-alcohol oxidase.

2.2. Materials and methods

Organism and media

All experiments were performed with *P. simplicissimum* CBS 170.90. The liquid medium (pH 5.4) contained (per liter): Na₂HPO₄, 0.65 g; KH₂PO₄, 2.5 g; NH₄Cl, 2.0 g; (NH₄)₂SO₄, 0.10 g; MgCl₂·6H₂O, 0.075 g; 50 % (wt/vol) poly(acrylic acid-co-maleic acid)

(PAMA; molecular weight 3,000), 1.0 g; and 0.2 ml of a trace elements solution as described by Vishniac and Santer (24). Cells were grown in 500 ml medium in 2-liter Erlenmeyer flasks. The flasks were incubated at 30 °C with shaking, and the mycelial pellets were harvested with a cheesecloth. Carbon sources were added at 0.1 % (w/v) (aromatic compounds) or 1.0 % (w/v) (nonaromatic compounds). When grown on nonaromatic compounds and aromatic acids the cells were harvested 2 days after inoculation. In all other growth experiments, the cells were harvested after 4 days. For collecting samples during growth on veratryl alcohol (0.1%) a 20-liter fermentor (15-liter working volume; 30 °C; 50 rpm; air flow: 0.4 liter/min) was used which was inoculated with 5 mycelial pellets of glucose-grown cells. The cells were harvested regularly by withdrawing 500 ml of the culture.

Preparation of cell extracts and protoplasts

Cell extracts were prepared by three 10 s sonications of washed cell suspensions (0.5 ml of 50 mM potassium phosphate [pH 7.0]) with cooling intervals of 50 s. Cell debris was removed by centrifugation. Protoplasts were prepared by the method of Witteveen et al. (26).

Analytical methods

Veratryl alcohol (1.0 g) was purified using a silica-column (2.5 by 19 cm). After the column was washed with 100 ml of petroleum ether (boiling point, 60 to 80 °C), veratryl alcohol was collected by elution with 100 ml of methanol. Gas chromatography-mass spectrometry analysis showed that this fraction was of high purity (>99.5 %). The protein content of cell extracts was determined by the method of Lowry et al. (13). High-pressure liquid chromatography (HPLC) analysis was performed at room temperature on a Hewlett Packard 1040-1050 series HPLC system with a Chromspher C₁₈ (100 by 4.6 mm) column (Chrompack). The eluent contained methanol, water, and acetic acid (33:66:1). For detection, a Waters 996 diode array detector was used. Stock solutions of a broad range of aromatic compounds (1.0 mM) were separately analyzed for their retention times and spectral characteristics, enabling identification of the formed degradation products (retention times [minutes]: veratryl alcohol, 2.65; veratraldehyde, 4.94; veratrate, 4.58; anisyl alcohol, 3.60; anisaldehyde, 7.27; anisate, 7.99; 4-(methoxymethyl)phenol, 3.40; 4-hydroxybenzaldehyde, 2.64; 4-hydroxybenzoate, 2.25; 3,4-dihydroxybenzoate, 1.61 ; vanillin, 2.98 and 4-hydroxybenzylalcohol, 1.64).

Biochemical analysis

The vanillyl-alcohol oxidase activity was assayed at 30 °C and pH 10.0 with vanillyl alcohol as the aromatic substrate (3). Catalase and peroxidase were assayed as described

previously (6). For peroxidase activity, 2,6-dimethoxyphenol was used as the electron donor. Glucose-6-phosphate dehydrogenase was assayed by the method of Bruinenberg et al. (1). Protocatechuate 3,4-dioxygenase activity was measured spectrophotometrically at 290 nm (9). Enzyme units are expressed as micromoles of substrate converted per minute. Sodium dodecyl sulfate (SDS)-polyacrylamide gelelectrophoresis was carried out in slab gels, essentially as described by Laemmli (11). For protein staining, Coomassie brilliant blue R-250 was used. For fluorescence detection of vanillyl-alcohol oxidase, the gel was incubated in 5% acetic acid solution for 5 min after electrophoresis. Upon illumination with UV light, vanillyl-alcohol oxidase is visible because of the fluorescence of the covalently bound flavin (3). To obtain sufficient fluorescence signal for photographing, five times the amount of protein was loaded compared to that in the protein stained gels.

Generation of antibodies

Polyclonal antibodies directed against vanillyl-alcohol oxidase and catalase-peroxidase from *P. simplicissimum* were generated and purified as described before (6). By using dot-blots the detection limit of both antibodies was estimated to be less than 10 pg. For detection of vanillyl-alcohol oxidase and catalase-peroxidase on Western-blots, an alkaline phosphatase based immunoassay was used. For molecular weight estimation prestained, SDS-polyacrylamide gel electroforesis standard proteins were used (Bio-Rad).

Chemicals

Aromatic compounds were from Aldrich except for vanillin and vanillyl alcohol, which were from Janssen Chimica. All other chemicals were of commercially available analytical grade.

2.3. Results

2.3.1. Growth of *P. simplicissimum* on veratryl alcohol

It was found in a previous study that *P. simplicissimum* is able to grow on veratryl alcohol as the sole carbon and energy source (2). During growth on this aromatic alcohol vanillyl-alcohol oxidase is induced (3). Because the commercially available veratryl alcohol contains some minor aromatic impurities (4 %), we decided to purify it to exclude any effect of these aromatic impurities on the induction pattern. However, when the fungus was grown on highly purified veratryl alcohol, the same level of induction of vanillyl-alcohol oxidase was found. Fig. 1 shows that vanillyl-alcohol oxidase activity was highest during growth. When all veratryl alcohol was depleted, the enzyme activity level dropped

significantly. Other measured enzyme activities, glucose-6-phosphate dehydrogenase and catalase, were present at a nearly constant level. As *P. simplicissimum* contains two different types of catalases, an atypical periplasmic catalase and a catalase-peroxidase (6), no conclusions can be drawn with respect to the time-dependent induction of each of these hydroperoxidases.

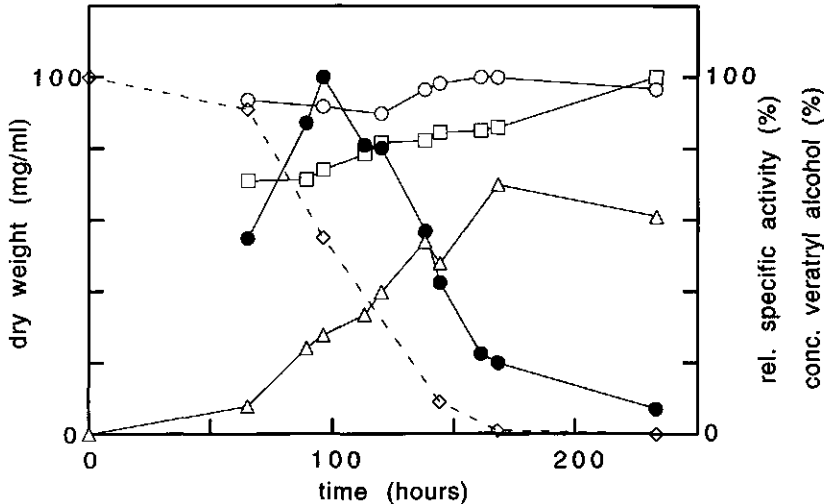


Figure 1. Growth of *P. simplicissimum* on veratryl alcohol (0.1 %, wt/vol) and some enzyme activities. Cells were grown in a 20-liter fermentor as described in Materials and Methods. Symbols: Δ, dry weight; ◊, veratryl alcohol; ○, glucose-6-phosphate dehydrogenase; ●, vanillyl-alcohol oxidase; ◻, catalase.

2.3.2. Subcellular localization

Protoplasts of *P. simplicissimum* cells were prepared to determine the subcellular location of vanillyl-alcohol oxidase. Preliminary results had indicated that both vanillyl-alcohol oxidase and catalase-peroxidase were not extracellular or cell wall localized (6). The measured activities of protoplast and cell extracts confirmed that both vanillyl-alcohol oxidase and catalase-peroxidase are intracellular enzymes (Table 1). The apparent increase in the peroxidase activity in protoplasts from veratryl alcohol-grown cells is caused by loss of the competing periplasmic catalase activity (6). When the fungus was grown on glucose, no vanillyl-alcohol oxidase activity was found (Table 1). Immunoblot detection confirmed this finding (see below). Extracts of glucose-grown cells contained periplasmic catalase activity but only minor amounts of catalase-peroxidase activity. This indicates that this enzyme is also induced by growth on veratryl alcohol. Western blot analysis confirmed the presence of some catalase-peroxidase in glucose-grown cells (data not shown).

Table 1. Specific enzyme activities in extracts of mycelium and protoplasts of *P. simplicissimum* cells grown on veratryl alcohol and glucose

Source of extract	activity ^a of:			
	G6PDH	VAO	CAT	PER
	(mU/mg)	(mU/mg)	(U/mg)	(U/mg)
Veratryl alcohol-grown cells				
Mycelium	360	81	154	0.22
Protoplast	386	78	93	0.34
Glucose-grown cells				
Mycelium	790	0	38	< 0.05
Protoplast	690	0	<1	< 0.05

^a G6PDH, glucose-6-phosphate dehydrogenase; VAO, vanillyl-alcohol oxidase; CAT, catalase; PER, peroxidase.

2.3.3. Induction of vanillyl-alcohol oxidase

To study the induction of vanillyl-alcohol oxidase in more detail, *P. simplicissimum* CBS 170.90 was grown on several aromatic compounds [phenylalanine, benzoate, 4-hydroxybenzoate, 3-hydroxybenzoate, vanillic acid, ferulic acid, caffeic acid, veratrate, veratryl alcohol, veratraldehyde, anisyl alcohol, vanillyl alcohol, homovanillyl alcohol, vanillylamine, vanillin, phenol, catechol, *p*-cresol, and 4-(methoxymethyl)phenol] and non-aromatic compounds (glucose, fructose, sucrose, oleate, and acetate). The fungus did not grow on 4-methoxyphenol, eugenol, isoeugenol, 4-ethylphenol, or 4-hydroxy-3-methoxypropylphenol under the conditions used in this study. Growth on the vanillyl-alcohol oxidase substrates vanillyl alcohol and vanillylamine did not result in any detectable vanillyl-alcohol oxidase activity. Activity could be detected only in extracts of cells grown on veratryl alcohol, anisyl alcohol or 4-(methoxymethyl)phenol. As can be seen from Fig. 2, the amount of enzyme induced by growth on these aromatic compounds is relatively high (Fig. 2., lanes B, D, and G). Purification of vanillyl-alcohol oxidase from anisyl alcohol-grown cells revealed that up to 5 % of the total protein may consist of vanillyl-alcohol oxidase (data not shown). This value is even higher than the value originally reported for veratryl alcohol-grown cells (3).

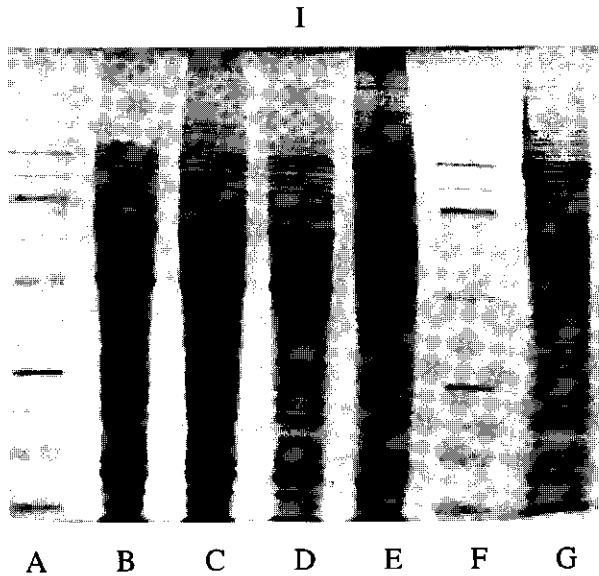
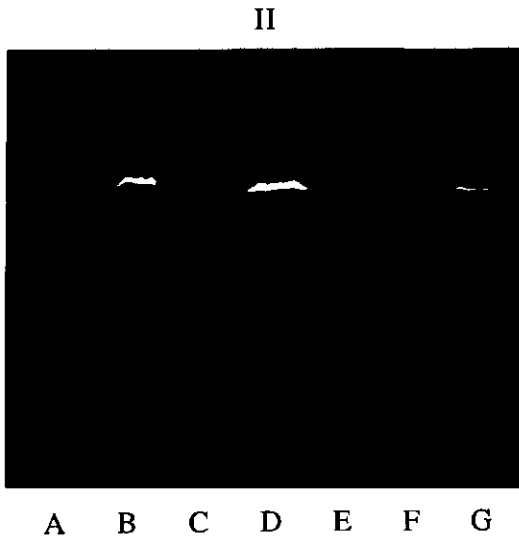


Figure 2. SDS-PAGE of extracts of *P. simplicissimum* cells grown on different substrates. Lanes: A and F, marker proteins (from top to bottom, phosphorylase *b*, 94 kDa; bovine serum albumin, 67 kDa; ovalbumine, 43 kDa; carbonic anhydrase, 30 kDa; trypsin inhibitor, 20 kDa; and α lactalbumin, 14 kDa); B to E and G, extracts of cells grown on veratryl alcohol (B), veratryl alcohol plus isoeugenol (0.01%) (C), anisyl alcohol (D), glucose (E), and 4-(methoxymethyl)phenol (G). The presence of vanillyl-alcohol oxidase (~65 kDa) is indicated by an arrow in panel (I) and was confirmed by fluorescence detection of a similarly loaded gel (II).



2.3.4. Degradation and accumulation of aromatic metabolites by whole cells

The degradation pathway of veratryl alcohol by *P. simplicissimum* was already established in an earlier report (2). To study the steps used by this fungus to degrade anisyl alcohol and 4-(methoxymethyl)phenol, a similar approach was used. Intact mycelia were

incubated with the above-mentioned phenols, and the accumulation of aromatic degradation products was analyzed by HPLC (Fig. 3). As a control, we analyzed the accumulation during veratryl alcohol degradation, which showed the same degradation products as described previously (2).

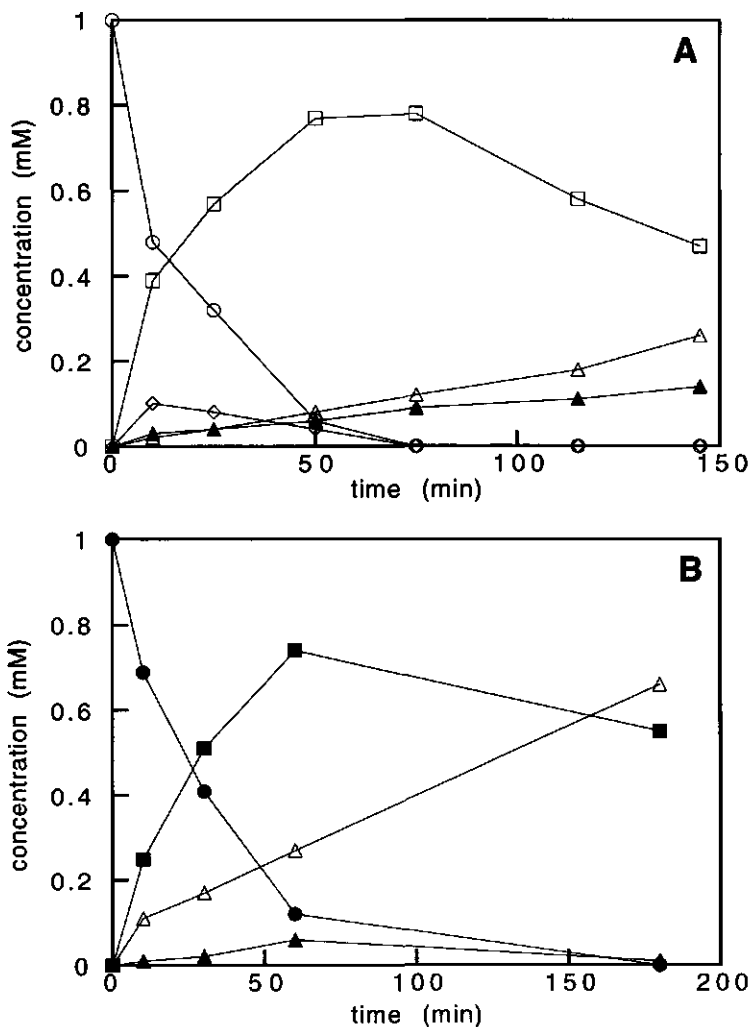


Figure 3. Consumption of anisyl alcohol (A) and 4-(methoxymethyl)phenol (B) and transient accumulation of degradation products. Incubation mixtures (50 ml) contained anisyl alcohol-grown washed cells (5 g [wet weight]) and 1 mM anisyl alcohol or 4-(methoxymethyl)phenol. Symbols: O, anisyl alcohol; ◊, anisaldehyde; ◻, anisate; Δ, 4-hydroxybenzoate; ▲, 3,4-dihydroxybenzoate; ●, 4-(methoxymethyl)phenol; ■, 4-hydroxybenzaldehyde.

As can be seen from Fig. 3, anisyl alcohol was readily degraded via two initial oxidation steps into the acid form, which was subsequently demethylated. After that, 4-hydroxybenzoate was hydroxylated to give 3,4-dihydroxybenzoate. Like the veratryl alcohol grown cells (2), anisyl alcohol- and 4-(methoxymethyl)phenol-grown cells contained protocatechuic 3,4-dioxygenase activity, catalyzing intradiol ring fission. Incubation of 4-(methoxymethyl)phenol-grown cells with 4-(methoxymethyl)phenol resulted in a rapid accumulation of 4-hydroxybenzaldehyde. Because demethylation of 4-(methoxymethyl)phenol is efficiently catalyzed by vanillyl-alcohol oxidase (5), this suggests that vanillyl-alcohol oxidase is involved in the initial degradation of 4-(methoxymethyl)phenol. By analogy to the degradation of veratryl alcohol and anisyl alcohol, 4-hydroxybenzaldehyde was oxidized to 4-hydroxybenzoate and converted to 3,4-dihydroxybenzoate to enter the β -ketoadipate pathway (19) (Fig. 4). An identical accumulation pattern of products for the degradation of 4-(methoxymethyl)phenol was found when anisyl alcohol-grown cells were used (Fig. 3).

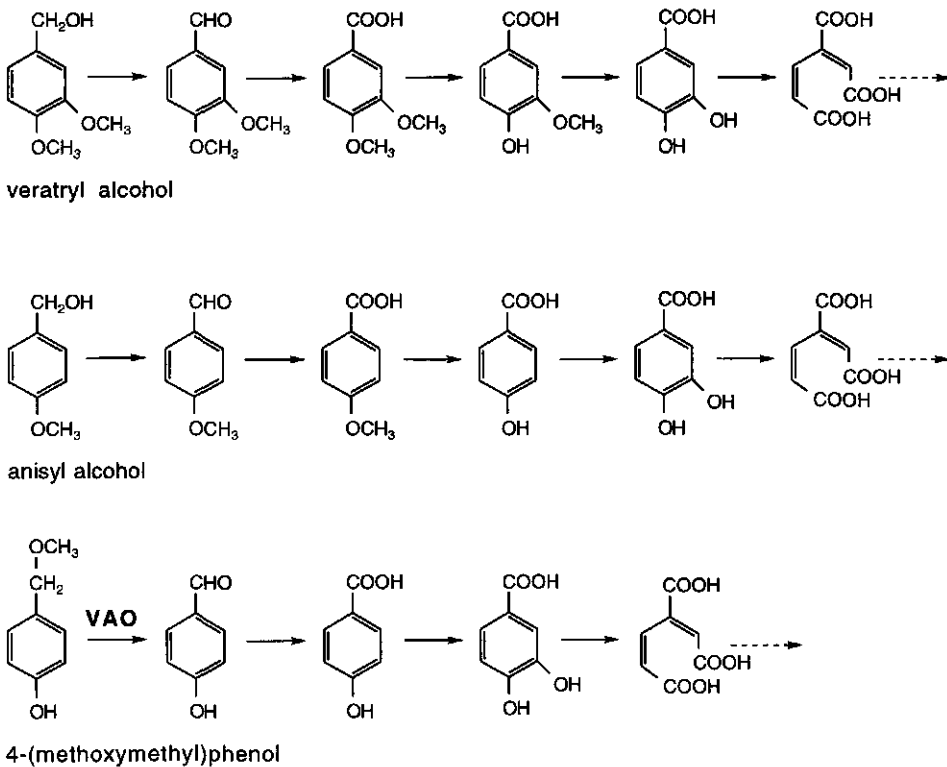


Figure 4. Degradation pathways of veratryl alcohol (2), anisyl alcohol, and 4-(methoxymethyl)phenol by *P. simplicissimum* CBS 170.90.

2.3.5. Effect of isoeugenol on induction of vanillyl-alcohol oxidase

A series of induction experiments were performed in which the fungus was grown in the absence or presence of isoeugenol. Isoeugenol is a strong competitive inhibitor for vanillyl-alcohol oxidase (5). These experiments resulted in some unexpected and interesting observations. When *P. simplicissimum* was grown on anisyl alcohol (0.1 %) or 4-(methoxymethyl)phenol (0.1 %) in the presence of isoeugenol (0.01%), no effect was found on the induction of vanillyl-alcohol oxidase or growth rate of the fungus. However, when *P. simplicissimum* was grown in veratryl alcohol-containing media to which isoeugenol (0.01 %) was added, no vanillyl-alcohol oxidase activity could be detected. Furthermore, SDS-polyacrylamide gel electrophoresis revealed that expression of the enzyme (65 kDa) was totally suppressed (Fig. 2, lane C). Only when antibodies were used could some vanillyl-alcohol oxidase be detected (Fig. 5).

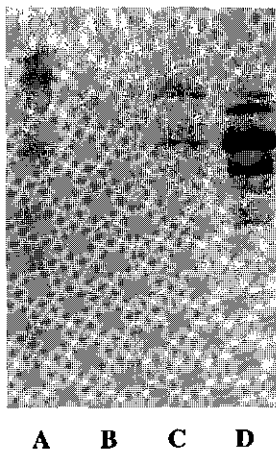


Figure 5.

Western-blot of cell-extracts (20 μ g) of *P. simplicissimum* CBS 170.90 grown on glucose (lane B); veratryl alcohol plus isoeugenol (0.01%) (lane C), and veratryl alcohol (lane D), using antibodies directed against purified vanillyl-alcohol oxidase. The arrow indicates the position of vanillyl-alcohol oxidase. Lane A contains prestained marker proteins (from top to bottom: phosphorylase *b*, 107 kDa; bovine serum albumin, 76 kDa; ovalbumine, 52 kDa; carbonic anhydrase, 36.8 kDa; trypsin inhibitor, 27.2 kDa; lysozyme, 19 kDa). Note that the apparent molecular mass of the prestained marker proteins differs from that of the unstained marker proteins (cf. Fig.2).

Apart from the band corresponding to native vanillyl-alcohol oxidase, some other minor bands were detected with antibodies. The smaller bands most probably reflect proteolytic degradation products of the enzyme because these fragments were also fluorescent. The larger bands may be cross-reactive proteins or precursor proteins of vanillyl-alcohol oxidase, and they have been observed previously (3). Although isoeugenol has a drastic effect on the induction of vanillyl-alcohol oxidase, its presence did not affect fungal growth, and the protein pattern of cell extracts was quite similar to the protein pattern of extracts of veratryl alcohol-grown cells in the absence of isoeugenol (Fig. 2, lane C). Except for the disappearance of vanillyl-alcohol oxidase, only one major difference could be clearly seen: the appearance of a protein band around 35 kDa. Similar effects were observed when lower isoeugenol concentrations (0.005% and 0.001%) were used.

2.4. Discussion

In this study, the degradation of anisyl alcohol and 4-(methoxymethyl)phenol by *P. simplicissimum* was investigated. Like veratryl alcohol, these aromatic compounds induce high levels of the covalent flavoprotein vanillyl-alcohol oxidase, while with a range of other growth substrates, no induction occurs. Growth on metabolites of the above-mentioned aromatics or growth on the vanillyl-alcohol oxidase substrates vanillyl alcohol and vanillylamine did not result in vanillyl-alcohol oxidase induction. Although the induction seems to be very strictly regulated, no rationale was found for the induction of vanillyl-alcohol oxidase by the two aromatic alcohols. The degradation pathways for veratryl alcohol and anisyl alcohol do not involve any step which can be catalyzed by vanillyl-alcohol oxidase, suggesting that the enzyme is superfluously induced. The non-functional presence of vanillyl-alcohol oxidase in *P. simplicissimum* is supported by the growth experiments with isoeugenol. The latter compound is a very potent inhibitor of vanillyl-alcohol oxidase activity (5) and is also known for its antifungal activity (17). Although isoeugenol is not degraded by *P. simplicissimum* and does not influence fungal growth on veratryl alcohol, it strongly suppresses the induction of vanillyl-alcohol oxidase. This drastic effect is not seen when *P. simplicissimum* is grown on anisyl alcohol or 4-(methoxymethyl)phenol as the sole carbon source. It is rather uncommon that an enzyme inhibitor causes the suppression of the respective enzyme. Isoeugenol may therefore compete on a genetic level with the inducer veratryl alcohol, whereas anisyl alcohol and 4-(methoxymethyl)phenol might have a higher affinity in triggering the expression of vanillyl-alcohol oxidase. To obtain further insight into the regulation of the vanillyl-alcohol oxidase gene, we are presently cloning the respective gene.

The initial demethylation step in the degradation of 4-(methoxymethyl)phenol by *P. simplicissimum* is catalyzed by vanillyl-alcohol oxidase. Furthermore, substrate specificity studies have revealed that this oxidase can readily convert substrates having relatively large substituents at the C_α-atom (5, 7). From this, we propose that 4-(methoxymethyl)phenol and analogs of this *p*-cresol methylether (e.g., ethylether) are plausible candidates as physiological substrates for this enzyme. To our best knowledge, 4-(methoxymethyl)phenol or analogous cresol ethers have never been described in the literature as being present in nature. It can, however, easily be envisaged that these phenolic compounds may be formed during the degradation of lignin, an aromatic polymer containing extensive ether bonds. This report describes for the first time a degradation pathway for 4-(methoxymethyl)phenol which involves a cleavage of an ether bond in the first step of degradation catalyzed by a flavoenzyme.

Together with the induction of vanillyl-alcohol oxidase in *P. simplicissimum*, an intracellular catalase-peroxidase is expressed. Recently, we postulated that induction of this

unusual peroxidase might be coupled to the induction of vanillyl-alcohol oxidase, because the latter enzyme produces hydrogen peroxide (6). However, this study shows that the induction of the catalase-peroxidase is not restricted to growth on aromatic compounds. So far, these enzymes, exhibiting both catalase and peroxidase activity, were mainly found in bacteria and show homology with the yeast cytochrome *c* peroxidase (25). Their peroxidatic activity is, however, relatively low, and their catalase activity is strongly inhibited by high concentrations of hydrogen peroxide (15), which might be the reason for their recent discovery in fungi (6). From this study, it is not clear which catalytic function of the catalase-peroxidase is operative in this fungus. Increased levels of catalase-peroxidase activity parallel with vanillyl-alcohol oxidase induction suggests that the catalase-peroxidase plays an essential role in the intracellular elimination of hydrogen peroxide. In this respect, it is worth mentioning that the homologous yeast cytochrome *c* peroxidase plays an essential role in the detoxification of hydrogen peroxide in the yeasts *Saccharomyces cerevisiae* and *Hansenula polymorpha* (23).

It would be interesting to determine whether the catalase-peroxidase from *P. simplicissimum* is located in peroxisomes like most eucaryotic catalases or in the mitochondria like yeast cytochrome *c* peroxidase. Also, it is interesting to know if vanillyl-alcohol oxidase is located in a specific organelle. Until now, all eucaryotic enzymes containing a covalently bound flavin have been localized in mitochondria or peroxisomes (14). The localization of vanillyl-alcohol oxidase and catalase-peroxidase might therefore give valuable information about their physiological role.

Acknowledgement

We thank Falko Drijfhout for excellent technical assistance.

2.5. References

1. Bruinenberg P.M., J.P. van Dijken and W.A. Scheffers (1983) An enzymic analysis of NADPH production in *Candida utilis*. *J. Gen. Microbiol.* **129**, 965-971.
2. De Jong E., E.E. Beuling, R.P. van der Zwan and J.A.M. de Bont (1990) Degradation of veratryl alcohol by *Penicillium simplicissimum*. *Appl. Microbiol. Biotechnol.* **34**, 420-425.
3. De Jong E., W.J.H. van Berkel, R.P. van der Zwan and J.A.M. de Bont (1992) Purification and characterization of vanillyl-alcohol oxidase from *Penicillium simplicissimum*. *Eur. J. Biochem.* **208**, 651-657.
4. Edlin D.A.N., A. Narbad, J.R. Dickinson and D. Lloyd (1995) The biotransformation of simple phenolic compounds by *Brettanomyces anomalus*. *FEMS Microbiol. Lett.* **125**, 311-316.
5. Fraaije M.W., C. Veeger and W.J.H. van Berkel (1995) Substrate specificity of flavin-dependent vanillyl-alcohol oxidase from *Penicillium simplicissimum*. *Eur. J. Biochem.* **234**, 271-277.
6. Fraaije M.W., H.P. Roubroeks, W.R. Hagen and W.J.H. van Berkel (1996) Purification and characterization of an intracellular catalase-peroxidase from *Penicillium simplicissimum*. *Eur. J. Biochem.* **235**, 192-198.

7. Fraaije M.W., F. Drijfhout, G. Meulenbelt and W.J.H. van Berkel (1996) Conversion of *p*-alkylphenols by vanillyl-alcohol oxidase, PH1. In R.M. Buitelaar (ed.), 6th Netherlands Biotechnology Congress 1996, Amsterdam, The Netherlands.
8. Fraaije R.H.B. and M.W. Fraaije (1995) Miocene bracket fungi (*Basidiomycetes*, *Aphyllphorales*) from the Netherlands. *Contr. Tert. Quatern. Geol.* **32**, 27-33.
9. Fujisawa, H. and O. Hayaishi (1968) Protocatechuate 3,4-dioxygenase. I. Crystallization and characterization. *J. Biol. Chem.* **243**, 2673-2681.
10. Hibbett D.S., D. Grimaldi and M.J. Donoghue (1995) Cretaceous mushrooms in amber. *Nature* **377**, 487.
11. Laemmli U.K. (1970) Cleavage of structural proteins during the assembly of the head of bacteriophage T4. *Nature* **227**, 680-685.
12. Launen L., L. Pinto, C. Wiebe, E. Kiehlmann and M. Moore (1995) The oxidation of pyrene and benzo[a]pyrene by nonbasidiomycete soil fungi. *Can. J. Microbiol.* **41**, 477-488.
13. Lowry O.H., N.J. Rosebrough, A.L. Farr and R.J. Randall (1951) Protein measurement with the folin phenol reagent. *J. Biol. Chem.* **193**, 265-275.
14. Mihalik S.J. and G.C. Mc Guinness (1991) Covalently-bound flavin in peroxisomal L-pipecolic acid oxidase from primates, p. 881-884. In B. Curti, S. Ronchi and G. Zannetti (ed.), *Flavins and Flavoproteins 1990*. W. de Gruyter, Berlin, New York.
15. Nadler V., Goldberg J. and A. Hochman (1986) Comparative study of bacterial catalases. *Biochim. Biophys. Acta* **882**, 234-241.
16. Patel T.R., N. Hameed and A.M. Martin (1990) Initial steps of phloroglucinol metabolism in *Penicillium simplicissimum*. *Arch. Microbiol.* **153**, 438-443.
17. Pauli A. and K. Knobloch (1987) Inhibitory effect of essential oil components on growth of food-contaminating fungi. *Z. Lebensm. Unters. Forsch.* **185**, 10-13.
18. Rodríguez A., A. Carnicero, F. Perestelo, G. De La Fuente, O. Milstein and M.A. Falcon (1994) Effect of *Penicillium chrysogenum* on lignin transformation. *Appl. Env. Microbiol.* **60**, 2971-2976.
19. Stanier R.Y. and L.N. Ornston (1973) The β -keto adipate pathway. *Adv. Microb. Physiol.* **9**, 89-151.
20. Tillet R. and J.R.L. Walker (1990) Metabolism of ferulic acid by *Penicillium* sp.. *Arch. Microbiol.* **154**, 206-208.
21. Van Berkel W.J.H., M.W. Fraaije and E. de Jong (1993) Process for producing 4-hydroxycinnamyl alcohols, patent application N.L. 93201975.5 of 0607-1993.
22. Van Berkel W.J.H., M.W. Fraaije, E. de Jong and J.A.M. de Bont. (1994) Vanillyl-alcohol oxidase from *Penicillium simplicissimum*: a novel flavoprotein containing $8\alpha(N^3\text{-histidyl})\text{-FAD}$, p. 799-802. In K. Yagi (ed.), *Flavins and flavoproteins 1993*. W. de Gruyter, Berlin, New York.
23. Verduyn C., M.L.F. Giuseppin, W.A. Scheffers and J.P. van Dijken (1988) Hydrogen peroxide metabolism in yeasts. *Appl. Environ. Microbiol.* **54**, 2086-2090.
24. Vishniac W. and M. Santer (1957) *The thiobacilli* *Bacteriol. Rev.* **21**, 195-213.
25. Welinder K.G. (1992) Superfamily of plant, fungal and bacterial peroxidases. *Curr. Opin. Struct. Biol.* **2**, 388-393.
26. Witteveen C.F.B., M. Veenhuis and J. Visser (1992) Localization of glucose oxidase and catalase activities in *Aspergillus niger*. *Appl. Environ. Microbiol.* **58**, 1190-1194.

3

Purification and characterization of an intracellular catalase-peroxidase from *Penicillium simplicissimum*

Marco W. Fraaije, Hanno P. Roubroeks, Wilfred R. Hagen and Willem J. H. van Berkel

European Journal of Biochemistry **235**, 192-198 (1996)

Abstract

The first dimeric catalase-peroxidase of eucaryotic origin, an intracellular hydroperoxidase from *Penicillium simplicissimum* which exhibited both catalase and peroxidase activities, has been isolated. The enzyme has an apparent molecular mass of about 170 kDa and is composed of two identical subunits. The purified protein has a pH optimum for catalase activity at 6.4 and for peroxidase at 5.4. Both activities are inhibited by cyanide and azide whereas 3-amino-1,2,4-triazole has no effect. 3,3'-Diaminobenzidine, 3,3'-dimethoxy-benzidine, guaiacol, 2,6-dimethoxyphenol and 2,2'-azinobis(3-ethylbenzothiazoline-6-sulfonic acid) all serve as substrates. The optical spectrum of the purified enzyme shows a Soret band at 407 nm. Reduction by dithionite results in the disappearance of the Soret band and formation of three absorption maxima at 440, 562 and 595 nm. The prosthetic group was identified as a protoheme IX and EPR spectroscopy revealed the presence of a histidine residue as proximal ligand.

In addition to the catalase-peroxidase, an atypical catalase which is active over a broad pH range was also partially purified from *P. simplicissimum*. This catalase is located in the periplasm and contains a chlorin-type heme as prosthetic group.

3.1. Introduction

Catalases are ubiquitous enzymes which have been isolated from a broad range of procaryotic and eucaryotic organisms. Most catalases described so far are tetramers with molecular masses ranging over 220-270 kDa with each subunit containing a protoheme as prosthetic group. These typical catalases are active in the pH range 5-10 and are specifically inactivated by 3-amino-1,2,4-triazole.

More recently, some intracellular hydroperoxidases have been described that have properties deviating from the above enzymes. Enzymes of this new class of hydroperoxidases exhibit both catalase as well as significant peroxidase activity and are therefore called catalase-peroxidases. Besides their different catalytic behaviour these enzymes also differ in their reduction by dithionite, the narrow pH range for maximal activity, inactivation by hydrogen peroxide and their insensitivity to 3-amino-1,2,4-triazole. Most of the catalase-peroxidases are tetramers isolated from bacteria (1-6). Those of *Bacillus stearothermophilus* (7), *Comamonas compransoris* (8), *Mycobacterium tuberculosis* (9) and *Streptomyces cyaneus* (10) exist as dimers. Furthermore, monomeric catalase-peroxidases have been purified from two halophilic archaeobacteria (11, 12). Until now the tetrameric catalase-peroxidase from the fungus *Septoria tritici* (13) is the only reported catalase-peroxidase of eucaryotic origin.

In this study we describe the purification and initial characterization of an intracellular catalase-peroxidase from the plectomycete *Penicillium simplicissimum*. When grown on veratryl alcohol, *P. simplicissimum* induces an intracellular vanillyl-alcohol oxidase which is a potential source of intracellular hydrogen peroxide (14). During the purification of this flavoprotein oxidase, we copurified a hydroperoxidase with some unusual properties. Based on its catalytic and physical properties this enzyme is designated as a catalase-peroxidase. Furthermore, evidence is presented that, in *P. simplicissimum*, an atypical periplasmic catalase containing a chlorintype heme as the prosthetic group is also expressed.

3.2. Materials and methods

General

3-Amino-1,2,4-triazole, 2,2'-azino-bis(3-ethylbenzothiazoline-6-sulfonic acid) (ABTS), Coomassie brilliant blue R250, 3,3'-diaminobenzidine, peroxidase from horseradish and lysing enzymes from *Trichoderma harzianum* were obtained from Sigma. Acrylamide and bisacrylamide were from Serva. Phenyl-Sepharose CL-4B, Superose 6 HR 10/30, Superdex 200 HR 10/30, Superdex PG-200, Q-Sepharose HI-LOAD and the low-molecular-mass calibration kit for SDS/PAGE were products of Pharmacia.

Hydroxyapatite was purchased from Bio-Rad. All other chemicals were of commercially available analytical grade.

Penicillium simplicissimum (Oudem.) Thom. CBS 170.90 was maintained at 4 °C on glucose/agar slants. The fungus was grown on veratryl alcohol as described before (14). A 20-l fermentor was used for cultivation. Cells were harvested five days after inoculation by filtration over a cheese cloth, washed with 50 mM potassium phosphate pH 7.0 and stored at -20 °C until use.

Enzyme purification

All purification steps were performed at 4 °C and 0.5 mM phenylmethylsulfonyl fluoride was added to the buffers used in purification. After thawing, 300 g wet cells were resuspended in 20 mM potassium phosphate pH 7.5 and disrupted by passage through a chilled French press. The resultant homogenate was clarified by centrifugation and adjusted to 20 % saturation with ammonium sulfate. After centrifugation the supernatant was applied to a phenyl-Sepharose column (33 × 2.6 cm) equilibrated with 20 mM potassium phosphate pH 7.5 containing 0.5 M ammonium sulfate. Following washing of the column, the catalase-peroxidase was eluted with 20 mM potassium phosphate pH 7.5. The active fraction was applied to a Q-Sepharose column (10 × 2.6 cm) equilibrated with 20 mM potassium phosphate pH 7.5. After washing, the enzyme was eluted with a linear gradient (0 - 1.0 M KCl in the starting buffer). Active fractions were concentrated and washed with 20 mM potassium phosphate pH 7.5 using an Amicon YM-30 ultrafiltration unit. The resulting enzyme preparation was then applied to a hydroxyapatite column (12 × 2.6 cm) equilibrated with 20 mM potassium phosphate pH 7.5 and eluted with the same buffer. In the final step the active fraction was concentrated by ultrafiltration to 8 ml and eluted over a Superdex PG-200 gelfiltration column (85 × 2.6 cm) equilibrated with 20 mM potassium phosphate pH 7.5. Active fractions showing optimal A407/A280 ratios were pooled, concentrated by ultrafiltration and stored at -70 °C.

Analytical methods

Catalase activity was routinely assayed spectrophotometrically at 25 °C by following the decrease in absorption at 240 nm ($\epsilon_{240} = 43.6 \text{ mM}^{-1}\text{cm}^{-1}$) of 10 mM H₂O₂ in 50 mM potassium phosphate pH 6.4. Peroxidase activity was measured spectrophotometrically in 50 mM potassium phosphate pH 5.4, 1.0 mM H₂O₂ and 0.5 mM 3,3'-diaminobenzidine. Furthermore, 3,3'-dimethoxybenzidine ($\epsilon_{460} = 11.3 \text{ mM}^{-1}\text{cm}^{-1}$; 15), guaiacol, 2,6-dimethoxyphenol ($\epsilon_{469} = 49.6 \text{ mM}^{-1}\text{cm}^{-1}$; 16) or 2,2'-azino-bis(3-ethylbenzothiazoline-6-sulfonic acid) were used as aromatic substrates. 1 U is defined as the amount of enzyme that catalyzes the oxidation of 1 μmol hydrogen peroxide min^{-1} under the assay conditions.

Absorption spectra were recorded at 25°C on an Aminco DW-2000 spectrophotometer. In reduction experiments, solutions were made anaerobic by alternate evacuation and flushing with argon. Enzyme reduction was achieved by adding sodium dithionite (final concentration 100 µM). EPR spectra were recorded on a Bruker ER 200D spectrometer with peripheral instrumentation and data acquisition as described before (17). Spectral simulation was done on an Intel 80486 based PC with a program written in FORTRAN (W.R. Hagen, unpublished). Ferrous PCP complexed with nitrite oxide was prepared as described by Cendrin et al. (12) except that the sodium salts were added in buffer solution.

Analytical gelfiltration utilized Superose-6 HR 10/30 as well as Superdex 200 HR 10/30 columns. These columns were calibrated with 50 mM potassium phosphate buffer at either pH 7.0 or pH 7.5, containing 100 mM sodium sulfate. Sedimentation-velocity measurements were performed essentially as described by Müller et al. (18) using a MSE Centriscan 75 analytical centrifuge. Scanning wavelengths of 280 and 400 nm were used. The sedimentation coefficient ($S_{20,w}$) determined at 20 °C in 50 mM potassium phosphate pH 7.0 was calculated from plots of $\ln r$ versus time and making appropriate viscosity corrections. The subunit molecular mass was determined by SDS-PAGE (19), using 12.5 % (w/v) acrylamide. PAGE on native enzyme was performed on a Phast-system (Pharmacia). Polyacrylamide gels were stained for peroxidase and catalase activity as previously described (3, 20). Purified PCP to be used in the generation of antibodies was electroeluted from SDS-PAGE gels with recoveries of 50-60%. Rabbits were immunized by subcutaneous injection of 200 µg protein and a booster injection (150 µg) 14 days later.

Protoplasts were prepared by the method of Witteveen et al. (21). Carbohydrate analysis was performed by the phenolic/sulfuric acid method using D-glucose as a standard (22). Protein concentrations were determined by the method of Lowry et al. (23) using bovine serum albumin as a standard.

3.3 Results

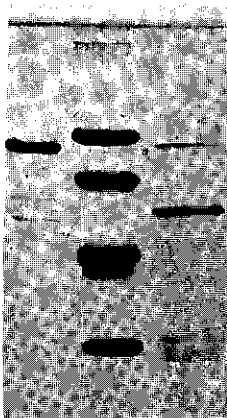
3.3.1 Purification and subcellular localization of enzymes

Extracts of *P. simplicissimum* cells grown on veratryl alcohol exhibit, besides vanillyl-alcohol oxidase activity (14), a relatively high catalase activity (150 - 250 U/mg). The activity in extracts of cells grown in glucose was considerably lower (50 - 100 U/mg) and no vanillyl-alcohol oxidase activity was present. Under both conditions no extracellular catalase could be detected.

Table 1. Purification scheme of catalase-peroxidase from *Penicillium simplicissimum*.

Step	Volume	Protein	Activity	Specific activity	Yield
	ml	mg	kU	U/mg	%
Cell extract	600	2000	499	250	100
Ammonium sulfate	720	1700	352	210	71
Phenyl-Sepharose	90	270	150	550	30
Q-Sepharose	40	130	145	1120	29
Hydroxyapatite	8	53	99	1870	20
Superdex 200	7	18	52	2960	10

Initial isolation of the hydroperoxidase from veratryl alcohol-grown cells showed that almost half of the catalase activity was not retained on phenyl-Sepharose (Table 1). Subsequent purification of this fraction by Q-Sepharose and Superdex PG-200 resulted in a partially purified 'green' catalase, designated as PAC, showing a major band of about 60 kDa by SDS/PAGE (Fig. 1, lane C). The hydroperoxidase fraction retained by phenyl-Sepharose was further purified in three steps (Table 1). SDS/PAGE of this catalase-peroxidase (PCP) showed a protein band of 83 kDa and some minor impurities (Fig. 1, lane A). Antiserum to the purified PCP showed no cross-reactivity towards any protein in the partially purified PAC fraction (data not shown). This indicates that the two isolated hydroperoxidases are structurally different.



A B C

Figure 1. SDS/PAGE results for purified hydroperoxidases from *P. simplicissimum*. Lane A, purified PCP; lane B, marker proteins (from top to bottom: phosphorylase *b*, 94 kDa; bovine serum albumin, 67 kDa; ovalbumin, 43 kDa; carbonic anhydrase, 30 kDa); lane C, partially purified PAC.

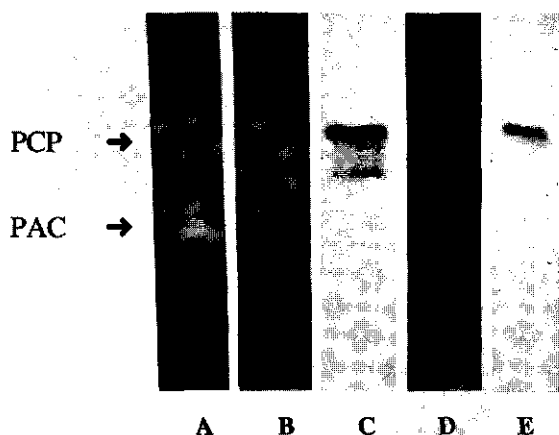


Figure 2. Catalase and peroxidase staining of PAGE sections of different enzyme preparations from *P. simplicissimum*. Lane A, extract of cells grown in veratryl alcohol stained for catalase activity; lanes B and C: purified PCP stained for (B) catalase activity and (C) peroxidase activity; lanes D and E, extract of protoplasts of cells grown on veratryl alcohol stained for (D) catalase activity and (E) peroxidase activity.

The presence of two catalases in *P. simplicissimum* was confirmed by catalase activity staining of protein subjected to PAGE. Extracts of cells grown on veratryl alcohol revealed two zones of catalase activity (Fig. 2, lane A), one of them weak and diffuse. In contrast, the purified catalase-peroxidase preparation (Fig. 2, lane B) showed only the diffuse component. This component also seen in extracts of protoplasts (Fig. 2, lane D) prepared from cells grown on veratryl alcohol was less diffuse. Staining of the same samples for peroxidase activity (Fig. 2, lane C and E) showed that the purified enzyme is also active as a peroxidase and therefore is a catalase-peroxidase. It can also be seen from Fig. 2 (lane B and C) that during purification a minor protein species is formed from the native PCP. Because this species is not observed in cell extracts (lane A) or protoplast preparations (lane E), the microheterogeneity of the purified enzyme may be due to chemical modification or limited proteolysis as noticed with the catalase-peroxidase from *Rhodopseudomonas capsulata* (24). The second catalase band present in cell extracts (lane A) corresponds to the partially purified 'green' catalase. This catalase was not observed in the protoplast extract and did not show any peroxidase activity. Therefore it most probably represents a periplasmic catalase. Activity measurements on protoplast extracts also indicated that after digestion of the cell wall the specific peroxidase activity is comparable to that of extracts of normal cells while catalase activity decreases significantly (data not shown). Cells grown in glucose-containing media showed almost no peroxidase activity, indicating that the catalase activity of these cells is due to the low expression of catalase-peroxidase and a more constitutive expression of the periplasmic catalase.

3.3.2. Catalytic properties

The activity of purified PCP from *P. simplicissimum* is strongly pH-dependent (Fig. 3). The optimum for catalase is about pH 6.4, whereas the peroxidase activity is optimal around pH 5.4. This different dependency is a common feature for catalase-peroxidases. The apparent K_m for H_2O_2 of the catalase activity of PCP at pH 6.4 was 10.8 mM. At a substrate concentration of 10 mM, PCP has a specific activity of 2960 U/mg which is rather high when compared with other catalase-peroxidases.

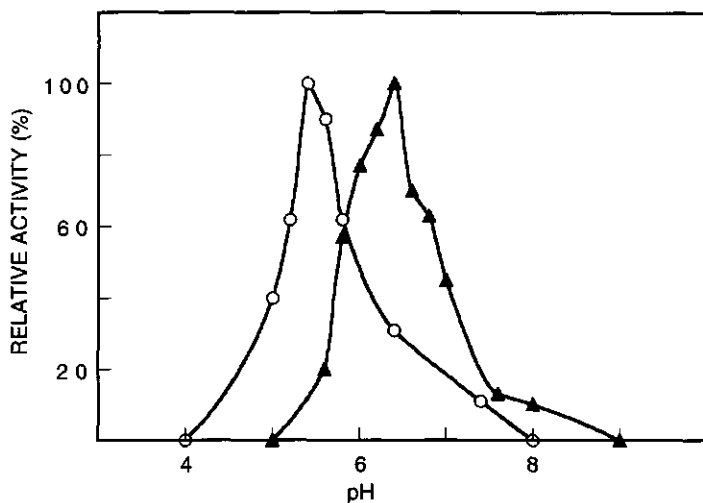


Figure 3. pH dependence of the catalase and peroxidase activity of PCP. The catalase (▲) and peroxidase (○) activity was determined in buffers of 50 mM potassium phosphate citric acid (pH 4.0-8.0) and 50 mM glycine (pH 8.0-10.5) at 25 °C. The relative activity is plotted against pH. 3,3'-Diaminobenzidine was used as electron donor in the peroxidase assay.

Table 2. Peroxidatic activity of PCP with several aromatic compounds.

Substrate	Detection wavelength	Specific activity
	nm	$\Delta A \cdot mg^{-1} \cdot min^{-1}$ (U/mg)
ABTS	415	150
2,6-dimethoxyphenol	469	77 (1.6)
3,3'-diaminobenzidine	460	16
3,3'-dimethoxybenzidine	460	28 (2.5)
guaiacol	450	7.5

PCP was also tested for its capability to oxidize certain aromatic compounds at pH 5.4 (Table 2). In addition to the compounds listed, NADPH, vanillyl alcohol and veratryl alcohol were also tested as electron donors. These compounds were not oxidized. The oxidation rate of 3,3'-dimethoxybenzidine is comparable with those of other catalase-peroxidases (3, 13). PCP is reversibly inhibited by potassium cyanide and sodium azide reaching 50% inhibition at 3 μ M and 17 μ M, respectively. PCP is not inactivated by 3-amino-1,2,4-triazole, a specific inhibitor of catalases (25). Incubation of PCP for 60 min with 20 mM 3-amino-1,2,4-triazole had no effect.

Stability tests performed at 37 °C showed that PCP is most stable at relatively high pH. At pH 5, all activity is lost within 5 min whereas no inactivation was observed between pH 7 and pH 9 at this temperature after a 10-h incubation. The enzyme remained fully active at pH 5 for more than 15 min at 25°C. The pH stability of PCP closely resembles that of the catalase-peroxidase from *Septoria tritici* (13).

The catalytic properties of the partially purified PAC were tested in some detail. This catalase has a very broad pH optimum for activity with more than 90 % of the maximum activity remaining between pH 5.0 and 9.5. This characteristic is shared by typical catalases. An apparent linear relationship was found between the catalase activity and H₂O₂ concentration in the substrate range 0-20 mM. The activity of partially purified PAC was 6000 U/mg at a substrate concentration of 20 mM.

3.3.3. Physical properties

The molecular mass and the subunit composition of PCP were determined by SDS/PAGE, gel-permeation chromatography and analytical ultracentrifugation. As mentioned above, the subunit mass of PCP is 83 \pm 3 kDa based on SDS/PAGE (Fig. 1). From analytical gel filtration under native conditions, an apparent molecular mass of 170 \pm 10 kDa was determined (Fig. 4). This value was nearly independent of the type of column or buffer used (see Materials and methods). Sedimentation velocity experiments at 0.1-0.5 mg/ml yielded single symmetric boundaries with a sedimentation coefficient, $S_{20,w}$ = 8.3 \pm 0.2 S. These results indicate that the enzyme is a homodimer with an average molecular mass of about 170 kDa. This is in the same range as reported for other dimeric catalase-peroxidases.

PCP does not contain a significant amount of carbohydrate. In contrast, the total content of neutral sugar of the partially purified PAC is approximately 12 %. These findings confirm the intracellular localization of both hydroperoxidases.

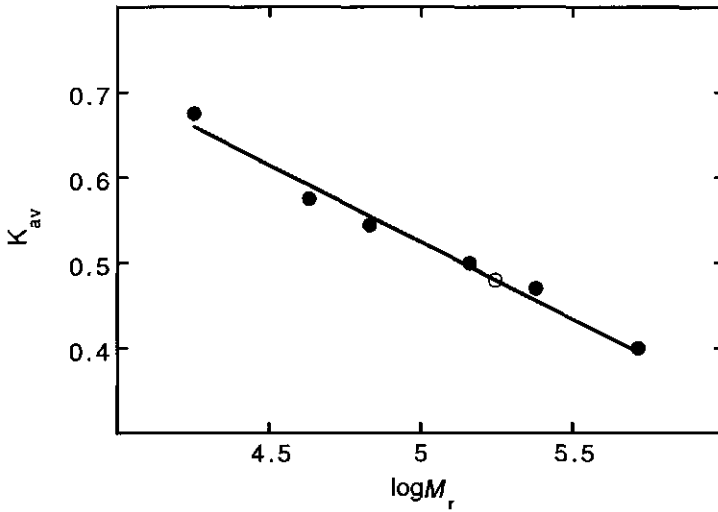


Figure 4. Analytical gel filtration of PCP. The molecular mass relation to the partition coefficient (K_{av}) of the catalase-peroxidase of *P. simplicissimum* (○) as determined on a Superose 6 HR 10/30 column equilibrated in 50 mM potassium phosphate pH 7.0. The marker proteins: vanillyl-alcohol oxidase from *P. simplicissimum* (520 kDa, [14]), beef liver catalase (240 kDa), yeast alcohol dehydrogenase (144 kDa), bovine serum albumin (67 kDa), ovalbumin (43 kDa) and myoglobin (17.8 kDa) were run in parallel (●). Each calibration point is the result of at least two independent determinations.

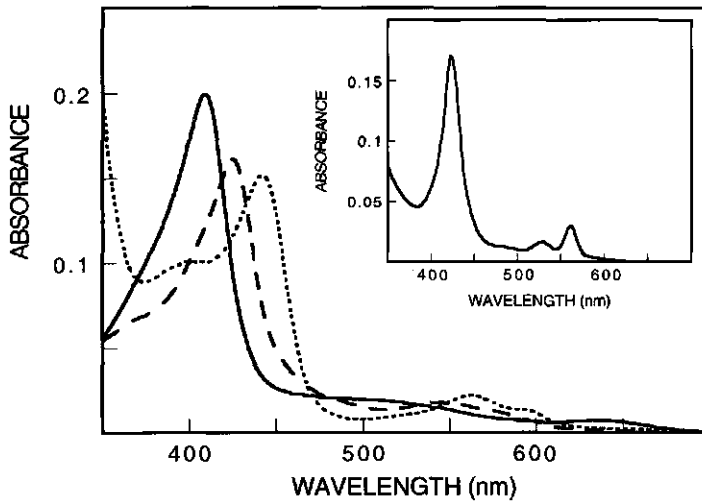


Figure 5. Spectral properties of oxidized and reduced PCP. The spectra of PCP (0.24 mg/ml) in potassium phosphate pH 7.0 were recorded at 25 °C; native enzyme (—); after the addition of 10 mM KCN (-----); after addition of 0.1 mM sodium dithionite (.....). The inset shows the pyridine hemochrome spectrum of PCP after reduction with dithionite in 2.1 M pyridine and 0.1 M NaOH.

PCP shows a typical high-spin ferric heme spectrum with a maximum at 407 nm and two shoulders at 510 nm and 638 nm (Fig. 5). A value of 0.43 for the ratio $A_{407\text{nm}}/A_{280\text{nm}}$ compares favorably with those reported for the bacterial catalase-peroxidases. Upon reduction with dithionite, the Soret band decreases and shifts to 440 nm with a new maximum appearing at 562 nm with a shoulder at about 595 nm. Addition of cyanide to the oxidized enzyme results in a shift of the Soret band to 423 nm and the appearance of an absorbance at 543 nm with a shoulder at 590 nm. These spectral properties closely resemble the optical characteristics of known catalase-peroxidases. The presence of a maximum at 543 nm for the cyanide complex suggests that the proximal heme ligand is a histidine (24). The inset of Fig. 5 shows the absorption spectrum of PCP after treatment with pyridine/NaOH. The pyridine hemochromogen spectrum obtained is identical to that of protoheme IX.

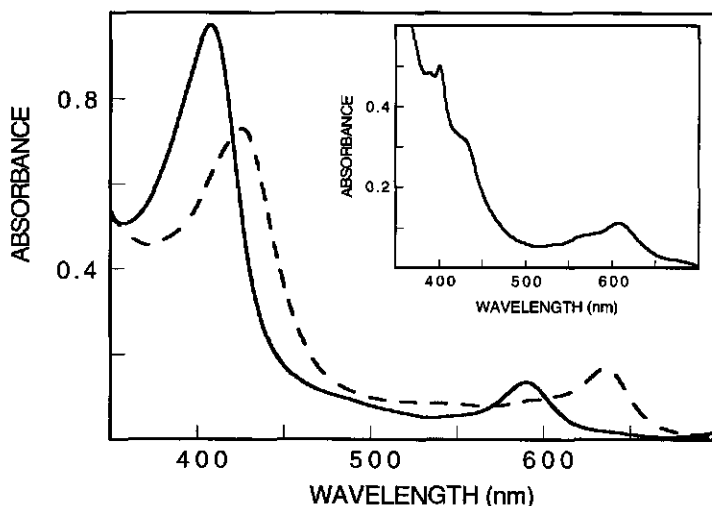


Figure 6. Spectral properties of partially purified PAC. The spectra of PAC (2 mg/ml) in potassium phosphate pH 7.0 were recorded at 25 °C; native enzyme (—); after the addition of 10 mM KCN (---). The inset shows the pyridine hemochrome spectrum after reduction with dithionite in 2.1 M pyridine and 0.1 M NaOH.

The absorption spectrum of the oxidized form of PAC differed from that of PCP by having an additional maximum at 590 nm which explains the greenish color of the enzyme solution (Fig. 6). In contrast to PCP, PAC was not reduced by dithionite. This insensitivity towards dithionite is a general property of the typical catalases. Furthermore, the inset of Fig. 6 shows that the pyridine hemochromogen spectrum of PAC has a maximum at 606 nm

with shoulders around 530 nm and 565 nm. This suggests that PAC contains a chlorin-type heme as prosthetic group (26). This unusual type of heme has been found in only a few proteins including tetrameric catalases from *Neurospora crassa* (26), *Klebsiella pneumonia* (20) and the hexameric catalase of *Escherichia coli* (27). In analogy with these enzymes, addition of cyanide to oxidized PAC results in a shift of the Soret band (425 nm) and the formation of a maximum at 636 nm (Fig. 6).

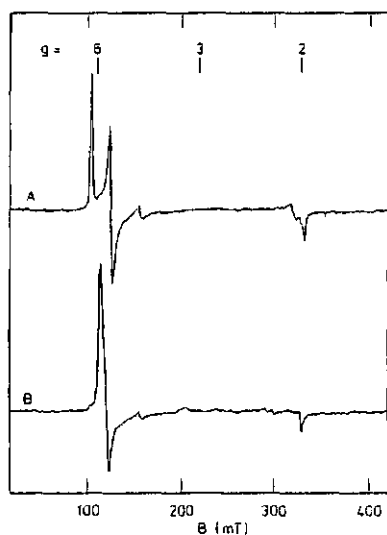


Figure 7. High-spin ferric heme EPR spectra of PAC and of PCP. Trace A, 8 mg/ml PAC in 100 mM potassium phosphate pH 7.0; trace B, 10 mg/ml PCP in 100 mM potassium phosphate pH 7.0. EPR conditions: microwave frequency, 9.18 GHz, microwave power, 5 mW; modulation frequency, 100 kHz; modulation amplitude, 0.63 mT; temperature, 14.5 K.

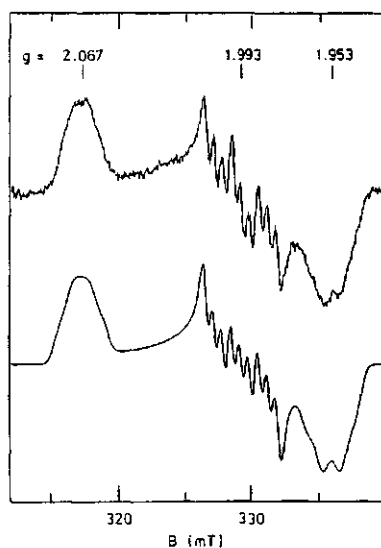


Figure 8. EPR and simulation spectra of the NO derivative of PCP. PCP (7.1 mg/ml) in 100 mM potassium phosphate pH 7.0 was incubated for 10 min after addition of sodium nitrite and sodium dithionite under a strict argon atmosphere at ambient temperature. EPR conditions: microwave frequency, 9.18 GHz, microwave power, 8 mW; modulation frequency, 100 kHz; modulation amplitude, 0.13 mT; temperature, 100 K. The spectrum (upper trace) is an average of nine scans. The simulation (lower trace) is based on 100x100 molecular orientations and assumes a rhombic $S=1/2$ spectrum with a Gaussian line shape in field space split by two nitrogen ($I=1$) nuclei (cf. Table 3).

EPR spectra confirmed that both PCP and PAC contain an $S = 5/2$ high spin ferric heme. With both hemoproteins one rhombic signal was found with resonances at about $g = 2$ and $g = 6$ (Fig. 7, Table 3). The spectrum of PAC (Fig. 7, trace A) showed an increased rhombicity compared to the spectrum of PCP (Fig. 7, trace B) consistent with

structural differences in ligation of the prosthetic groups. Interestingly, for both spectra the average value of g_x and g_y is significantly less than 6.0. This is indicative for quantum-mechanical mixing with a low lying $S = 3/2$ state, and has been noted for other peroxidases (28). The spectrum of PCP also shows a minor low-spin heme component with $g_z = 3.2$.

Nitrous oxide is a heme ligand which can be used to determine the nature of the proximal ligand of hemoproteins by EPR measurements. Because PAC can not be reduced by dithionite only the EPR spectrum of reduced PCP complexed with nitrous oxide could be obtained (Fig. 8). This protein has lost the signals in the $g = 6$ region and exhibits one with rhombic symmetry around $g = 2$ (Table 3) which is characteristic for low-spin ferrous heme NO complexes ($S = 1/2$). A triplet of signals is seen in the g_z region from hyperfine interaction with the ^{14}N nucleus ($I = 1$) of NO. An additional weaker hyperfine splitting of these three lines was observed which can be explained by the presence of an additional nitrogen coordinating to the ferrous ion (29). Simulation as a rhombic $S = 1/2$ spectrum with the presence of two nitrogen nuclei resulted in a very good fit (Fig. 8). This hyperfine coupling pattern indicates that in PCP the proximal ligand is most probably a histidine residue as suggested above.

Table 3. EPR parameters of ferric PAC/PCP and the ferrous NO derivative of PCP. The parameters for the Fe(II)-NO complex were determined in the computer simulation of Fig. 8. The other g -values were obtained from the spectra recorded in Fig. 7

Enzyme	Form	g_x	g_y	g_z
PAC	high-spin ferric	5.41	6.48	1.98
PCP	high-spin ferric	5.60	5.90	2.00
	low-spin ferric	n.d.	n.d.	3.22
PCP ferrous-NO		2.067	1.953	1.993
	Value	Other values (mT)		
		x	y	z
	line width	0.7	0.7	0.38
	hyperfine splittings from:			
	NO	1.0	1.2	2.05
	histidine	0.65	0.65	0.65

3.4 Discussion

In this study we describe the (partial) purification of two structurally distinctive hydroperoxidases from the plectomycete *Penicillium simplicissimum*, an intracellular catalase-peroxidase (PCP) and a periplasmic atypical catalase (PAC). The first catalase-peroxidase of eucaryotic origin was recently purified from the fungus *Septoria tritici* (13). This catalase-peroxidase resembles PCP by its spectral and catalytical properties. A major difference between the two enzymes is their oligomeric structure. Whereas PCP from *P. simplicissimum* is a homodimer of 170 kDa, the catalase-peroxidase from *S. tritici* is a homotetramer with a molecular mass of 244 kDa (13). Spectral properties indicate that both eucaryotic catalase-peroxidases contain histidine as proximal heme ligand which is a common feature of catalase-peroxidases and all heme-containing peroxidases. In this study EPR experiments confirmed the presence of a histidine as proximal ligand in PCP.

Sequence similarity studies have revealed that bacterial catalase-peroxidases consist of two domains which have similarities with yeast cytochrome *c* peroxidase (30). Thus catalase-peroxidases appear to have evolved from an ancestral peroxidase and are therefore members of the plant peroxidase superfamily. As PCP is the second fungal catalase-peroxidase described, it seems likely that this type of hydroperoxidases is not restricted to a bacterial peroxidase family as proposed by Welinder (31) but forms a more widespread family consisting of both prokaryotic and eucaryotic members.

In addition to a catalase-peroxidase, a catalase is also present in *P. simplicissimum* which is active over a broad pH range and can not be reduced by dithionite. This catalase contains an uncommon chlorin-type heme. This type of prosthetic group has recently been extensively studied (32) and has been found only in three other catalases.

The presence of multiple catalases has been observed in other fungi. Three different catalases were detected in *Neurospora crassa* (33) and four in *Aspergillus niger* (21). In *A. niger* two catalases are located peripheral to the outer cell membrane. Furthermore, cell extracts of the fungal wheat pathogen *S. tritici* contained, in addition to a catalase-peroxidase, two additional catalases (13). Eucaryotic catalases are commonly located in peroxisomes but have also been found in the periplasm of the ligninolytic fungus *Phanerochaete chrysosporium* (34) and the cell wall of the plectomycete *A. niger* (21). Furthermore, it is known that catalases can be excreted by fungi, especially by *Penicillia* and *Aspergilli*, in high quantities (35, 36). In *P. simplicissimum* an atypical catalase is located outside the cell membrane. This 'green' catalase presumably eliminates external hydrogen peroxide.

The PCP of *P. simplicissimum* may be involved in detoxification processes. It is highly expressed when grown on veratryl alcohol which coincides with the induction of the flavoprotein oxidase, vanillyl-alcohol oxidase (14). Induction of both enzymes suggests that

the hydrogen peroxide formed by the flavoprotein is either destroyed or used for some catabolic process by the catalase-peroxidase. Preliminary results suggest that both PCP and vanillyl-alcohol oxidase are located in peroxisomes which is a further indication that the physiological functions of these enzymes are linked. A similar peroxisomal oxidase/peroxidase couple is present in methylotrophic yeasts. In these organisms methanol oxidase and catalase both oxidize methanol to form formaldehyde using oxygen and hydrogen peroxide, respectively as electron acceptor (37). However, the question of whether PCP *in vivo* is mainly active as a catalase or a peroxidase and its relation to vanillyl-alcohol oxidase remains to be elucidated.

3.5 References

1. Claiborne, A. & Fridovich, I. (1979) Purification of the o-dianisidine peroxidase from *Escherichia coli* B, *J. Biol. Chem.* **254**, 4245-4252.
2. Nadler, V., Goldberg, I. & Hochman, A. (1986) Comparative study of bacterial catalases, *Biochim. Biophys. Acta* **882**, 234-241.
3. Hochman, A. & Goldberg, I. (1991) Purification and characterization of a catalase-peroxidase and a typical catalase from the bacterium *Klebsiella pneumonia*, *Biochim. Biophys. Acta* **1077**, 299-307.
4. Yumoto, I., Fukumori, Y. & Yamanaka, T. (1990) Purification and characterization of catalase from a facultative alkalophilic *Bacillus*, *J. Biochem. (Tokyo)* **108**, 583-587.
5. Morris, S.L., Nair, J. & Rouse D.A. (1992) The catalase-peroxidase of *Mycobacterium intracellulare*: nucleotide sequence analysis and expression in *Escherichia coli*, *J. Gen. Microbiol.* **138**, 2363-2370.
6. Brown-Peterson, N.J. & Salin, M.L. (1993) Purification of a catalase-peroxidase from *Halobacterium halobium*: characterization of some unique properties of the halophilic enzyme, *J. Bacteriol.* **175**, 4197-4202.
7. Loprasert, S., Negoro, S. & Okada, H. (1988) Thermostable peroxidase from *Bacillus stearothermophilus*, *J. Gen. Microbiol.* **134**, 1971-1976.
8. Nies, D. & Schlegel, H.G. (1982) Catalase from *Comamonas compransoris*, *J. Appl. Microbiol.* **28**, 311-319.
9. Diaz, G.A. & Wayne, L.G. (1974) Isolation and characterization of catalase produced by *Mycobacterium tuberculosis*, *Am. Rev. Resp. Disease* **110**, 312-319.
10. Mliki, A. & Zimmermann, W. (1992) Purification and characterization of an intracellular peroxidase from *Streptomyces cyaneus*, *Appl. Env. Microbiol.* **58**, 916-919.
11. Fukumori, Y., Fujiwara, T., Okada-Takahashi, Y., Mukohata & Yamanaka, T. (1985) Purification and properties of a peroxidase from *Halobacterium halobium* L-33, *J. Biochem. (Tokyo)* **98**, 1055-1061.
12. Cendrin, F. Jouve, H.M., Gaillard, J., Thibault, P. & Zaccari, G. (1994) Purification and properties of a halophilic catalase-peroxidase from *Haloarcula marismortui*, *Biochim. Biophys. Acta* **1209**, 1-9.
13. Levy, E., Eyal, Z. & Hochman (1992) Purification and characterization of a catalase-peroxidase from the fungus *Septoria tritici*, *Arch. Biochem. Biophys.* **296**, 321-327.
14. De Jong, E., van Berkel, W.J.H., van der Zwan, R.P. & de Bont, J.A.M. (1992) Purification and characterization of vanillyl-alcohol oxidase from *Penicillium simplicissimum*, *Eur. J. Biochem.*, **208**, 651-657.
15. Hammel, K.E. & Tardone, P.J. (1988) The oxidative 4-dechlorination of polychlorinated phenols is catalyzed by extracellular fungal lignin oxidases, *Biochemistry* **27**, 6563-6568.
16. Wariishi, H., Valli, K. & Gold, M.H. (1992) Manganese(II) oxidation by manganese peroxidase from the basidiomycete *Phanerochaete chrysosporium* - Kinetic mechanism and role of chelators, *J. Biol. Chem.* **267**, 23688-23695.

17. Pierik, A.J., & Hagen, W.R. (1991) $S = 9/2$ EPR signals are evidence against coupling between the siroheme and the Fe/S cluster prosthetic groups in *Desulfovibrio vulgaris* (Hildenborough) dissimilatory sulfite reductase, *Eur. J. Biochem.* **195**, 505-516.
18. Müller, F., Voordouw, G., van Berkel, W.J.H., Steennis, P.J., Visser, S. & van Rooyen, P.J. (1979) A study of *p*-hydroxybenzoate hydroxylase from *Pseudomonas fluorescens*, *Eur. J. Biochem.* **101**, 235-244.
19. Laemmli, U.K. (1970) Cleavage of structural proteins during the assembly of the head of bacteriophage T4, *Nature* **227**, 680-685.
20. Goldberg, I. & Hochman, A. (1989) Purification and characterization of a novel type of catalase from the bacterium *Klebsiella pneumonia*, *Biochim. Biophys. Acta* **991**, 330-336.
21. Witteveen, C.F.B., Veenhuis, M. & Visser, J. (1992) Localization of glucose oxidase and catalase activities in *Aspergillus niger*, *Appl. Env. Microbiol.* **58**, 1190-1194.
22. Ashwell, G. (1966) *Methods in enzymol.* **8**, 85-95.
23. Lowry, O. H., Rosebrough, N. J., Farr, A. L. & Randall, R. J. (1951) Protein measurement with the folin phenol reagent, *J. Biol. Chem.* **193**, 265-275.
24. Hochman, A. & Shemesh, A. (1987) Purification and characterization of a catalase-peroxidase from the photosynthetic bacterium *Rhodospseudomonas capsulata*, *J. Biol. Chem.* **262**, 6871-6876.
25. Margoliash, E., Novogrodsky, A. & Schejter, A. (1960) Irreversible reaction of 3-amino-1,2,4-triazole and related inhibitors with the protein of catalase, *Biochem. J.* **74**, 339-348.
26. Jacob, G.S. & Orme-Johnson, W.H. (1979) Catalase of *Neurospora crassa*. 1. Induction, purification and physical properties, *Biochemistry* **18**, 2967-2975.
27. Loewen, P.C., Switala, J., von Ossowski, I., Hillar, A., Christie, A., Tattrie, B. & Nicholls, P. (1993) Catalase HPII of *Escherichia coli* catalyzes the conversion of protoheme to *cis*-heme d, *Biochemistry* **32**, 10159-10164.
28. Maltempo, M.M. & Moss, T.H. (1976) The spin $3/2$ state and quantum spin mixtures in haem proteins, *Q. Rev. Biophys.* **9**, 181-215.
29. Yonetani, T., Yamamoto, H., Erman, J.E., Leigh, J.S. & Reed, G.H. (1972) Electromagnetic properties of hemoproteins, *J. Biol. Chem.* **247**, 2447-2455.
30. Welinder, K.G. (1991) Bacterial catalase-peroxidases are gene duplicated members of the plant peroxidase superfamily, *Biochim. Biophys. Acta* **1080**, 215-220.
31. Welinder, K.G. (1992) Superfamily of plant, fungal and bacterial peroxidases, *Curr. Opin. Struct. Biol.* **2**, 388-393.
32. Bracete, A.M., Kadkhodayan, S., Sono, M., Huff, A.M., Zhuang, C., Cooper, D.K., Smith, K.M., Chang, C.K. & Dawson, J.H. (1994) Iron chlorin-reconstituted histidine-ligated heme proteins as models for naturally occurring iron chlorin proteins: magnetic circular dichroism spectroscopy as a probe of iron chlorin coordination structure, *Inorg. Chem.* **33**, 5042-5049.
33. Chary, P. & Natvig, D.O. (1989) Evidence for three differentially regulated catalase genes in *Neurospora crassa*: effects of oxidative stress, heat shock and development, *J. Bacteriol.* **171**, 2646-2652.
34. Forney, L.J., Reddy, C.A. & Pankratz, H.S. (1982) Ultrastructural localization of hydrogen peroxide production in ligninolytic *Phanerochaete chrysosporium* cells, *Appl. Env. Microbiol.* **44**, 732-736.
35. Chaga, G.S., Medin, A.S., Chaga, S.G. & Porath, J.O. (1992) Isolation and characterization of catalase from *Penicillium chrysogenum*, *J. Chromatogr.* **604**, 177-183.
36. Nishikawa, Y., Kawata, Y. & Nagai, J. (1993) Effect of Triton X-100 on catalase production by *Aspergillus terreus* IFO6123, *J. Ferment. Bioeng.* **76**, 235-236.
37. Kawaguchi, T., Ueda, M. & Tanaka, A. (1989) Efficient expression of peroxidatic activity of catalase in the coupled system with glucose oxidase - A model of yeast peroxisomes, *Biocatalysis* **2**, 273-282.

4

Subcellular localization of vanillyl-alcohol oxidase in *Penicillium simplicissimum*

Marco W. Fraaije, Klaas A. Sjollema, Marten Veenhuis and Willem J.H. van Berkel

FEBS Letters 422, 65-68 (1998)

Abstract

Growth of *Penicillium simplicissimum* on anisyl alcohol, veratryl alcohol or 4-(methoxymethyl)phenol, is associated with the synthesis of relatively large amounts of the hydrogen peroxide producing flavoprotein vanillyl-alcohol oxidase (VAO). Immunocytochemistry revealed that the enzyme has a dual location namely in peroxisomes and in the cytosol. The C-terminus of the primary structure of VAO displays a WKL-COOH sequence which might function as a peroxisomal targeting signal type 1 (PTS1). As VAO activity results in production of hydrogen peroxide also the subcellular location of a recently characterized co-inducible catalase-peroxidase was studied. As VAO, this hydroperoxidase is distributed throughout the cytosol and peroxisomes.

4.1. Introduction

In 1992, a novel flavoprotein, vanillyl-alcohol oxidase (VAO), was isolated from the fungus *Penicillium simplicissimum* CBS 170.90 which can oxidize a wide variety of phenolic compounds (1, 2). The enzyme is specifically induced when the fungus is grown on veratryl alcohol, anisyl alcohol or 4-(methoxymethyl)phenol (3). We have recently demonstrated that 4-(methoxymethyl)phenol represents a 'natural' inducer as VAO catalyzes the first step in the degradation of this phenolic methylether. However, with veratryl alcohol and anisyl alcohol, induction appears to be redundant for growth although the enzyme is produced in high quantities.

VAO is a homo-octameric covalent flavoprotein with each subunit harboring a histidyl bound FAD (1). Recently, we have solved the crystal structure of VAO confirming the covalent bond between His422 and the FAD cofactor (4). Covalently bound flavin cofactors have been found in about 25 other enzymes while several hundred flavin dependent enzymes are known (5). At present, the rationale for covalent flavinylation is still unclear. In the bacterial trimethylamine dehydrogenase, containing a cysteinyl bound FMN, the covalent linkage seems to prevent chemical modification of the flavin leading to inactivation (6). For *p*-cresol methylhydroxylase, it was suggested that the linkage of FAD to a tyrosine residue results in a more efficient electron flow from the reduced flavin to the cytochrome subunit (7). However, it has also been suggested that covalent flavinylation may improve the *in vivo* stability of the enzyme or that it may be beneficial for the organism in times of decreased levels of available flavin (5).

Until now, eight eukaryotic covalent flavoproteins have been localized. It was found that all these enzymes are located in distinct cell organelles: monoamine oxidase, succinate dehydrogenase, dimethylglycine dehydrogenase, sarcosine dehydrogenase (8) and D-arabinono-1,4-lactone oxidase (9) are contained in mitochondria, L-gulonono- γ -lactone oxidase is located in the endoplasmic reticulum (10), L-pipecolic acid oxidase and sarcosine oxidase in peroxisomes (11, 12), and the plant reticuline oxidoreductase in vesicles (13). For rat dimethylglycine dehydrogenase and yeast succinate dehydrogenase it was reported that covalent attachment of the FAD cofactor is stimulated when the precursor protein is imported and proteolytically processed in the mitochondria (8, 14). However, covalent flavinylation of these enzymes can also occur in the cytoplasm and holoenzyme can be imported in the mitochondria as well.

The present work describes an immunocytochemical study to determine the intracellular distribution of VAO in mycelium of *P. simplicissimum* CBS 170.90. Recently, we also purified a catalase-peroxidase from this fungus which represents the first characterized dimeric catalase-peroxidase of eukaryotic origin (15). As VAO activity generates hydrogen peroxide as side-product and induction of VAO coincides with an

elevated synthesis of this catalase-peroxidase, the induction and subcellular localization of catalase-peroxidase activity was studied as well.

4.2. Materials and methods

Microorganism and cultivation

All experiments were performed with *P. simplicissimum* CBS 170.90. Cells were grown as described earlier (3). For immunocytochemical experiments, cells were harvested during the logarithmic growth phase (48 h after inoculation when grown on anisyl alcohol and 24 h after inoculation when grown on glucose).

Enzyme assays

The vanillyl-alcohol oxidase activity was assayed at 30 °C and pH 10.0 with vanillyl alcohol as the aromatic substrate (1). Catalase and peroxidase activities were assayed as described previously (15). For peroxidase activity, 2,6-dimethoxyphenol was used as the electron donor. Glucose-6-phosphate dehydrogenase was assayed by the method of Bruinenberg et al. (16). L-glutamate dehydrogenase was determined by measuring the decrease of absorbance at 340 nm after adding 50 µl aliquots of enzyme to 950 µl 20 mM α -ketoglutarate, 0.5 mM NADPH, 100 mM HEPES pH 7.5.

Cell fractionation

Several methods were tested for the isolation of protoplasts. Invariably, with all tested lysing enzymes the efficiency of protoplast formation was very low, presumably due to a very rigid cell wall. Therefore, lysis of protoplasts by osmotic shock was not feasible. Grinding cells with quartz-sand, as described for *Neurospora crassa* (17), did neither result in efficient cell disruption. Finally, cells (10 g) were disrupted under liquid nitrogen by grinding frozen mycelia. For thawing, 75 ml 5 mM MES pH 6.0, 1.0 M sorbitol was added. After filtration with a cheese cloth, the solution was centrifuged at 16000 g for 5 min at 4 °C. The pellet was carefully resuspended in 5 mM MES pH 6.0, 1.0 M sorbitol and applied to a 25-60% sucrose gradient in 5 mM MES pH 6.0. Gradients were centrifuged (100 min, 32.000 rpm) in a swinging bucket rotor (TST 4114 rotor, Centrikon T-1055 centrifuge).

Polyclonal antibodies

Rabbit polyclonal antibodies against VAO and catalase-peroxidase were obtained as described earlier (15). The antisera were purified by incubation with glucose-grown mycelia to remove aspecific cell wall binding components. Subsequently, the antisera were further

purified by hydrophobic interaction chromatography using a phenyl-Sepharose column (elution gradient: 0.6 - 0 M ammonium sulfate in 20 mM potassium phosphate pH 7.5).

Immunocytochemical experiments

Immunocytochemistry was performed on ultrathin sections of Unicryl (British Biocell International) embedded cells, using purified polyclonal antibodies and goat anti-rabbit IgG conjugated to gold (Amersham, UK), basically according to the method of Slot and Geuze (18).

4.3. Results

4.3.1. Enzyme induction

Earlier studies have shown that VAO activity is induced when *P. simplicissimum* is grown on some specific aromatic compounds (3). It was also observed that, during growth on veratryl alcohol, relatively high amounts of a dimeric catalase-peroxidase were produced in parallel with production of an atypical catalase (15). As VAO activity results in the generation of hydrogen peroxide as a side-product, these enzymes may represent the response of the organism to eliminate this toxic compound. Table 1 shows that with all tested growth substrates the atypical catalase is produced at a rather constant level, while the catalase-peroxidase is present at a higher level when the fungus is grown on aromatic compounds. The induction of catalase-peroxidase is highest during growth on the VAO-inducing growth substrates. However, from the data of Table 1, it is clear that the synthesis of catalase-peroxidase activity is not that strictly regulated as that of VAO.

Table 1. Growth substrate dependent induction of VAO, catalase and peroxidase activity in *P. simplicissimum*.

growth substrate	VAO ^a	atypical catalase ^b	catalase-peroxidase ^c
anisyl alcohol	74.5	36.5	55.9
veratryl alcohol	69.8	38.7	56.6
vanillyl alcohol	<1	27.1	31.8
vanillic acid	<1	50.4	31.9
homovanillyl alcohol	<1	48.3	33.8
glucose	<1	25.4	5.0

^a VAO activity in mU/mg, ^b atypical catalase activity in U/mg (as measured at pH 8.5),

^c catalase activity of catalase-peroxidase in U/mg (= catalase activity measured at pH 6.4 corrected for activity of atypical catalase activity at pH 8.5 (see (15)).

4.3.2. Cell fractionation studies

Fig. 1 shows the distribution of various *P. simplicissimum* enzyme activities after sucrose density centrifugation of an organellar pellet prepared from cells grown on veratryl alcohol. Activity of the mitochondrial marker enzyme L-glutamate dehydrogenase was primarily found in protein fractions with a density of 1.15 g/cm³. The three other enzyme activities tested showed a bimodal distribution. The relative high level of activity in the 1.21-1.24 g/cm³ density fractions indicated that these enzymes are compartmentalized. Activity of these enzymes observed in the lower density fractions may originate from organelle leakage, possibly due to the relatively harsh method for cell breakage. A similar bimodal distribution of catalase activity has been observed before (19, 20). The relatively high catalase activity in the lower density fractions of the gradient, as compared to the peroxidase activity in these fractions, may in part also result from some residual atypical catalase activity.

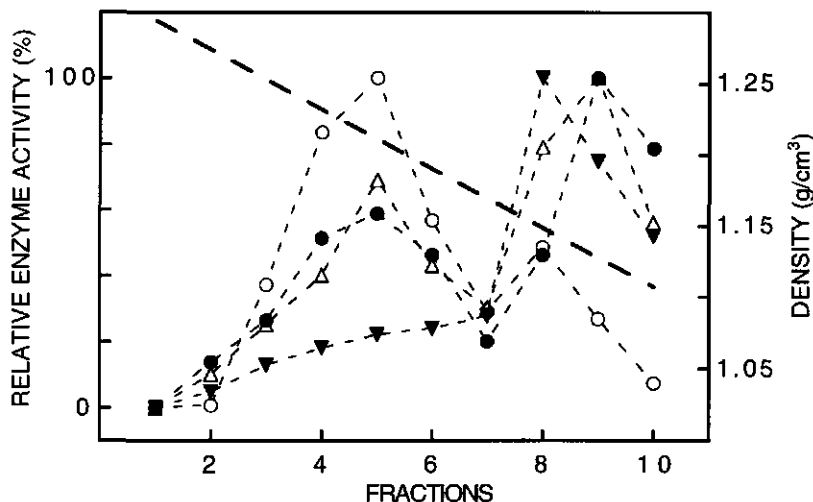


Figure 1. Distribution of VAO (Δ), peroxidase (O), catalase (\bullet) and L-glutamate dehydrogenase (\blacktriangledown) activity in a 25-60% (w/v) sucrose gradient (— — —) after sucrose density centrifugation.

4.3.3. Immunocytochemical localization

Western blot analysis have shown that the antisera raised against VAO and catalase-peroxidase are specific for the corresponding proteins (3). By using the purified polyclonal antibodies, the subcellular localization of both VAO and catalase-peroxidase was determined (see Materials and Methods section). Fig. 2A shows the labeling pattern on ultrathin

sections of anisyl alcohol-grown cells, using purified α -VAO antibodies. It is evident that the labeling is not restricted to a specific cell compartment, but localized on the peroxisomal matrix and the cytosol as well, including the nuclei. Fig. 2A also shows that significant label is absent on other cell compartments, including the mitochondria. In accordance with the absence of VAO activity, no significant labeling was observed in glucose-grown control cells (Fig. 2B).

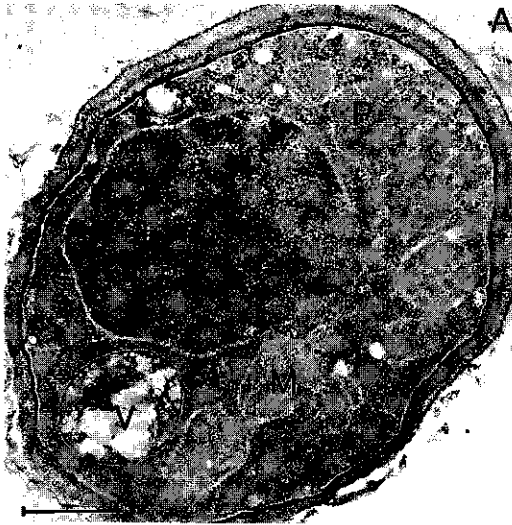
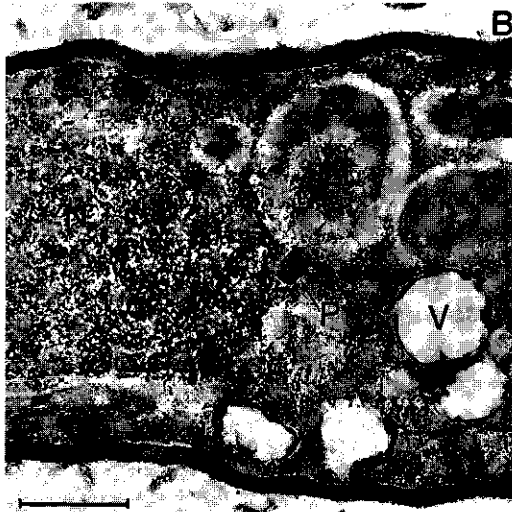


Figure 2.

Immunogold labeling of VAO in anisyl alcohol- (A) and glucose-grown (B) *P. simplicissimum* cells (P, peroxisome; M, mitochondrion; N, nucleus; V, vacuole; bar represents 0.5 μ m).



Using antibodies raised against catalase-peroxidase, an identical subcellular labeling pattern was observed: predominantly peroxisomes and cytosol were labeled on both glucose- and anisyl alcohol-grown cells (Fig. 3). These results are in line with the fact that glucose does not induce VAO production whereas catalase-peroxidase is expressed under all tested growth conditions (Table 1).

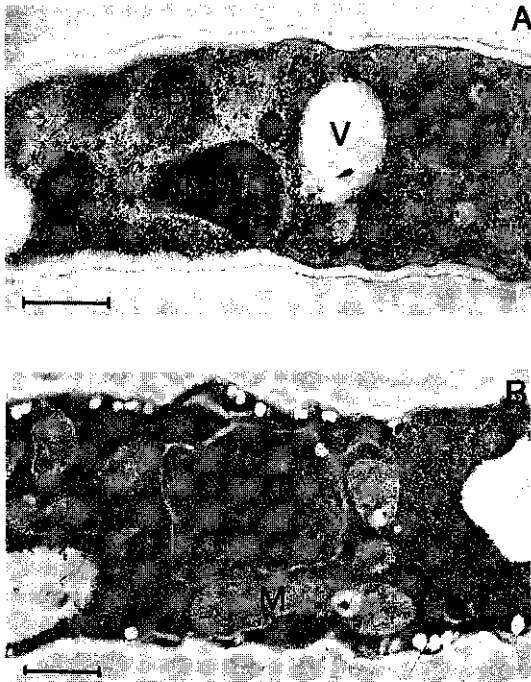


Figure 3. Immunogold labeling of catalase-peroxidase in anisyl alcohol- (A) and glucose-grown (B) *P. simplicissimum* cells (P, peroxisome; N, nucleus; M, mitochondrion; V, vacuole; bar represents 0.5 μm).

4.4. Discussion

In this study, we have shown that the covalent flavoprotein VAO has a bimodal distribution and is located in peroxisomes and the cytosol of *P. simplicissimum*. The peroxisomal localization of VAO was not unexpected as it is known that various hydrogen peroxide-producing flavoenzymes, e.g. sarcosine oxidase (12), D-amino acid oxidase (21), alcohol oxidase (22) and acyl-CoA oxidase (23) are compartmentalized in these organelles. Moreover, being a substrate inducible enzyme, VAO shows several features which are typical for many peroxisomal matrix enzymes. As a significant amount of VAO was localized in peroxisomes, the primary structure of VAO (24) was analyzed for the presence

of a peroxisomal targeting signal (PTS). It was found that at the extreme C-terminus a WKL-COOH tripeptide sequence is present which resembles the well-known PTS1, characterized by the SKL-COOH consensus sequence (25). Most of the reported fungal flavin-dependent oxidases contain a PTS1 (21, 26-31) although for acyl CoA oxidases other targeting mechanisms may be operative (23). Therefore, it is likely that the VAO C-terminal sequence represents a novel PTS1 variant. As only part of the protein is located in peroxisomes, translocation may not be fully efficient due to a limited recognition of this PTS1 variant. As an alternative, the partial translocation of VAO into peroxisomes may be caused by a relatively fast rate of VAO synthesis exceeding the import capacity. Another striking observation with respect to the subcellular location of VAO is the fact that a large portion of VAO is present in the nuclei. The presence of hydrogen-peroxide generating activity in nuclei is remarkably as this could lead to deleterious effects. However, peroxisomal matrix enzymes including H₂O₂-producing enzymes also accumulate in nuclei of *per*-mutants of methylotrophic yeast (32) and it is still not known how the cell deals with this potentially hazardous event. In line with this, the presence of VAO in the cytosol may indicate that the translocation of VAO within the cell is not optimally regulated. A rationale behind this could be that the VAO gene is a result of a relatively recent gene transfer. The plasmid-encoded flavocytochrome *p*-cresol methylhydroxylase isolated from *Pseudomonas putida* is a possible candidate for such an event as this enzyme is highly homologous to VAO: both the primary sequence and 3-D structure are very similar to VAO (4, 7).

Generally, hydrogen peroxide produced in peroxisomes is efficiently eliminated by the action of peroxisomal catalase activity. However, hydrogen peroxide producing and degrading enzymes have also been detected in other cell compartments. For example, the mammalian monoamine oxidase is localized in mitochondria and in several fungi, flavin-dependent oxidases are excreted. *Aspergillus niger* produces large amounts of the extracellular glucose oxidase resulting in acidification of the medium (33). Other organisms, like the fungus *Talaromyces flavus* and the red alga *Chondrus crispus*, produce extracellular sugar oxidases as a defense system generating extracellular toxic hydrogen peroxide (34, 35). For white-rot fungi, the extracellular production of hydrogen peroxide by action of flavin-dependent oxidases is crucial to sustain the enzymatic lignin degradation mechanism (36). Previously, we have shown that *P. simplicissimum* produces two hydroperoxidases; an atypical periplasmic catalase and an intracellular catalase-peroxidase (15). By cell fractionation and immunolocalization we have established that the catalase-peroxidase is located throughout the cell and thereby may decompose the hydrogen peroxide produced by VAO. An increase in production of catalase-peroxidase concurrent with VAO induction is in keeping with this hypothesis. It has been shown that, due to a low affinity for hydrogen peroxide, catalases only function in the degradation of hydrogen peroxide when it is present at the site of its generation, e.g. in peroxisomes. However, for catalase-peroxidases the

physiological electron donor it is not yet known and, consequently, its efficiency for peroxidase reactions is also unknown. Cytochrome *c* peroxidase plays an essential role in the intracellular degradation of hydrogen peroxide in yeasts (37). As catalase-peroxidases show sequence homology with cytochrome *c* peroxidase (38), these hydroperoxidases may be effective alternatives in decomposing subcellularly produced hydrogen peroxide.

VAO represents the first example of a covalent flavoprotein which is not strictly compartmentalized. The presence of active octameric VAO in both peroxisomes and cytosol demonstrates that for this enzyme no specific organelle-bound assembly factors are required for flavinylation and oligomerization/activation. This is in contrast with the FAD-containing alcohol oxidases from methylotrophic yeasts which in WT cells only assemble into octamers after import of FAD-lacking monomers in the peroxisomes and subsequent FAD binding (39). The self-assembly and autoflavinylation of VAO is in keeping with the production of active enzyme in heterologous hosts like *A. niger* and *Escherichia coli* (24).

Acknowledgement

We thank Jan Schel (Department of Plant Cytology and Morphology, WAU) for his support and interest.

4.5. References

1. De Jong, E., van Berkel, W.J.H., van der Zwan, R.P. and de Bont, J.A.M. (1992) Purification and characterization of vanillyl-alcohol oxidase from *Penicillium simplicissimum*, *Eur. J. Biochem.* **208**, 651-657.
2. Fraaije, M.W., Veeger, C. and van Berkel, W.J.H. (1995) Substrate specificity of flavin-dependent vanillyl-alcohol oxidase from *Penicillium simplicissimum*. *Eur. J. Biochem.* **234**, 271-277.
3. Fraaije, M.W., Pikkemaat, M. and van Berkel, W.J.H. (1997) Enigmatic gratuitous induction of the covalent flavoprotein vanillyl-alcohol oxidase in *Penicillium simplicissimum*. *Appl. Environ. Microbiol.* **63**, 435-439.
4. Mattevi, A., Fraaije, M.W., Mozzarelli, A., Olivi, L., Coda, A. and van Berkel, W.J.H. (1997) Crystal structures and inhibitor binding in the octameric flavoenzyme vanillyl-alcohol oxidase: the shape of the active-site cavity controls substrate specificity, *Structure* **5**, 907-920.
5. Decker, K.F. (1993) Biosynthesis and function of enzymes with covalently bound flavin. *Annu. Rev. Nutr.* **13**, 17-41
6. Mewies, M., Basran, J., Packman, L.C., Hille, R. and Scrutton, N.S. (1997) Involvement of a flavin iminoquinone methide in the formation of 6-hydroxyflavin mononucleotide in trimethylamine dehydrogenase: a rationale for the existence of 8 α -methyl and C6-linked covalent flavoproteins. *Biochemistry* **36**, 7162-7168.
7. Kim, J., Fuller, J.H., Kuusk, V., Cunane, L., Chen, Z., Mathews, F.S. and McIntire, W.S. (1995) The cytochrome subunit is necessary for covalent FAD attachment to the flavoprotein subunit of *p*-cresol methylhydroxylase. *J. Biol. Chem.* **270**, 31202-31209.
8. Otto, A., Stolz, M., Sailer, H. and Brandsch, R. (1996) Biogenesis of the covalently flavinylated mitochondrial enzyme dimethylglycine dehydrogenase. *J. Biol. Chem.* **271**, 9823-9829.
9. Huh, W.K., Kim, S.T., Yang, K.S., Seok, Y.J., Hah, Y.C., Kang, S.O. (1994) Characterisation of D-arabinono-1,4-lactone oxidase from *Candida albicans* ATCC 10231. *Eur. J. Biochem.* **225**, 1073-1079.

10. Yagi, K. and Nishikimi, M. (1994) L-gulonolactone oxidase - cDNA cloning and elucidation of the genetic defect in a mutant rat with osteogenic disorder. In: *Flavins and Flavoproteins 1993* (Yagi, K. ed.) pp. 799-802, W. de Gruyter, Berlin.
11. Mihalic, S.J. and McGuinness, M.C. (1991) Covalently-bound flavin in peroxisomal L-pipecolic acid oxidase from primates. In: *Flavins and Flavoproteins 1990* (Curti, B., Ronchi, S. and Zanetti, G. eds.) pp. 881-884, W. de Gruyter, Berlin.
12. Reuber, B.E., Karl, C., Reimann, S.A., Mihalik, S.J. and Dodt, G. (1997) Cloning and expression of a mammalian gene for a peroxisomal sarcosine oxidase. *J. Biol. Chem.* **272**, 6766-6776.
13. Kutchan, T.M. and Dittrich, H. (1995) Characterization and mechanism of the berberine bridge enzyme, a covalently flavinylated oxidase of benzophenanthridine alkaloid biosynthesis in plants. *J. Biol. Chem.* **270**, 24475-24481.
14. Robinson, K.M. and Lemire, B.D. (1996) Covalent attachment of FAD to the yeast succinate dehydrogenase flavoprotein requires import into mitochondria, presequence removal, and folding. *J. Biol. Chem.* **271**, 4055-4060.
15. Fraaije, M.W., Roubroeks, H.P., Hagen, W.R. and van Berkel, W.J.H. (1996) Purification and characterization of an intracellular catalase-peroxidase from *Penicillium simplicissimum*. *Eur. J. Biochem.* **235**, 192-198.
16. Bruinenberg, P.M., van Dijken, J.P. and Scheffers, W.A. (1983) An enzymic analysis of NADPH production in *Candida utilis*. *J. Gen. Microbiol.* **129**, 965-971.
17. Kionka, C. and Kunau, W.H. (1985) Inducible β -oxidation pathway in *Neurospora crassa*. *J. Bacteriol.* **161**, 153-157.
18. Slot, J.W. and Geuze, H.J. (1984) Gold markers for single and double immunolabeling of ultrathin cryosections. In: *Immunolabeling for electron microscopy* (Polack, J.M. and Varndell, I.M. eds.) pp. 129-142, Elsevier, Amsterdam.
19. Goodman, J.M. (1985) Dihydroxyacetone synthase is an abundant constituent of the methanol-induced peroxisome of *Candida boidinii*. *J. Biol. Chem.* **260**, 7108-7113.
20. Kamasawa, N., Ohtsuka, I., Kamada, Y., Ueda, M., Tanaka, A. and Osumi, M. (1996) Immunoelectron microscopic observation of the behaviors of peroxisomal enzymes inducibly synthesized in an n-alkane-utilizable yeast cell, *Candida tropicalis*. *Cell. Struct. Funct.* **21**, 117-122.
21. Pilone Simonetta, M., Perotti, M.E. and Pollegioni, L. (1991) D-amino acid oxidase expressed under induction conditions is enzymatically active in microperoxisomes of *Rhodotorula gracilis*. In: *Flavins and Flavoproteins 1990* (Curti, B., Ronchi, S. and Zanetti, G. eds.) pp. 167-170, W. de Gruyter, Berlin.
22. Veenhuis, M., van Dijken, J.P., Pilon, S.A.F. and Harder, W. (1978) Development of crystalline peroxisomes in methanol-grown cells of the yeast *Hansenula polymorpha* and its relation to environmental conditions. *Arch. Microbiol.* **117**, 153-163.
23. Small, G.M., Szabo, L.J. and Lazarow, P.B. (1988) Acyl-CoA oxidase contains two targeting sequences each of which can mediate protein import into peroxisomes. *EMBO J.* **7**, 1167-1173.
24. Benen, J.A.E., Wagemaker, M.J.M., Sánchez-Torres, P., Fraaije, M.W., van Berkel, W.J.H. and Visser, J. (1998) Molecular cloning, sequencing and overexpression of the *vao* gene from *Penicillium simplicissimum* CBS 170.90 encoding vanillyl-alcohol oxidase and purification of the gene-product, *J. Biol. Chem.*, in press.
25. Gould, S.J., Keller, G.A., Hosken, N., Wilkinson, F. and Subramani, S. (1989) A conserved tripeptide sorts proteins to peroxisomes. *J. Cell Biol.* **108**, 1657-1664.
26. Yoshida, N., Sakai, Y., Isogai, A., Fukuya, H., Yagi, M., Tani, Y. and Kato, N. (1996) Primary structure of fungal fructosyl amino acid oxidases and their application to the measurement of glycosylated proteins. *Eur. J. Biochem.* **242**, 499-505.
27. Takahashi, M., Pischetsrieder, M., Monnier, V.M. (1997) Molecular cloning and expression of amadoriase isoenzyme (fructosyl amine: oxygen oxidoreductase, EC 1.5.3) from *Aspergillus fumigatus*. *J. Biol. Chem.* **272**, 12505-12507.
28. Isogai, T., Ono, H., Ishitani, Y., Kojo, H., Ueda, Y. and Kohsaka, M. (1990) Structure and expression of cDNA for D-amino acid oxidase active against cephalosporin C from *Fusarium solani*. *J. Biochem. (Tokyo)* **108**, 1063-1069.
29. Faotto, L., Pollegioni, L., Ceciliani, F., Ronchi, S., Pilone, M.S. (1995) The primary structure of D-amino acid oxidase from *Rhodotorula gracilis*. *Biotech. Lett.* **17**, 193-198.
30. Schilling, B. and Lerch, K. (1995) Cloning, sequencing and heterologous expression of the monoamine oxidase gene from *Aspergillus niger*. *Mol. Gen. Genet.* **247**, 430-438.

31. Hansen, H., Didion, T., Thiemann, A., Veenhuis, M. and Roggenkamp, R. (1992) Targeting sequences of the major peroxisomal proteins in the methylotrophic yeast *Hansenula polymorpha*. *Mol. Gen. Genet.* **235**, 269-278.
32. Van der Klei, I.J., Hilbrands, R.E., Swaving, G.J., Waterham, H.R., Vrieling, E.G., Titorenko, V.I., Cregg, J.M., Harder, W. and Veenhuis, M. (1995) The *Hansenula polymorpha* PER3 is essential for the import of PTS1 proteins into the peroxisomal matrix. *J. Biol. Chem.* **270**, 17229-17236.
33. Witteveen, C.F.B., Veenhuis, M. and Visser, J. (1992) Localization of glucose oxidase and catalase activities in *Aspergillus niger*. *Appl. Environ. Microbiol.* **58**, 1190-1194.
34. Sullivan, J.D. and Ikawa, M. (1973) Purification and characterization of hexose oxidase from the red alga *Chondrus crispus*. *Biochim. Biophys. Acta.* **309**, 11-20.
35. Stosz, S.K., Fravel, D.R. and Roberts, D.P. (1996) In vitro analysis of the role of glucose oxidase from *Talaromyces flavus* in biocontrol of the plant pathogen *Verticillium dahliae*. *Appl. Environ. Microbiol.* **62**, 3183-3186.
36. Ander, P. and Marzullo, L. (1997) Sugar oxidoreductases and veratryl alcohol oxidases as related to lignin degradation. *J. Biotechnol.* **53**, 115-131.
37. Verduyn, C., Giuseppin, M.L.F., Scheffers, W.A. and van Dijken, J.P. (1988) Hydrogen peroxide metabolism in yeasts. *Appl. Environ. Microbiol.* **54**, 2086-2090.
38. Welinder, K.G. (1991) Bacterial catalase-peroxidases are gene duplicated members of the plant peroxidase superfamily. *Biochim. Biophys. Acta* **1080**, 215-220.
39. Evers, M.E., Titorenko, V., Harder, W., van der Klei, I. and Veenhuis, M. (1996) Flavin adenine dinucleotide binding is the crucial step in alcohol oxidase assembly in the yeast *Hansenula polymorpha*. *Yeast* **12**, 917-923.

5

Substrate specificity of flavin-dependent vanillyl-alcohol oxidase from *Penicillium simplicissimum*

Evidence for the production of 4-hydroxycinnamyl alcohols from 4-allylphenols

Marco W. Fraaije, Cees Veeger and Willem J.H. van Berkel

European Journal of Biochemistry **234**, 271-277 (1995)

Abstract

The substrate specificity of the flavoprotein vanillyl-alcohol oxidase from *Penicillium simplicissimum* was investigated. Vanillyl-alcohol oxidase catalyzes besides the oxidation of 4-hydroxybenzyl alcohols, the oxidative deamination of 4-hydroxybenzylamines and the oxidative demethylation of 4-(methoxymethyl)phenols. During the conversion of vanillylamine to vanillin, a transient intermediate, most probably vanillylimine, is observed.

Vanillyl-alcohol oxidase weakly interacts with 4-hydroxyphenylglycols and a series of catecholamines. These compounds are converted to the corresponding ketones. Both enantiomers of (nor)epinephrine are substrates for vanillyl-alcohol oxidase, but the *R* isomer is preferred.

Vanillyl-alcohol oxidase is most active with chavicol and eugenol. These 4-allylphenols are converted to coumaryl alcohol and coniferyl alcohol, respectively. Isotopic labeling experiments show that the oxygen atom inserted at the C γ atom of the aromatic side chain is derived from water. The 4-hydroxycinnamyl alcohol products and the substrate analog isoeugenol are competitive inhibitors of vanillyl alcohol oxidation.

The binding of isoeugenol to the oxidized enzyme perturbs the optical spectrum of protein-bound FAD. pH-dependent binding studies suggest that vanillyl-alcohol oxidase preferentially binds the phenolate form of isoeugenol ($pK_a < 6$, 25 °C). From this and the high pH optimum for turnover, a hydride transfer mechanism involving a *p*-quinone methide intermediate is proposed for the vanillyl-alcohol oxidase catalyzed conversion of 4-allylphenols.

5.1. Introduction

Several fungi produce aryl-alcohol oxidases that are involved in the biodegradation of lignin, the most abundant aromatic biopolymer (de Jong et al., 1994). The monomeric aryl-alcohol oxidases are excreted by basidiomycetes and contain non-covalently bound FAD as a prosthetic group (Guillén et al., 1992). By catalyzing the oxidation of the secondary metabolites veratryl alcohol (3,4-dimethoxybenzyl alcohol) and anisyl alcohol (4-methoxybenzyl alcohol), the extracellular aryl-alcohol oxidases generate hydrogen peroxide, which is an essential substrate for the ligninolytic process (de Jong et al., 1994).

In a previous report, we described a novel type of aryl-alcohol oxidase isolated from the ascomycete *Penicillium simplicissimum* (de Jong et al., 1992). This intracellular enzyme catalyzes the oxidation of vanillyl alcohol (4-hydroxy-3-methoxybenzyl alcohol) to vanillin (4-hydroxy-3-methoxybenzaldehyde) and is a homooctamer with each subunit containing 8α -(N^3 -histidyl)-FAD as a covalently bound prosthetic group. Urea unfolding has shown that the enzyme is also active as a dimer (van Berkel et al., 1994). Vanillyl-alcohol oxidase from *P. simplicissimum* is induced when the fungus is grown upon veratryl alcohol as the sole carbon source. As veratryl alcohol is not a substrate for the oxidase (de Jong et al., 1992) and vanillyl alcohol seems not to be an intermediate in the degradation of veratryl alcohol (de Jong et al., 1990), the physiological role of the enzyme remains to be solved.

The extracellular aryl-alcohol oxidases have an acidic pH optimum thereby oxidizing a variety of non-activated or methoxylated aromatic alcohols (Sannia et al., 1991; Guillén et al., 1992). In contrast, vanillyl-alcohol oxidase from *P. simplicissimum* has a basic pH optimum and acts solely on 4-hydroxybenzyl alcohols (de Jong et al., 1992). In this report, we have studied the substrate specificity of vanillyl-alcohol oxidase to a greater extent. It is demonstrated that the enzyme acts on a wide range of 4-hydroxybenzylic compounds. The nature of the reaction intermediates and products allows some conclusions about the reaction mechanism of vanillyl-alcohol oxidase. Some preliminary results have been presented elsewhere (van Berkel et al., 1994).

5.2. Materials and methods

General

Catalase, glutamate dehydrogenase and NADPH were from Boehringer. Eugenol (4-allyl-2-methoxyphenol), isoeugenol (2-methoxy-4-propenylphenol), chavicol (4-allylphenol), safrole [4-allyl-1,2-(methylenedioxy)benzene], and isosafrole [1,2-(methylenedioxy)-4-propenylbenzene] were from Quest. Vanillin and vanillyl alcohol were products of Janssen Chimica and adrenalone (3',4'-dihydroxy-2-methylaminoacetophone)

was purchased from Fluka. Alcohol oxidase, *R*-norepinephrine [α -(aminomethyl)-3,4-dihydroxybenzyl alcohol], *R,S*-epinephrine [3,4-dihydroxy- α -(methylaminomethyl)benzyl alcohol] and *R*-epinephrine were products of Sigma (Bornem, Belgium). *S*-norepinephrine, $H_2^{18}O$ (10 mol/100 mol ^{18}O) and all other chemicals were obtained from Aldrich.

P. simplicissimum (Oudem.) Thom. CBS 170.90 (ATCC 90172) was grown essentially as described earlier (de Jong et al., 1990), except that a 20-l fermentor was used for cultivation. Vanillyl-alcohol oxidase was purified to apparent homogeneity as described previously (de Jong et al., 1992). A single band, stained with Coomassie brilliant blue R250 (Serva) was observed after SDS/PAGE.

Analytical methods

Mass spectra were determined using a Hewlett Packard HP 5890 GC equipped with a 30-m DB17 column and a HP 5970 MSD, essentially as described before (de Jong et al., 1992). Samples were prepared by extraction of reaction mixtures with diethylether and injected without derivization into the GC/MS. Reaction mixtures, containing 10 μ mol substrate and 0.2 U enzyme in 2 ml 50 mM glycine/NaOH, pH 10.0, were incubated at 30°C for 8 h.

For HPLC experiments, an Applied Biosystems 400 pump and a Waters 996 photodiode array detector were used. The column (100 mm \times 4.6 mm) filled with ChromSpher C₁₈ (3 μ m particles) was from Chrompack. The conversion of monoamines was analyzed by gradient elution using 0-80% methanol in 2% acetic acid.

1H -NMR spectra were recorded with a Bruker AMX-500 MHz spectrometer. NMR samples were prepared as for mass spectroscopy experiments, dried after diethylether extraction, and dissolved in deuterated chloroform.

Enzyme concentrations were determined spectrophotometrically using a molar absorption coefficient $\epsilon_{439} = 12.5 \text{ mM}^{-1} \text{ cm}^{-1}$ for protein-bound FAD (de Jong et al., 1992). The substrate specificity of vanillyl-alcohol oxidase was routinely tested by following absorption spectral changes after the addition of a catalytic amount of enzyme. Vanillyl-alcohol oxidase activity was assayed at 30 °C, pH 10.0, by recording the formation of product or by following oxygen consumption using a Clark electrode (de Jong et al., 1992). Vanillin production was measured at 340 nm ($\epsilon_{340} = 22.8 \text{ mM}^{-1} \text{ cm}^{-1}$). The formation of 4-hydroxycinnamyl alcohols from 4-allylphenols was recorded at 325 nm [4-hydroxy-3-methoxycinnamyl alcohol (coniferyl alcohol): $\epsilon_{325} = 7.5 \text{ mM}^{-1} \text{ cm}^{-1}$] or 310 nm [4-hydroxycinnamyl alcohol (coumaryl alcohol): $\epsilon_{310} = 5.5 \text{ mM}^{-1} \text{ cm}^{-1}$], respectively. The production of hydrogen peroxide was determined by measuring oxygen levels before and after addition of 150 U catalase. Ammonia and methanol were enzymically determined using glutamate dehydrogenase (Bergmeyer, 1970) and alcohol oxidase (Geissler et al., 1986), respectively.

Absorption spectra were recorded at 25 °C on an automated Aminco DW-2000 spectrophotometer. Binding studies as a function of pH were performed in 50 mM citric acid/sodium phosphate (pH 4-5), 50 mM sodium phosphate (pH 6-8), and 50 mM glycine/NaOH (pH 9-11). Dissociation constants of enzyme/inhibitor complexes were determined from flavin absorption difference spectra by titration of a known concentration of enzyme with the desired inhibitor. The ionization state of enzyme-bound isoeugenol was monitored at 320 nm by recording absorption spectra of 10 µM enzyme in the absence or presence of the inhibitor. Both sample and reference cell were titrated with known concentrations of isoeugenol, diluted in the appropriate buffer. Titration results were analyzed by non-linear least square fitting using the FORTRAN *numerical recipes* subroutine package (Press et al., 1986) of KALEIDAGRAPH (Adelbeck Software).

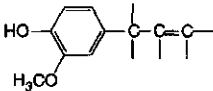
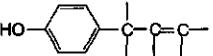
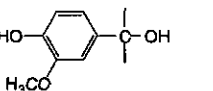
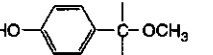
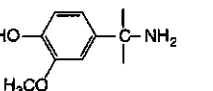
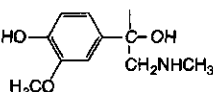
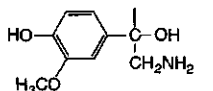
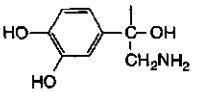
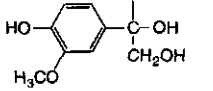
5.3. Results

5.3.1. Substrate specificity

Initial characterization of vanillyl-alcohol oxidase from *P. simplicissimum* has revealed that the substrate specificity of this flavoenzyme is different from that of the extracellular FAD-dependent aryl-alcohol oxidases (de Jong et al., 1992). Besides catalyzing the conversion of vanillyl alcohol to vanillin, vanillyl-alcohol oxidase was reported to act solely on 4-hydroxybenzyl alcohol. This and the inhibitory effect of cinnamyl alcohol (3-phenyl-2-propene-1-ol) (de Jong et al., 1992) prompted us to investigate the catalytic versatility of vanillyl-alcohol oxidase in more detail by introducing substituents at the C_α atom of the benzyl moiety of the substrate. Different novel types of substrates were found. In addition to the oxidation of simple 4-hydroxybenzyl alcohols, vanillyl-alcohol oxidase from *P. simplicissimum* catalyzed the conversion of α-(aminomethyl)-4-hydroxybenzyl alcohols, 4-hydroxyphenylglycols, 4-hydroxybenzylamines, 4-(methoxymethyl)phenols, and 4-allylphenols (Table 1).

In agreement with earlier observations (de Jong et al., 1992), no activity or inhibition was found with homovanillyl alcohol (4-hydroxy-3-methoxy-phenethyl alcohol). Furthermore, hydroxylated aromatic acids like 4-hydroxyphenylacetic acid, 4-hydroxymandelic acid, 4-hydroxyphenylglycine, 4-hydroxyphenylpyruvic acid, and tyrosine were not substrates for this flavoenzyme. Table 1 shows that vanillyl-alcohol oxidase is specific for 4-hydroxybenzylic compounds. No activity or inhibition was observed with 4-aminobenzylamine, 4-nitrobenzyl alcohol and allylbenzene. Furthermore, substituted allylbenzenes like 4-allylanisole (4-methoxy-allylbenzene), safrole, and isosafrole were not converted by vanillyl-alcohol oxidase.

Table 1. Steady-state kinetic parameters for vanillyl-alcohol oxidase from *P. simplicissimum*. All experiments were performed at 25 °C in 50 mM glycine/NaOH buffer pH 10.0. Methanephrine, normetanephrine, norepinephrine, and 4-hydroxy-3-methoxyphenylglycol were tested as racemic mixtures. Norepinephrine was assayed in the presence of ascorbate (10 mM) to prevent auto-oxidation of the substrate.

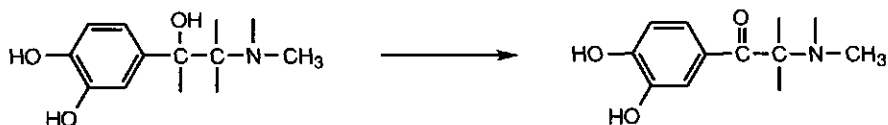
Substrate	Structure	K_m μM	k_{cat} s^{-1}	k_{cat}/K_m $10^3 \text{ s}^{-1}\text{M}^{-1}$
Eugenol		4.9	13.0	2700
Chavicol		4.8	6.5	1400
Vanillyl alcohol		290	5.4	19
4-(Methoxymethyl)phenol		65	5.3	82
Vanillylamine		240	1.3	5.4
Methanephrine		1600	0.8	0.5
Normetanephrine		1400	0.7	0.5
Norepinephrine		2900	0.3	0.1
4-Hydroxy-3-methoxyphenylglycol		6000	3.6	0.6

5.3.2. Catalytic properties

Table 1 shows the steady-state kinetic parameters of vanillyl-alcohol oxidase with some newly investigated substrates and with vanillyl alcohol as a reference. With all substrates, turnover of vanillyl-alcohol oxidase is optimal around pH 10. This suggests that the phenolate forms of the substrates may play an important role in catalysis (see also below). From Table 1, it is evident that the 4-allylphenols eugenol and chavicol are the best substrates. No activity or inhibition of vanillyl-alcohol oxidase was observed in the presence of 4-allyl-2,6-dimethoxyphenol. This suggests that the presence of an additional *ortho* methoxy substituent introduces steric constraints. From Table 1, it can also be observed that the catecholamine derivatives metanephrine [4-hydroxy-3-methoxy- α -(methylaminomethyl)-benzyl alcohol], normetanephrine [α -(aminomethyl)-4-hydroxy-3-methoxybenzyl alcohol] and norepinephrine are poor substrates for vanillyl-alcohol oxidase. In analogy, vanillyl-alcohol oxidase slowly reacted with epinephrine, octopamine [α -(aminomethyl)-4-hydroxybenzyl alcohol], and synephrine [4-hydroxy- α -(methylaminomethyl)benzyl alcohol] ($k_{\text{cat}} < 0.3 \text{ s}^{-1}$). The kinetic parameters for these compounds were not studied in further detail.

5.3.3. Identification of reaction products

Vanillyl alcohol oxidase is active with 4-hydroxybenzyl alcohols substituted at the C_{α} atom (Table 1). The enzymic oxidation of (nor)metanephrine, (nor)epinephrine, and 4-hydroxy-3-methoxyphenylglycol resulted in the formation of an absorption peak around 350 nm resembling the optical spectrum of vanillin. As an example, the spectral changes induced upon oxidation of normetanephrine are recorded in Fig. 1. For a more thorough product identification, the enzymatic conversion of *R*-epinephrine was followed by HPLC analysis using diode array detection. The retention time and absorption spectrum of the aromatic product were identical to those of adrenalone (3',4'-dihydroxy-2-methylaminoacetophenone) indicating oxidation of the C_{α} hydroxyl group:



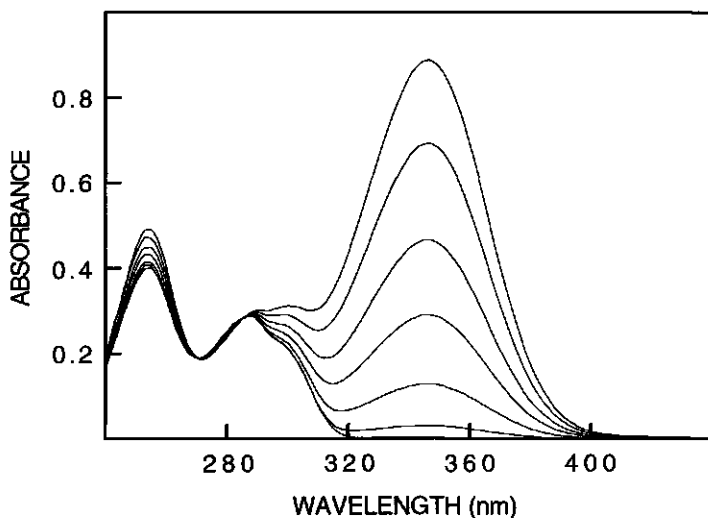


Figure 1. Spectral changes observed upon oxidation of normetanephrine by vanillyl-alcohol oxidase from *P. simplicissimum*. The reaction mixture contained 0.1 mM normetanephrine in 1.0 ml 50 mM glycine/NaOH, pH 10. Spectra (from bottom to top) were recorded at $t = 0, 1, 5, 15, 30, 60,$ and 120 min at 25°C after the addition of 0.62 nmol vanillyl-alcohol oxidase.

By oxidizing the α -hydroxy group of catecholamines, vanillyl-alcohol oxidase differs from the flavin-dependent monoamine oxidases. The latter enzymes preferably convert the catecholamines by oxidative deamination (Singer, 1991). Another interesting feature of the vanillyl-alcohol-oxidase-catalyzed conversion of catecholamines is the stereospecificity of the reaction. Experiments with pure enantiomers showed that the oxidation rate of *S*-norepinephrine (at 2.0 mM and 4.0 mM) is only 30% with respect to the oxidation rate of the *R* isomer (100%). With epinephrine the same preference was observed: the *R* isomer was significantly faster oxidized than the *S* isomer (tested as the racemic mixture).

Vanillyl-alcohol oxidase was also active with 4-hydroxybenzylamines (Table 1). Besides vanillylamine (4-hydroxy-3-methoxybenzylamine), 3,4-dihydroxybenzylamine was oxidized, though at a slower rate (k_{cat} about 0.9 s^{-1}). With the latter substrate, estimation of kinetic parameters was complicated by the instability of this compound. Mass spectral analysis revealed that vanillyl-alcohol oxidase converts vanillylamine to vanillin. As expected for oxidative deamination, conversion of vanillylamine resulted in the production of stoichiometric amounts of hydrogen peroxide and ammonia. When recording the enzymic oxidation of vanillylamine spectrophotometrically, initially an absorption increase was observed around 390 nm (Fig. 2). This transient peak gradually changed into the spectrum of vanillin. The extent and rate of formation of the spectral intermediate was dependent on temperature and enzyme concentration (data not shown). These findings suggest the initial formation of vanillylimine which is subsequently hydrolyzed non-enzymically:

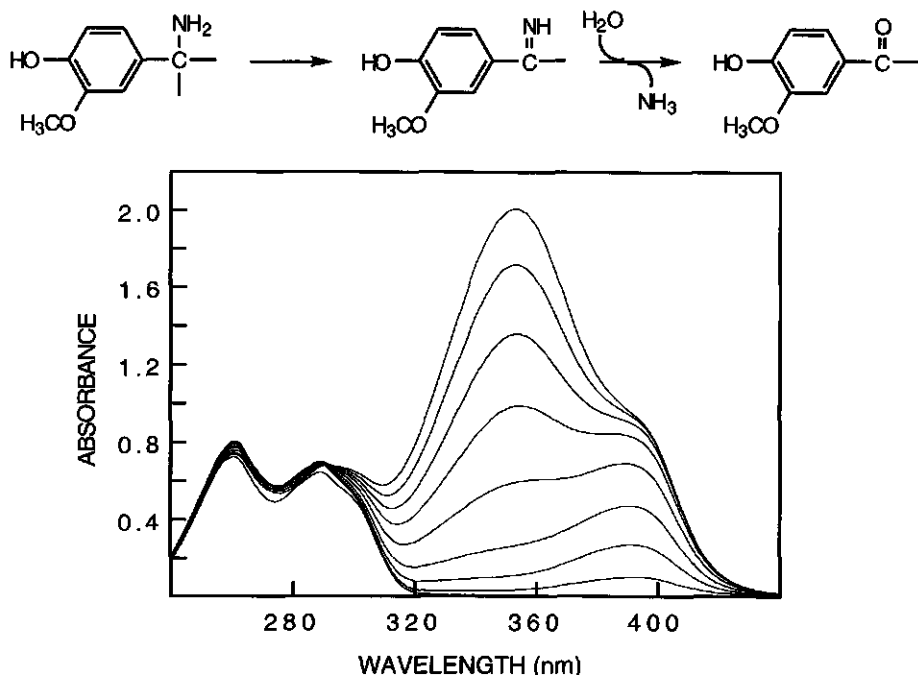


Figure 2. Spectral changes observed upon oxidation of vanillylamine by vanillyl-alcohol oxidase from *P. simplicissimum*. The reaction mixture contained 0.2 mM vanillylamine in 1.0 ml 50 mM glycine/NaOH, pH 10. Spectra (from bottom to top) were recorded at $t = 0, 1, 2, 5, 10, 15, 20, 25,$ and 30 min at 25°C after the addition of 0.31 nmol vanillyl-alcohol oxidase.

In analogy to the conversion of vanillylamine to vanillin, vanillyl-alcohol oxidase catalyzed the formation of 4-hydroxybenzaldehyde from 4-(methoxymethyl)phenol (compare Table 1). The oxidative demethylation of 4-(methoxymethyl)phenol was evidenced by mass spectral analysis of the aromatic product ($\{M\}^+ = 122$). Enzymic analysis with alcohol oxidase from *Candida boidinii* revealed that the conversion of 4-(methoxymethyl)phenol by vanillyl-alcohol oxidase involved the stoichiometric production of methanol, indicating fission of the ether bond.

Eugenol and chavicol are the best substrates for vanillyl-alcohol oxidase. Fig. 3A shows the absorption spectral changes observed during the conversion of eugenol by vanillyl-alcohol oxidase. The final spectrum obtained resembled the absorption spectrum of coniferyl alcohol as recorded at pH 10 (Fig. 3B). The actual formation of coniferyl alcohol was confirmed by $^1\text{H-NMR}$ (Rothen and Schlosser, 1991) and mass spectral analysis. The mass spectrum of the aromatic product was identical to that of authentic coniferyl alcohol; molecular ion at m/z (relative intensity) $\{M\}^+ 180$ (64.7%) and the following diagnostic fragments with more than 30% abundance: 137 (100%), 124 (59.0%) and 91 (46.9%). In a similar way, the product of the enzymic conversion of chavicol was identified as coumaryl

alcohol. This product contained the molecular ion at m/z (relative intensity) $[M]^+$ 150 (39.3%) and the following diagnostic fragments had more than 30% abundance: 107 (100%), 94 (50.9%) and 77 (30.6%).

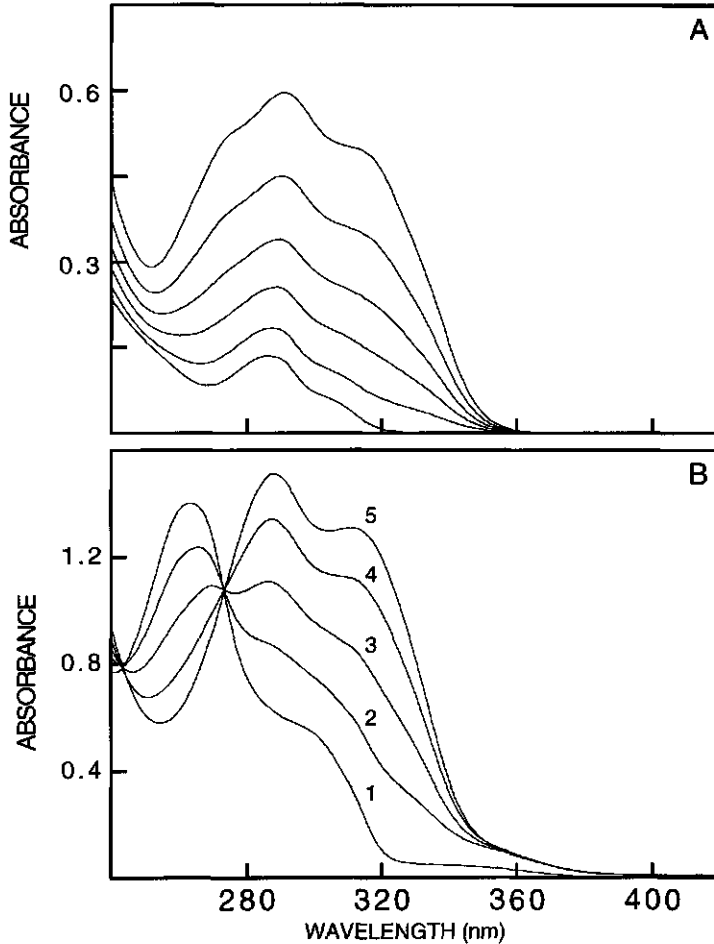


Figure 3. Spectral changes observed upon oxidation of eugenol by vanillyl-alcohol oxidase from *P. simplicissimum*. (A) The reaction mixture contained 0.1 mM eugenol in 1.0 ml 50 mM glycine/NaOH, pH 10. Spectra (from bottom to top) were recorded at $t = 0, 0.5, 1.5, 3, 5,$ and 10 min at 25°C after the addition of 0.03 nmol vanillyl-alcohol oxidase. (B) Reference spectra at 25°C of 0.1 mM conferyl alcohol recorded at pH values of 7.0 (1), 9.1 (2), 9.6 (3), 10.2 (4), and 12.0 (5).

During the enzymic conversion of eugenol to conferyl alcohol, the consumption of oxygen was coupled to the production of stoichiometric amounts of hydrogen peroxide. This suggests that the oxygen atom incorporated in conferyl alcohol is derived from water. This was tested by performing the enzymic conversion of eugenol in the presence of 10 % H_2^{18}O . Mass spectral analysis of the formed product yielded a spectrum similar to the

spectrum of coniferyl alcohol except for the presence of an additional peak with a mass of 182 (10 % relative to $\{M^+\}$ 180). This result confirms the involvement of water as a reactant in the enzymic production of coniferyl alcohol from eugenol:

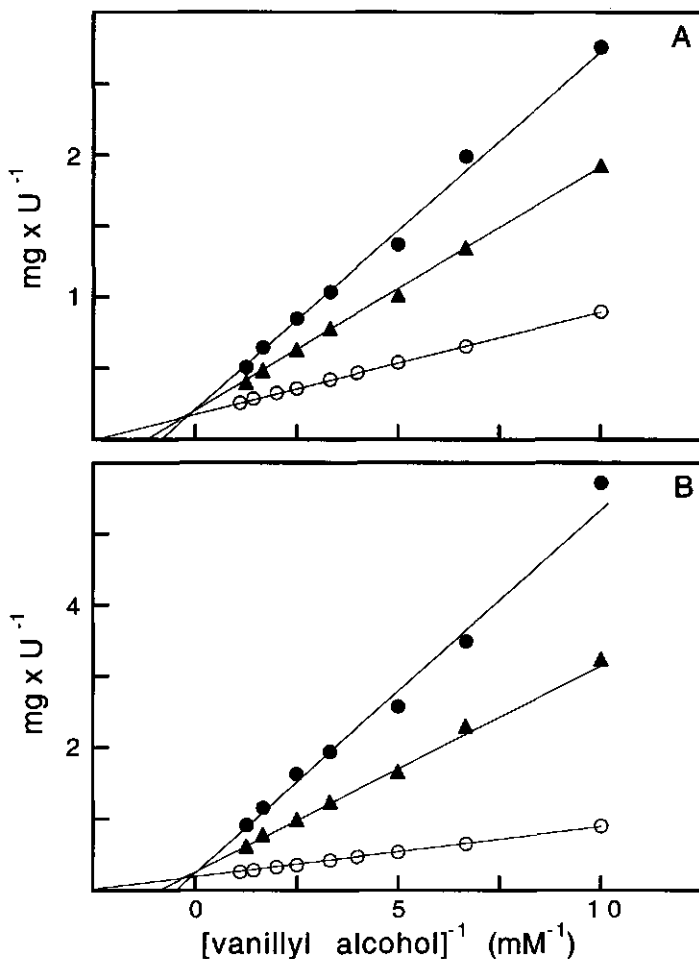
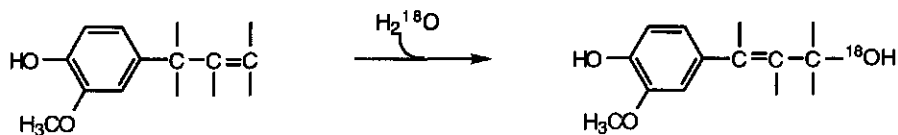


Figure 4. Competitive inhibition of vanillyl-alcohol oxidase from *P. simplicissimum*. The activity of vanillyl-alcohol oxidase was measured by the increase of absorbance at 340 nm (25°C, 50 mM glycine/NaOH, pH 10) with vanillyl alcohol as the variable substrate. All fits have R values > 0.995 . (A) The presence of the following are indicated: no inhibitor (O); 50 μ M coniferyl alcohol (\blacktriangle); 100 μ M coniferyl alcohol (\bullet). (B) The presence of the following are indicated: no inhibitor (O); 50 μ M isoeugenol (\blacktriangle); 100 μ M isoeugenol (\bullet).

5.3.4. Binding studies

Previously we reported that cinnamyl alcohol is a competitive inhibitor of vanillyl-alcohol oxidase (de Jong et al., 1992). Consequently, it was of interest to study the inhibitory effect of the 4-hydroxycinnamyl alcohols produced from enzymic conversion of eugenol and chavicol. Coniferyl alcohol is a strong competitive inhibitor of vanillyl alcohol oxidation ($K_i = 31 \pm 6 \mu\text{M}$) (Fig. 4A). The binding of coniferyl alcohol to the oxidized enzyme was confirmed by absorption difference spectroscopy. At pH 10, the binding of coniferyl alcohol resulted in small perturbations of the absorption spectrum of protein-bound FAD (data not shown). From the absorption differences at 490 nm a dissociation constant, $K_d = 9 \pm 2 \mu\text{M}$ was estimated for the binary enzyme-inhibitor complex. The binding of coniferyl alcohol was fully reversible as evidenced from the absorption spectrum recorded after gel filtration of the enzyme-coniferyl alcohol complex.

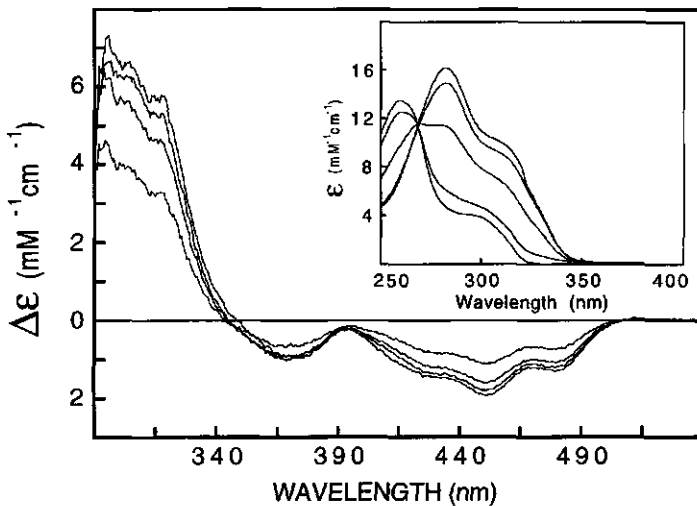


Figure 5. Absorption difference spectra observed upon binding of isoegenol to vanillyl-alcohol oxidase from *P. simplicissimum*. The absorption spectra were recorded at 25 °C in 50 mM sodium phosphate, pH 7.0. Both sample cell (containing 10 μM enzyme) and reference cell were titrated with isoegenol. The curves shown are the difference spectra, the corrected enzyme spectra in the presence of 15, 30, 44, and 59 μM isoegenol, minus the enzyme spectrum in the absence of isoegenol. The inset shows the spectral properties of free isoegenol as a function of pH. From bottom to top: absorption spectrum of isoegenol at pH 5.0, 9.0, 10.0, 11.0, and 12.4, respectively.

The substrate isomer isoegenol was another potent competitive inhibitor of vanillyl-alcohol oxidase. Fig. 4B shows the inhibition pattern obtained with vanillyl alcohol as the variable substrate. From the data of Fig. 4B an inhibition constant of $K_i = 13 \pm 5 \mu\text{M}$ at pH 10 was estimated. Tight binding of isoegenol to the oxidized enzyme was confirmed by difference spectroscopy. At pH 7.0, isoegenol reversibly perturbed the flavin

absorption spectrum of vanillyl-alcohol oxidase with a maximal hypochromic shift around 450 nm (Fig. 5). Binding followed simple binary complex formation with a dissociation constant of $K_d = 24 \pm 4 \mu\text{M}$ and a maximum value of about $-1.8 \text{ mM}^{-1}\text{cm}^{-1}$ for the molar difference absorption coefficient at 450 nm.

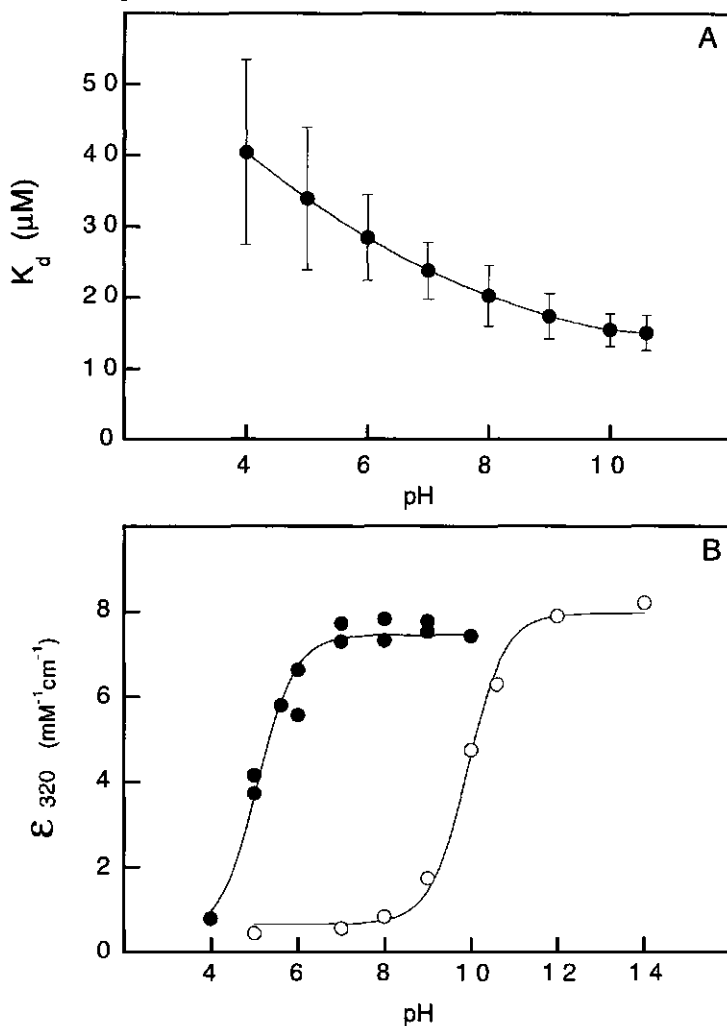


Figure 6. The pH dependence of the dissociation constant and ionization state of the binary complex between vanillyl-alcohol oxidase and isoeugenol. 10 μM Enzyme was titrated with isoeugenol at 25 °C. Absorption changes were monitored as described in the legend of Fig. 5. For buffers used and other experimental details, see the Materials and methods section. (A) pH dependence of the dissociation constant of the complex between vanillyl-alcohol oxidase and isoeugenol. (B) The effect of pH on the molar absorption coefficient at 320 nm: at saturating concentrations of isoeugenol with vanillyl-alcohol oxidase (●); with free isoeugenol (○).

The difference spectra recorded in Fig. 5 also show that binding of isoeugenol to vanillyl-alcohol oxidase at pH 7.0 results in a large increase in absorbance around 320 nm. The

shape and intensity of this peak, together with the minimal absorbance of the enzyme in this region (de Jong et al., 1992), are consistent with the formation of the phenolate form of the inhibitor (see Fig. 5). Since the pK_a of isoeugenol free in solution is about 9.8 (Fig. 5), this suggests that the binding of isoeugenol to the oxidized enzyme perturbs the phenolic pK_a of the inhibitor. This was studied in more detail by titration of the enzyme with isoeugenol at various pH values. These experiments revealed that the shape and intensity of the flavin difference spectrum (340-500 nm, Fig. 5) are nearly pH independent. From the absorption changes at 450 nm and over the entire pH interval studied, the binding of isoeugenol was described by simple binary complex formation, yielding dissociation constants ranging from $K_d = 40 \pm 13 \mu\text{M}$ at pH 4 to $K_d = 15 \pm 3 \mu\text{M}$ at pH 10 (Fig. 6A). In contrast to the flavin difference spectrum, the intensity of the difference absorbance around 320 nm strongly changed with pH and in accordance with the dissociation constants reported above. Fig. 6B shows the pH dependence of the molar absorption differences at 320 nm at saturating concentrations of isoeugenol. An apparent pK_a value of 5.0 was estimated from the experimental data with a maximum difference absorption coefficient of $\Delta\epsilon_{\text{max}} = 7.5 \text{ mM}^{-1}\text{cm}^{-1}$ at 320 nm. The low pK_a observed for the enzyme-isoeugenol complex suggests that binding of substrates to vanillyl-alcohol oxidase involves the interaction between an acidic amino acid side chain and the phenolic moiety of the substrate.

5.4. Discussion

The results presented in this study show that vanillyl-alcohol oxidase from *P. simplicissimum* is specific for 4-hydroxybenzylic compounds. This clearly discriminates the enzyme from the extracellular aryl-alcohol oxidases isolated from basidiomycetes (Guillén et al., 1992). Vanillyl-alcohol oxidase catalyzes besides the oxidation of (complex) 4-hydroxybenzyl alcohols, the oxidative demethylation of 4-(methoxymethyl)phenols, the oxidative deamination of 4-hydroxybenzylamines, and the oxidative hydration of 4-allylphenols. The enzymic conversion of eugenol is of special industrial interest in view of the production of natural flavour compounds (van Berkel et al., 1993).

The type of oxidation reaction catalyzed by vanillyl-alcohol oxidase is determined by the substituents at the C_α atom of the aromatic substrate. The introduction of a bulky substituent in the 4-hydroxybenzyl alcohols results in relatively low but significant oxidation rates. The high K_m values and the partial enantioselective conversion of at least two of these compounds suggest some steric limitations. It is evident, however, that additional data on the individual reaction steps are needed to determine which parameters dictate the rate of substrate oxidation.

Pseudomonas putida (Hopper and Taylor, 1977; McIntire et al., 1981; Reeve et al., 1989). These $\alpha_2\beta_2$ flavocytochromes convert their substrates by subsequent dehydrogenation and hydration but cannot act with oxygen as electron acceptor. Instead, the electrons are transferred one at a time from the flavin to a heme on a separate subunit (Mathews et al., 1991). The 4-alkylphenol methylhydroxylases are most active with 4-alkylphenols but also convert 4-hydroxybenzyl alcohol and eugenol (Reeve et al., 1989). Unfortunately, with these enzymes no attempt was made to identify the product of the conversion of eugenol.

From the present study, the question arises of whether the term vanillyl-alcohol oxidase is appropriate as it does not cover the catalytic versatility of this fungal flavoenzyme. According to the substrate specificity and catalytic efficiency, one might argue that a more appropriate name would be 4-allylphenol oxidase. It is doubtful, however, whether the antiseptic 4-allylphenols are physiological substrates of the enzyme. Nevertheless, the *in vitro* formation of the monolignols, coniferyl alcohol and coumaryl alcohol, by this flavoenzyme is noteworthy. Plants are thought to be the only organisms to produce these precursors for the biosynthesis of lignans or the lignin polymer (Paré et al., 1994). In this respect, it is interesting to note that vanillyl-alcohol oxidase is not able to oxidize 4-allyl-2,6-dimethoxyphenol to form the third lignin building block, sinapyl alcohol (4-hydroxy-3,5-dimethoxycinnamyl alcohol).

Vanillyl-alcohol oxidase from *P. simplicissimum* is an inducible intracellular octameric flavoprotein oxidase. These features may indicate that this oxidase is a peroxisomal enzyme like the alcohol oxidases from methylotrophic yeasts (Borst, 1989; Müller et al., 1992). Similar octameric alcohol oxidases, acting on primary alcohols, were recently isolated from several fungi (Danneel et al., 1994). Most eukaryotic covalent flavoproteins studied so far are localized in mitochondria (Mihalik and McGuinness, 1991). Ultrastructural localization of vanillyl-alcohol oxidase will hopefully shed more light on the physiological role of this 8α -(N^3 -histidyl)-FAD-containing flavoenzyme.

Acknowledgements

The authors are grateful to dr. E. de Jong for helpful discussions in preparing the manuscript. We also thank dr. J.J.M. Vervoort for help in NMR experiments and C.J. Theunis for technical assistance in mass spectral analysis.

5.5. References

- Bergmeyer, H.U. (1970) *Methoden der enzymatischen Analyse*, pp. 1749-1752, Verlag Chemie, Weinheim.
 Borst, P. (1989) Peroxisome biogenesis revisited, *Biochim. Biophys. Acta* **1008**, 1-13.
 Curti, B., Ronchi, S. & Simonetta, M.P. (1992) D- and L-amino acid oxidases, in *Chemistry and biochemistry of flavoenzymes* (Müller, F., ed.) vol.3, pp. 69-94, CRC Press, Boca Raton.

- Danneel, H.-J., Reichert, A. & Giffhorn, F. (1994) Production, purification and characterization of an alcohol oxidase of the ligninolytic fungus *Peniophora gigantea*, *J. Biotechnol.* **33**, 33-41.
- De Jong, E., Beuling, E.E., van der Zwan, R.P. & de Bont, J.A.M. (1990) Degradation of veratryl alcohol by *Penicillium simplicissimum*, *Appl. Microbiol. Biotechnol.* **34**, 420-425.
- De Jong, E., van Berkel, W.J.H., van der Zwan, R.P. & de Bont, J.A.M. (1992) Purification and characterization of vanillyl-alcohol oxidase from *Penicillium simplicissimum*: a novel aromatic alcohol oxidase containing covalently FAD, *Eur. J. Biochem.* **208**, 651-657.
- De Jong, E., Field, J.A. & de Bont, J.A.M. (1994) Aryl alcohols in the physiology of ligninolytic fungi, *FEMS Microbiol. Rev.* **13**, 153-188.
- Geissler, J., Ghisla, S. & Kroneck, P.M.H. (1986) Flavin-dependent alcohol oxidase from yeast, *Eur. J. Biochem.* **160**, 93-100.
- Guillén, F., Martínez, A.T. & Martínez, M. J. (1992) Substrate specificity and properties of the aryl-alcohol oxidase from the ligninolytic fungus *Pleurotus eryngii*, *Eur. J. Biochem.* **209**, 603-611.
- Hopper, D.J. & Taylor, D.G. (1977) The purification and properties of *p*-cresol-(acceptor) oxidoreductase (hydroxylating), a flavocytochrome from *Pseudomonas putida*, *Biochem. J.* **167**, 155-162.
- Kwok, F. & Churchich, J.E. (1992) Pyridoxine-5-P oxidase, in *Chemistry and biochemistry of flavoenzymes* (Müller, F., ed.) vol.3, pp. 1-20, CRC Press, Boca Raton.
- Mathews, F.S., Chen, Z-W, Bellamy, H.D. & McIntire, W.S. (1991) Three-dimensional structure of *p*-cresol methylhydroxylase (flavocytochrome c) from *Pseudomonas putida* at 3.0 Å resolution, *Biochemistry* **30**, 238-247.
- McIntire, W.S., Edmondson, D.E., Hopper, D.J. & Singer, T.P. (1981) 8 α -(*o*-Tyrosyl)flavin adenine dinucleotide, the prosthetic group of bacterial *p*-cresol methylhydroxylase, *Biochemistry* **20**, 3068-3075.
- Mihalik, S.J. & McGuinness, M.C. (1991) Covalently-bound flavin in peroxisomal l-pipecolic acid oxidase from primates, in *Flavins and flavoproteins 1990* (Curti, B., Ronchi, S. & Zanetti, G., eds) pp. 881-884, W. de Gruyter, Berlin, New York.
- Müller, F., Hopkins, T.R., Lee, J. & Bastiaens, P.I.H. (1992) Methanol oxidase, in *Chemistry and biochemistry of flavoenzymes* (Müller, F., ed.) vol. 3, pp. 95-119, CRC Press, Boca Raton.
- Paré, P.W., Wang, H.-B., Davin, L.B. & Lewis, N.G. (1994) (+)-Pinoresinol synthase : a stereoselective oxidase catalyzing 8,8'-lignan formation in *Forsythia intermedia*, *Tetrahedron Lett.* **35**, 4731-4734.
- Press, W.H., Flannery, B.P., Teukolsky, S.A. & Vetterling, W.T. (1986) *Numerical recipes: the art of scientific computing*, Cambridge University Press, Cambridge.
- Reeve, C.D., Carver, M.A. & Hopper, D.J. (1989) The purification and characterization of 4-ethylphenol methylene-hydroxylase, a flavocytochrome from *Pseudomonas putida* JD1, *Biochem. J.* **263**, 431-437.
- Rothen, L. & Schlosser, M. (1991) A one-pot synthesis of coumaryl, coniferyl and sinapyl alcohol, *Tetrahedron Lett.* **32**, 2475-2476.
- Sannia, G., Limongi, P., Cocca, E., Buonocore, F., Nitti, G. & Giardina, P. (1991) Purification and characterization of a veratryl alcohol oxidase enzyme from the lignin degrading basidiomycete *Pleurotus ostreatus*, *Biochim. Biophys. Acta* **1073**, 114-119.
- Sherry, B. & Abeles, R.H. (1985) Mechanism of action of methanol oxidase, reconstitution of methanol oxidase with 5-deazaflavin, and inactivation of methanol oxidase by cyclopropanol, *Biochemistry* **24**, 2594-2605.
- Silverman, R.B. (1984) Effect of α -methylation on inactivation of monoamine oxidase by *N*-cyclopropylbenzylamine, *Biochemistry* **23**, 5206-5213.
- Singer, T.P. (1991) Monoamine oxidases, in *Chemistry and biochemistry of flavoenzymes* (Müller, F., ed.) vol.2, pp. 437-470, CRC Press, Boca Raton.
- Van Berkel, W.J.H., Fraaije, M.W. & de Jong, E. (1993) Process for producing 4-hydroxycinnamyl alcohols, patent application N.L. 93201975.5 of 0607-1993.
- Van Berkel, W.J.H., Fraaije, M.W., de Jong, E. & de Bont, J.A.M. (1994) Vanillyl-alcohol oxidase from *Penicillium simplicissimum* : a novel flavoprotein containing 8 α -(*N*³-histidyl)-FAD, in *Flavins and flavoproteins 1993* (Yagi, K., ed.) pp. 799-802, W. de Gruyter, Berlin, New York.
- Williams, R.F., Shinkai, S.S. & Bruce, T.C. (1977) Kinetics and mechanism of the 1,5-dihydroflavin reduction of carbonyl compounds and the flavin oxidation of alcohols. 4. Interconversion of formaldehyde and methanol, *J. Am. Chem. Soc.* **99**, 921-931.

6

Catalytic mechanism of the oxidative demethylation of 4-(methoxymethyl)phenol by vanillyl-alcohol oxidase

Evidence for formation of a *p*-quinone methide intermediate

Marco W. Fraaije and Willem J.H. van Berkel

Journal of Biological Chemistry **272** (29), 18111-18116 (1997)

Abstract

The catalytic mechanism for the oxidative demethylation of 4-(methoxymethyl)phenol by the covalent flavoprotein vanillyl-alcohol oxidase was studied. Using H_2^{18}O , it was found that the carbonylic oxygen atom from the product 4-hydroxybenzaldehyde originates from a water molecule. Oxidation of vanillyl alcohol did not result in any incorporation of ^{18}O .

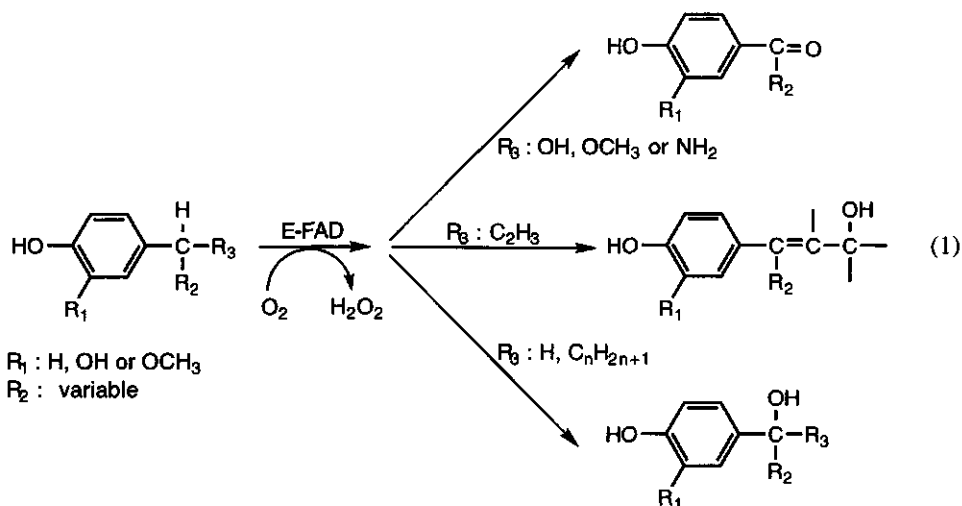
Enzyme-monitored turnover experiments revealed that for both substrates a process involving flavin reduction is rate determining. During anaerobic reduction of vanillyl-alcohol oxidase by 4-(methoxymethyl)phenol, a relatively stable spectral intermediate is formed. Deconvolution of its spectral characteristics showed a typical pH-independent absorption maximum at 364 nm ($\epsilon_{364\text{nm}} = 46 \text{ mM}^{-1}\text{cm}^{-1}$). A similar transient species was observed upon anaerobic reduction by vanillyl alcohol.

The rate of flavin reduction and synchronous intermediate formation by 4-(methoxymethyl)phenol is 3.3 s^{-1} and is fast enough to account for turnover (3.1 s^{-1}). The anaerobic decay of the intermediate was too slow (0.01 s^{-1}) to be of catalytical relevance. The reduced binary complex is rapidly reoxidized ($1.5 \times 10^5 \text{ M}^{-1}\text{s}^{-1}$) and is accompanied with formation and release of product. Oxidation of free-reduced enzyme is an even faster process ($3.1 \times 10^5 \text{ M}^{-1}\text{s}^{-1}$).

The kinetic data for the oxidative demethylation of 4-(methoxymethyl)phenol are in accordance with a ternary complex mechanism in which the reduction rate is rate-limiting. It is proposed that, upon reduction, a binary complex is produced composed of the *p*-quinone methide of 4-(methoxymethyl)phenol and reduced enzyme.

6.1. Introduction

Vanillyl-alcohol oxidase (VAO, EC 1.1.3.13) from *Penicillium simplicissimum* is a novel flavoprotein which acts on a wide range of 4-hydroxybenzylic compounds (1, 2). VAO is a homo-octamer, with each subunit containing 8α -(N^3 -histidyl)-FAD as a prosthetic group (3). During catalysis, the flavin cofactor is first reduced and subsequently reoxidized by molecular oxygen to yield hydrogen peroxide. In addition to the oxidation of aromatic alcohols also, demethylation, deamination, and hydroxylation reactions are being catalyzed as shown in Equation 1. By its versatile catalytic potential, VAO may develop as a useful biocatalyst for applications in the fine chemical industry (4).



VAO is readily induced in *P. simplicissimum* by growth on veratryl alcohol (3). Although the enzyme is produced in relatively high amounts, the physiological role of the enzyme remained obscure for some time as VAO is not involved in the degradation of this aromatic alcohol. Only recently, it was found that the VAO-mediated oxidative demethylation of 4-(methoxymethyl)phenol is of metabolic relevance (5). When *P. simplicissimum* is grown on this phenolic methylether, VAO is induced and catalyzes the first step of the degradation pathway of 4-(methoxymethyl)phenol. Furthermore, analogs of 4-(methoxymethyl)phenol can easily be envisaged as physiological substrates enabling this ascomycetous fungus to cope with a wide variety of lignin decomposition products (5).

Previous studies have revealed some interesting mechanistic properties of VAO. A striking feature of all substrates is the necessity of a *p*-hydroxyl group that is probably a prerequisite for binding. Moreover, a large pK_a shift observed upon binding of the

competitive inhibitor isoeugenol indicates that substrates become deprotonated upon binding (1). For the reaction of VAO with the substrate eugenol, it was established that the oxygen atom incorporated into the formed product coniferyl alcohol is derived from water. From these results, a catalytic mechanism for the hydroxylation of eugenol was proposed which involves formation of a *p*-quinone methide intermediate (1). A similar catalytic mechanism has been proposed for the hydroxylation of 4-alkylphenols by the flavocytochrome, *p*-cresol methylhydroxylase (6). So far, no real evidence has ever been presented for the formation of *p*-quinone methide intermediates during flavin-mediated reactions. We have suggested that hydride transfer to the oxidized flavin cofactor following deprotonation of the substrate would be a feasible sequence of reactions leading to the formation of the labile *p*-quinone methide intermediate (1). Hydride transfer mechanisms have been proposed for several other flavin-dependent oxidases like methanol oxidase (7) and cholesterol oxidase (8). Recently, Mattevi *et al.* (9) provided evidence from crystallographic studies that, for D-amino acid oxidase also, a hydride transfer is a likely event during catalysis. Because well diffracting crystals of VAO have been obtained, we aim to relate the catalytic properties of this flavoenzyme with the crystal structure in the near future (10).

In this paper, we report on the kinetic and catalytic mechanism of VAO with the physiological substrate 4-(methoxymethyl)phenol. Evidence from rapid reaction studies is presented which shows that the hydroxylation of phenolic compounds by VAO involves the formation of a *p*-quinone methide intermediate. Vanillyl alcohol (4-hydroxy-3-methoxybenzyl alcohol; $R_1=OCH_3$, $R_2=H$ and $R_3=OH$ in Equation 1) was included as a model substrate in this study to examine both an oxidative demethylation and an alcohol oxidation reaction.

6.2. Materials and methods

Enzymes and reagents

VAO was purified from *Penicillium simplicissimum* as described by De Jong *et al.* (3) with the modification that a 200-l fermentor was used for cultivation and that cells were disrupted using a Manton-Gaulin homogenizer. The ratio A_{280}/A_{439} for the purified enzyme was 11.0. Glucose oxidase (grade II) and catalase were from Boehringer. $H_2^{18}O$ (97 mol/100 mol ^{18}O) was obtained from Campro (Veenendaal, The Netherlands). Vanillyl alcohol, vanillin (4-hydroxy-3-methoxybenzaldehyde), 4-hydroxybenzaldehyde and 4-(methoxymethyl)phenol were purchased from Aldrich.

Analytical methods

All experiments were performed at 25°C in 50 mM phosphate buffer, pH 7.5, unless stated otherwise. VAO concentrations were calculated from the molar absorption coefficient of the oxidized form ($\epsilon_{439\text{nm}} = 12.5 \text{ mM}^{-1}\text{cm}^{-1}$ (3)).

Isotope labeling experiments

For ^{18}O incorporation experiments, 195 μl of H_2^{18}O was added to 400 μl of 1.0 mM substrate solutions. After addition of VAO (25 μl , 200 μM) and catalase (5 μl , 100 μM) the samples were incubated for 5 minutes at 25°C and subsequently twice extracted with 500 μl diethylether. After evaporation, the samples were analyzed by GC/MS. GC/MS analysis was performed on a Hewlett Packard HP 5973 MSD and HP 6090 GC equipped with a HP-5 column.

Steady-state kinetics

Steady state kinetic experiments were performed essentially as described earlier (1). Vanillyl alcohol and 4-(methoxymethyl)phenol activity were determined spectrophotometrically by recording the formation of vanillin ($\epsilon_{340\text{nm},\text{pH}7.5} = 14.0 \text{ mM}^{-1}\text{cm}^{-1}$) and 4-hydroxybenzaldehyde ($\epsilon_{340\text{nm},\text{pH}7.5} = 10.0 \text{ mM}^{-1}\text{cm}^{-1}$), respectively. Oxygen concentrations were varied by mixing buffers saturated with 100% nitrogen and 100% oxygen in different ratios.

Stopped-flow kinetics

Stopped-flow kinetics were carried out with a Hi-Tech SF-51 apparatus equipped with a Hi-Tech M300 monochromator diode-array detector (Salisbury, United Kingdom). Spectral scans were collected each 10 ms. For accurate estimation of rate constants single wavelength kinetic traces were recorded at 439 nm using a Hi-Tech SU-40 spectrophotometer. In anaerobic experiments, solutions were flushed with argon and contained glucose (10 mM) and glucose oxidase (0.1 μM) to ensure anaerobic conditions. To determine the maximal rate of enzyme reduction by 4-(methoxymethyl)phenol and vanillyl alcohol, apparent rates were determined at five different substrates concentrations. To obtain accurate estimations of reduction rate constants observed during anaerobic reduction by vanillyl-alcohol, measurements were also performed at 355 nm and 393 nm. Deconvolution analysis of spectral data was performed using the Specfit Global Analysis program version 2.10 (Spectrum Software Assn., Chapel Hill, NC). Solutions containing reduced enzyme (5 μM) were prepared by titrating argon flushed enzyme solutions with dithionite. For generation of the reduced enzyme intermediate complex, the enzyme was anaerobically mixed with a 1.5-fold excess of 4-(methoxymethyl)phenol. Reoxidation of reduced enzyme was measured by monitoring the increase in absorption at 439 nm after

mixing with molecular oxygen. Reduced enzyme (5.0 μM) was mixed with varying concentrations of molecular oxygen (10, 21, 50 and 100 % saturation) to determine the second-order rate constants for the reoxidation of protein-bound flavin.

For enzyme-monitored turnover experiments (11), air-saturated enzyme and substrate solutions were mixed in the stopped-flow instrument after which the redox state of the flavin cofactor was recorded at 439 nm.

6.3. Results

6.3.1. Isotope labeling experiments

In a previous report we already identified the products formed from 4-(methoxymethyl)phenol and vanillyl alcohol as their corresponding aldehydes (1). In this study, H_2^{18}O was used to test the involvement of water in the VAO-mediated conversion of 4-(methoxymethyl)phenol and vanillyl alcohol. Substrate solutions (containing 30% H_2^{18}O (w/w)) were incubated for 5 minutes in the presence of a catalytical amount of enzyme. Blank reactions with the aromatic products 4-hydroxybenzaldehyde and vanillin revealed that, under these conditions, less than 5% of the carbonylic oxygen atoms had exchanged with H_2^{18}O .

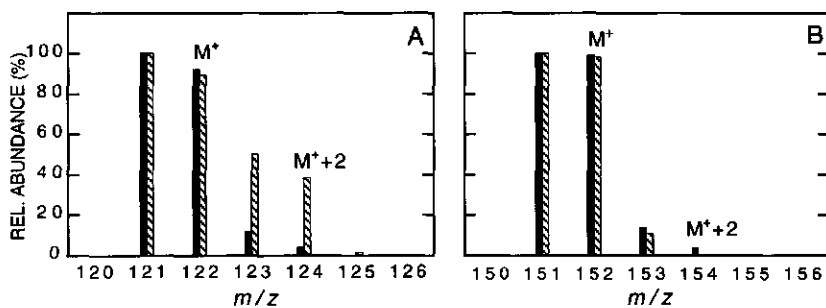


Figure 1. Incorporation of ^{18}O from water during conversion of 4-(methoxymethyl)phenol (A) and vanillyl alcohol (B) by VAO. Only mass peaks around M^+ are shown. Mass spectral data of the unlabelled aromatic aldehydes were as described before (3).

For the VAO-mediated conversion of 4-(methoxymethyl)phenol, it was found that the aromatic product 4-hydroxybenzaldehyde was fully hydroxylated by action of water ($97 \pm 4\%$) (Fig. 1). The incorporation of ^{18}O confirms an earlier finding (1) that conversion of 4-(methoxymethyl)phenol by VAO results in cleavage of the methoxyl group

as methanol. The VAO catalyzed oxidation of vanillyl alcohol to vanillin did not result in significant ^{18}O incorporation (Fig. 1). This shows that with this alcoholic substrate water is not involved in the enzymatic reaction.

6.3.2. Steady-state kinetics

By measuring the VAO activity upon varying the concentration of oxygen at different 4-(methoxymethyl)phenol concentrations, a set of parallel Lineweaver-Burk plots was obtained. This suggests that for this reaction a ping-pong mechanism may be operative. Parallel line kinetics can, however, also occur in some limited cases of a ternary complex mechanism where some specific rate constants are relatively small (12, 13). Fig. 2 shows a secondary plot of the extrapolated turnover rates at saturating oxygen concentrations *versus* the concentration of 4-(methoxymethyl)phenol. From this, the steady state kinetic parameters with 4-(methoxymethyl)phenol could be calculated (Table 1). The steady state kinetic parameters for vanillyl alcohol were similarly determined (again showing series of parallel secondary plots) and were in the same range as for 4-(methoxymethyl)phenol ($k_{\text{cat}} = 3.3 \text{ s}^{-1}$, $K_{m,S} = 160 \mu\text{M}$, $K_{m,O_2} = 28 \mu\text{M}$). The relatively high K_m value for vanillyl alcohol might result from the more polar character of the benzylic moiety compared to 4-(methoxymethyl)phenol (1).

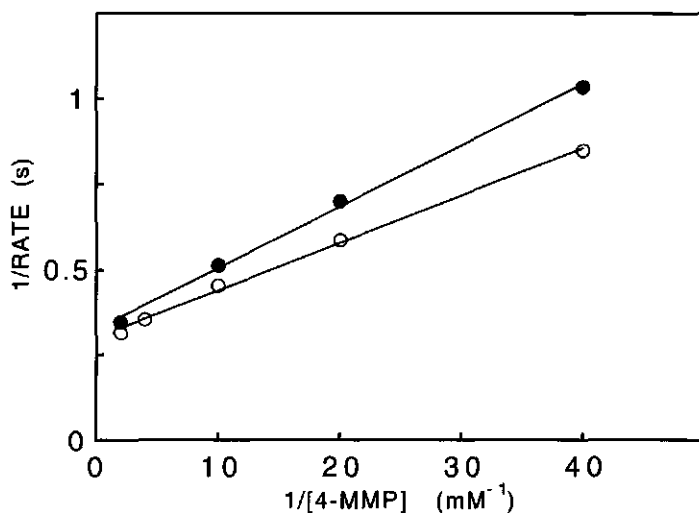


Figure 2. Double-reciprocal plot of steady-state kinetic measurements (●) and anaerobic reductive half-reaction with 4-(methoxymethyl)phenol (○). For the steady-state kinetic data, the turnover rates at saturating oxygen concentrations were determined from secondary plots using several substrate concentrations (25, 50, 100, and 500 μM) with varying oxygen concentrations.

By measuring the redox state of the flavin cofactor during catalysis (enzyme-monitored turnover) information can be obtained about the rate-limiting step (11). For this, the enzyme was aerobically mixed in the stopped-flow apparatus with a high concentration of substrate. It should be noted here that due to the low solubility of vanillyl alcohol and 4-(methoxymethyl)phenol, the substrate concentrations (500 μM) were not fully saturating. During turnover, the absorbance at 439 nm was monitored to detect the amount of oxidized enzyme present. Fig. 3 shows that with both substrates most of the enzyme is in the oxidized state during turnover. The fraction of oxidized enzyme for both substrates was almost identical, 0.86 for 4-(methoxymethyl)phenol and 0.91 for vanillyl alcohol (Fig. 3). This suggests that processes involving flavin reduction are slower than those of the oxidative part of the catalytic cycle.

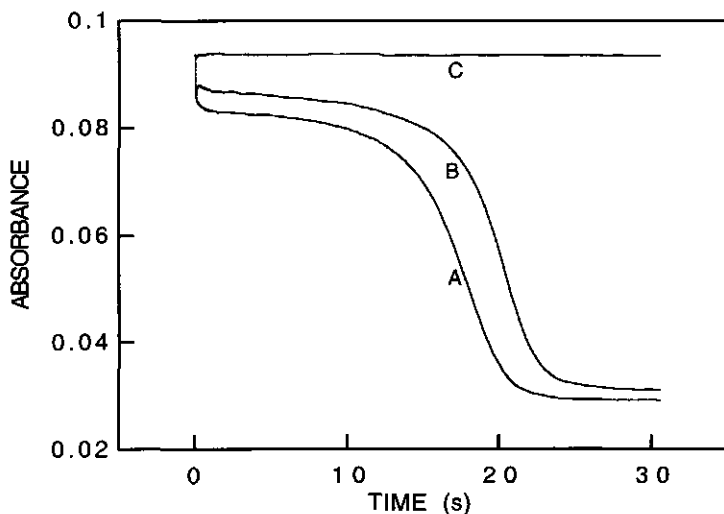


Figure 3. Enzyme-monitored turnover of VAO with 4-(methoxymethyl)phenol and vanillyl alcohol. The enzyme (7.5 μM) was reacted in the stopped-flow instrument with 500 μM 4-(methoxymethyl)phenol (trace A) and vanillyl alcohol (trace B). During the reaction, the absorbance at 439 nm was monitored. Trace C was the result of mixing the enzyme with buffer.

6.3.3. Reductive half-reaction

To study the reductive half-reaction of VAO, the oxidized enzyme was mixed with substrate in the stopped-flow spectrophotometer under anaerobic conditions. Reduction of VAO by 4-(methoxymethyl)phenol was a monophasic process when monitored at 439 nm. Diode-array detection revealed that anaerobic enzymatic reaction with 4-(methoxymethyl)phenol resulted in the formation of a species with an intense absorption maximum at 364 nm ($\epsilon_{364\text{nm}} = 46 \text{ mM}^{-1}\text{cm}^{-1}$) (Fig. 4).

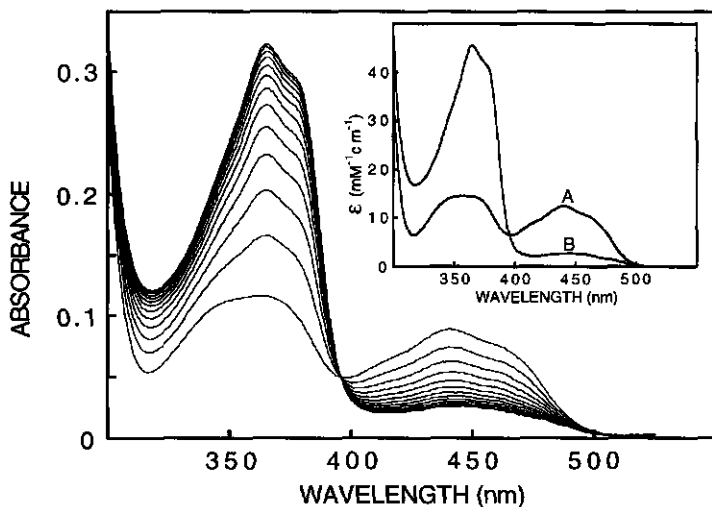
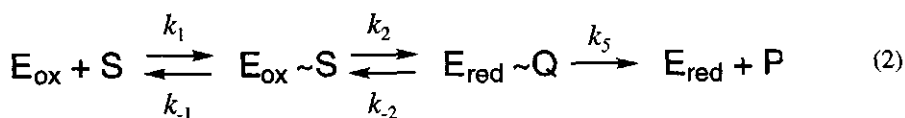


Figure 4. Spectral changes observed upon anaerobic mixing of VAO (7.0 μM) with 4-(methoxymethyl)phenol (500 μM , 25°C, pH 7.5). Original spectral scans are shown from 5.6 msec to 965.6 ms with intervals of 80 msec. The inset shows spectra obtained after deconvolution of the original spectral scans where spectrum (A) represents the initial spectrum of oxidized enzyme and spectrum (B) shows the formed spectral intermediate. The data were fit with a one-exponential function ($A \rightarrow B$) resulting in a rate of 3.0 s^{-1} .

During this process, the flavin becomes fully reduced as evidenced by the decrease in absorbance at 439 nm. This indicates that the rate of the reverse reaction must be relatively small. The rate of flavin reduction at saturated substrate concentrations was in the same range as the turnover rate (Table 1). pH-Dependent anaerobic reductions by 4-(methoxymethyl)phenol revealed that the spectral properties of the formed intermediate were not influenced between pH 6.8 and pH 7.9. Furthermore, reduction at the tested pH values did not result in a significant change of the rate of reduction. When the spectral changes were followed on a longer time scale ($>20 \text{ s}$), a very slow decay of the high absorbance intermediate was observed. The resulting spectrum could be characterized as the composite of reduced enzyme and the product 4-hydroxybenzylaldehyde. Indicative for aldehyde formation was the increase in absorbance around 335 nm, which was even more pronounced at higher pH due to deprotonation of the phenolic group ($\text{p}K_{\text{a}}$ 4-hydroxybenzaldehyde = 7.6). The rate of aldehyde formation under anaerobic conditions was estimated to be 0.01 s^{-1} , which is too slow to be of catalytical relevance. The results obtained from the anaerobic reduction of VAO with 4-(methoxymethyl)phenol are consistent with the following Equation 2,



where Q represents the high absorbance intermediate.

Reduction of VAO by vanillyl alcohol showed biphasic absorption traces at 439 nm. Diode array analysis revealed that during reduction an intermediate spectrum is formed with a typical absorption maximum at 362 nm (Fig. 5, A and B).

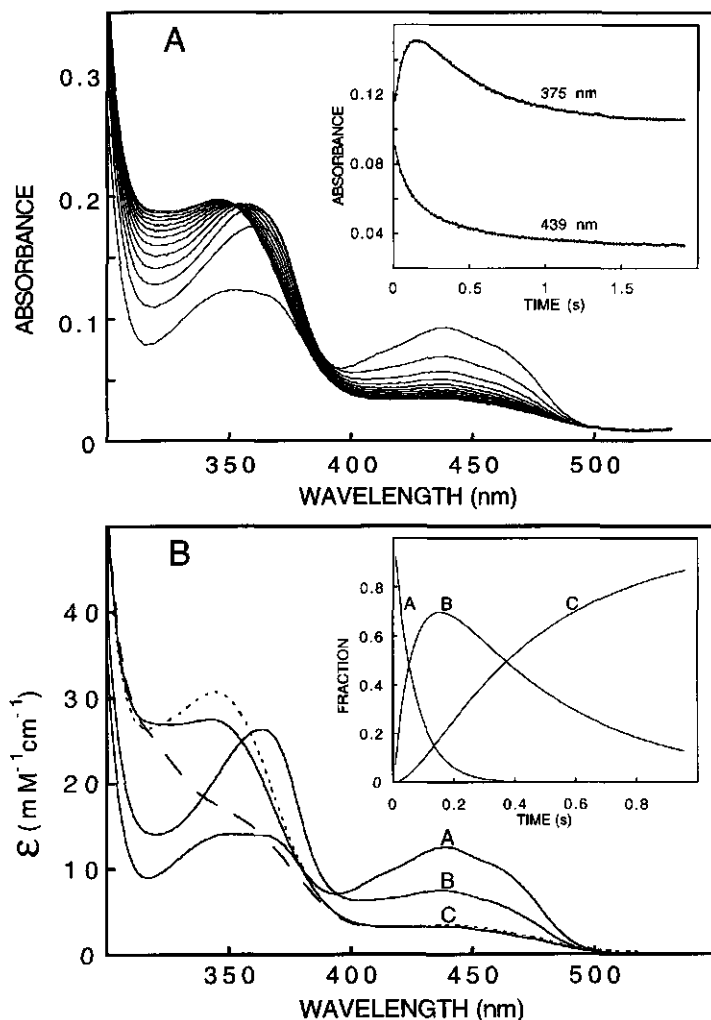


Figure 5. A, Spectral changes observed upon anaerobic mixing of VAO ($7.0 \mu\text{M}$) with vanillyl alcohol ($500 \mu\text{M}$, 25°C , pH 7.5). Original spectral scans are shown from 5.6 msec to 965.6 ms with intervals of 80 msec. The inset shows the original data monitored at 375 nm and 439 nm (pH 7.5) using diode-array detection showing the biphasic nature of the reduction reaction.

B. Spectra obtained from deconvolution of spectral changes caused by anaerobic reduction of VAO ($7.0 \mu\text{M}$) by vanillyl alcohol ($500 \mu\text{M}$, 25°C , pH 7.5). A consecutive irreversible model ($\text{A} \rightarrow \text{B} \rightarrow \text{C}$) was used to fit the data resulting in apparent rates of 14 and 2.2 s^{-1} for the two respective reductive phases. Upon reaction with vanillyl alcohol, the original spectrum A transforms to B and subsequently C is formed. When the same reaction was performed at pH 6.8 or pH 7.9 (50 mM phosphate buffer), only the final spectrum (C) significantly changed (shown by broken line and dashed line respectively). The inset shows the simulated concentrations of the three components during the anaerobic reduction by vanillyl alcohol.

As can be seen from Fig. 5A, this intermediate decayed rapidly to yield fully reduced enzyme. For accurate kinetic data, rate constants of both reductive phases were determined at various substrate concentrations by monitoring the reaction at isosbestic points (393 nm and 355 nm, see Fig. 5B). It was found that the first rapid phase was an order of magnitude faster compared to the slow phase ($k_{\text{red1}} = 24 \text{ s}^{-1}$, $K_d = 270 \text{ }\mu\text{M}$ compared to $k_{\text{red2}} = 3.5 \text{ s}^{-1}$, $K_d = 150 \text{ }\mu\text{M}$; Fig. 6).

Using a consecutive irreversible reaction model in which the first reaction corresponds to the fast process, spectral deconvolution produced well defined spectra for the initial, intermediate, and final components (Fig. 5B, traces A, B, and C). As can be seen from Fig. 5B the distinctive absorption maximum of the intermediate spectrum formed in the first phase showed some resemblance with the intermediate spectrum formed by anaerobic reduction of VAO with 4-(methoxymethyl)phenol (see Fig. 4 inset). This analogy was confirmed by performing the anaerobic reduction experiments with vanillyl alcohol at different pH values (Fig. 5B). As with 4-(methoxymethyl)phenol, no significant effect of pH on the observed reduction rates was observed. Furthermore, these studies again showed that in contrast to the transient intermediate spectrum, the final spectrum is pH-dependent. This indicates that the final product vanillin is formed only in the second step as the spectral properties of the final spectrum agree nicely with formation of vanillin ($\text{p}K_a = 7.5$, $\lambda_{\text{max}} = 345 \text{ nm}$). Furthermore, in the case of vanillyl alcohol, the flavin apparently is only partially reduced when the high absorbance intermediate is formed as the absorbance at 439 nm is relatively high after the first reductive phase (Fig. 5B).

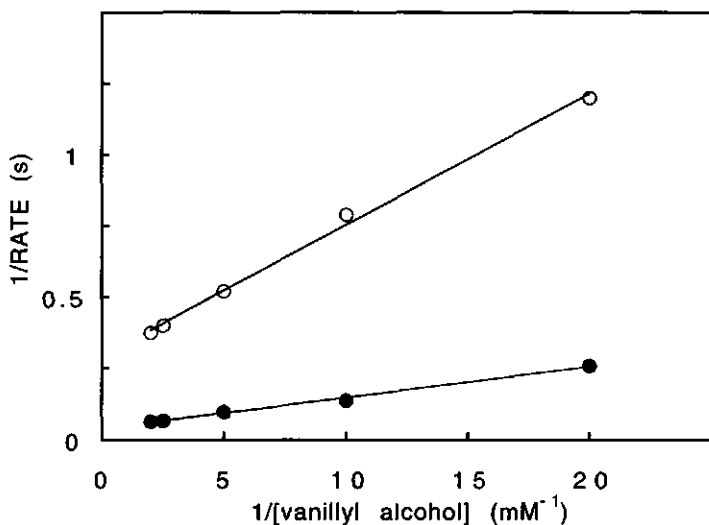
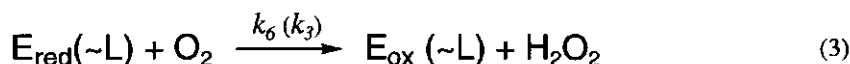


Figure 6. Double-reciprocal plot of the two reduction rates observed during the anaerobic reductive half-reaction of VAO with vanillyl alcohol (●: k_{red1} , ○: k_{red2}).

6.3.4. Oxidative half-reaction

To measure the rate of reoxidation, reduced VAO was mixed with molecular oxygen in the stopped-flow spectrophotometer, and the increase of the flavin absorbance at 439 nm was monitored. Reoxidation of free-reduced VAO was a monophasic reaction resulting in formation of fully oxidized enzyme. By varying the concentration of oxygen it was found that reoxidation of free reduced VAO is a fast bimolecular process ($3.1 \times 10^5 \text{ M}^{-1}\text{s}^{-1}$) as has been found for other flavoprotein oxidases (14).



For flavoprotein oxidases, the rate of enzyme reoxidation can significantly be influenced by bound ligands (L in Equation 3) (15). For instance, in case of D-amino acid oxidase from yeast, it was reported that reoxidation of free-reduced enzyme is not of catalytical significance as it is significantly slower than the turnover rate. Only the rate for reoxidation of the reduced enzyme product complex was high enough to account for the observed turnover rate, which is in agreement with the proposed ternary complex mechanism (16). When the reoxidation rate of reduced VAO was studied in the presence of vanillyl alcohol or its product vanillin, the rates of flavin reoxidation were significantly lower as compared with free-reduced enzyme (1.4×10^5 and $1.1 \times 10^5 \text{ M}^{-1}\text{s}^{-1}$, respectively).

As reduction by 4-(methoxymethyl)phenol resulted in a relatively stable reduced enzyme-intermediate complex ($E_{\text{red}}\sim Q$), the rate of reoxidation of this complex was measured as well. Therefore, after reducing VAO by 4-(methoxymethyl)phenol, the reduced complex was mixed in the stopped-flow apparatus with oxygen to measure the rate of formation of oxidized enzyme. It was found that the complex readily reacted with oxygen in a fast monophasic process reoxidizing the flavin with simultaneous product formation as evidenced by the increase of absorbance at 335 nm. By varying the oxygen concentration the second order rate constant for reoxidation of the reduced enzyme intermediate complex was estimated to be $1.5 \times 10^5 \text{ M}^{-1}\text{s}^{-1}$. Similar values for the rate of reoxidation have been reported for other flavin dependent oxidases (15-18). The apparent turnover rate with 4-(methoxymethyl)phenol during steady-state conditions is much slower as the rate of reoxidation. Evidently, reoxidation is not determining the rate of catalysis in case of 4-(methoxymethyl)phenol, which is in agreement with the enzyme monitored turnover results.

Table 1. Kinetic constants for the reaction of 4-(methoxymethyl)phenol with vanillyl-alcohol oxidase from *P. simplicissimum* (pH 7.5, 25°C).

Constant	Experimental	Calculated
k_{-1}/k_1	48 μM	
$k_2 (=k_{\text{red}})$	3.3 s^{-1}	
k_{-2}	~ 0	
k_3^{a}	$1.5 \times 10^5 \text{ M}^{-1}\text{s}^{-1}$	$1.4 \times 10^5 \text{ M}^{-1}\text{s}^{-1}$
k_4^{b}		50 s^{-1}
k_5	0.01 s^{-1}	
k_6	$3.1 \times 10^5 \text{ M}^{-1}\text{s}^{-1}$	
k_{cat}	3.1 s^{-1}	
$K_{\text{m}}(\text{S})^{\text{c}}$	55 μM	45 μM
$K_{\text{m}}(\text{O}_2)^{\text{d}}$	24 μM	21 μM

^a: $k_3 = k_{\text{cat}}/K_{\text{m}}(\text{O}_2)$, ^b: k_4 calculated from $k_{\text{cat}} = k_2 \cdot k_4 / (k_2 + k_4)$,

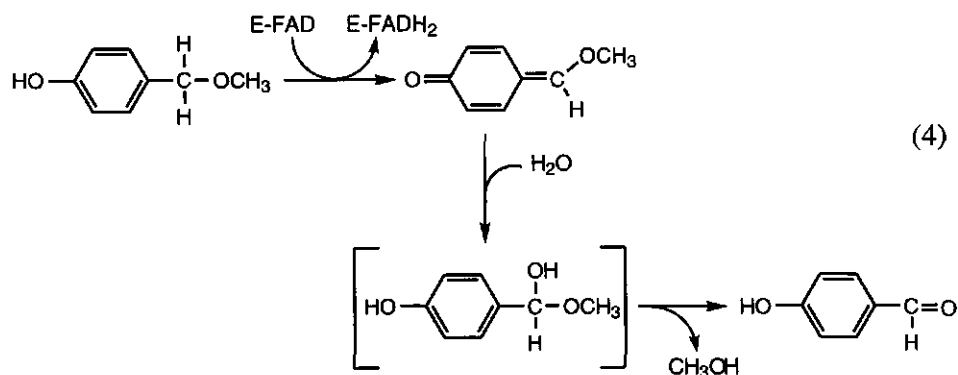
^c: $K_{\text{m}}(\text{S}) = k_4(k_{-1} + k_2) / k_1(k_2 + k_4)$, ^d: $K_{\text{m}}(\text{O}_2) = k_4(k_2 + k_{-2}) / k_3(k_2 + k_4)$

6.4. Discussion

The experiments described here represent the first study on the kinetic mechanism of VAO catalyzed reactions. Furthermore, evidence is presented for the participation of *p*-quinone methides in the catalytic mechanism of VAO. Previously, we proposed a reaction mechanism for the conversion of eugenol by VAO, which included formation of a *p*-quinone methide intermediate (1). Addition of water to this putative electrophilic intermediate would result in the formation of the product coniferyl alcohol. From isotopic labeling experiments, we have demonstrated in the present study the involvement of water during the VAO catalyzed demethylation of 4-(methoxymethyl)phenol. VAO-mediated demethylation of this physiological substrate resulted in the introduction of an oxygen atom originating from a water molecule. This indicates that during catalysis the substrate is activated, after which water can attack the C_{α} -atom. In contrast, with vanillyl alcohol, no oxygen atom derived from water is introduced into the aromatic product vanillin.

The rapid reaction data presented in this paper showed the formation of intermediate reduced enzyme complexes during the reductive half-reaction. Anaerobic reduction of VAO by 4-(methoxymethyl)phenol revealed the formation of an eminently stable intermediate with

typical spectral properties ($\epsilon_{364\text{nm}} = 46 \text{ mM}^{-1}\text{cm}^{-1}$). The spectral characteristics of the intermediate binary complex did not resemble any known flavoprotein oxidase complex. Intermediate complexes formed during catalysis of, for example, lactate monooxygenase (19) and D-amino acid oxidase (20) have specific absorbances above 500 nm and are due to a charge transfer interaction between the reduced enzyme and product. The formation of a flavin adduct as intermediate in the reaction of VAO with 4-(methoxymethyl)phenol is rather unlikely as the spectral properties of the intermediate complex do not resemble any known flavin adduct spectrum (21). However, the spectral properties of the formed intermediate generated during the anaerobic reaction of VAO with 4-(methoxymethyl)phenol closely resembled reported spectra of several *p*-quinone methides of structural analogs of the phenolic substrate ($\lambda_{\text{max}} \sim 360 \text{ nm}$, $\epsilon \sim 40 \text{ mM}^{-1}$) as obtained by chemical synthesis or flash photolysis of the corresponding phenols (22-26). However, spectra of the *p*-quinone methides of vanillyl alcohol and 4-(methoxymethyl)phenol have never been described. These compounds are highly unstable because of the lack of an electron donating group to stabilize the electrophilic methide carbon atom. The data presented here for VAO-mediated conversion of 4-(methoxymethyl)phenol are all consistent with formation of a *p*-quinone methide intermediate, which subsequently will react with water. The *p*-quinone methide formed from this substrate is highly stabilized in the active site as long as the enzyme remains reduced. This suggests that the active site of the reduced enzyme intermediate complex is solvent inaccessible. Upon reoxidation of the flavin, the *p*-quinone methide intermediate rapidly reacts with water, indicating that during this process local structural changes occur leading to a more solvent accessible active site. The *p*-quinone methide is hydrated to form the unstable hemiacetal product of 4-(methoxymethyl)phenol, which decomposes rapidly to give 4-hydroxybenzaldehyde (Equation 4). The presence of reduced glutathione during turnover of 4-(methoxymethyl)phenol did not influence the stoichiometric formation of the aldehyde product, indicating that hydration of the formed *p*-quinone methide occurs in the enzyme active site.



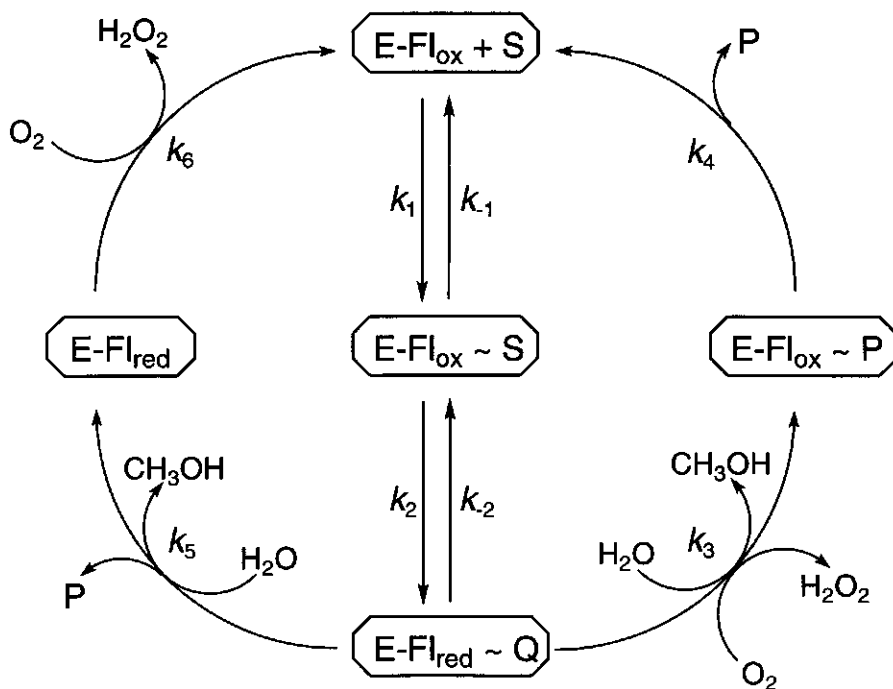
With vanillyl alcohol also, a transient intermediate spectrum was observed during anaerobic reduction with similar spectral characteristics as with 4-(methoxymethyl)phenol. However, with vanillyl alcohol, only half of the flavin is reduced when the maximal amount of the high absorbance intermediate is formed, indicating that the intermediate is already decomposed when the enzyme is fully reduced. When the decay of the intermediate during the second reductive phase is acknowledged, the molar absorption coefficient of the intermediate may well resemble that of the 4-(methoxymethyl)phenol *p*-quinone methide intermediate. The instability of the formed vanillyl alcohol *p*-quinone methide may well explain why during oxidation of this alcohol water is not involved in the formation of the aldehyde product. Decay of the initial intermediate formed may correspond to the autocatalytic decomposition of the vanillyl alcohol *p*-quinone methide leading to vanillin. The biphasic reduction can be interpreted to result from two reactive conformations of the enzyme of which one is able to reduce the flavin rapidly while the other conformation is slow in reduction. In view of this, it is worthy to note that VAO is an octamer composed of relatively stable dimers (27). Another explanation for the partial reduction observed with vanillyl alcohol is a reversible reduction of the flavin by vanillyl alcohol, which results in an equilibrium of oxidized and reduced enzyme in anaerobic reduction experiments. When $k_2 \approx k_{-2}$, the ratio of oxidized and reduced enzyme will be 0.5, leading to an apparent partial reduction as shown in Fig. 5. The second phase observed during the reductive half-reaction might then represent product release, which would also result in total reduction of the flavin. In that case, the turnover rate for vanillyl-alcohol oxidation would be determined by product release, which has also been found for several other flavoprotein oxidases (11, 13). However, analysis of the substrate dependent reduction rates revealed that the reversible step of reduction must be very small ($k_{-2} < 0.5 \text{ s}^{-1}$) and is too small to explain the relatively high amount of oxidized enzyme present after the first phase of flavin reduction. Furthermore, enzyme-monitored turnover experiments showed that the enzyme is mainly in the oxidized state (91%) during steady-state turnover. As a consequence, with vanillyl alcohol, a reductive step is limiting the turnover rate also.

From the rapid reaction kinetic parameters obtained in this study, it can be concluded that VAO catalyzes the oxidative demethylation of 4-(methoxymethyl)phenol via a ternary complex mechanism. Also, the parallel lines pattern of Lineweaver-Burk plots found for the steady-state kinetics are in accordance with a ternary complex mechanism as k_2 is negligible small and k_3 is relatively large (Table 1). Because k_5 is very small, only a small portion of enzyme will react via a ping-pong mechanism as represented by the left cycle in scheme I. From single turnover experiments, it could be deduced that the rate of flavin reduction, eq. formation of the binary complex ($k_2 = 3.3 \text{ s}^{-1}$), is by far the rate determining step in catalysis ($k_{\text{cat}} = 3.1 \text{ s}^{-1}$). The enzyme-monitored turnover results are also consistent with the proposed kinetic mechanism. When the formation of the Michaelis-Menten complex is a

relatively fast process (at infinite substrate concentrations), the ratio of enzyme in the oxidized state during steady-state can be calculated by the following.

$$\frac{E_{\text{ox}}}{E_{\text{total}}} = \frac{1/k_2 + 1/k_4}{1/k_2 + 1/k_3 + 1/k_4} \quad (5)$$

For 4-(methoxymethyl)phenol, the calculated ratio is 0.92 ($k_2 = 3.0 \text{ s}^{-1}$ at $500 \mu\text{M}$) which compares quite well with the experimental obtained value of 0.86. This indicates that the mechanism based calculated rate of product release ($k_4 = 50 \text{ s}^{-1}$) is a reasonable approximation. Taken together, the kinetic data are consistent with a ternary complex mechanism including (right cycle of scheme I) (1) formation of a Michaelis-Menten complex, (2) flavin reduction and synchronous formation of the reduced enzyme intermediate complex, (3) reoxidation of the reduced enzyme complex by molecular oxygen with the concomitant conversion of the intermediate to form the final product, and (4) product release completing the catalytic cycle.



Scheme 1. Proposed kinetic mechanism for the oxidative demethylation of 4-(methoxymethyl)phenol by vanillyl-alcohol oxidase. ($E\text{-Fl}_{\text{ox}}$ = oxidized VAO, $E\text{-Fl}_{\text{red}}$ = reduced VAO, S = 4-(methoxymethyl)phenol, Q = *p*-quinone methide of S , P = 4-hydroxybenzaldehyde).

Although a ternary complex mechanism is operative with 4-(methoxymethyl)phenol, with vanillyl alcohol, the reaction may also follow a ping-pong mechanism (represented by the left cycle in scheme 1). With this substrate, the binary reduced enzyme intermediate complex readily decomposes to form product without prior reoxidation of the flavin. In both cases, the rate of substrate-mediated flavin reduction is mainly limiting the overall rate of catalysis.

From the results presented in this study, it can be concluded that VAO efficiently converts the transient formed *p*-quinone methides. Quinone methides are highly electrophilic compounds and are thought to be involved in several toxicological processes. Studies have shown that formation of analogous quinone methides can result in (cyto)toxic effects by forming covalent bonds with cellular nucleophiles like proteins or DNA (25, 28). Preliminary release of the reactive product intermediate formed by VAO would also result in spontaneous reactions with water or other nucleophiles and could therefore *in vivo* elicit possible deleterious effects. Clearly, efficient hydration of the *p*-quinone methide in the active site of the enzyme is a prerequisite for the microorganism to exclude potential toxic effects.

Acknowledgement

The authors want to thank Prof. Dr. N.C.M. Laane for critically reading the manuscript.

6.5. References

1. Fraaije, M.W., Veeger, C. & van Berkel, W.J.H. (1995) Substrate specificity of flavin-dependent vanillyl-alcohol oxidase from *Penicillium simplicissimum*. *Eur. J. Biochem.* **234**, 271-277.
2. Fraaije, M.W., Drijfhout, F., Meulenbeld, G.H., van Berkel, W.J.H. & Mattevi, A. (1997) Vanillyl-alcohol oxidase from *Penicillium simplicissimum*: reactivity with *p*-cresol and preliminary structural analysis, in *Flavins and flavoproteins XII* (Stevenson, K., Massey, V., and Williams, C., eds.) pp 261-264, University Press, Calgary.
3. De Jong, E., van Berkel, W.J.H., van der Zwan, R.P. & de Bont, J.A.M. (1992) Purification and characterization of vanillyl-alcohol oxidase from *Penicillium simplicissimum*. *Eur. J. Biochem.* **208**, 651-657.
4. Van Berkel, W.J.H., Fraaije, M.W. & de Jong, E. (1997) Process for producing 4-hydroxycinnamyl alcohols. European Patent application 0710289B1.
5. Fraaije, M.W., Pikkemaat, M. and van Berkel, W.J.H. (1997) Enigmatic gratuitous induction of the covalent flavoprotein vanillyl-alcohol oxidase in *Penicillium simplicissimum*. *Appl. Environ. Microbiol.* **63**, 435-439.
6. Hopper, D.J. (1976) The hydroxylation of *p*-cresol and its conversion to *p*-hydroxy-benzaldehyde in *Pseudomonas putida*. *Biochem. Biophys. Res. Commun.* **69**, 462-468.
7. Menon, V., Hsieh, C-T. & Fitzpatrick, P.F. (1995) Substituted alcohols as mechanistic probes of alcohol oxidase. *Bioorg. Chem.* **23**, 42-53.
8. Li, J., Vrieling, A. Brick, P. & Blow, D.M. (1993) Crystal structure of cholesterol oxidase complexed with flavin adenine dinucleotide dependent alcohol oxidases. *Biochemistry* **32**, 11507-11515.

9. Mattevi, A., Vanoni, M.A., Todone, F., Rizzi, M., Teplyakov, A., Coda, A., Bolognesi, M. & Curti, B. (1996) Crystal structure of D-amino acid oxidase: a case of active site mirror-image convergent evolution with flavocytochrome *b₂*. *Proc. Nat. Acad. Sc.* **93**, 7496-7501.
10. Mattevi, A., Fraaije, M.W., Coda, A. & van Berkel, W.J.H. (1997) Crystallization and preliminary X-ray analysis of the flavoenzyme vanillyl-alcohol oxidase from *Penicillium simplicissimum*. *Proteins: Structure, Function and Genetics* **27**, 601-603.
11. Gibson, Q. H., Swoboda, B.E.P. & Massey, V. (1964) Kinetics and mechanism of action of glucose oxidase. *J. Biol. Chem.* **239**, 3927-3934.
12. Palmer, G. & Massey, V. (1968) Mechanisms of Flavoprotein Catalysis. In: *Biological Oxidations* (Singer, T. P., eds.), pp. 263-300, Wiley, New York.
13. Porter, D.J.T., Voet, J.G. & Bright, H.J. (1977) Mechanistic features of the D-amino acid oxidase reaction studied by double stopped flow spectrophotometry. *J. Biol. Chem.* **252**, 4464-4473.
14. Massey, V. (1994) Activation of molecular oxygen by flavins and flavoproteins. *J. Biol. Chem.* **269**, 22459-22462.
15. Tan, A.K. & Ramsay, R.R. (1993) Substrate-specific enhancement of the oxidative half-reaction of monoamine oxidase. *Biochemistry* **32**, 2137-2143.
16. Pollegioni, L., Langkau, B., Tischer, W., Ghisla, S. & Pilone, M.S. (1993) Kinetic mechanism of D-aminoacid oxidases from *Rhodotorula gracilis* and *Trichonopsis variabilis*. *J. Biol. Chem.* **268**, 13850-13857.
17. Geissler, J., Ghisla, S. & Kroneck, P.M.H. (1986) Flavin-dependent alcohol oxidase from yeast. *Eur. J. Biochem.* **160**, 93-100.
18. Maeda-Yorita, K., Aki, K., Sagai, H., Misaki, H. & Massey, V. (1995) L-lactate oxidase and L-lactate monooxygenase: Mechanistic variations on a common structural theme. *Biochimie* **77**, 631-642.
19. Lockridge, O., Massey, V. & Sullivan, P.A. (1972) Mechanism of action of the flavoenzyme lactate oxidase. *J. Biol. Chem.* **247**, 8097-8106.
20. Massey, V. & Ghisla, S. (1974) Role of charge-transfer interactions in flavoprotein catalysis. *Ann. N.Y. Acad. Sci.* **227**, 446.
21. Ghisla, S., Massey, V. & Choong, Y.S. (1979) Covalent adducts of lactate oxidase. *J. Biol. Chem.* **254**, 10662-10669.
22. Filar, L.J. & Winstein, S. (1960) Preparation and behavior of simple quinone methides. *Tetrahedron Lett.* **25**, 9-16.
23. Leary, G. (1972) The chemistry of reactive lignin intermediates. Part I. Transients in coniferyl alcohol photolysis. *J.C.S. Perkin II*, 640-642.
24. Diao, L., Yang, C. & Wan, P. (1995) Quinone methide intermediates from the photolysis of hydroxybenzyl alcohols in aqueous solution. *J. Am. Chem. Soc.* **117**, 5369-8370.
25. Thompson, D., Norbeck, K., Olsson, L-I., Despina, C-T, Van Der Zee, J. & Moldéus, P. (1989) Peroxidase-catalyzed oxidation of eugenol: formation of a cytotoxic metabolite(s). *J. Biol. Chem.* **264**, 1016-1021.
26. Thompson, D.C. & Perera, K. (1995) Inhibition of mitochondrial respiration by a para-quinone methide. *Bioch. Biophys. Res. Comm.* **209**, 6-11.
27. Fraaije, M.W., Mattevi, A. & van Berkel, W.J.H. (1997) Mercuration of vanillyl-alcohol oxidase from *Penicillium simplicissimum* generates inactive dimers. *FEBS Lett.* **402**, 33-35.
28. Thompson, D.C. Perera, K. & London, R. (1995) Quinone methide formation from *para* isomers of methylphenol (cresol), ethylphenol, and isopropylphenol: relationship to toxicity. *Chem. Res. Toxicol.* **8**, 55-60.

7

Enantioselective hydroxylation of 4-alkylphenols by vanillyl-alcohol oxidase

Falko P. Drijfhout, Marco W. Fraaije, Hugo Jongejan,
Willem J.H. van Berkel and Maurice C. R. Franssen

Biotechnology and Bioengineering, in press

Abstract

Vanillyl-alcohol oxidase (VAO) from *Penicillium simplicissimum* catalyzes the enantioselective hydroxylation of 4-ethylphenol, 4-propylphenol and 2-methoxy-4-propylphenol into 1-(4'-hydroxyphenyl)ethanol, 1-(4'-hydroxyphenyl)propanol, and 1-(4'-hydroxy-3'-methoxyphenyl)propanol, respectively, with an *ee* of 94% for the R-enantiomer. The stereochemical outcome of the reactions was established by comparing the chiral GC retention times of the products to those of chiral alcohols obtained by the action of the lipases from *Candida antarctica* and *Pseudomonas cepacia*. Isotope labeling experiments revealed that the oxygen atom incorporated into the alcoholic products is derived from water. During the VAO-mediated conversion of 4-ethylphenol/4-propylphenol, 4-vinylphenol/4-propenylphenol are formed as side products. With 2-methoxy-4-propylphenol as a substrate, this competing side reaction is nearly abolished, resulting in less than 1% of the vinylic product, isoeugenol. The VAO-mediated conversion of 4-alkylphenols also results in small amounts of phenolic ketones indicative for a consecutive oxidation step.

7.1. Introduction

The enantioselective oxidation of aromatic compounds for the production of chiral synthons and other fine chemicals by various kinds of biocatalysts has received much attention during the last years (Crosby, 1991; Stinson, 1995; Zaks and Dodds, 1995). Relatively little is known about the enzymatic enantioselective hydroxylation of prochiral alkylphenols. It has been well established that certain bacterial flavocytochromes catalyze the oxygen-independent asymmetric synthesis of 1-(4'-hydroxyphenyl)alkanols from 4-alkylphenols (McIntire et al., 1984; Bossert et al., 1989; Reeve et al., 1989), but their use in biotechnology applications is limited by the need of artificial electron acceptors. Oxidation reactions of 4-alkylphenols by heme-dependent enzymes like cytochrome P450 and horseradish peroxidase have also been reported (Thompson et al., 1989, 1995). However, heme-based oxidations of 4-alkylphenols result in the formation of highly unstable *p*-quinone methides, leading to aspecific polymers as the main products.

Recently, we described a novel flavoprotein from *Penicillium simplicissimum* acting on aromatic compounds which uses oxygen as mild reoxidant and is relatively stable (van Berkel et al., 1994, Fraaije et al., 1995). This enzyme, referred to as vanillyl-alcohol oxidase (VAO), is a homooctamer of 520 kDa with each subunit containing 8α -(*N*³-histidyl)FAD as a covalently bound prosthetic group (de Jong et al., 1992). Besides oxidizing vanillyl alcohol to vanillin, VAO is also able to hydroxylate, deaminate, and demethylate a variety of phenolic compounds (Fraaije et al., 1995).

The reaction mechanism of flavoprotein-mediated hydroxylation of 4-alkylphenols has been studied to some extent. The hydroxylation of 4-ethylphenol by the bacterial flavocytochrome *p*-cresol methylhydroxylase (PCMH) from *Pseudomonas putida* has been proposed to involve the initial formation of an enzyme-bound *p*-quinone methide product intermediate (Hopper, 1976; McIntire and Bohmont, 1987). Addition of water then results in the formation of 1-(4'-hydroxyphenyl)ethanol (Hopper, 1978). A similar reaction mechanism has been proposed for the VAO-catalyzed conversion of 4-allylphenols and is supported by the observation that the competitive inhibitor isoeugenol binds in its deprotonated form (Fraaije et al., 1995). Formation of the *p*-quinone methide is followed by an enzyme mediated addition of water to the electrophilic methide moiety. Recently, we obtained from rapid reaction studies the first spectral evidence for the formation of *p*-quinone methide intermediates in VAO catalyzed reactions (Fraaije and van Berkel, 1997).

In this report we focus on the stereochemistry of the VAO-mediated hydroxylation of 4-alkylphenols. It is demonstrated that VAO is very enantioselective in the hydroxylation of 4-ethylphenol, 4-propylphenol and 2-methoxy-4-propylphenol. Furthermore, as 4-vinylphenols are well-known flavour compounds (Edlin et al., 1995), attention was paid to the accumulation of these side products as well.

7.2. Materials and methods

GC analysis was performed on a Fisons 8160 gas chromatograph equipped with a FID ($T = 260\text{ }^{\circ}\text{C}$). The chiral column used was a 30 m β -Dex fused silica capillary column (0.25 mm internal diameter; film thickness 0.25 μm), having permethylated β -cyclodextrin as the chiral stationary phase. H_2 was used as carrier gas; flow = 0.7 ml min^{-1} . The initial temperature was 80 $^{\circ}\text{C}$. After sample injection, the temperature was raised 7 $^{\circ}\text{C min}^{-1}$ up to 150 $^{\circ}\text{C}$ (130 $^{\circ}\text{C}$ for (R,S)-1-(4'-hydroxy-3'-methoxyphenyl)propanol), which was held until all products were detected.

GC/MS experiments were performed on a Hewlett Packard (HP) 5890 gas chromatograph with a 30 m DB-17 column and a HP 5970 MSD. The initial temperature was 80 $^{\circ}\text{C}$. After injection, the temperature was raised 7 $^{\circ}\text{C min}^{-1}$ up to 240 $^{\circ}\text{C}$. Mass spectrum of 4-vinylphenol, m/z (rel. abundance): 120 (M^+ , 100), 119 (24), 91 (49), 65 (23), 39 (20). Mass spectrum of 4-propenylphenol, m/z (rel. abundance): 134 (M^+ , 100), 133 (85), 107 (37), 105 (48), 91 (22), 79 (21), 77 (38), 51 (25), 39 (29).

HPLC analysis was performed on a Spark Holland instrument with the use of a Gynkotek M480 pump and an Applied Biosystems 759A doublebeam UV/vis detector. The column used was an S5-ODS 2 (250 mm \times 4.6 mm). The solvent used was methanol/water (1:1) at a flow rate of 0.9 ml min^{-1} . Aromatic compounds were detected at 276 nm. The integrator used was an HP 3395.

^1H NMR spectra were recorded on a Bruker AC-200 (200 MHz) spectrometer. Samples were dissolved either in pyridine- d_5 or CDCl_3 (with TMS as internal standard). Optical rotation was measured on a Perkin-Elmer 241 polarimeter. Elemental analysis was carried out on a Carlo Erba elemental analyser 1106.

Chemicals

4-Hydroxyacetophenone, imidazole and vanillin were products of Janssen Chimica; 4-ethylphenol, 4-propylphenol, *tert*-butyldimethylsilyl chloride (TBDMSCl), 2-methoxy-4-propylphenol, and H_2^{18}O were obtained from Aldrich. Ethyl bromide was obtained from Merck. 4-Vinylphenol was purchased from Lancaster. Tetrabutylammonium fluoride (TBAF) (1 M in tetrahydrofuran) was from Acros. All solvents used were distilled before use.

(R,S)-1-(4'-hydroxyphenyl)ethanol

To a stirred solution of 3.4 g (0.025 mol) of *p*-hydroxyacetophenone in 50 ml of methanol was added a solution of sodium borohydride (0.57 g, 0.015 mol of NaBH_4 in 10 ml of 0.2 M NaOH) at a rate of 0.5 ml min^{-1} , with occasional cooling to keep the temperature at 18–25 $^{\circ}\text{C}$. The reaction was followed by TLC with chloroform/methanol

(20:1) as eluent. When the reaction was complete, most of the methanol was removed by evaporation and the residue was diluted with 100 ml of water. The mixture was extracted with ether, after which the ether layer was washed with water and dried over magnesium sulphate. The ether was removed by evaporation, yielding a mixture of (R,S)-1-(4'-hydroxyphenyl)ethanol and residual 4-hydroxyacetophenone. 4-Hydroxyacetophenone was removed by washing with chloroform, yielding 300 mg of pure (R,S)-1-(4'-hydroxyphenyl)ethanol.

Mp 130.6-131 °C (mp 132-133 °C for R/S mixture; McIntire et al., 1984); ^1H NMR (d_5 -pyridine) δ_{H} (ppm): 1.67 (d, 3H, -CH₃), 5.16 (q, 1H, CH), 7.23 and 7.57 (2 x d, 4H, Ar-H). Mass spectrum, m/z (rel. abundance): 138 (M⁺, 26), 123 (100), 95 (76), 77 (56), 65 (23), 43 (41), 39 (28); HRMS calcd for C₆H₁₀O₂ m/z 138.0681, found m/z 138.0681. Elemental anal. calcd for C₈H₁₀O₂: C, 69.54; H, 7.30. Found: C, 69.81; H, 7.42. These values are all in accordance with the values reported by Everhart and Craig (1991).

(R,S)-1-(4'-hydroxyphenyl)propanol

To a stirred solution of 3.75 g (0.025 mol) of 4-hydroxypropiophenone in 50 ml of methanol was added a solution of sodium borohydride (0.57 g, 0.015 mol of NaBH₄ in 10 ml of 0.2 M NaOH) at a rate of 0.5 ml min⁻¹, with occasional cooling to keep the temperature at 18-25 °C. The next steps in the synthesis were the same as for the synthesis of (R,S)-1-(4'-hydroxyphenyl)ethanol. In the final step, the product was purified by silica column chromatography yielding 1.2 g of pure (R,S)-1-(4'-hydroxyphenyl)propanol.

^1H NMR (CDCl₃) δ_{H} (ppm): 0.90 (t, 3H, CH₃), 1.73-1.80 (m, 2H, CH₂), 4.55 (t, 1H, CH), 6.77 and 7.14 (2 x d, 4H, Ar-H). Mass spectrum, m/z (rel. abundance): 152 (M⁺, 10), 123 (100), 95 (51), 77 (41), 39 (16).

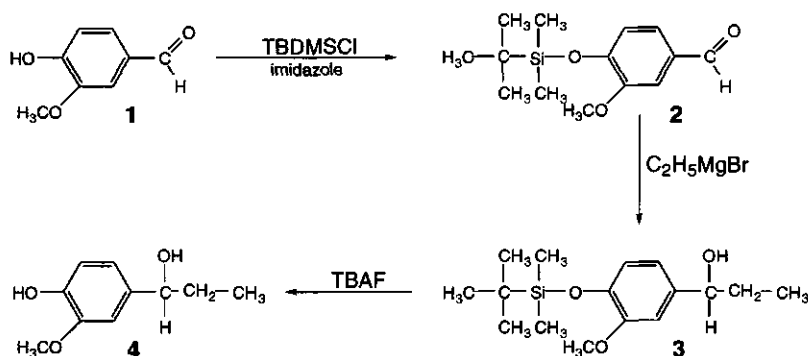


Figure 1. Scheme for the synthesis of 1-(4'-hydroxy-3'-methoxyphenyl)propanol.

(R,S)-1-(4'-hydroxy-3'-methoxyphenyl)propanol (Fig. 1)

4-[(1-*tert*-butyl-1,1-dimethylsilyloxy]-3-methoxybenzaldehyde (**2**): To a stirred solution of 2 g (13.2 mmol) 4-hydroxy-3-methoxybenzaldehyde (**1**) in 20 ml of DMF were added 1.79 g (26.4 mmol) of imidazole and 2.38 g (15.8 mmol) of TBDMSCl. The mixture was stirred at room temperature under a nitrogen atmosphere for 40 h and then poured into 80 ml of water. The mixture was extracted twice with 100 ml of petroleum ether (bp 40-60 °C), which was subsequently washed with 100 ml of brine, dried over MgSO₄, and evaporated, yielding 3.75 g of **2** as a yellow oil which was used for the Grignard reaction without further purification.

¹H NMR (CDCl₃) δ_H (ppm): 0.21 (s, 6H, Si-CH₃), 1.03 (s, 9H, C₄H₉), 3.89 (s, 3H, OCH₃) 6.95-7.41 (m, 3H, Ar-H), 9.86 (s, 1H, CHO). Mass spectrum, *m/z* (relative intensity): 209 (M⁺-C₄H₉, 81), 195 (18), 194 (100), 193 (44), 59 (23), 57 (17), 41 (29), 29 (31).

1-[4-[(1-*tert*-butyl-1,1-dimethylsilyloxy]-3-methoxyphenyl]propanol (**3**): In a three-necked flask equipped with a reflux condenser, dropping funnel, and a stirrer, was placed 0.36 g of magnesium turnings. To this was added anhydrous ether (dried over sodium) until all the magnesium turnings were covered. The whole setup was under a nitrogen atmosphere. A small crystal of I₂ was added, after which a few drops of ethyl bromide were added until the reaction started. Hereafter, 1.64 g of ethyl bromide in 20 ml of anhydrous ether was dropped to the stirred solution as rapidly as the refluxing of the ether allowed. When all the ethyl bromide was added, the reaction was stirred for another hour.

A solution of 3.5 g of **2** in 20 ml of anhydrous ether was dropped to the stirred Grignard reagent. When all of **2** was added, the reaction mixture was heated (with gentle boiling) for another hour. The reaction mixture was poured into a solution of 10 g of NH₄Cl in 120 ml of crushed ice. The resulting mixture was extracted twice with 150 ml of ether and washed with 100 ml of brine. The ether was evaporated, yielding 3.03 g of **3** as a yellow oil which was used without further purification.

¹H NMR (CDCl₃) δ_H (ppm): 0.17 (s, 6H, Si-CH₃), 0.92 (t, 3H, CH₃), 1.02 (s, 9H, C₄H₉), 1.78-1.86 (m, 2H, CH₂), 3.89 (s, 3H, OCH₃), 4.55 (t, 1H, CH), 6.73-6.88 (m, 3H, Ar-H). Mass spectrum, *m/z* (relative intensity): 239 (M⁺-C₄H₉, 61), 195 (100), 167 (22), 75 (18), 73 (30), 59 (21), 57 (25), 41 (21), 29 (31).

(R,S)-1-(4'-hydroxy-3'-methoxyphenyl)propanol (**4**): To a stirred solution of 2.0 g **3** in 40 ml of dry DMF was added 16 ml of TBAF (1M in tetrahydrofuran). The reaction mixture was stirred at room temperature until the reaction was complete (90 min). The resulting green mixture was poured into 50 ml of water and extracted twice with 100 ml of ether. The ether was washed with brine, dried over Na₂SO₄, and evaporated. Purification

of the reaction product by silica column chromatography (eluent: 5% MeOH in CHCl₃) gave 0.46 g (20%) of (R,S)-1-(4'-hydroxy-3'-methoxyphenyl)propanol.

¹H NMR (CDCl₃) δ_H (ppm): 0.91 (t, 3H, CH₃), 1.73-1.87 (m, 2H, CH₂), 3.89 (s, 3H, OCH₃), 4.55 (t, 1H, CH), 6.77-6.90 (m, 3H, Ar-H). Mass spectrum, *m/z* (relative intensity): 182 (M⁺, 23), 153 (92), 125 (38), 93 (100), 65 (52), 53 (16), 39 (19), 29 (33), 27 (28); HRMS calcd for C₈H₁₄O₃ *m/z* 182.0943, found *m/z* 182.0943.

Enzymes

Vanillyl-alcohol oxidase (EC 1.1.3.7) was purified from *P. simplicissimum* (Oudem.) Thom. CBS 170.90 (ATCC 90172) as described by Fraaije et al. (1995). Lipase (EC 3.1.1.3) from *Pseudomonas cepacia* was a gift from Biocatalysts Ltd. (Pontypridd, UK). Lipase from *Candida rugosa* was purchased from Sigma, and lipase B from *Candida antarctica* was a generous gift from Boehringer (Mannheim, Germany).

Enzyme kinetics

VAO activity was measured at pH 10.0 by spectrophotometrically recording the formation of aromatic product at 260 nm (to determine *K_m* values) and by following oxygen consumption using a Clark electrode (to determine *k_{cat}* values) (Fraaije et al., 1995).

Enzymatic conversion of 4-alkylphenols

The reaction mixture containing 1.0 mM 4-ethylphenol in 50 mM glycine/NaOH buffer pH 10.0, and 0.05 U of VAO in 2 ml was incubated for 3 h at 30 °C. Product samples were prepared by extraction of the reaction mixture with two times 1.0 ml of ether. After evaporation, the products were dissolved in 10 µl of methanol and analyzed using GC and GC/MS. For larger scale accumulation of the alcohol product formed after the enzymatic conversion of 4-ethylphenol, 15 mg of 4-ethylphenol and 100 µg of VAO in 50 ml of 50 mM glycine/NaOH (pH 10.0) was incubated at 30 °C. Samples of 0.5 ml were extracted with 1 ml of ether and analyzed by HPLC. When all 4-ethylphenol was consumed, another 15 mg of 4-ethylphenol was added. Further additions of 4-ethylphenol were made to a total of 100 mg. Isolation of the products was done essentially according to Reeve et al. (1990). The reaction mixture was extracted two times with 100 ml of ether, dried over Na₂SO₄, and evaporated. The solid obtained was washed with 20 ml of light petroleum (bp 40-60 °C) to remove 4-ethylphenol and 4-vinylphenol and with 20 ml of chloroform to remove 4-hydroxyacetophenone, yielding 33.2 mg (28%) of 1-(4'-hydroxyphenyl)ethanol. The conditions for the enzymatic conversion of 4-propylphenol and 2-methoxy-4-propylphenol were the same as for the oxidation of 4-ethylphenol. A large scale conversion was also performed for 2-methoxy-4-propylphenol. After extraction, the alcohol product was purified by column chromatography (eluent: 5%

MeOH in CHCl_3), yielding 52 mg (45%) of 1-(4'-hydroxy-3'-methoxyphenyl)propanol as a yellow oil.

For ^{18}O incorporation experiments, 0.5 ml samples of 1.0 mM 4-ethylphenol were freeze-dried and resuspended in 0.5 ml of 33% w/w H_2^{18}O . After addition of vanillyl-alcohol oxidase (100 μg) the samples were incubated for 3 h at 25 °C. Hereafter, the samples were extracted twice with 0.5 ml of ether, evaporated, and analyzed by GC/MS.

Establishment of the absolute configurations of chiral products

The absolute configurations of the hydroxyalkylphenols produced by VAO were determined using a chiral GC column in combination with the well-established stereoselectivity of the lipases from *P. cepacia* and *C. antarctica*, essentially according to the procedure of Reeve et al. (1990). A typical experiment is described below.

Racemic 1-(4'-hydroxyphenyl)ethanol was injected on a β -cyclodextrin chiral GC column. The enantiomers were well separated, giving peaks at 49.3 and 51.2 min. Subsequently, this alcohol was enzymatically esterified with vinyl acetate. Racemic 1-(4'-hydroxyphenyl)ethanol (40 mg) was dissolved in 2 ml of freshly distilled vinyl acetate and 100 mg of lipase from *P. cepacia* was added. The mixture was incubated at 28 °C. At regular time intervals, the lipase was removed by centrifugation and the supernatant was analyzed on the chiral column. During the first 50 h of the reaction, the peak at 49.3 min decreased whereas the area of the peak at 51.2 min remained unchanged. Earlier studies of *P. cepacia* lipase have revealed that it very selectively reacts with secondary alcohols having the 3D-structure as shown below in Fig. 2 (Kazlauskas et al., 1991; Cygler et al., 1994). This means in our case that the lipase preferably reacts with the R-alcohol, leaving the S-alcohol unchanged. From these results, we could assign the R-structure to the peak at 49.3 min and the S-configuration to the peak at 51.2 min. Injection of the product obtained by VAO-mediated hydroxylation of 4-ethylphenol on the chiral GC column under the same conditions showed a large peak at 49.3 min and a very small one at 51.2 min, which leads to the conclusion that VAO produces R-1-(4'-hydroxyphenyl)ethanol with 94% *ee*.

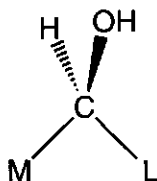


Figure 2. Stereochemical preference of *P. cepacia* lipase toward secondary alcohols. 'L' represents a large substituent; 'M' represents a medium-sized substituent.

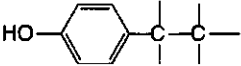
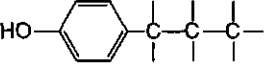
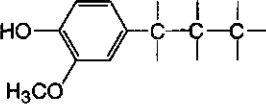
An identical experiment with racemic 1-(4'-hydroxyphenyl)propanol and *P. cepacia* lipase gave peaks at 61.2 and 62.5 min; the peak at 61.2 min decreased during incubation with the lipase and vinyl acetate. The main product of the reaction of 4-propylphenol with VAO displayed a peak at 61.2 min, which means that VAO produces R-1-(4'-hydroxyphenyl)propanol (94% *ee*).

Since both *P. cepacia* and *C. rugosa* lipase were unreactive toward 1-(4'-hydroxy-3'-methoxyphenyl)propanol, the lipase of *Candida antarctica* was used. This enzyme is also very stereoselective toward secondary alcohols and has the same stereochemical preference as the other two lipases according to literature (Uppenberg et al., 1995). Indeed, in our hands *C. antarctica* lipase displayed the same stereochemical preference for 1-(4'-hydroxyphenyl)ethanol as *P. cepacia* lipase, i.e. the peak of the R-isomer decreased during incubation with the lipase and vinyl acetate. Racemic 1-(4'-hydroxy-3'-methoxyphenyl)propanol gave peaks at 139.7 and 144.6 min; *C. antarctica* lipase-mediated esterification in vinyl acetate resulted in a decrease of the peak at 139.7 min while the area of the peak at 144.6 min remained unchanged. Incubation of VAO with 2-methoxy-4-propylphenol gave a large peak at 139.7 min and a small one at 144.6 min, so VAO produces R-1-(4'-hydroxy-3'-methoxyphenyl)propanol (94% *ee*).

7.3. Results

Steady-state kinetics were performed in order to determine the catalytic efficiency of VAO with 4-alkylphenols. The kinetic parameters for 4-ethylphenol, 4-propylphenol, and 2-methoxy-4-propylphenol (Table 1) were in the same range as reported for other VAO substrates (Fraaije et al., 1995).

Table 1. Kinetic parameters for the conversion of 4-alkylphenols by vanillyl-alcohol oxidase from *P. simplicissimum* (pH 10.0, 25 °C).

substrate		k_{cat}	K_{m}
		s^{-1}	μM
4-ethylphenol		2.7	7
4-propylphenol		3.9	3
2-methoxy-4-propylphenol		4.8	<10

HPLC analysis showed that two major products are formed during the enzymatic oxidation of 4-ethylphenol. GC/MS and ^1H NMR analysis revealed that one of these major products is 1-(4'-hydroxyphenyl)ethanol (78%). The other major product was 4-vinylphenol (18%) according to GC/MS analysis. The vinylic product was not formed by autocatalysis as prolonged incubation of either 4-ethylphenol or 1-(4'-hydroxyphenyl)ethanol in the absence of VAO did not result in the formation of 4-vinylphenol. Conversion of 4-ethylphenol also resulted in some formation of 4-hydroxyacetophenone (4%) indicative of some subsequent VAO-mediated oxidation of the formed alcohol.

Similar results as with 4-ethylphenol were obtained for the VAO-catalyzed conversion of 4-propylphenol. This reaction resulted in the formation of 1-(4'-hydroxyphenyl)propanol (78%), 4-propenylphenol (18%), and 1-(4'-hydroxyphenyl)propanone (4%). HPLC, GC/MS, and ^1H NMR analysis revealed that 2-methoxy-4-propylphenol was mainly converted by VAO into 1-(4'-hydroxy-3'-methoxyphenyl)propanol. In contrast to the above-mentioned reactions, only minor amounts (< 1%) of the unsaturated product, isoeugenol, and 1-(4'-hydroxy-3'-methoxyphenyl)propanone were formed in this case.

In order to identify the origin of the oxygen atom incorporated in the alcohol product, conversion of 4-ethylphenol by VAO was performed in H_2^{18}O -enriched buffer. The mass spectrum of 1-(4'-hydroxyphenyl)ethanol, isolated from the reaction mixture enriched with H_2^{18}O , resulted in an additional ion at m/z 140 (= $\text{M}^+ + 2$) (Fig. 3). This indicates that the incorporated oxygen atom is derived from water. The labeled alcohol represented 34% of the total amount of alcohol product, which is in good agreement with the 33% enrichment of H_2^{18}O in the reaction mixture.

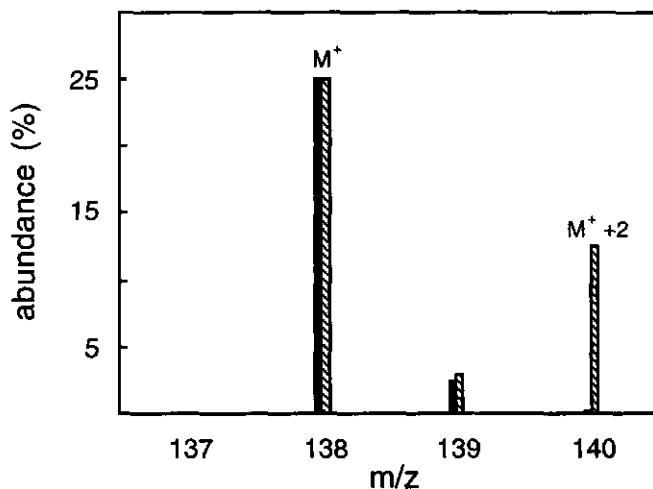


Figure 3. Mass spectra (M^+ -peak) of 1-(4'-hydroxyphenyl)ethanol obtained after incubation of 4-ethylphenol with VAO in the absence (solid bars) or presence (striped bars) of H_2^{18}O .

The absolute configuration of the chiral alcohols formed during the VAO-mediated conversion of 4-alkylphenols was determined using a chiral GC-column and lipase from *P. cepacia* and *C. antarctica*. These lipases specifically esterify the R-isomer of secondary alcohols (see Reeve et al., 1990, and Kazlauskas et al., 1991, for *P. cepacia* lipase and Uppenberg et al., 1995, for *C. antarctica* lipase). This procedure revealed that hydroxylation of 4-ethylphenol occurs enantioselectively, giving the (R)-isomer with an *ee* of 94%. Optical purity analysis of purified 1-(4'-hydroxyphenyl)ethanol ($[\alpha]_{D}^{20} = +40.1^\circ$) resulted in an *ee* of 82% (Everhart and Craig, 1991). ^1H NMR revealed that this apparent lower *ee* resulted from the presence of some 4-hydroxyacetophenone. The positive optical rotation is in accordance with the optical rotation measured by Reeve et al. (1990) and Everhart and Craig (1991), confirming that (R)-1-(4'-hydroxyphenyl)ethanol is the main product formed from 4-ethylphenol. Furthermore, the melting point of the purified alcohol (148-151 °C) again confirmed enantioselective hydroxylation (mp for one enantiomer, 157 °C (Everhart and Craig, 1991); mp for R/S mixture, 130.6-131 °C (see Materials and Methods)).

Stereochemical analysis of the 4-hydroxybenzylic alcohols formed from 4-propylphenol and 2-methoxy-4-propylphenol again revealed a 94% *ee* in favour of the R-isomer. Lipase treatment showed that VAO predominantly hydroxylates 4-propylphenol to the R-enantiomer of 1-(4'-hydroxyphenyl)propanol.

7.4. Discussion

This paper reports on the asymmetric synthesis of optically active short-chain 1-(4'-hydroxyphenyl)alkanols by the covalent flavoprotein vanillyl-alcohol oxidase from *P. simplicissimum*. Hydroxylation of 4-ethylphenol resulted in the enantioselective formation of (R)-1-(4'-hydroxyphenyl)ethanol with an *ee* of 94%. For the hydroxylation of 4-propylphenol and 2-methoxy-4-propylphenol also an *ee* of 94% for the R-isomer was found. Previous studies have shown that the bacterial flavocytochromes PCMH (McIntire and Bohmont, 1987) and 4-ethylphenol methylenehydroxylase (EPMH) (Reeve et al., 1990), both isolated from *P. putida* strains, also enantioselectively hydroxylate 4-ethylphenol. In case of PCMH, (S)-1-(4'-hydroxyphenyl)ethanol was formed with an *ee* of 31.2% when phenazine methosulphate was used as electron acceptor (McIntire et al., 1984), whereas an *ee* of 94% for the S-isomer was found with cytochrome *c* as electron acceptor (McIntire and Bohmont, 1987). On the other hand, more similar with VAO, EPMH catalyzes the hydroxylation of 4-ethylphenol into (R)-1-(4'-hydroxyphenyl)ethanol with an *ee* of 98% (Reeve et al., 1990). However, no data have been reported for the enantioselectivity of the bacterial flavocytochromes with 4-propylphenols.

Using H_2^{18}O it was found that in the VAO-catalyzed reactions, the oxygen atom introduced in the alcohol product originates from water. This is in line with the reaction mechanism postulated for the VAO-mediated conversion of 4-(methoxymethyl)phenol (Fraaije and van Berkel, 1997), involving the initial formation of a *p*-quinone methide product intermediate. As the addition of water to the *p*-quinone methide is enzyme-mediated (Fraaije and van Berkel, 1997), it is apparent that the reaction with prochiral 4-alkylphenols results in optical active products (Fig. 4).

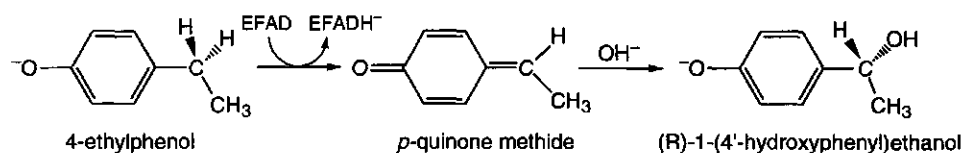


Figure 4. Proposed mechanism for the hydroxylation of 4-ethylphenol by vanillyl-alcohol oxidase (EFAD, oxidized enzyme; EFADH⁻, reduced enzyme).

During the VAO-catalyzed conversion of 4-alkylphenols, 4-vinyl phenols are formed as side products (Fig. 5). McIntire and Bohmont (1987) have suggested that the formation of these unsaturated compounds might result from the rearrangement of the *p*-quinone methide intermediate. Interestingly, almost no isoeugenol was formed in the VAO-mediated conversion of 2-methoxy-4-propylphenol. This shows that introduction of substituents in the substrate aromatic ring may influence the absolute yield of chiral product formed. Rapid reaction studies have indicated that the electrophilic *p*-quinone methide product intermediates become stabilized in the active site of the reduced enzyme to a different extent, depending on the substrate, and that nucleophilic attack by water to these intermediates only occurs after flavin reoxidation (Fraaije et al., 1997). This suggests that the differences in the extent of formation of unsaturated products from 4-propylphenol and 2-methoxy-4-propylphenol result from subtle changes in susceptibility of the corresponding *p*-quinone methide intermediates toward rearrangement in the active site of the reduced enzyme.

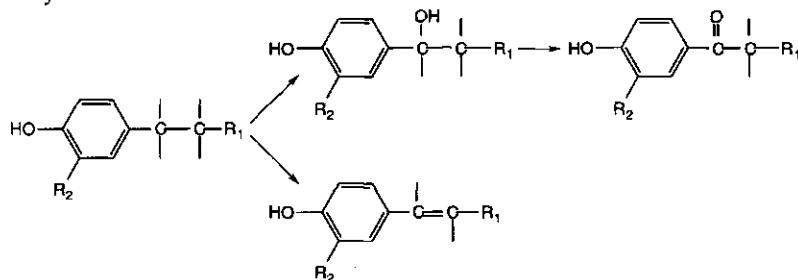


Figure 5. Reaction pathway for the conversion of short-chain 4-alkylphenols catalyzed by VAO (4-ethylphenol, $\text{R}_1, \text{R}_2 = \text{H}$; 4-propylphenol, $\text{R}_1 = \text{CH}_3$, $\text{R}_2 = \text{H}$; 2-methoxy-4-propylphenol, $\text{R}_1 = \text{CH}_3$, $\text{R}_2 = \text{OCH}_3$).

VAO oxidizes 4-hydroxybenzylalcohols and catecholamines to the corresponding aldehydes or ketones (Fraaije et al., 1995). However, during the conversion of 4-alkylphenols, VAO produces only limited amounts of 4-hydroxyacetophenones. The inefficient formation of these compounds may be caused by the relatively weak binding of the 1-(4'-hydroxyphenyl)alkanols and the fact that the vinylic side products act as strong competitive inhibitors (Fraaije et al., 1995). A similar inhibition by 4-vinylphenol was reported in case of PCMH (McIntire and Bohmont, 1987). Because nearly no isoeugenol is formed from 2-methoxy-4-propylphenol, another likely explanation for the low yield of 4-hydroxyacetophenones is that VAO may be enantioselective in oxidizing preferably the S-isomers of 1-(4'-hydroxyphenyl)alkanols, while the R-isomers are predominantly formed.

Recently, the crystal structure of VAO has been determined in the native state and in complex with several inhibitors (Mattevi et al., 1997). These studies clearly established that the structure of the VAO subunit closely resembles that of the flavoprotein subunit of PCMH (Mathews et al., 1991). The crystal structure has provided a rationale for the poor reactivity of VAO toward 4-methylphenol (Fraaije et al., 1997), the physiological substrate of PCMH. Upon binding of 4-methylphenol, a covalent adduct is formed between the substrate and the reduced flavin which is rather stable under aerobic conditions (Mattevi et al., 1997). Steric constraints imposed by the shape of the active-site cavity most likely prevent such an adduct formation with more bulkier 4-alkylphenols, which is consistent with the present results.

In summary, this study strongly supports an earlier conclusion (Fraaije et al., 1995) that the reaction mechanism of VAO is similar to PCMH and EPMH. However, several marked differences exist between the catalytic properties of the bacterial flavocytochromes and VAO. These differences include the substrate specificity and the nature of the electron acceptor involved in flavin reoxidation. In view of potential biotechnological applications, it should be stressed that, opposite to the flavocytochromes, VAO does not need an artificial electron acceptor for flavin reoxidation but uses dioxygen instead. Therefore, like glucose oxidase (Wilson and Turner, 1992) and D-amino acid oxidase (Butò et al., 1994), VAO can be classed among an emerging group of flavoprotein oxidases that catalyze transformations of industrial relevance.

7.5. References

- Bossert, I.D., Whited, G., Gibson, D.T., Young, L.Y. (1989) Anaerobic oxidation of *p*-cresol mediated by a partially purified methylhydroxylase from a denitrifying bacterium. *J. Bacteriol.* **171**, 2956-2962.
- Butò, S., Pollegioni, L., D'Angurio, L., Pilone, M.S. (1994) Evaluation of D-amino acid oxidase from *Rhodotorula gracilis* for the production of α -keto acids: A reactor system. *Biotechnol. Bioeng.* **44**, 1288-1294.

- Crosby, J. (1991) Synthesis of optically active compounds: a large scale perspective. *Tetrahedron* **47**, 4789-4841.
- Cyglter, M., Grochulski, P., Kazlauskas, R.J., Schrag, J.D., Bouthiller, F., Rubin, B., Serreqi, A.N., Gupta, A.K. (1994) A structural basis for the chiral preference of lipases. *J. Am. Chem. Soc.* **116**, 3180-3186.
- De Jong, E., van Berkel, W.J.H., van der Zwan, R.P., de Bont, J.A.M. (1992) Purification and characterization of vanillyl-alcohol oxidase from *Penicillium simplicissimum*. *Eur. J. Biochem.* **208**, 651-657.
- Edlin, D.A.N., Narbad, A., Dickinson, J.R., Lloyd, D. (1995) The biotransformation of simple phenolic compounds by *Brettanomyces anomalus*. *FEMS Microbiol. Lett.* **125**, 311-316.
- Everhart, E.T., Craig, J.C. (1991) A facile general route to enantiomeric 1-(4'-hydroxyphenyl)alkanols, and an improved synthesis of 4-vinylphenol. *J. Chem. Soc. Perkin Trans. 1*, 1701-1707.
- Fraaije, M.W., Veeger, C., van Berkel, W.J.H. (1995) Substrate specificity of flavin-dependent vanillyl alcohol oxidase from *Penicillium simplicissimum*. *Eur. J. Biochem.* **234**, 271-277.
- Fraaije, M.W., Drijfhout, F.P., Meulenbelt, G., van Berkel, W.J.H., Mattevi, A. (1997) Vanillyl-alcohol oxidase from *Penicillium simplicissimum*: Reactivity with *p*-cresol and preliminary structural analysis, pp. 261-264. In: K. Stevenson, V. Massey, and Ch. Williams, Jr. (eds.), *Flavins and Flavoproteins XII*, University Press, Calgary, Canada.
- Fraaije, M.W., van Berkel, W.J.H. (1997) Catalytic mechanism of the oxidative demethylation of 4-(methoxymethyl)phenol by vanillyl-alcohol oxidase. *J. Biol. Chem.* **272**, 18111-18116.
- Hopper, D.J. (1976) The hydroxylation of *p*-cresol and its conversion to *p*-hydroxybenzaldehyde in *Pseudomonas putida*. *Biochem. Biophys. Res. Commun.* **69**, 462-468.
- Hopper, D.J. (1978) Incorporation of [¹⁸O]water in the formation of *p*-hydroxybenzyl alcohol by the *p*-cresol methylhydroxylase from *Pseudomonas putida*. *Biochem. J.* **175**, 345-347.
- Kazlauskas, R.J., Weissflog, A.N.E., Rappaport, A.T., Cuccia, L.A. (1991) A rule to predict which enantiomer of a secondary alcohol reacts faster in reactions catalyzed by cholesterol esterase, lipase from *Pseudomonas cepacia* and lipase from *Candida rugosa*. *J. Org. Chem.* **56**, 2656-2665.
- Mattevi, A., Fraaije, M.W., Mozarelli, A., Olivi, L., Coda, A., van Berkel, W.J.H. (1997) Crystal structures and inhibitor binding in the octameric flavoenzyme vanillyl-alcohol oxidase: the shape of the active-site cavity controls substrate specificity. *Structure* **5**, 907-920.
- Mathews, F.S., Chen, Z.-W., Bellamy, H.D., McIntire, W.S. (1991) Three-dimensional structure of *p*-cresol methylhydroxylase (flavocytochrome *c*) from *Pseudomonas putida* at 3.0 Å resolution. *Biochemistry* **30**, 238-247.
- McIntire, W.S., Hopper, D.J., Craig, J.C., Everhart, E.T., Webster, R.V., Causer, M.J., Singer, T.P. (1984) Stereochemistry of 1-(4'-hydroxyphenyl)ethanol produced by hydroxylation of 4-ethylphenol by *p*-cresol methylhydroxylase. *Biochem. J.* **224**, 617-621.
- McIntire, W.S., Bohmont, C. (1987) The chemical and stereochemical course of oxidation of 4-ethylphenol and other 4-alkylphenols by *p*-cresol methylhydroxylase, pp. 677-686. In: D.E. Edmondson and D.B. McCormick (eds.), *Flavins and Flavoproteins IX*, W. de Gruyter, Berlin.
- Reeve, C.D., Carver, M.A., Hopper, D.J. (1989) The purification and characterization of 4-ethylphenol methylhydroxylase, a flavoprotein from *Pseudomonas putida* JD1. *Biochem. J.* **263**, 431-437.
- Reeve, C.D., Carver, M.A., Hopper, D.J. (1990) Stereochemical aspects of the oxidation of 4-ethylphenol by the bacterial enzyme 4-ethylphenol methylenehydroxylase. *Biochem. J.* **269**, 815-819.
- Stinson, S.C. (1995) Chiral drugs. *Chem. Eng. News* **73**, 44-74.
- Thompson, D., Norbeck, K., Olsson, L.-I., Despina, C.-T., Van Der Zee, J., Moldéus, P. (1989) Peroxidase-catalyzed oxidation of eugenol: Formation of a cytotoxic metabolite(s). *J. Biol. Chem.* **264**, 1016-1021.
- Thompson, D.C., Perera, K., London, R. (1995) Quinone methide formation from *para* isomers of methylphenol (cresol), ethylphenol, and isopropylphenol: relationship to toxicity. *Chem. Res. Toxicol.* **8**, 55-60.
- Uppenberg, J., Öhrner, N., Norin, M., Hult, K., Kleywegt, G.J., Patkar, S., Waagen, V., Anthonsen, T., Jones, T.A. (1995) Crystallographic and molecular-modeling studies of lipase B from *Candida antarctica* reveal a stereospecificity pocket for secondary alcohols. *Biochemistry* **34**, 16838-16851.
- van Berkel, W.J.H., Fraaije, M.W., de Jong, E., de Bont, J.A.M. (1994) Vanillyl-alcohol oxidase from *Penicillium simplicissimum*: A novel flavoprotein containing 8 α -(N³-histidyl)-FAD, pp. 799-802. In: K. Yagi (ed.), *Flavins and Flavoproteins XI*, W. de Gruyter, Berlin.
- Wilson, R., Turner, A.P.F. (1992) Glucose oxidase: An ideal enzyme. *Biosens. Bioelectr.* **7**, 165-185.
- Zaks, A., Dodds, D.R. (1995) Chloroperoxidase-catalyzed asymmetric oxidations: Substrate specificity and mechanistic study. *J. Am. Chem. Soc.* **117**, 10419-10424.

8

Kinetic mechanism of vanillyl-alcohol oxidase with short-chain 4-alkylphenols

Marco W. Fraaije, Robert H.H. van den Heuvel,
Jules C.A.A. Roelofs and Willem J.H. van Berkel

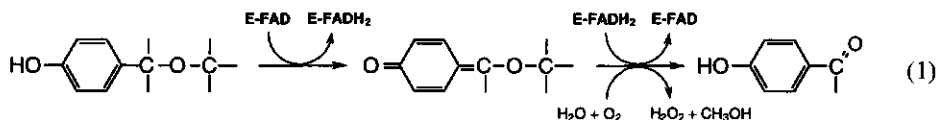
Submitted to *European Journal of Biochemistry*

Abstract

The kinetic mechanism of vanillyl-alcohol oxidase with 4-methylphenol, 4-ethylphenol, 4-propylphenol and their C_α-deuterated analogs has been studied at pH 7.5 and 25°C. Conversion of 4-methylphenol is extremely slow (0.005 s⁻¹) while the enzyme is largely in the reduced form during turnover. 4-Ethylphenol and 4-propylphenol are efficiently converted while the enzyme is mainly in the oxidized form during turnover. The deuterium isotope effect on the rate of turnover ranges from 7 to 10. With all three 4-alkylphenols, flavin reduction appeared to be a reversible process with the rate of reduction being in the same range as the rate for the reverse reaction. During the reductive half-reaction of VAO with 4-ethylphenol and 4-propylphenol, a transient intermediate is formed with an absorbance maximum at 330 nm. This intermediate has been tentatively identified as the *p*-quinone methide of the aromatic substrate in complex with reduced enzyme. It is concluded that VAO catalysis with 4-ethylphenol and 4-propylphenol favors an ordered sequential binding mechanism in which the reduced enzyme-*p*-quinone methide binary complex reacts rapidly with oxygen. With both substrates, the rate of flavin reduction determines the turnover rate. With 4-methylphenol a step involved in the reoxidation of the flavin is rate limiting. From recent crystallographic data (Mattevi, A., Fraaije, M.W., Mozzarelli, A., Olivi, L., Coda, A. & van Berkel, W.J.H. (1997) *Structure* 5, 907-920), it is proposed that this step involves the decomposition of a covalent adduct between 4-methylphenol and flavin N5.

8.1. Introduction

Vanillyl-alcohol oxidase (VAO) is a covalent flavoprotein isolated from *Penicillium simplicissimum*, a filamentous fungus capable of growing on a wide variety of aromatic compounds (De Jong et al, 1990; Fraaije et al., 1997a). The enzyme is a rather stable homooctamer with each 65 kDa subunit containing a 8α -(N^3 -histidyl)-FAD molecule (De Jong et al., 1992; Fraaije et al., 1997b). VAO is active with a wide range of *para*-substituted phenolic compounds (Fraaije et al., 1995), but the physiological function of the enzyme is not fully understood. Based on induction experiments, 4-(methoxymethyl)phenol has been proposed to represent the physiological substrate (Fraaije et al., 1997a). A detailed kinetic study with this phenolic methylether has pointed to a ternary complex mechanism in which flavin reduction is the rate-limiting step in catalysis (Fraaije and van Berkel, 1997c). The reaction of VAO with 4-(methoxymethyl)phenol involves the initial formation of a binary complex of reduced enzyme and the *p*-quinone methide of 4-(methoxymethyl)phenol. This complex then reacts with molecular oxygen, reoxidising the flavin, and after water addition of the *p*-quinone methide, the products 4-hydroxybenzaldehyde and methanol are formed (Equation 1).



The reaction mechanism of VAO has some properties in common with that of *p*-cresol methylhydroxylase (PCMH) (McIntire et al., 1984). This bacterial flavocytochrome converts a wide range of 4-alkylphenols first into 4-hydroxybenzyl alcohols and subsequently into 4-hydroxybenzaldehydes. In contrast to VAO, flavin reoxidation in PCMH involves the transfer of electrons to a tightly bound cytochrome subunit (McIntire et al., 1985).

The crystal structure of VAO has recently been solved at 2.5 Å resolution (Mattevi et al., 1997). Each VAO monomer consists of two domains; one creating a binding site for the ADP moiety of the FAD molecule while the other domain covers the active center which is located between the two domains. The structure shows that the isoalloxazine ring of the flavin makes a covalent bond with His422. Furthermore, the active site is located in the interior of the protein and contains an anion binding pocket facilitating the deprotonation of phenolic substrates. Based on the structures of several VAO-inhibitor complexes it could be invoked that the distance between the C_α -atom of aromatic substrates and the reactive N5 of the isoalloxazine ring is about 3.5 Å. Equally close to the C_α -atom of the inhibitors is the side chain of Asp170, which function is so far unclear. The structure of the VAO monomer

is very similar to that of the flavoprotein subunit of PCMH (McIntire et al., 1991; Kim et al., 1995). Most active site residues are conserved but intriguingly, Asp170 of VAO is replaced by Ser in PCMH (Benen et al., 1997).

The parent substrate of PCMH, 4-methylphenol, is a very poor substrate for VAO (Fraaije et al., 1997d). The crystallographic analysis of VAO has suggested that this might be related to the formation of a covalent adduct between the C α -atom of 4-methylphenol and flavin N5. In view of this, it was of interest to address the kinetic mechanism of VAO with short-chain 4-alkylphenols. In this study, 4-methylphenol, 4-ethylphenol and 4-propylphenol were used as model substrates and the deuterium kinetic isotope effects for the overall and reductive half-reactions were determined. For this purpose, an improved method for the synthesis of C α -deuterated 4-alkylphenols was developed.

8.2. Materials and methods

General

4-Methylphenol, 4-ethylphenol, 4-propylphenol, methyl-4-hydroxybenzoate, 4-hydroxyacetophenone, 4-hydroxypropiophenone, LiAlD $_4$, *t*-butyldimethylsilylchloride, imidazole, D $_2$ O and AlCl $_3$ were from Aldrich. Glucose oxidase (grade II) was from Boehringer. Vanillyl-alcohol oxidase from *P. simplicissimum* (ATCC 90172) was purified as described before (De Jong et al., 1992; Fraaije et al., 1995). VAO concentrations were calculated from the molar absorption coefficient of the oxidized flavin ($\epsilon_{439} = 12.5 \text{ mM}^{-1}\text{cm}^{-1}$ (De Jong et al., 1992)).

Analytical methods

HPLC experiments were performed with a Lichrospher RP8 (4.6×150 mm) reverse phase column, connected to an Applied Biosystems 400 pump and a Waters 996 photodiode-array detector. Products were eluted with a mixture of methanol, water and acetic acid (33:66:1) at 1 ml min $^{-1}$. GC/MS analysis was performed on a Hewlett Packard HP 5973 MSD and HP 6090 GC equipped with a HP-5 column. The initial temperature was 80°C. After injection the temperature was raised 7°C min $^{-1}$ up to 240°C. ^1H NMR spectra were recorded on a Bruker AC-200 (200 MHz) spectrometer. Samples were dissolved either in pyridine- d_5 or CDCl $_3$ containing TMS as internal standard.

Steady-state kinetic experiments were carried out essentially as described earlier (Fraaije et al., 1995). Kinetic experiments were performed at 25°C in 50 mM potassium phosphate buffer, pH 7.5, unless stated otherwise. Oxygen consumption was measured with a Clark electrode (De Jong et al., 1992). Conversion of 4-ethylphenol and 4-propylphenol was followed by the increase of absorbance at 260 nm. Formation of

4-hydroxybenzaldehyde from 4-methylphenol was measured at 340 nm ($\epsilon_{340} = 10.0 \text{ mM}^{-1}\text{cm}^{-1}$). Absorption spectra were recorded at 25 °C on an automated Aminco DW-2000 spectrophotometer.

Stopped-flow kinetic studies were carried out with a Hi-Tech SF-51 apparatus equipped with a Hi-Tech M300 monochromator diode-array detector (Salisbury, England). Spectra were scanned in the 300-550 nm wavelength range with a scan time of 10 ms. Deconvolution analysis of spectral data was performed using the Specfit Global Analysis program version 2.10 (Spectrum Software Ass., Chapel Hill, N.C., U.S.A.). Single wavelength kinetic traces were recorded using a Hi-Tech SU-40 spectrophotometer. All concentrations mentioned concerning stopped-flow experiments are those after mixing. In anaerobic experiments, solutions were flushed with argon and contained glucose (10 mM) and glucose oxidase (0.1 μM) to ensure anaerobic conditions. For enzyme-monitored turnover experiments (Gibson et al., 1984), air-saturated enzyme (5 μM) and substrate (1.0 mM) solutions were mixed in the stopped-flow instrument after which the redox state of the flavin cofactor was recorded at 439 nm.

Synthesis of 4-methylphenol- $\alpha,\alpha,\alpha\text{-d}_3$

4.6 g (0.030 mol) Methyl 4-hydroxybenzoate, 4.0 g (0.060 mol) imidazole and 5.3 g (0.035 mol) *t*-butyldimethylsilylchloride in 120 ml dimethylformamide was stirred under nitrogen for 72 hours. The mixture was subsequently diluted with 200 ml water and extracted with 2 \times 200 ml petroleum ether (bp 40-60°C). The ether layer was washed with water and dried over magnesium sulphate. The ether was removed by evaporation, yielding a yellow oil of methyl-4-([1-*t*-butylsilyl]oxy)-benzoate (yield 96%, $^1\text{H NMR}$ (CDCl_3) δ_{H} (ppm) 0.3 (t, 6H, CH_3), 1.0 (s, 12H, *t*-butyl), 1.6 (s, 3H, CH_3), 6.8 (d, 2H, Ar), 7.0 (d, 2H, Ar). Mass spectrum, m/z (rel. abundance): 266 (M^+ , 10), 235 (6), 209 (100), 135 (29), 91 (15), 73 (8), 59 (13)).

4.0 g (0.015 mol) Methyl 4-([1-*t*-butylsilyl]oxy)-benzoate and 1.6 g (0.012 mol) AlCl_3 in 20 ml ether was dropwise added to a stirred solution containing 4.8 g (0.036 mol) AlCl_3 and 2.0 g (0.048 mol) LiAlD_4 in 180 ml ether. The mixture was refluxed for 70 hours after which some D_2O was added to remove remaining LiAlD_4 . After acidification with H_2SO_4 , the solution was extracted by 2 \times 150 ml ether. The ether was removed by evaporation and in the final step, the deuterated product was purified by silica column chromatography (eluent: dichloromethane/ethyl acetate 4:1) yielding 1.37 g of pure 4-methylphenol- $\alpha,\alpha,\alpha\text{-d}_3$ (pale yellow oil): yield 82%, $^1\text{H NMR}$ (CDCl_3) δ_{H} (ppm) 5.1 (s, 1H, OH), 6.7 (d, 2H, Ar), 7.0 (d, 2H, Ar). Mass spectrum, m/z (rel. abundance): 111 (M^+ , 100), 110 (68), 109 (58), 93 (7), 82 (21), 77 (20), 63 (4), 53 (10)).

Synthesis of 4-ethylphenol- α,α -d₂ and 4-propylphenol- α,α -d₂

4-Ethylphenol- α,α -d₂ and 4-propylphenol- α,α -d₂ were synthesized essentially as described above, starting from 4-hydroxyacetophenone and 4-hydroxypropiophenone, respectively. Pure 4-ethylphenol- α,α -d₂ (1.62 g, yellowish crystals) was obtained with a yield of 87%: ¹H NMR (CDCl₃) δ _H (ppm) 1.2 (s, 3H, -CH₃), 5.1 (s, 1H, -OH), 6.8 (d, 2H, Ar), 7.1 (d, 2H, Ar). Mass spectrum, *m/z* (rel. abundance): 124 (M⁺, 41), 110 (12), 109 (100), 79 (13), 66 (3), 53 (4). Pure 4-propylphenol- α,α -d₂ (0.79 g, pale yellow liquid) was obtained with a yield of 38%, ¹H NMR (CDCl₃) δ _H (ppm) 1.0 (t, 3H, -CH₃), 1.6 (q, 2H, -CH₂-), 5.0 (s, 1H, -OH), 6.8 (d, 2H, Ar), 7.1 (d, 2H, Ar). Mass spectrum, *m/z* (rel. abundance): 138 (M⁺, 34), 109 (100), 93 (3), 79 (17), 53 (4).

8.3. Results

8.3.1. Steady-state kinetics

In a previous study, we have shown that VAO can oxidize a wide range of phenolic compounds with a maximal turnover rate ranging from 1 to 10 s⁻¹ (Fraaije et al., 1995). Table 1 shows that both 4-ethylphenol and 4-propylphenol are converted at a similar rate. With these 4-alkylphenols and using stopped-flow spectrophotometry, it was found that during steady-state the enzyme is mainly in the oxidized form. Enzyme-monitored turnover experiments revealed that with ethylphenol, 69% of the enzyme was in the oxidized state while with 4-propylphenol, 63% was in the oxidized state during turnover. When the deuterated isomers were used, an increase in the amount of oxidized enzyme during catalysis was observed (90% and 82 % oxidized VAO for 4-ethylphenol- α,α -d₂ and 4-propylphenol- α,α -d₂, respectively). Furthermore, the turnover rates for these compounds revealed a relatively large kinetic isotope effect (Table 1). This suggests that, for both 4-ethylphenol and 4-propylphenol, a step involving flavin reduction is limiting the rate of overall catalysis.

Conversion of both 4-ethylphenol and 4-propylphenol by VAO leads to a mixture of the corresponding benzylic alcohol and alkenylic phenol in a ratio of approximately 4:1 (Drijfhout et al., 1997). HPLC product analysis revealed that deuteration of C_α has no effect on the ratio of aromatic products. When the reaction with 4-ethylphenol was performed in D₂O, no significant effect was seen on the ratio of aromatic products as well. However, using equimolar amounts of H₂O and D₂O, a 15% increase of the rate of turnover was observed.

Table 1. Steady-state kinetic parameters for the reaction of VAO with short-chain [α - ^1H]- and [α - ^2H]-4-alkylphenols (pH 7.5, 25°C). All values of kinetic parameters have a standard error <10%.

Substrate	k_{cat}	K_{m}	$k_{\text{cat}}/K_{\text{m}}$
	s^{-1}	μM	$\text{mM}^{-1}\text{s}^{-1}$
[α - ^1H]-4-methylphenol	0.0050	31	0.16
[α - ^2H]-4-methylphenol	0.0007	n.d.	-
<i>Isotope effect ($^1\text{H}/^2\text{H}$)</i>	7	-	-
[α - ^1H]-4-ethylphenol	2.5	9.0	300
[α - ^2H]-4-ethylphenol	0.24	11	22
<i>Isotope effect ($^1\text{H}/^2\text{H}$)</i>	10	0.8	13
[α - ^1H]-4-propylphenol	4.2	3.7	1100
[α - ^2H]-4-propylphenol	0.56	3.0	190
<i>Isotope effect ($^1\text{H}/^2\text{H}$)</i>	7.5	1.2	6.2

n.d. : not determined

Conversion of 4-methylphenol by VAO leads to formation of 4-hydroxybenzaldehyde as final aromatic product (Fraaije et al., 1997d). Analogous to PCMH catalysis (Hopper, 1976) and the VAO-mediated conversion of other 4-alkylphenols (Drijfhout et al., 1997), this reaction most probably involves two consecutive substrate oxidation steps. Table 1 shows that VAO oxidizes 4-methylphenol at an exceptional low rate. Therefore, the enzyme was mixed with 4-methylphenol under aerobic conditions, and the redox state of the flavin was monitored spectrophotometrically (Fig. 1). It was found that the enzyme is mainly (58%) in the reduced state during turnover (Fig. 1, spectrum 2) while product is continuously formed as evidenced by the increase in absorbance at 330 nm (Fig. 1, spectrum 3). Moreover, in separate experiments, oxygen consumption could be detected during a long period of time confirming continuous turnover. The apparent reduction of the flavin during turnover was even more pronounced at higher pH values and, at pH 9.4, VAO became almost fully reduced (Fig. 1, spectrum 4). The spectrum of the reduced enzyme species was strikingly different from free reduced enzyme (Fraaije and van Berkel, 1997c) showing a typical absorbance maximum at 352 nm with a molar absorption coefficient of $7.6 \text{ mM}^{-1}\text{cm}^{-1}$. Recently, evidence was obtained from X-ray crystallography that VAO can form a stable 4-methylphenol-flavin N5 adduct (Mattevi et al., 1997). Therefore, the apparent reduction of the flavin may reflect formation of this adduct and its slow decay might limit the turnover rate. As the enzyme is mainly in a reduced state during catalysis at

pH 7.5, the relatively large isotope effect on k_{cat} (Table 1) is difficult to interpret. Apparently, a reaction step leading to oxidized enzyme is rate limiting and its velocity is influenced by deuterium replacement of the C_{α} -hydrogens of 4-methylphenol. When VAO was mixed with deuterated 4-methylphenol, an increase of oxidized enzyme was observed (77 % in the oxidized state), indicating that the rate of reduction is partially limiting the rate of overall catalysis.

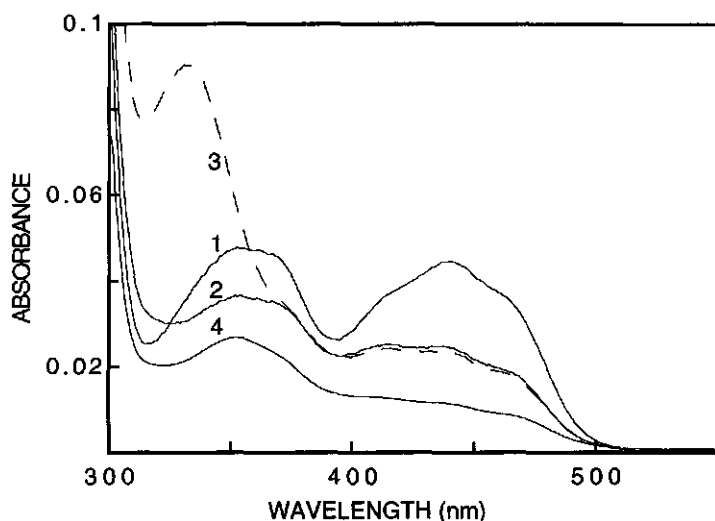
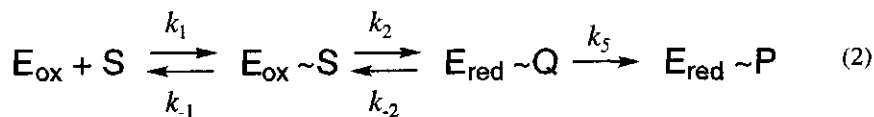


Figure 1. Spectral changes observed upon reaction of VAO with 4-methylphenol. VAO (3.6 μM) was aerobically mixed with 4-methylphenol (500 μM) and spectra were recorded after reaching an apparent equilibrium of the redox state. Before the addition of 4-methylphenol (1). After 1 min incubation at pH 7.5 (2). After 7.5 min incubation at pH 7.5 (3). After 1 min incubation at pH 9.4 (4). Spectra were recorded at 25°C.

8.3.2. Reductive half-reaction

The anaerobic reduction reaction of VAO can be described by the following equation (Fraaije and van Berkel, 1997c),



where E_{ox} represents oxidized enzyme, E_{red} represents reduced enzyme, S represents substrate, Q represents intermediate product and P represents final product.

When VAO and 4-ethylphenol were mixed in the stopped-flow spectrophotometer under anaerobic conditions, a fast decrease of absorbance at 439 nm was observed, indicative for flavin reduction. The reaction traces could satisfactorily be fitted assuming a

biphasic process with rate constants at saturating substrate concentrations $k_{fast} = 3.6 \text{ s}^{-1}$ and $k_{slow} = 0.3 \text{ s}^{-1}$, respectively. The secondary process was too slow to account for the turnover rate (2.5 s^{-1}) and therefore is probably of no catalytic importance. When we examined the substrate concentration dependence of the two phases of the reaction it appeared that the slow component (k_{slow}) is not dependent on the substrate concentration while the other component (k_{fast}) reached a finite value at the lowest substrate concentrations measured (Fig. 2). When the kinetic data for k_{fast} were analyzed, a best fit was obtained using the procedure of Strickland et al. (1975) which includes an apparent 'initial' reduction rate at infinite low substrate concentrations indicating a reversible process ($k_{-2} > 0$, Equation 2). By this approach a reduction rate of 2.5 s^{-1} (k_2) was determined while the reversible step occurs at a rate of 1.1 s^{-1} (k_{-2}) (Fig. 2, Table 2). In analogy with our previous study on the reaction of VAO with vanillyl alcohol, we assume that k_{slow} reflects the decay of the formed binary complex of $E_{red} \sim Q$ (k_3 in Equation 2) (Fraaije and van Berkel, 1997c).

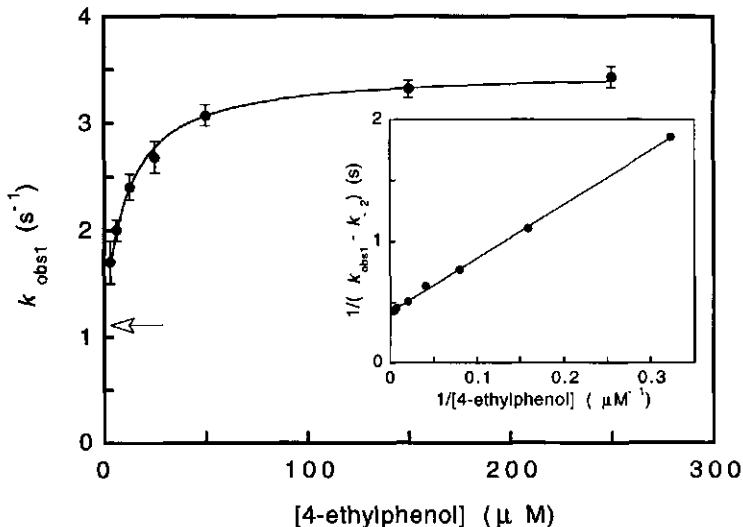


Figure 2. Observed reduction rates (k_{obs1}) of VAO with varying concentrations of 4-ethylphenol. The anaerobic reduction experiments were performed at 25°C and pH 7.5. Flavin reduction was monitored at 439 nm. The arrow indicates the value found for the reverse reduction rate. In the inset, the double-reciprocal plot of the kinetic data (corrected for k_{-2}) is shown.

With 4-ethylphenol- α,α - d_2 , again a biphasic reduction was observed with markedly decreased rates for both steps ($k_{fast} = 1.3 \text{ s}^{-1}$ and $k_{slow} = 0.05 \text{ s}^{-1}$ at a substrate concentration of 0.5 mM). However, accurate determination of the rate of the fast phase was hampered by the fact that the absorbance decrease, and therefore the extent of reduction in the first phase, was significantly decreased. Furthermore, both rate constants appeared to be independent of the substrate concentration. This again is in line with a model in which

the first step represents a reversible reduction of the flavin. With 4-ethylphenol- $\alpha,\alpha\text{-d}_2$, the slow rate of reduction results in an equilibrium in which most of the enzyme is in the oxidized state as $k_2 < k_{-2}$ and hence a small decrease in absorbance during the first phase is observed. Using the fraction of oxidized enzyme present at the end of the first reductive step (corresponding to $k_2/(k_{-2}+k_2)$), both k_2 and k_{-2} can be determined. For this, we determined the apparent reduction rate ($k_{\text{fast}} = k_2+k_{-2}$) and the redox state of the enzyme at the end of the reduction, at saturating conditions. Using this method, we could calculate the reduction rate ($k_2 = 0.3 \text{ s}^{-1}$) and the rate of the reverse step ($k_{-2} = 1.0 \text{ s}^{-1}$), the latter being similar to the rate found with 4-ethylphenol (Table 2). The molecular origin of the relatively large kinetic isotope effect on k_3 (Equation 2) is unclear. With yeast D-amino acid oxidase a similar unidentified isotope effect was observed (Pollegioni et al., 1997). In that case, it was suggested that it might be ascribed to a step involving substrate conversion/product dissociation.

Table 2. Stopped-flow kinetic results of the reductive half-reaction of VAO with short-chain 4-alkylphenols (pH 7.5, 25°C).

Substrate	k_2 s^{-1}	k_{-2} s^{-1}	$K_d (=k_{-1}/k_1)$ μM	k_5 s^{-1}
$[\alpha\text{-}^1\text{H}]\text{-4-methylphenol}$	0.076 ± 0.015	0.086 ± 0.013	42 ± 15	---
$[\alpha\text{-}^2\text{H}]\text{-4-methylphenol}^a$	0.008 ± 0.002	0.04 ± 0.01	n.d.	---
<i>Isotope effect ($^1\text{H}/^2\text{H}$)</i>	9.5	2	---	---
$[\alpha\text{-}^1\text{H}]\text{-4-ethylphenol}$	2.5 ± 0.3	1.1 ± 0.2	10 ± 2	0.3
$[\alpha\text{-}^2\text{H}]\text{-4-ethylphenol}^a$	0.3 ± 0.1	1.0 ± 0.1	n.d.	0.05
<i>Isotope effect ($^1\text{H}/^2\text{H}$)</i>	10	1.1	---	6
$[\alpha\text{-}^1\text{H}]\text{-4-propylphenol}$	4.4 ± 0.4	1.6 ± 0.3	0.8 ± 0.2	1
$[\alpha\text{-}^2\text{H}]\text{-4-propylphenol}^a$	0.5 ± 0.1	1.6 ± 0.2	n.d.	0.2
<i>Isotope effect ($^1\text{H}/^2\text{H}$)</i>	9	1.0	---	5

^a : rates determined from the ratio of $E_{\text{ox}}/E_{\text{total}} (=k_2/(k_{-2}+k_2))$, with $k_{\text{obs}1}=k_2+k_{-2}$ at the end of the first reductive process.

To verify the reversibility of reduction of VAO by 4-ethylphenol and to monitor spectral changes during the reductive half-reaction, diode-array detection was used in the stopped-flow experiments. In Fig. 3A, the spectral course (300 - 550 nm) observed during the anaerobic reduction of VAO by 4-ethylphenol is shown. Analysis of these data clearly showed that an initial fast reductive process is followed by a relatively slow secondary process (Fig. 3B).

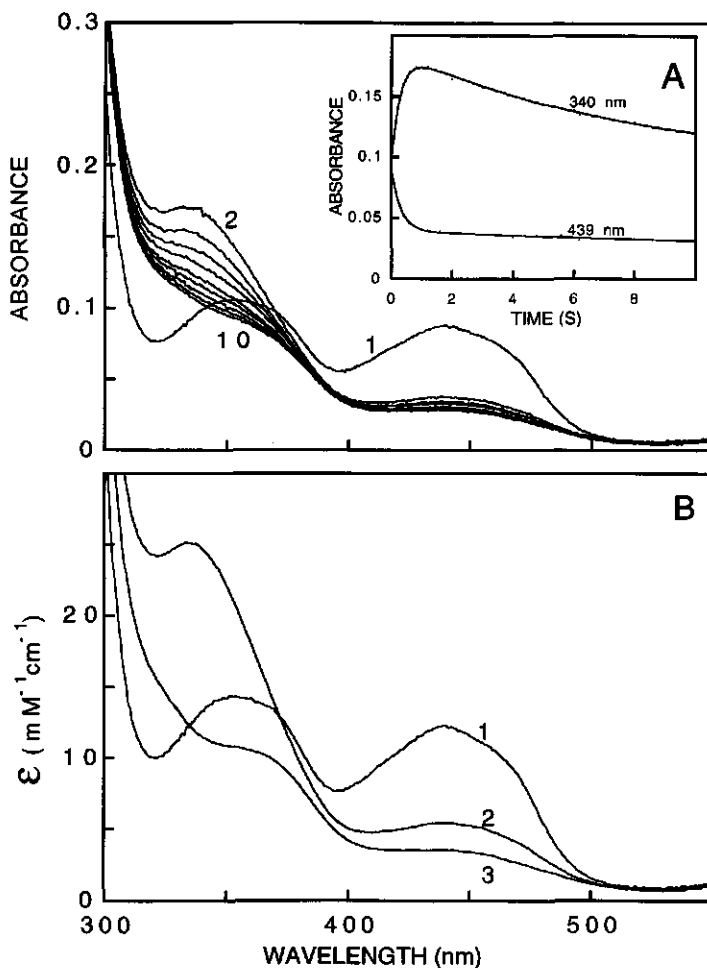


Figure 3. Anaerobic half-reaction of VAO with 4-ethylphenol.

A. Spectral changes observed upon anaerobic mixing of VAO ($7.6 \mu\text{M}$) with 4-ethylphenol ($500 \mu\text{M}$) (pH 7.5, 25°C). Original spectral scans are shown from 5.6 ms (1) to 18 s with intervals of 2 s (2-10). The inset shows the original data monitored at 340 nm and 439 nm showing the biphasic nature of the reduction reaction.

B. Spectra obtained from deconvolution of spectral changes shown in Fig 3A. A consecutive irreversible model ($\text{A} \rightarrow \text{B} \rightarrow \text{C}$) was used to fit the data resulting in apparent rates of 3.4 s^{-1} and 0.12 s^{-1} for the two observed reductive phases. Upon reaction of VAO with 4-ethylphenol, the original spectrum (1) transforms to (2) and subsequently (3) is formed.

Except for the decrease of absorbance at 439 nm, indicative for flavin reduction, also a marked increase in absorbance around 330 nm was observed during the first process (Spectrum 2; Fig. 3B). Based on studies with 4-(methoxymethyl)phenol (Fraaije et al., 1997c), this intermediate spectrum ($\epsilon_{330} = 25 \text{ mM}^{-1} \text{ cm}^{-1}$) is ascribed to the formation of a

binary complex between reduced enzyme and the *p*-quinone methide of 4-ethylphenol. This is substantiated by data of Bolton et al. (1995) who have synthesized a *p*-quinone methide of a 4-ethylphenol analogue which exhibits an absorbance maximum at 322 nm. In the second slow process the absorbance at 330 nm decreases (Spectrum 3, Fig. 3B) and a spectrum is formed which shows some resemblance with the 4-methylphenol generated reduced enzyme species (Spectrum 4, Fig. 1). Using the fraction of oxidized enzyme formed after the first process (spectrum 2 in Fig. 3B), the rate of reduction (k_2) and the reverse reaction (k_{-2}) could be determined (assuming that spectrum 3 in Fig. 3B represents fully reduced enzyme). Using the absorbance values at 439 nm (Fig. 3A), k_2 and k_{-2} were 2.6 s^{-1} and 0.8 s^{-1} , respectively. These values agree well with the data obtained using the single wavelength acquisition mode.

Similar results as observed for the reductive half-reaction with 4-ethylphenol were obtained when VAO was anaerobically mixed with 4-propylphenol. Again, the kinetic data were consistent with a model which includes reversible reduction ($k_{-2} > 0$). For 4-propylphenol, a relatively low value for the dissociation constant of the Michaelis complex (k_{-1}/k_1) was found while all other kinetic parameters, including the isotope effects on k_2 and k_3 , were in the same range as found for 4-ethylphenol (Table 2). The transient intermediate formed with 4-propylphenol had an absorbance maximum around 330 nm and from the kinetic analysis a molar absorption coefficient, $\epsilon_{330} = 22 \text{ mM}^{-1}\text{cm}^{-1}$ could be calculated. This, and the fact that the *p*-quinone methide of a 4-propylphenol analogue exhibits an absorbance maximum at 326 nm (Bolton et al., 1995), supports that a *p*-quinone methide intermediate is formed upon anaerobic reduction of VAO by 4-propylphenol.

The solvent isotope effect on the rate of enzyme reduction with 4-ethylphenol was also determined. In 50 % D_2O , a similar increase in the initial rate of flavin reduction was found as with the steady-state experiments ($k_2 = 2.8 \text{ s}^{-1}$). The origin of this stimulating effect is difficult to explain but confirms that flavin reduction does not involve fission of a hydrogen bond originating from a water molecule. However, the observed stimulation of activity by D_2O may also mask a true solvent isotope effect.

Anaerobic reduction of VAO by 4-methylphenol was a slow and monophasic process (Fig. 4). The rate of reduction (k_{fast}) was dependent on the substrate concentration and ranged from 0.11 to 0.15 s^{-1} (25 - 250 μM 4-methylphenol). The kinetic data concerning k_{fast} were again analyzed using the procedure of Strickland et al. (1975). The observation that reduction by 4-methylphenol did not lead to fully reduced enzyme is in line with this model which includes a reversible reduction (Equation 2). A maximal reduction rate of 0.076 s^{-1} (k_2) was determined while the reversible step occurs at a maximal rate of 0.086 s^{-1} (k_{-2}) (Table 2). With [α - ^2H]-4-methylphenol the rate of reduction (k_{fast}) significantly decreased (Fig. 4). Furthermore, the extent of reduction also decreased indicating that the rate of reduction (k_2) decreased to a greater extent as the rate of the reversible reduction

(k_2). Because of the small changes in absorbance and k_{fast} upon changing the substrate concentration, the dissociation constant for the Michaelis complex (k_{-1}/k_1) could not accurately be determined. However, it is expected that this parameter will be in the same range as for the non-deuterated substrate. Again, using the fraction of oxidized enzyme formed as a result of reduction by deuterated 4-methylphenol (corresponding to the ratio of $k_2/(k_{-2}+k_2)$) at 250 μM , k_2 could be calculated. Assuming that the dissociation constant for the Michaelis complex is not significantly affected by deuteration, the rate of reduction could be calculated (Table 2). A relatively large deuterium kinetic isotope effect was seen on the rate of reduction (k_2) while the rate of the reverse reaction was only slightly affected.

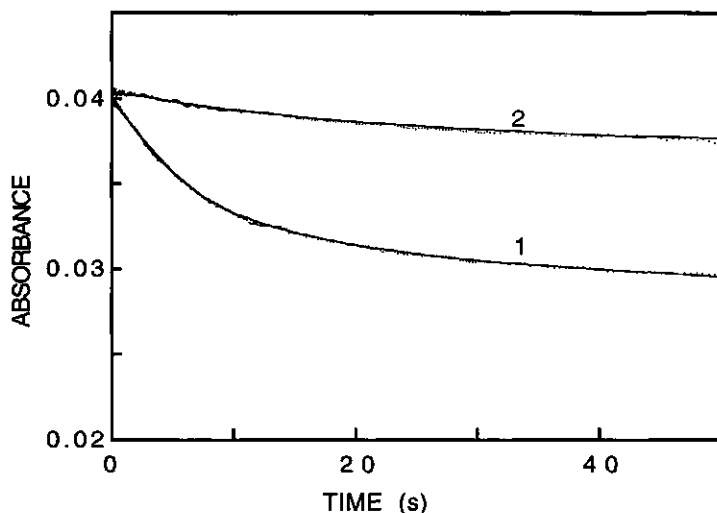


Figure 4. Spectral changes observed upon anaerobic mixing of VAO (3.3 μM) with 75 μM [α - ^1H]-4-methylphenol (trace 1) or [α - ^2H]-4-methylphenol (trace 2) when monitored at 439 nm (pH 7.5, 25°C). The data (dotted lines) could satisfactorily be fitted according to a monophasic process (dark lines) yielding apparent reaction rates of 0.133 s^{-1} (1) and 0.045 s^{-1} (2), respectively.

8.4. Discussion

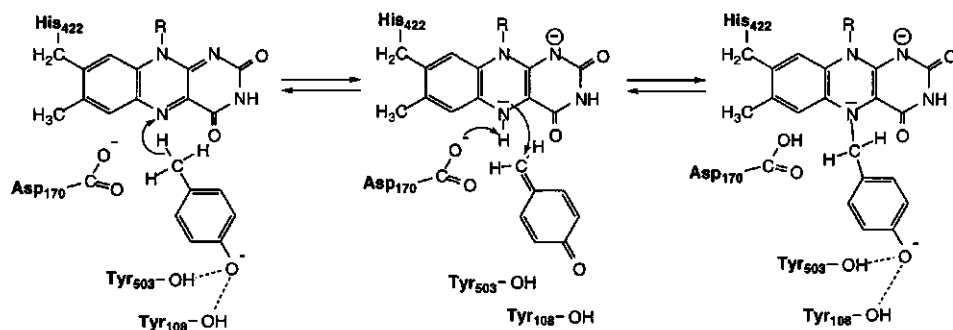
In this study we have described the kinetic mechanism of VAO with short-chain 4-alkylphenols. For the reactions with 4-ethylphenol and 4-propylphenol, it was clearly shown that flavin reduction is rate limiting in overall catalysis. The flavin reduction rates for the non-deuterated and deuterated forms of these substrates are similar to the corresponding k_{cat} values and the enzyme is predominantly in the oxidized state during turnover. During the reductive half-reaction, a transient intermediate is formed which is ascribed to the binary complex between reduced enzyme and the *p*-quinone methide of the alkylphenols. Addition of water to these quinoid species preferentially occurs after flavin reoxidation, after which

product release completes the catalytic cycle. The kinetic mechanism of VAO with 4-ethylphenol and 4-propylphenol is slightly different from that of 4-(methoxymethyl)phenol (Fraaije and van Berkel, 1997c). With the latter substrate, the *p*-quinone methide intermediate is considerably stabilized in the active site of the reduced enzyme, resulting in a true ternary complex mechanism (Fraaije and van Berkel, 1997c). With the alkylphenols, a more rapid decomposition of the reduced enzyme-*p*-quinone methide complex and concomitant product release may cause part of the enzyme molecules to obey a ping-pong mechanism. A similar sequence of events was reported for the reaction with vanillyl-alcohol (Fraaije and van Berkel, 1997a).

The crystal structure of VAO has revealed that the active site is located in the interior of the protein and is shielded from solvent (Mattevi et al., 1997). This corresponds to the observed enantioselective hydroxylation of 4-alkylphenols (Drijfhout et al., 1997), which is indicative for an enzyme mediated nucleophilic attack of water at the methide carbon. From the crystallographic data we have suggested that charge balancing between the side chain of Arg504 and the anionic reduced flavin might favor the stabilization of the neutral substrate quinone. Upon flavin reoxidation, this charge balancing is lost, facilitating water attack. However, in the enzymatic reaction with 4-ethylphenol or 4-propylphenol, addition of water to the quinone intermediate is less efficient than with 4-(methoxymethyl)phenol and significant amounts of vinylic phenols are formed (Drijfhout et al., 1997). It is not clear whether this competing side reaction results from a relatively rapid rearrangement of the 4-alkylphenol *p*-quinone methide intermediates or is related to the water accessibility of the active site. In this respect it is interesting to note that in the reaction of VAO with 2-methoxy-4-propylphenol, hardly any vinylic product is formed (Drijfhout et al., 1997).

In the reaction of VAO with 4-methylphenol a rather slow reduction of the flavin was observed which was, however, too fast to account for the rate of overall catalysis. Moreover, with this substrate the enzyme is mainly in the reduced state during turnover, particularly at high pH. A plausible explanation for the stabilization of the reduced form of the enzyme may lie in the observation that VAO can form a flavin-methylphenol adduct (Mattevi et al., 1997). Crystals soaked with 4-methylphenol revealed a covalent bond between the C α of the substrate and the N5 of the isoalloxazine ring. The spectrum of the reduced enzyme species obtained during the aerobic conversion of 4-methylphenol at pH 9.4 showed a relatively low absorbance around 320 nm and closely resembled the spectrum of the 4-methylphenol soaked VAO crystals (Mattevi et al., 1997). Moreover, the recently identified flavin N5 adduct in nitroalkane oxidase (Gadda et al., 1997) shows very similar spectral properties. A possible mechanism which would account for flavin adduct formation is given in Scheme 1. It is proposed that during conversion of 4-methylphenol a flavin adduct is formed which only slowly decomposes to form product and hence is limiting turnover. Crystallographic analysis have suggested that for more bulky 4-alkylphenols,

formation of a N5 adduct is prevented by steric constraints (Mattevi et al., 1997). This corresponds to the far higher turnover rates observed with 4-ethyl- and 4-propylphenol.



Scheme 1. Proposed mechanism for the formation of a 4-methylphenol-FAD adduct in VAO.

Reduction of VAO by short-chain 4-alkylphenols is not very efficient as also the reverse reaction can proceed at a considerable rate. A similar reversible reduction was recently reported for yeast D-amino acid oxidase (Pollegioni et al., 1997). In contrast, with the natural substrate 4-(methoxymethyl)phenol, no significant reverse reduction of VAO occurs (Fraaije and van Berkel, 1997c). With the homologous enzyme PCMH also a reversible reduction of the flavin was observed upon reaction with 4-ethylphenol, but the rate of reduction was several orders of magnitude higher (McIntire et al., 1987). With VAO and similar to PCMH, almost no kinetic deuterium isotope effect on k_2 was observed. Apparently, the hydrogen or deuterium abstracted from C_α of the substrate during reduction of the flavin is not necessarily involved in the reverse reaction. Possibly, there is an alternative source of hydrogen or the transferred hydrogen may be quickly exchanged. A possible residue involved in this may be Asp170 which side chain is located close to the C_α -atom of the substrate and the N5 atom of the isoalloxazine ring (Mattevi et al., 1997).

In PCMH, a fast intramolecular electron transfer to the cytochrome renders reoxidized flavin after which product is released (McIntire et al., 1987). Recently, it was reported that the 8α -O-tyrosyl-FAD phenolic ether bond in PCMH may facilitate electron transfer to the cytochrome subunit (Kim et al., 1995). As VAO does not contain a cytochrome subunit and is not involved in the biodegradation of 4-alkylphenols (Fraaije et al., 1997), it may be concluded that VAO is a true flavoprotein oxidase which fortuitously mediates the (enantioselective) hydroxylation of 4-alkylphenols via the transient stabilization of their corresponding *p*-quinone methides. With the availability of the VAO structure it will be stimulating to unravel the substrate specificity and oxygen reactivity of this flavoenzyme in further detail.

Acknowledgements

We are indebted to Maurice Franssen and Hugo Jongejan (Wageningen Agricultural University) for their help during the synthesis of deuterated substrates. We also thank Marleen Verheul (NIZO, Ede) and Andrea Mattevi (University of Pavia) for fruitful discussions.

8.5. References

- Bolton, J.L., Comeau, E. & Vukomanovic, V. (1995) The influence of 4-alkyl substituents on the formation and reactivity of 2-methoxy-quinone methides: evidence that the extended π -conjugation dramatically stabilizes the quinone methide formed from eugenol, *Chem.-Biol. Interact.* **95**, 279-290.
- Bolton, J.L., Wu, H.M. & Hu, L.Q. (1996) Mechanism of isomerization of 4-*O*-propyl-quinone to its tautomeric *p*-quinone methide, *Chem. Res. Toxicol.* **9**, 109-113.
- De Jong, E., van Berkel, W.J.H., van der Zwan, R.P. & De Bont, J.A.M. (1992) Purification and characterization of vanillyl-alcohol oxidase from *Penicillium simplicissimum*, *Eur. J. Biochem.* **208**, 651-657.
- Drijfhout, F.P., Fraaije, M.W., Jongejan, H., van Berkel, W.J.H. and Franssen, M.C.R. (1998) Enantioselective hydroxylation of 4-alkylphenols by vanillyl-alcohol oxidase, *Biotechnol. Bioeng.*, in press.
- Fraaije, M.W., Veeger, C. & van Berkel, W.J.H. (1995) Substrate specificity of flavin-dependent vanillyl-alcohol oxidase from *Penicillium simplicissimum*, *Eur. J. Biochem.* **234**, 271-277.
- Fraaije, M.W., Pikkemaat, M. & van Berkel, W.J.H. (1997a) Enigmatic gratuitous induction of the covalent flavoprotein vanillyl-alcohol oxidase in *Penicillium simplicissimum*, *Appl. Environ. Microbiol.* **63**, 435-439.
- Fraaije, M.W., Mattevi, A. & van Berkel, W.J.H. (1997b) Mercuration of vanillyl-alcohol oxidase from *Penicillium simplicissimum* generates inactive dimers, *FEBS Lett.* **402**, 33-35.
- Fraaije, M.W. and van Berkel, W.J.H. (1997c) Catalytic mechanism of the oxidative demethylation of 4-(methoxymethyl)phenol by vanillyl-alcohol oxidase, *J. Biol. Chem.* **272**, 18111-18116.
- Fraaije, M.W., Drijfhout, F., Meulenbeld, G.H., van Berkel, W.J.H. & Mattevi, A. (1997d) Vanillyl-alcohol oxidase from *Penicillium simplicissimum*: Reactivity with *p*-cresol and preliminary structural analysis, in *Flavins and flavoproteins XII* (Stevenson, K., Massey, V., and Williams, C.H. jr, eds.), pp. 261-264, University Press, Calgary.
- Gadda, G., Edmondson, D.E., Russell, D.H. & Fitzpatrick, P.F. (1997) Identification of the naturally occurring flavin of nitroalkane oxidase from *Fusarium oxysporum* as a 5-nitrobutyl-FAD and conversion of the enzyme to the active FAD-containing form, *J. Biol. Chem.* **272**, 5563-5570.
- Hopper, D.J. (1976) The hydroxylation of *p*-cresol and its conversion to *p*-hydroxybenzaldehyde in *Pseudomonas putida*, *Biochem. Biophys. Res. Commun.* **69**, 462-468.
- Kim, J., Fuller, J.H., Kuusk, V., Cunane, L., Chen, Z., Mathews, F.S. and McIntire, W.S. (1995) The cytochrome subunit is necessary for covalent FAD attachment to the flavoprotein subunit of *p*-cresol methylhydroxylase, *J. Biol. Chem.* **270**, 31202-31209.
- Mattevi, A., Fraaije, M.W., Mozzarelli, A., Olivi, L., Coda, A. & van Berkel, W.J.H. (1997) Crystal structures and inhibitor binding in the octameric flavoenzyme vanillyl-alcohol oxidase: the shape of the active-site cavity controls substrate specificity, *Structure* **5**, 907-920.
- Mathews, F.S., Chen, Z.-W., Bellamy, H.D. & McIntire, W.S. (1991) Three-dimensional structure of *p*-cresol methylhydroxylase (flavocytochrome *c*) from *Pseudomonas putida* at 3.0 Å resolution, *Biochemistry* **30**, 238-247.
- McIntire, W.S., Hopper, D.J., Craig, J.C., Everhart, E.T., Webster, R.V., Causer, M.J. & Singer, T.P. (1984) Stereochemistry of 1-(4'-hydroxyphenyl)ethanol produced by hydroxylation of 4-ethylphenol by *p*-cresol methylhydroxylase, *Biochem. J.* **224**, 617-621.
- McIntire, W.S., Hopper, D.J. Hopper & Singer, T.P. (1985) *p*-Cresol methylhydroxylase: assay and general properties, *Biochem. J.* **228**, 325-335.
- McIntire, W.S., Hopper, D.S. & Singer, T.P. (1987) Steady-state and stopped-flow kinetic measurements of the primary deuterium isotope effect in the reaction catalyzed by *p*-cresol methylhydroxylase, *Biochemistry* **26**, 4107-4117.
- Pollegioni, L., Blodig, W. & Ghisla, S. (1997) On the mechanism of D-amino acid oxidase, *J. Biol. Chem.* **272**, 4924-4934.
- Strickland, S., Palmer, G. and Massey, V. (1975) Determination of dissociation constants and specific rate constants of enzyme-substrate (or protein-ligand) interactions from rapid reaction kinetic data, *J. Biol. Chem.* **250**, 4048-4052.

9

Mercuration of vanillyl-alcohol oxidase from *Penicillium simplicissimum* generates inactive dimers

Marco W. Fraaije, Andrea Mattevi and Willem J.H. van Berkel

FEBS Letters **402**, 33-35 (1997)

Abstract

Vanillyl-alcohol oxidase (EC 1.1.3.7) from *Penicillium simplicissimum* was modified with *p*-mercuribenzoate. One cysteine residue reacts rapidly without loss of enzyme activity. Three sulfhydryl groups then react in an 'all or none process' involving enzyme inactivation and dissociation of the octamer into dimers. The inactivation reaction is slowed down in the presence of the competitive inhibitor isoeugenol and fully reversible by treatment of the modified enzyme with dithiothreitol. Vanillyl-alcohol oxidase is more rapidly inactivated at low enzyme concentrations and protected from mercuration by antichaotropic salts. It is proposed that subunit dissociation accounts for the observed sensitivity of vanillyl-alcohol oxidase crystals towards mercury compounds.

9.1. Introduction

Vanillyl-alcohol oxidase (VAO) from *Penicillium simplicissimum* catalyzes the oxidation of vanillyl-alcohol to vanillin with the simultaneous reduction of molecular oxygen to hydrogen peroxide (1). The enzyme is a homooctamer of 0.5 MDa with each subunit containing 8α -(N^3 -histidyl)-FAD as a covalently bound prosthetic group (1). Based on the production of 4-hydroxycinnamyl alcohols from 4-allylphenols we have proposed that the reaction mechanism of VAO involves the formation of a *p*-quinone methide product intermediate (2). To relate the chemical mechanism to protein function we have undertaken the X-ray analysis of VAO (3). A major problem hampering the structure determination proved to be the high sensitivity of the VAO crystals towards mercury and other heavy atom compounds. Therefore, we have studied the reactivity towards mercury of VAO in solution. In this paper, evidence is provided that mercuriation of VAO involves the dissociation into dimers.

9.2. Materials and Methods

Enzyme purification

Vanillyl-alcohol oxidase from *Penicillium simplicissimum* (ATCC 90172) was purified as described (1, 2).

Analytical methods

Absorption spectra were recorded at 25 °C on an Aminco DW-2000 spectrophotometer. The concentration of VAO was determined spectrophotometrically using a molar absorption coefficient $\epsilon_{439} = 12.5 \text{ mM}^{-1} \text{ cm}^{-1}$ for protein-bound FAD (1). VAO substrates and competitive inhibitors have been described elsewhere (2). VAO activity was assayed at 25 °C, pH 9.5 by following the conversion of vanillyl alcohol to vanillin ($\epsilon_{340} = 22.8 \text{ mM}^{-1} \text{ cm}^{-1}$) at 340 nm.

Chemical modification

4-Hydroxymercuribenzoate was obtained from Aldrich. Mercuriation of VAO was performed at 25 °C in 50 mM Hepes pH 7.5. Incubation mixtures contained 1-10 μM VAO and 100-300 μM mercurial reagent. Aliquots were withdrawn from the incubation mixtures at intervals and assayed for residual enzyme activity. Reactivation of mercurated VAO was achieved by the addition of 10 mM dithiothreitol. After a 2 h incubation at room temperature the activity of the enzyme was fully restored.

Incorporation of 4-hydroxymercuribenzoate into VAO was followed spectrophotometrically at 250 nm, using a molar difference absorption coefficient of $7.6 \text{ mM}^{-1}\text{cm}^{-1}$ to quantify the formation of mercaptide bonds (4). Two-compartment cells were used with a total pathlength of 0.875 cm (5). Both sample and reference cell contained 0.8 ml of 20 μM enzyme in 50 mM Hepes pH 7.5, in one compartment and 0.8 ml of 250 μM 4-hydroxymercuribenzoate in the same buffer in the other compartment. After recording a baseline, the reaction was initiated by mixing the solutions in the sample cell. The absorbance changes were followed by scanning spectra from 240-540 nm at a scan speed of 5 nm/s. At time-intervals, aliquots were withdrawn from the sample cell and assayed for enzyme activity.

Analytical gel filtration

Analytical gel filtration at room temperature was performed on a Superdex 200 HR 10/30 column (Pharmacia ÅKTA system). Samples (50 μl) were eluted in 50 mM potassium phosphate pH 7.0, containing 150 mM KCl, at a flow rate of 1.0 ml/min. Protein peaks were detected at 220 nm. Calibration proteins used were ferritin (450 kDa), catalase (232 kDa), alcohol dehydrogenase (144 kDa), lipoamide dehydrogenase (100 kDa), *p*-hydroxybenzoate hydroxylase (88 kDa), bovine serum albumin (67 kDa), ovalbumin (43 kDa), chymotrypsinogen (25 kDa) and cytochrome c (12.3 kDa). The analysis of the oligomeric state of VAO was done essentially as described in (6).

9.3. Results

9.3.1 Inactivation of VAO by 4-hydroxymercuribenzoate

Incubation of VAO with 4-hydroxymercuribenzoate led to complete loss of enzyme activity. The inactivation reaction followed pseudo-first-order kinetics and was slowed down in the presence of the competitive inhibitor isoeugenol (Fig. 1). The activity could be fully restored by treatment of the modified enzyme with 10 mM dithiothreitol. VAO was protected from inactivation by 4-hydroxymercuribenzoate in the presence of 0.5 M sodium chloride (Fig. 1). A similar protective effect was displayed by 0.2 M ammonium sulfate. Fig. 1 also shows that the rate of VAO inactivation by 4-hydroxymercuribenzoate increased at lower enzyme concentrations.

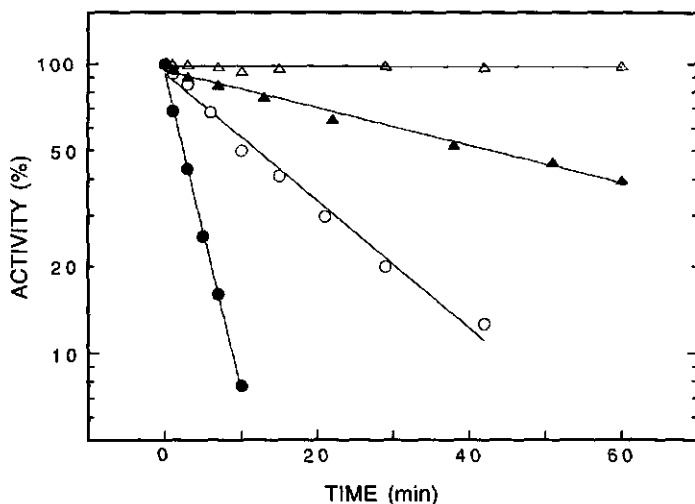


Figure 1. Time-dependent inactivation of VAO by 4-hydroxymercuribenzoate. The temperature was 25 °C. VAO in 50 mM HEPES pH 7.5 was incubated with 200 μM 4-hydroxymercuribenzoate: 1 μM VAO (●); 10 μM VAO (○); 10 μM VAO in the presence of 200 μM isoeugenol (▲); 10 μM VAO in the presence of 0.5 M sodium chloride (△).

9.3.2 Incorporation of 4-hydroxymercuribenzoate into VAO

The incorporation of 4-hydroxymercuribenzoate into VAO was quantified by combined spectrophotometric and activity measurements. Fig. 2 shows that the time-dependent development of the difference spectrum involved absorbance changes around 250 and 280 nm and in the flavin-absorbing region. Isobestic points were observed at 305 and 450 nm. The kinetics at 280 nm and in the flavin-absorbing region were monophasic and parallel to those of the inactivation reaction (cf. Fig. 1). From the absorbance changes at 250 nm, indicative for the formation of mercaptide bonds (4), it can be concluded that about four cysteine residues are modified in VAO by 4-hydroxymercuribenzoate (inset Fig. 2). One cysteine reacts rapidly without significant loss of enzyme activity. About three cysteines then react more slowly leading to complete inactivation (inset Fig. 2). When the incorporation of 4-hydroxymercuribenzoate into VAO was studied in the presence of 0.2 M ammonium sulfate, nearly no absorbance changes occurred at 280 nm and in the flavin-absorbing region. About one cysteine residue was mercurated under these conditions as evidenced from the absorbance changes at 250 nm (not shown).

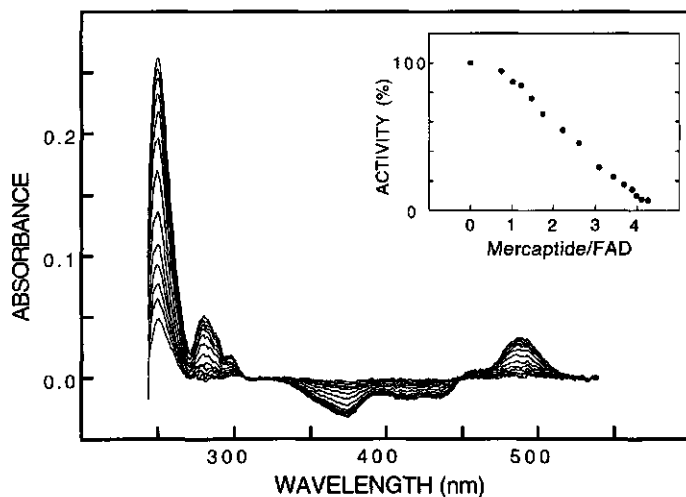


Figure 2. Difference spectra observed during the inactivation of 10 μM VAO by 125 μM 4-hydroxymercuribenzoate in 50 mM HEPES, pH 7.5. Spectra are shown, recorded 1, 3, 5, 8, 12, 19, 31, 47, 61, 75, 90, 105 and 120 min after mixing. In the inset, the formation of mercaptide bonds is plotted as a function of residual VAO activity.

9.3.3 Quaternary structure of native and 4-hydroxymercuribenzoate treated VAO

Fig. 3A shows that treatment of VAO with 4-hydroxymercuribenzoate resulted in octamer dissociation. From running calibration proteins in parallel it was established that mercuration of VAO involved the formation of dimers. The VAO dimers were inactive and the kinetics of subunit dissociation strongly resembled that of the inactivation reaction (cf. Fig. 1). Inactive dimers were also formed when VAO was treated with 4-hydroxymercuribenzoate in the presence of isoeugenol. Binding of isoeugenol however inhibited the rate of dimer formation and the fraction of octamers remaining paralleled the fraction of residual enzyme activity. The 4-hydroxymercuribenzoate induced dissociation of VAO octamers was fully reversible as evidenced by treatment of the modified enzyme with dithiothreitol (not shown).

No subunit dissociation was observed when VAO was incubated with 4-hydroxymercuribenzoate in the presence of 0.2 M ammonium sulfate or 0.5 M sodium chloride. Analytical gel filtration revealed that this might be related to the stabilization of the octameric state. Fig. 3B shows that lowering the concentration of the native enzyme resulted in a considerable increase in the fraction of dimers. In agreement with urea

unfolding experiments (10), the dimers were also active. Addition of 0.2 M ammonium sulfate to 1 μ M VAO strongly shifted the octamer-dimer equilibrium in favor of the octameric state (Fig. 3B).

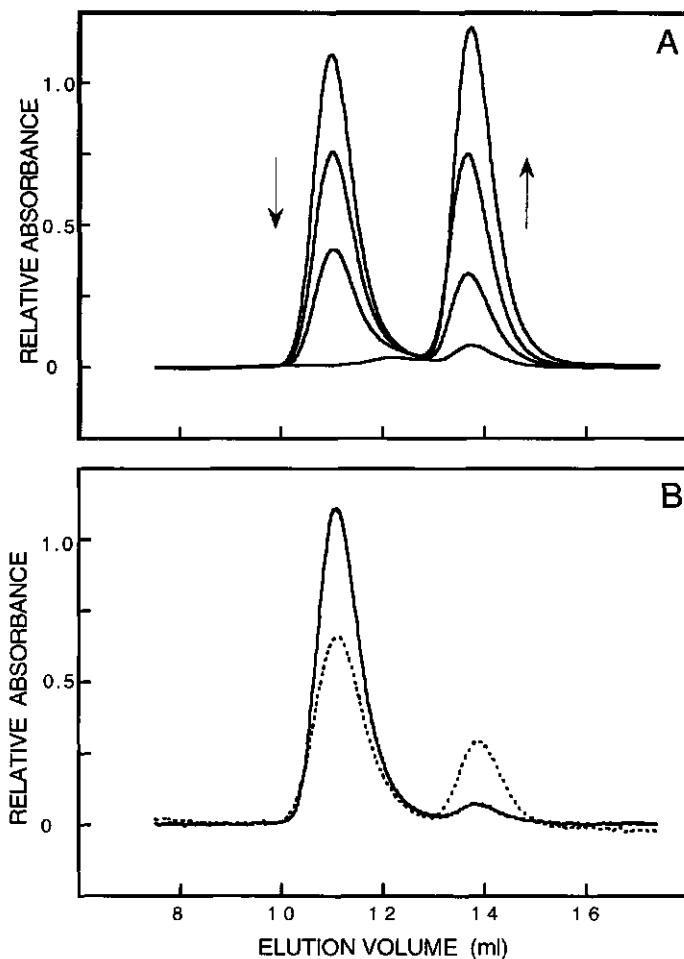


Figure 3. Quaternary structure of native and mercurated VAO. (A) 10 μ M VAO in 50 mM Hepes pH 7.5 was incubated at 25 $^{\circ}$ C with 200 μ M 4-hydroxymercuribenzoate. Superdex 200 HR elution profiles are shown, recorded 0, 10, 30 and 60 min after mixing. The arrows indicate the decrease and increase in the amount of octamers and dimers, respectively. (B) Elution profiles of 1 μ M native VAO in 50 mM Hepes pH 7.5, preincubated in the absence (broken line) or presence (continuous line) of 0.2 M ammonium sulfate.

9.4. Discussion

VAO represents a novel type of flavoprotein oxidase (2) and its X-ray structure is presently determined by the method of multiple isomorphous replacement (3). In soaking experiments with mercury compounds we noticed that the VAO crystals are sensitive towards structural changes, influencing the crystal packing. In this paper evidence is provided that mercuration of VAO involves quaternary structural changes causing the stabilization of dimers. Similar mercury-induced quaternary structural changes have been reported with other oligomeric enzymes like muscle phosphorylase (7), hemerythrin (8) and aspartate transcarbamoyltransferase (9). The formation of VAO dimers is in line with results from urea unfolding (10) and the observation that the enzyme octamer has 422 symmetry (3).

Mercuration of VAO resulted in complete inactivation and was accompanied with significant changes in the spectral properties of the covalently bound flavin. Because the inactivation of VAO involved the modification of three cysteine residues it is at present not clear whether these spectral perturbations are directly related to subunit dissociation. Although the inhibitory effect of isoeugenol may point to the modification of a cysteine residue in the vicinity of the substrate binding site, the assignment of modification sites has to await the elucidation of the X-ray structure.

VAO was more rapidly inactivated at low enzyme concentrations and the enzyme was protected from mercuration in the presence of antichaotropic salts. This suggests that the mercuration of VAO dimers shifts the octamer-dimer equilibrium of the native enzyme towards the dimeric state. In contrast to the native enzyme, octamerization of mercurated VAO was not stimulated in the presence of antichaotropic salts. This indicates that at least one of the cysteine residues is located near the dimer-dimer interface. Because VAO crystals grow in low salt (3) it is proposed that subunit dissociation accounts for the observed sensitivity of VAO crystals towards mercury compounds.

9.5. References

1. de Jong, E., van Berkel, W.J.H., van der Zwan, R.P. and de Bont, J.A.M. (1992) *Eur. J. Biochem.* **208**, 651-657.
2. Fraaije, M.W., Veeger, C. and van Berkel, W.J.H. (1995) *Eur. J. Biochem.* **234**, 271-277.
3. Mattevi, A., Fraaije, M.W., Coda, A. and van Berkel, W.J.H. (1996) *Proteins: Structure, Function and Genetics* **27**, 601-603.
4. Boyer, P.D. (1959) *The Enzymes* **1**, 511-588.
5. van Berkel, W.J.H., Weijer, W.J., Müller, F., Jekel, P.A. and Beintema, J.J. (1984) *Eur. J. Biochem.* **145**, 245-256.
6. Ostendorf, R., Auerbach, G. and Jaenicke, R. (1996) *Protein Sci.* **5**, 862-873.
7. Madsen, N.B. and Cori, C.F. (1956) *J. Biol. Chem.* **223**, 1055-1066.
8. Keresztes-Nagy S. and Klotz, I.M. (1963) *Biochemistry* **2**, 923-927.
9. Gerhart, J.C. and Schachman, H.K. (1965) *Biochemistry* **4**, 1054-1062.
10. van Berkel, W.J.H., Fraaije, M.W., de Jong, E. and de Bont, J.A.M. (1994) in: *Flavins and Flavoproteins 1993* (Yagi, K. ed.) pp. 799-802, W. de Gruyter, Berlin.

10

Crystal structures and inhibitor binding in the octameric flavoenzyme vanillyl-alcohol oxidase: the shape of the active-site cavity controls substrate specificity

Andrea Mattevi, Marco W. Fraaije, Andrea Mozzarelli,
Luca Olivi, Alessandro Coda and Willem J.H. van Berkel

Structure 5, 907-920 (1997) (modified version)

Abstract

Background: Lignin degradation leads to formation of a broad spectrum of aromatic molecules, which can be used by various fungal micro-organisms as their sole source of carbon. When grown on phenolic compounds, *Penicillium simplicissimum* induces the strong expression of a flavin-containing vanillyl-alcohol oxidase (VAO). The enzyme catalyses the oxidation of a vast array of substrates, ranging from aromatic amines to 4-alkylphenols. VAO is a member of a novel class of widely distributed oxidoreductases, which use flavin adenine dinucleotide (FAD) as a cofactor covalently bound to the protein. We have carried out the determination of the structure of VAO in order to shed light on the most interesting features of these novel oxidoreductases, such as the functional significance of covalent flavinylation and the mechanism of catalysis.

Results: The crystal structure of VAO has been determined in the native state and in complexes with four inhibitors. The enzyme is an octamer with 42 symmetry; the inhibitors bind in a hydrophobic, elongated cavity on the *si* side of the flavin molecule. Three residues, Tyr108, Tyr503 and Arg504 form an anion-binding subsite, which stabilises the phenolate form of the substrate. The structure of VAO complexed with the inhibitor 4-(1-heptenyl)phenol shows that the catalytic cavity is completely filled by the inhibitor, explaining why alkylphenols bearing aliphatic substituents longer than seven carbon atoms do not bind to the enzyme.

Conclusions: The shape of the active-site cavity controls substrate specificity by providing a 'size exclusion mechanism'. Inside the cavity, the substrate aromatic ring is positioned at an angle of 18° to the flavin ring. This arrangement is ideally suited for a hydride transfer reaction, which is further facilitated by substrate deprotonation. Burying the substrate beneath the protein surface is a recurrent strategy, common to many flavoenzymes which effect substrate oxidation or reduction via hydride transfer.

10.1. Introduction

Lignin is the most abundant aromatic biopolymer on earth. In addition to conferring strength to the plants, it provides a barrier against microbial attack and protects cellulose from hydrolysis. Among the relatively few organisms able to degrade lignin, white-rot fungi are particularly efficient in carrying out the lignolytic process, which has been described as an "enzymatic combustion" (1) due to the broad substrate specificity of the enzymes involved. Lignin degradation results in the production of various aromatic molecules, which can be used as source of carbon by soil inhabitants, such as several basidiomycetes and ascomycetes. The aryl alcohol oxidases, a wide group of flavin adenine dinucleotide (FAD-)dependent enzymes which produce hydrogen peroxide through the oxidation of their aromatic substrates, are crucial for the degradation of the secondary metabolites derived from the lignolytic process (2). Recently, we have isolated from the ascomycete *Penicillium simplicissimum* a novel type of aryl alcohol oxidase, vanillyl alcohol oxidase (VAO) (3,4), which consists of eight identical subunits each comprising 560 amino acids and a molecule of 8α -(N^3 -histidyl)-FAD as covalently bound prosthetic group. A noticeable feature of VAO is its strikingly broad substrate specificity. In fact, besides the vanillyl-alcohol (4-hydroxy-3-methoxybenzyl alcohol) oxidation to vanillin (4-hydroxy-3-methoxybenzaldehyde; Fig. 1a), VAO is able to carry out the oxidative demethylation of 4-(methoxymethyl)phenol to 4-hydroxybenzaldehyde (Fig. 1b), the oxidative deamination of vanillylamine to vanillin and the conversion of eugenol (4-allyl-2-methoxyphenol) to coniferyl alcohol (4-hydroxy-3-methoxycinnamyl alcohol) (4). In spite of this wide spectrum of activity, two features common to the VAO catalysed reactions can be identified: the reaction is thought to be initiated by the oxidation of the substrate C α atom resulting in a *p*-quinone methide intermediate (Fig. 1a and 1b); and the reduced flavin is reoxidised by molecular oxygen, with the production of a hydrogen peroxide molecule.

A thorough characterisation of the VAO substrate specificity has revealed that the enzyme can bind aromatic compounds bearing aliphatic groups of variable size, ranging from a small methyl group to an aliphatic chain of up to seven carbon atoms (5). Moreover, the *ortho* substituent can be either a H, OH or OCH₃ group, whereas a hydroxyl substituent *para* to the aliphatic chain is strictly required for binding (4). This ability of VAO to convert a wide range of substrates has led to the speculation that *in vivo* the enzyme may be involved in the degradation of several metabolites. The fact that the expression of VAO is strongly induced by the presence of 4-(methoxymethyl)phenol in the growth medium, however, suggests that the main physiological role (6) of the enzyme is that of degrading this compound, leading to the production of methanol and 4-hydroxybenzaldehyde (Fig. 1b).

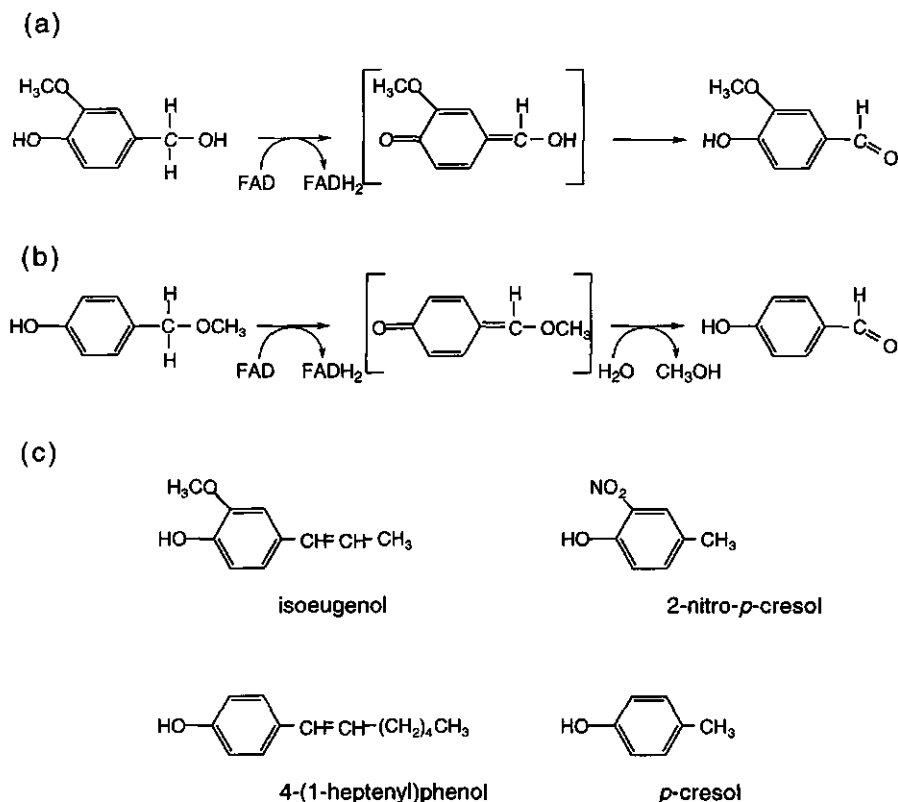


Figure 1. Substrate and inhibitors of VAO. Examples of different reactions catalysed by VAO are: (a) the oxidation of vanillyl alcohol to vanillin and (b) the oxidative demethylation of 4-(methoxymethyl)phenol. The catalysed reactions are thought to proceed through a *p*-quinone methide intermediate shown in square brackets. The reduced FAD is reoxidised by molecular oxygen (not shown). (c) Chemical structure of the competitive inhibitors and active-site ligands employed for the crystallographic analysis.

Analysis of the primary sequence (Benen *et al.*, personal communication) has revealed that VAO belongs to a recently discovered family of FAD-dependent oxidoreductases (7,8). The other known members of this family are D-lactate dehydrogenase, 6-hydroxy-D-nicotine oxidase, L-gulono- γ -lactone oxidase and *p*-cresol methylhydroxylase (PCMH). These proteins, which catalyse a wide range of chemical reactions, share a weak sequence homology. Particularly, PCMH is a well-characterised flavocytochrome whose three-dimensional structure has been reported (9,10). Despite a 26% sequence identity (Benen *et al.*, personal communication), PCMH differs from VAO in two major aspects: in PCMH the FAD cofactor is covalently bound to a tyrosine rather than to a histidine residue; and the reduced cofactor is reoxidised by electron transfer to the heme group and not by molecular oxygen as in VAO (9).

The covalent linkage of the FAD cofactor to the protein is a feature common to most members of the VAO-related oxidoreductase family (7). Although covalent flavinylation has been observed in many flavoproteins, the mechanism of formation and the functional role of the covalent bond are poorly understood (10,11). In this respect, the VAO related oxidoreductases are particularly attractive for study as they portray different types of flavinylation such as the 8α -(O-Tyrosyl)-FAD of PCMH, 8α -(N^1 -histidyl)-FAD of L-gulonolactone oxidase and the 8α -(N^3 -histidyl)-FAD of VAO and 6-hydroxy-D-nicotine oxidase.

In the framework of a project devoted to the analysis of flavoenzyme structure and function (12,13), we describe the crystal structure of VAO in the native state and in complexes formed with the competitive inhibitors isoeugenol (2-methoxy-4-(1-propenyl)phenol), *p*-cresol (4-methylphenol), 2-nitro-*p*-cresol, and with the reaction product 4-(1-heptenyl)phenol (Fig. 1c). The crystallographic analysis has been accompanied by a microspectrophotometric investigation, aimed at the precise determination of the FAD redox state in the various crystal complexes. These studies are the first step towards the characterisation of the most interesting features of VAO, such as the mechanism and functional role of the covalent flavinylation, the mechanism of FAD-mediated substrate oxidation and the possibility of exploiting the enzyme for the synthesis of compounds of industrial relevance (14). In this regard, it is of note that the gene encoding VAO has been cloned (Benen *et al.*, personal communication) paving the way to protein engineering studies.

10.2. Materials and methods

Crystallisation and crystal soaking

Crystals of VAO were obtained from a solution containing 6% w/v PEG 4000 0.1 M sodium acetate/HCl pH 4.6, using the hanging-drop vapour diffusion method. The crystals belong to space group I4 with cell dimensions $a=b=141$ Å, $c=133$ Å (Table 1). The asymmetric unit contains two VAO subunits related by a non-crystallographic axis perpendicular to the crystallographic *c* axis (26). Preparation of the heavy atom derivatives was hampered by extreme sensitivity of the crystals towards heavy atom containing compounds. Only one suitable derivative was obtained, by soaking a crystal for one hour in a solution containing 0.1 mM mercury acetate. The fragility of VAO crystals probably relates to fact that modification with *p*-mercuribenzoate leads to octamer dissociation and enzyme inactivation (16).

In contrast to the sensitivity towards heavy atom reagents, exposure to active-site ligands did not cause any damage to the crystals. Thus, all the VAO-ligand complexes could

be prepared by soaking in ligand saturated solutions containing 10% w/v PEG 4000, 0.1 M sodium acetate/HCl pH 4.6.

Table 1. Data collection and phasing statistics.

	Soaking time*	Cell axes a=b, c (Å)	Observations	Unique reflections	
Room temp					
Native		140.5, 132.9	86175	20541	
Mercury acetate	1 hour	141.8, 133.5	48825	19231	
2-Nitro- <i>p</i> -cresol	7 days	140.6, 132.5	43741	21522	
Heptenylphenol	1 month	141.0, 133.4	41329	17633	
100K					
Native		130.2, 133.5	330030	38274	
<i>p</i> -Cresol	7 days	128.8, 130.8	193846	27926	
Isoeugenol	7 days	128.4, 130.2	175968	23480	
	Resolution (Å) ⁺	Completeness (%) ⁺	R _{merge} (%) [‡]	R _{iso} (%) [§]	Phasing power [#]
Room temp					
Native	3.2	98.1 (95.5)	10.4 (30.0)		
Mercury acetate	3.2	90.7 (88.3)	8.2 (30.2)	31.4	1.4
2-Nitro- <i>p</i> -cresol	3.1	94.3 (90.1)	6.2 (27.4)	14.0	
Heptenylphenol	3.3	90.7 (86.1)	11.1 (33.9)	15.9	
100K					
Native	2.5	98.9 (98.3)	8.8 (21.0)		
<i>p</i> -Cresol	2.7	95.4 (84.2)	9.7 (31.2)	31.1	
Isoeugenol	2.8	90.6 (83.1)	11.8 (32.2)	27.4	

Data collected at room temperature were measured on an in-house rotating anode, using an RAXIS II imaging plate. Data collected at 100K were measured either at ELETTRA or DESY synchrotron beam lines (see text) using a 180 mm diameter Hendrix-Lentfer imaging plate system. * The concentration of mercury acetate used for the soaking experiment was 0.2 mM; all other soaking experiments were carried out with ligand-saturated solutions. + The values relating to the highest resolution shell are given in brackets. ‡ $R_{\text{merge}} = \sum |I_j - \langle I_j \rangle| / \sum \langle I_j \rangle$, where I_j is the intensity of an observation of reflection j and $\langle I_j \rangle$ is the average intensity for reflection j . § $R_{\text{iso}} = \sum |F_{\text{ph}}| - |F_{\text{p}}| / \sum |F_{\text{p}}|$, where F_{ph} is the structure-factor amplitude for the derivative or ligand-bound crystal and F_{p} is the structure-factor amplitude of a native crystal. The R_{iso} values were calculated with structure-factor amplitudes measured at the same temperature. # Phasing-power = root mean square ($|F_{\text{h}}|/E$), where F_{h} is the calculated structure-factor amplitude due to the heavy atoms and E is the residual lack of closure error.

Data collection

The data sets used for the single-isomorphous-replacement (SIR) phasing calculations and the analysis of the 4-(1-heptenyl)phenol and 2-nitro-*p*-cresol complexes were collected at room temperature using a Raxis II imaging plate system equipped with a Rigaku 200 rotating anode CuK α X-ray source. The images were evaluated using a modified version of MOSFLM (program written by AGW Leslie), whereas the CCP4 suite of programs (27) was used for data reduction (Table 1). The data employed for refinement of the native,

isoeugenol and *p*-cresol structures were collected at 100 K using synchrotron radiation. Data for the native enzyme and *p*-cresol complex were measured at the X-ray diffraction beam line of ELETTRA (Trieste, Italy), while the data set for the VAO—iseoeugenol complex was collected at the BW7B beam line of the EMBL outstation at DESY (Hamburg, Germany). In all cryocrystallographic experiments, 25% w/v PEG 400 was used as cryoprotectant. The data were integrated and scaled with the programs DENZO and SCALEPACK (28). Freezing resulted in a substantial reduction of the unit cell parameters, the length of the *a* and *b* axes being decreased from 141 Å to about 128 Å (Table 1).

SIR phasing and molecular replacement

The data sets used for the SIR phasing calculations were collected at room temperature (Table 1). The difference Patterson map for the mercury derivative was solved using the Patterson superposition option of SHELXS-90 (29). The six heavy-atom sites are close to the sidechains of Cys447, Cys470 and Cys495 of both subunits. The parameters of the mercury sites were refined with the program MLPHARE of the CCP4 package (27). The resulting 3.2 Å SIR phases allowed the local twofold axis to be positioned in the unit cell by means of the "real space translation function" option of GLRF (30). An envelope around the protein could be calculated from a local correlation map (31). The SIR phases were then improved by twofold averaging and solvent flattening using the program DM (32). However, the resulting map was uninterpretable.

While carrying out structure determination, preliminary sequence data suggested an homology between VAO and PCMH (9). Therefore, molecular replacement was attempted using a polyaniline search model derived from the partially refined structure of the PCMH subunit (10; FS Mathews, personal communication). A cross-rotation function calculated with the room temperature native data set resulted in two peaks at 3.3 σ and 3.1 σ above the mean (33). A phased translation function (34) employing the SIR phases was then calculated. Both solutions of the cross-rotation function produced a peak at 10 σ level (second peak at 5 σ), making the interpretation of the phased translation function straightforward. The translated subunits were related by a non-crystallographic symmetry (NCS) operator identical to that previously identified on the basis of the SIR phases, confirming the accuracy of the solution. The properly oriented and translated coordinates of the search model were then subjected to a few cycles of TNT (35) refinement. The resulting model was employed for a molecular replacement calculation using the 100 K data set (Table 1). This procedure revealed that the operator relating the atomic coordinates of the 100 K and room temperature structures correspond to a rotation defined by the polar angles $\kappa=1.7^\circ$, $\phi=96.0^\circ$, $\psi=81.3^\circ$ and a translation $T_x=-8.5$ Å, $T_y=-3.3$ Å, $T_z=1.9$ Å.

Multicrystal density averaging

The large differences between the unit cell parameters of the room temperature and cryocooled crystals (Table 1) raised the possibility of treating them as two different crystal forms in a multicrystal density averaging procedure (36). For this purpose, a protein envelope was defined on the basis of the PCMH coordinates, whereas the starting electron-density maps were derived from the SIR phases. The multicrystal averaging calculations were performed with the program DMMULTI (32) and resulted in a clearly interpretable map. In particular, taking as reference the refined model phases, the mean error of the multicrystal averaged phases is 51° , which is 21° lower than the 72° error of the SIR-twofold averaged phases. It must be stressed that the PCMH coordinates were employed for envelope definition but not for phase calculation, so that the multicrystal averaged maps were completely free of model bias. Freezing did not cause any significant change in the three-dimensional structure despite the large change in the unit cell parameters. In fact, after refinement of the atomic models (see below), the rms differences between the C α atoms of the room temperature and low temperature structures (Tables 1 and 2) turn out to be smaller than 0.41 Å.

Crystallographic refinement

Least squares refinement was carried out with TNT (35) while the program O (37) was used for manual rebuilding of the model. Progress of the refinement was monitored by means of the free R-factor (38), calculated from a set of randomly chosen 1000 reflections omitted from the least squares calculations. Strict NCS constraints were applied to all protein atoms, so that the two crystallographically independent subunits were kept identical. During refinement, the benzene ring and the pyrimidine ring of the flavin were restrained to be planar, but the central ring was allowed to bend or twist. This procedure was applied in order to allow the flavin to adopt a nonplanar conformation. Solvent molecules were included if they had suitable stereochemistry, after inspection of the difference electron-density maps (Table 2). In all investigated complexes, strong and well-defined density peaks allowed modelling the active-site ligands (Fig. 7 and 9). Only in the case of the VAO-iso Eugenol complex, the third carbon atom of the propenyl chain (Fig. 1c) was not well-defined in the density. This probably reflects the presence of a mixture of *cis* and *trans* isomers in the soaking solution, which both bind to the enzyme (4).

The refinement statistics are reported in Table 2. Out of 560 residues of each subunit, only the N-terminal five residues lack continuous density. In the native structure, residues 42-46 are not well defined in density and were not included in the final model. PROCHECK analysis shows that all refined models have stereochemical parameters well within the normal values found in protein structures (Table 2). The Ramachandran plot

shows no residues in the disallowed regions, while 95% of the amino acids fall in the core regions defined by Kleywegt and Jones (39).

Atomic superpositions and model analysis were carried out using programs of the CCP4 package (27). The drawings were generated with the program MOLSCRIPT (40). The program VOIDOO (19) was employed for detection of cavities within the structure.

Table 2. Refinement statistics.

VAO complex	native	<i>p</i> -cresol	isoeugenol	2-nitro- <i>p</i> -cresol	4-heptenyl-phenol
Resolution (Å)*	10.0-2.5	100.0-2.7	100.0-3.1	100.0-3.1	100.0-3.3
Rfactor (%)	22.1	22.2	21.5	20.6	22.5
R _{free} (%) (1000 reflections)	29.7	29.3	29.5	24.9	26.8
Number of protein atoms ⁺	2×4408	2×4452	2×4455	2×4455	2×4458
Number of water molecules	320	107	38	0	0
Rmsd for ideal values [‡]					
bond lengths (Å)	0.016	0.015	0.017	0.006	0.010
bond angles (°)	3.3	3.5	3.1	2.2	2.5
trigonal atoms (Å)	0.010	0.008	0.011	0.006	0.008
planar groups (Å)	0.009	0.009	0.009	0.006	0.006
non bonded atoms (Å)	0.047	0.065	0.064	0.030	0.039
ΔB bonded atoms (Å ²)	7.4	7.2	7.0	8.4	8.4

* All measured reflections were used for refinement (no σ cut-off). ⁺ Refinement was carried out with strict noncrystallographic symmetry constraints (two identical subunits); in all structures, the N-terminal residues (1-5) were disordered and not visible in the electron density maps. Moreover, in the native structure residues 42-46 have poorly defined density and were not included in the final model. [‡] The root mean square deviation (rmsd) from ideal values were calculated using the program TNT (35).

Microspectrophotometric studies and Cl⁻ binding

Single crystal absorption spectra (20) were obtained using a Zeiss MPM800 microspectrophotometer, with crystals in their soaking solution placed in a flow cell with quartz windows. Care was taken to carry out the spectrophotometric experiments in the same conditions employed for the preparation of the crystals used in the data collection. The dissociation constant and the effect of Cl⁻ on the enzyme activity were measured by spectrophotometric assays, as described (4,5).

Accession numbers

The atomic coordinates have been deposited with the Protein Data Bank. The accession codes are 1VAO (native enzyme), 2VAO (VAO—*isoeugenol*), 1AHU (VAO—*p*-cresol), 1AHV (VAO—*nitro-p*-cresol) and 1AHZ (VAO—4-(1-heptenyl)phenol).

10.3. Results and discussion

10.3.1. X-ray analysis

The three-dimensional structure of native VAO has been determined at 2.5 Å resolution using a combination of molecular replacement, isomorphous replacement and density modification techniques. A key step in the structure determination was the application of a phase refinement procedure in which the electron density maps calculated with data collected at room temperature and at 100 K were averaged. In this way, the phase error was decreased from 72° to 51°. The refined native structure (Table 2) has been used as initial model for the refinement of four enzyme•ligand complexes. In all cases, the electron density maps allowed an unambiguous location of the ligand within the enzyme active-site. Inhibitor binding did not induce any significant conformational change, with rms deviations from all C α atoms of the native structure of 0.41 Å, 0.39 Å, 0.37 Å, 0.37 Å for the VAO—2-nitro-*p*-cresol, the VAO—*p*-cresol, the VAO—iso Eugenol and VAO—4-(1-heptenyl)-phenol complexes, respectively. For the description of the overall structure, we shall refer to the native enzyme model, in view of the higher resolution of the relative diffraction data.

10.3.2. Overall structure

Each VAO subunit is made up by two domains (Fig. 2). The larger domain (residues 6-270 and 500-560) forms the FAD binding site and consists of one antiparallel and one mixed β -sheet surrounded by six α helices. The smaller cap domain (residues 271-499) covers the FAD isoalloxazine ring and encompasses a large seven-stranded antiparallel β -sheet flanked on both sides by a total of seven α -helical regions (Fig. 3a). The overall structure of the VAO subunit closely resembles that of PCMH, as indicated by an rms deviation of 1.2 Å for 470 C α atom pairs (31% sequence identity for the amino acids used in the superposition). An in-depth comparison between VAO and PCMH (10) must await the completion of the crystallographic refinement of the PCMH structure.

In addition to the similarity with PCMH, there are a few other lines of evidence to suggest that the folding topology of VAO is shared by other FAD-dependent enzymes. Firstly, PCMH and VAO are members of the family of FAD-dependent oxidoreductases which share a weak, but significant, sequence similarity; these enzymes are therefore likely to display structural similarities (7,8). Secondly, the VAO folding topology resembles that of MurB, a flavoenzyme involved in the biosynthesis of the bacterial cell wall (15). In particular, the FAD-binding domains of VAO and MurB can be superimposed with an rms deviation of 3.9 Å for 256 C α atom pairs (13% sequence identity). This similarity, however, does not extend to the other parts of the structures, the cap domain of VAO being

unrelated to the substrate-binding domain present in MurB (15). Therefore, the FAD-binding domain observed in VAO may be viewed as a sort of "cofactor binding unit" employed by various flavoenzymes, otherwise differing in the rest of their three-dimensional structure.

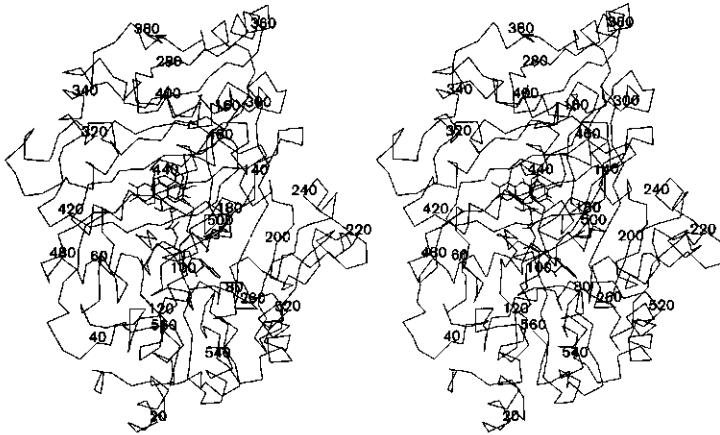


Figure 2. The structure of the VAO subunit. Stereoview of the C α trace of the subunit; every twentieth C α atom is labelled with the residues number. The drawing was produced using the coordinates of the VAO—isoeugenol complex.

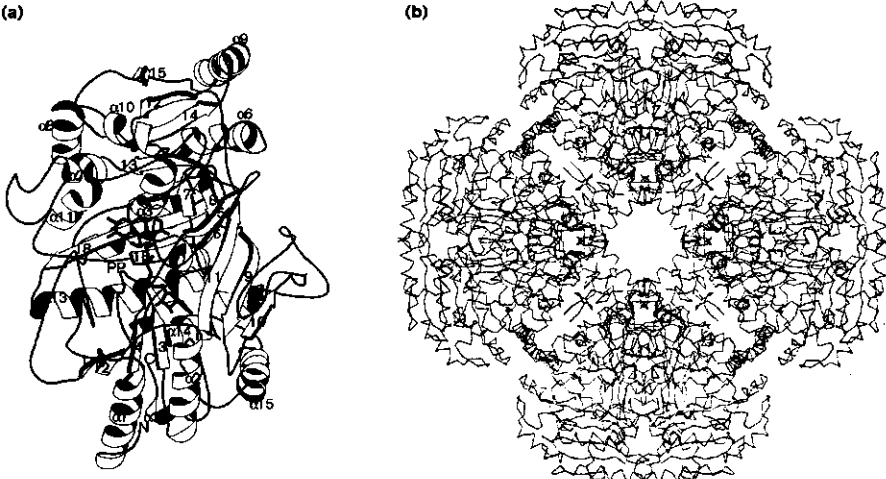


Figure 3. (a) Ribbon drawing of the VAO subunit. The β strands are labelled sequentially by numbers, whereas the α helices are indicated by α followed by a number. FAD is shown in ball-and-stick representation; the position of the PP loop (residues 99-110) is highlighted. (b) The quaternary structure of VAO. C α trace of the eight subunits forming the VAO octamer, viewed along the fourfold axis.

In solution, VAO is an octamer of eight identical subunits. Analysis of the crystal packing reveals that this oligomeric arrangement is maintained in the tetragonal crystals used for structure determination. The octamer has 42 symmetry, with the molecular fourfold axis being coincident with the crystallographic *c* axis. The oligomer can be described as a tetramer of dimers (Fig. 3b) in which each dimer is stabilised by extensive intersubunit contacts, as indicated by the burial of 18% (3950 Å²) of the monomer accessible surface area upon dimer formation. In contrast to the strength of the monomer-monomer interactions, the dimer-dimer contact area is limited to a restricted number of residues. Upon octamer formation, only 5% (1200 Å²) of the monomer accessible surface area becomes buried. This is in keeping with the observation that, in the presence of chaotropic agents, the octamer dissociates to fully active dimers (16).

10.3.3. FAD binding

A cofactor molecule is bound by the FAD domain of each subunit (Fig. 3a). Except for the ribose moiety, all cofactor atoms are solvent inaccessible, being involved in a number of interactions with the protein (Fig. 4). A major role in FAD binding is played by residues 99-110, which form a coil region connecting β strands 3 to 4 (Fig. 3a). This loop (called the "PP loop" in Fig. 3a) contributes to the binding of the adenine portion of FAD and compensates for the negative charge of the cofactor through the formation of hydrogen bonds between the backbone nitrogen atoms of residues Ser101, Ile102, Gly103, Arg104 and Asn105 and the pyrophosphate oxygen atoms (Fig. 4).

VAO is the first enzyme of known structure in which the isoalloxazine ring is linked to the protein by a covalent bond between the flavin C8M atom and the N ϵ 2 atom of His422 (Figs. 4 and 5). The covalent linkage does not perturb the flavin conformation, which is planar. In addition to the covalent bond, the isoalloxazine ring forms several hydrogen bonds with the protein (Figs. 4 and 5). In particular, two charged sidechains interact with the flavin ring: Arg504 and Asp170. Arg504 is engaged in hydrogen bond formation with the flavin O2 atom; as in many flavoenzymes (17), the proximity of a positive charge to the N1-C2=O2 locus stabilises the anionic form of the cofactor which is generated upon reduction (3). More unusual is the second interacting charged residue, Asp170, which is located only 3.5 Å from the flavin N5 position (Fig. 4). It cannot be excluded that in the crystal structure Asp170 may be protonated, given the low pH (4.6) of the crystallisation medium. Asp170 is, however, within hydrogen-bonding distance of Arg398, whose positive charge should favour deprotonation of the aspartic acid carboxylic group. In particular, Asp170 should be ionised at the high pH values (around pH 10) at which VAO turnover is optimal for all investigated substrates (4,5). The proximity of a negatively charged group to the N5 atom is intriguing, as in many flavin-dependent oxidoreductases of

known structure the N5 atom is in contact with a hydrogen-bond donor rather than an acceptor (18). The positioning of Asp170 is such that it could stabilise the reduced flavin by interacting with the protonated N5 atom of the reduced cofactor, thus increasing the FAD redox potential. The protonation state of Asp170, however, may change during catalysis (see below), making the role of this residue in the modulation of the cofactor redox properties even more enigmatic.

The electron-density maps of the native enzyme show a strong peak at $\sim 3.5 \text{ \AA}$ from the *re* side of the flavin. We have interpreted this feature as due to a bound Cl^- ion held in position by the interactions with the backbone nitrogen atoms of Asp170 and Leu171 (Fig. 5). This interpretation is supported by the fact that Cl^- binds to VAO with a dissociation constant (K_d) of 140 mM. Remarkably, in spite of the vicinity to the cofactor, Cl^- binding has only a marginal effect on the enzyme activity, slightly decreasing V_{max} to 80% of its normal value.

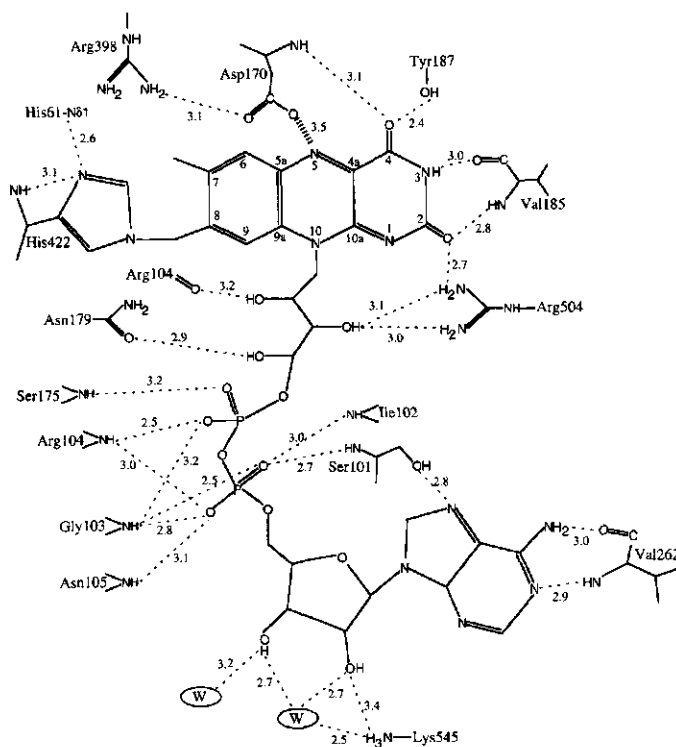


Figure 4. Schematic diagram of the protein-FAD interactions. Hydrogen bonds are indicated by dashed lines. The interatomic distances are shown in Å and refer to the native VAO structure. The Asp170-N5 contact is highlighted because of its particular relevance for the catalytic reaction.

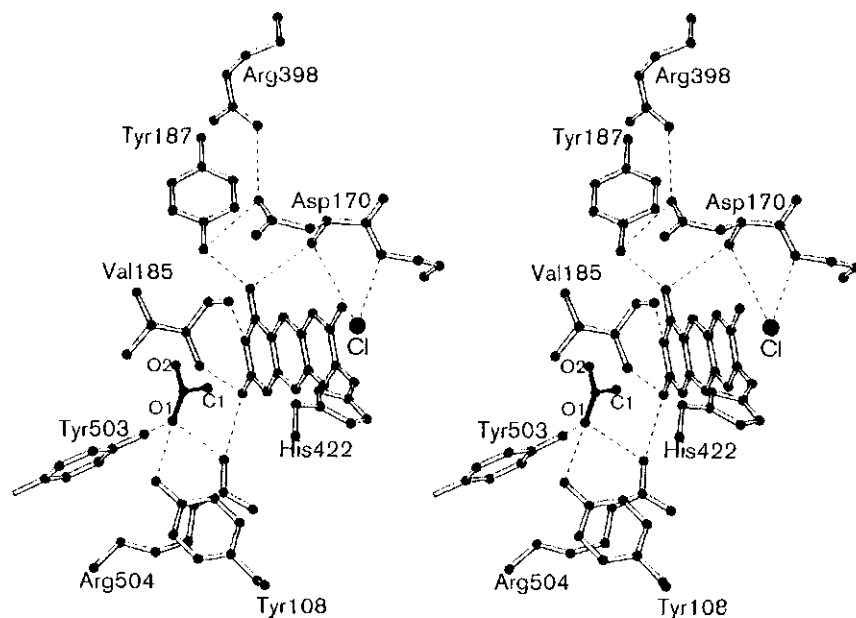


Figure 5. Stereoview drawing of the active-site residues and isoalloxazine ring in the native VAO structure. The putative acetate ion (see text) is shown in black ball-and-stick form; hydrogen bonds are represented by dashed lines. With respect to Figure 2, the molecule has been rotated by 30° about the vertical axis.

10.3.4. Catalytic centre

The VAO catalytic centre (Fig. 5) is located on the *si* side of the flavin ring and is delimited mainly by hydrophobic and aromatic residues. In the native enzyme, the active-site is occupied by a number of ordered solvent molecules. Furthermore, an electron-density peak, too large to be accounted for by a water molecule, has been tentatively assigned to an acetate ion, which is located 4.1 Å from the flavin ring and is hydrogen bonded to the sidechains of Tyr108, Tyr503 and Arg504 (Fig. 5).

A surprising feature emerging from the analysis of the three-dimensional structure of VAO is that the active-site is completely solvent inaccessible. In fact, the shape of the catalytic centre is that of a closed elongated cavity having a volume (19) of approximately 200 Å³ (Fig. 6). Inspection of the protein structure does not suggest any obvious structural element, whose conformational change may allow substrate admission into the active-site. In this context, it is remarkable that all VAO—inhibitor complexes were generated by soaking experiments, indicating that the conformational changes required for substrate binding are tolerated by the crystal lattice.

methoxy group would collide against Phe424 and Ile468, thus preventing binding to the enzyme.

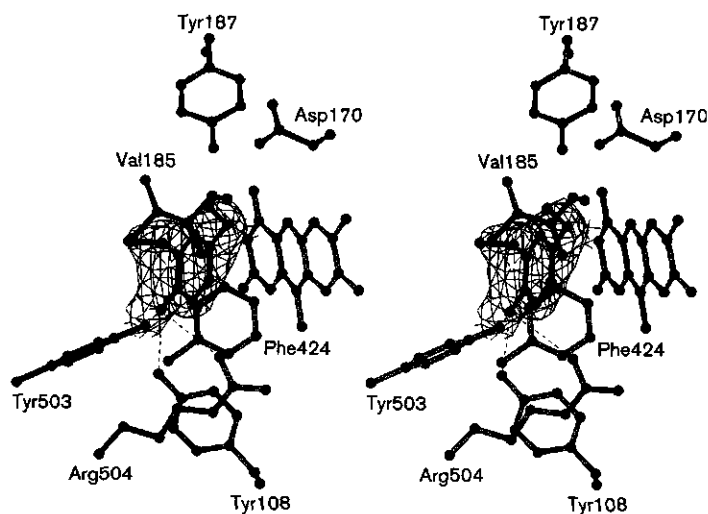


Figure 7. Stereoview drawing of the $2F_0-F_c$ map for isoeugenol bound to VAO; the contour level is 1σ . The isoeugenol atoms were omitted from the phase calculation, but otherwise the coordinates of the final model were used for structure-factor calculation. The dashed lines outline the hydrogen bonds between the inhibitor and the protein. The orientation of the figure is the same as for Figure 5.

10.3.7. The VAO—*p*-cresol adduct

p-Cresol (Fig. 1c) is a slowly catalysed substrate of VAO ($k'_{cat}=0.01\text{ s}^{-1}$) and its binding results in the stabilisation of an intermediate complex in which the flavin is reduced (5). This fact is particularly noticeable because such a complex is stable in the presence of oxygen, which normally reoxidises the cofactor very quickly. Given these peculiar properties, the reactivity of *p*-cresol towards the crystalline enzyme was investigated by single crystal microspectrophotometry (20). In agreement with the solution studies, the spectra indicated that *p*-cresol binding results in the generation of a reduced form of the cofactor (Fig. 8). Remarkably, the reaction proceeds very slowly, the FAD reduction being completed only after more than two days. Such a slow speed does not seem to be an intrinsic property related to the crystalline state, as dithionite is able to reduce the crystalline enzyme within a few seconds (Fig. 8). Moreover, the differences between the spectra of the crystals soaked in dithionite and *p*-cresol, indicate substantial variations in the structure and environment of the reduced flavin. In particular, in the VAO—*p*-cresol complex, the absorption maximum around 370 nm and the residual absorbance at 439 nm are consistent with the formation of a covalent adduct between the substrate and the flavin N5 atom (21).

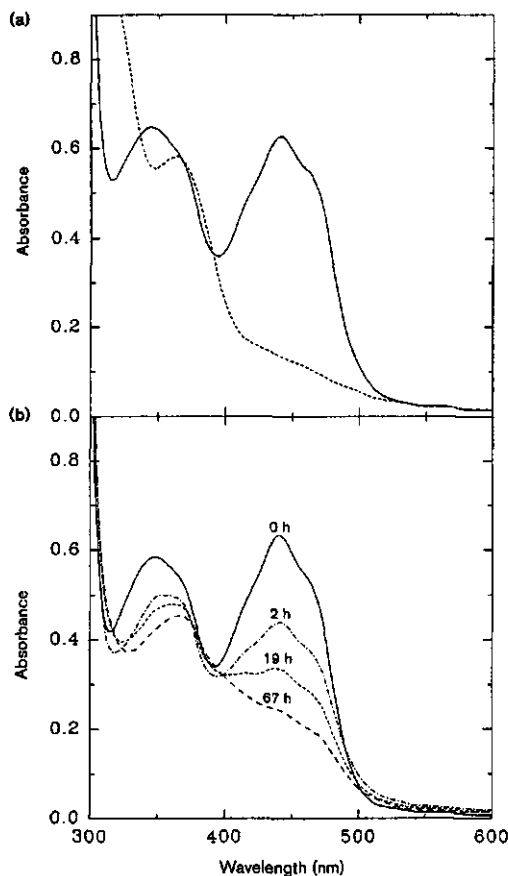


Figure 8. Polarised absorption spectra of VAO crystals. Polarised absorption spectra were recorded along two perpendicular directions on a crystal face that shows very weak birefringence. As the two spectra were very similar, only spectra recorded in one direction are presented. (a) Single crystal polarised absorption spectra of VAO crystals suspended in a solution containing 100 mM sodium acetate pH 4.6, 12% w/v PEG 4000 in absence (continuous line) and presence (dashed line) of sodium dithionite. The removal of dithionite led to the recovery of the oxidised enzyme (not shown). (b) Polarised absorption spectra of VAO crystals soaked in *p*-cresol were recorded 0, 2, 19 and 67 hours after starting the soaking experiment. After 67 hours, crystals were suspended in the same soaking solution but containing sodium dithionite; no spectral changes were observed (not shown). When these crystals were suspended in the standard storage solution (containing no *p*-cresol), spectra indicated a slow recovery of the oxidised enzyme.

The electron-density map of enzyme—*p*-cresol complex (Fig. 9) revealed a strong peak located on the flavin *si* side and connected to the cofactor N5 position by a stretch of continuous density. In the light of the microspectrophotometric data, this feature was taken as an indication of a covalent adduct between the *p*-cresol methyl group and the flavin N5 atom (Fig. 9). Adduct formation is associated to a distortion of the flavin ring, which deviates from planarity with an angle between the dimethylbenzene and the pyrimidine rings of 8.2° . Except for the flavin distortion, however, the presence of the adduct does not induce any conformational change in the active-site, the rms difference from the catalytic residues of the native structure being 0.39 \AA .

VAO is unusual in that it does not react with sulphite (3), which forms an N5 covalent adduct in most flavin-dependent oxidases (17). The structure of the VAO—*p*-cresol complex shows that the N5-bound C α atom is located 3.4 \AA from Asp170. Thus, a sulphite group covalently bound to the flavin would make a highly unfavourable contact with Asp170, suggesting that electrostatic repulsion of this acidic sidechain is the likely cause of the unusual lack of reactivity of VAO towards sulphite.

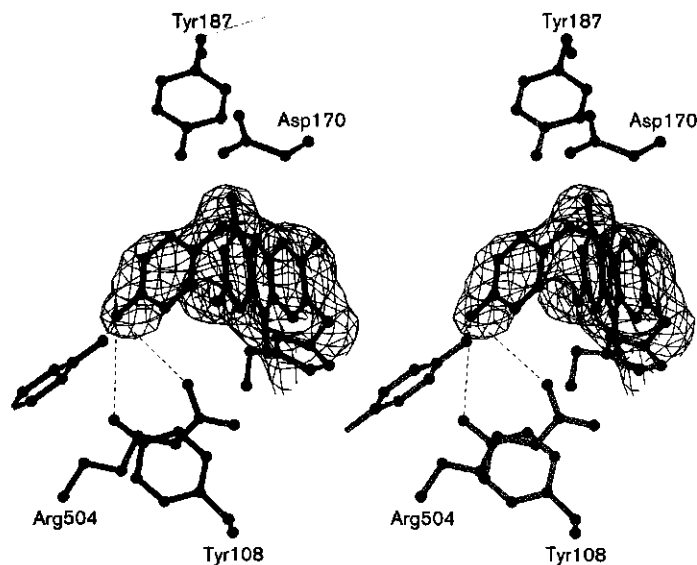


Figure 9. Stereoview drawing of $2F_o-F_c$ map for the FAD-*p*-cresol adduct; the contour level is 1σ . The inhibitor and flavin atoms were omitted from phase calculation, but otherwise the coordinates of the final model were used for structure-factor calculation. The dashed lines depict the hydrogen bonds between *p*-cresol and the protein atoms.

10.3.8. The catalytic mechanism

Kinetic and spectroscopic studies (4,22) suggest that substrate oxidation proceeds via direct hydride transfer from the $C\alpha$ atom to N5 of the FAD. Formation of the resulting *p*-quinone methide intermediate (Fig. 1a) is thought to be facilitated by the preferential binding of the phenolate form of the substrate (pK_a of isoeugenol < 6). The VAO—*isoeugenol* (Fig. 7) and VAO—2-nitro-*p*-cresol complexes reveal that the enzyme achieves hydride transfer by positioning the ligand $C\alpha$ atom 3.5 Å from N5. Moreover, the inhibitor hydroxyl oxygen is hydrogen bonded to three residues, Arg504, Tyr503 and Tyr108, which are ideally located to stabilise the phenolate negative charge (Figs. 7 and 10). The propensity of these sidechains for binding anionic molecules is further underlined by the presence, in the native structure, of an acetate ion directly interacting with the phenolate-binding cluster (Fig. 6).

Under anaerobic conditions, reaction with 4-(methoxymethyl)phenol leads to a stable reduced enzyme—*p*-quinone methide complex (Fig. 10) (22). Only after exposure to oxygen and consequent FAD reoxidation, is the reaction completed with synthesis and release of the final oxidised product (Fig. 10). The three-dimensional structure of VAO suggest that charge balancing between the flavin, the quinone intermediate and Arg504 may determine the sequence of the catalytic steps. In fact, in addition to the interaction with the

phenolate oxygen, Arg504 is well positioned to stabilise a negative charge on the N1-C2=O2 locus of the anionic reduced cofactor (Figs. 4 and 5). Flavin C2, however, is located $\sim 4 \text{ \AA}$ from the expected position of the oxygen atom of the *p*-quinone methide molecule bound to the reduced enzyme (Fig. 7). Therefore, in the reduced enzyme, electrostatic repulsion by the negative charge of the flavin C2 locus should prevent formation of the phenolate ion, thus stabilising the quinone form of the intermediate (Fig. 10). On the contrary, upon flavin reoxidation, Arg504 is deprived of an anionic partner, triggering the development of a negative charge on the quinone oxygen atom (Fig. 10). In this way, the electrophilicity of the methide carbon is increased, facilitating hydroxylation (as for the 4-(methoxymethyl)phenol; Fig. 10) or deprotonation (as for vanillyl-alcohol, Fig. 1a) of the intermediate, producing the final product.

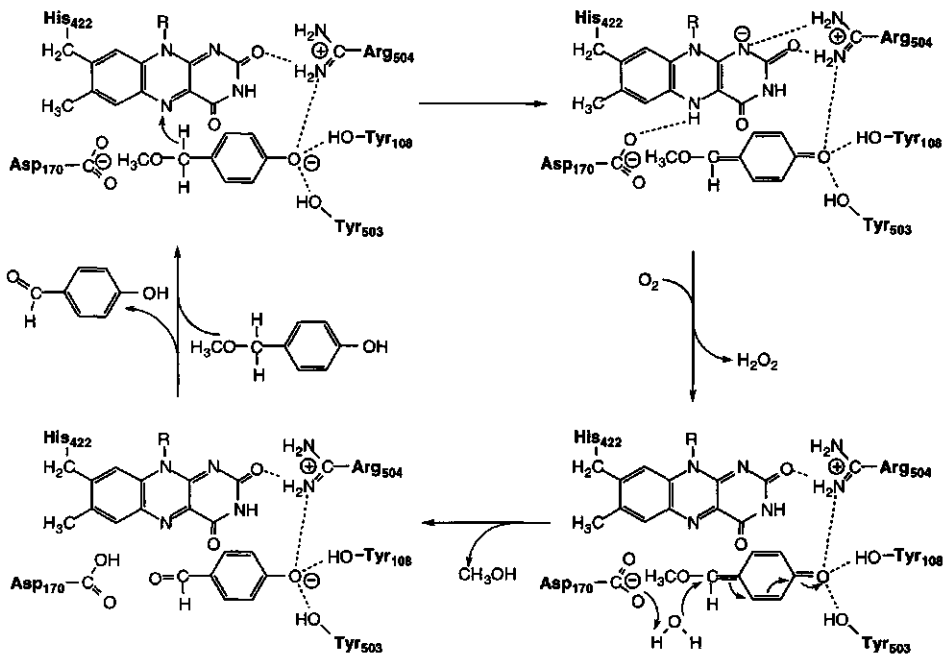


Figure 10. The reaction mechanism for the oxidation of 4-(methoxymethyl)-phenol. In the first step, the substrate is oxidised via a direct hydride transfer from the substrate C_{α} atom to N5 of the flavin. The reduced cofactor is then reoxidised by molecular oxygen with the production of a hydrogen peroxide molecule. In the next step, the *p*-quinone-methoxymethide intermediate is hydroxylated by a water molecule, possibly activated by Asp170. The resulting 4-hydroxybenzaldehyde and methanol products are released.

In all VAO structures investigated, the flavin N5 atom is within $3.4\text{--}3.6 \text{ \AA}$ of the sidechain of Asp170 (Figs. 4 and 7). This sidechain could function in catalysis as an active-site base, either activating the water attacking the substrates undergoing hydroxylation

(e.g. 4-(methoxymethyl)phenol; Fig. 10) or deprotonating the *p*-quinone methide intermediate in the case of substrates being dehydrogenated by the enzyme (e.g. vanillyl-alcohol, Fig. 1a). It cannot, however, be excluded that the p*K*_a of Asp170 is shifted upwards by the enzyme, so that the sidechain is protonated, simply acting as hydrogen bond donor to flavin N5. It is evident that site-directed mutagenesis experiments need to be carried out in order to resolve the enigmatic role of this unusually located aspartate residue.

Reaction of the crystalline enzyme with *p*-cresol results in a stable covalent adduct between this substrate analogue and the reduced flavin (Figs. 8 and 9). Stabilisation of the phenolate ion is expected to facilitate the nucleophilic attack of the methyl carbon on the flavin N5 position, leading to covalent adduct formation. Moreover, the sidechain of Asp170 could function as the base which abstracts the *p*-cresol α proton. Comparison between the VAO—isoeugenol and VAO—*p*-cresol complexes reveals an interesting difference in the orientation of the aromatic ring of the two ligands. The covalent bond forces *p*-cresol to be oriented towards the cofactor, making an angle of 34° with the flavin, whereas isoeugenol is less tilted with respect to the FAD, with an angle of 18° between the inhibitor and isoalloxazine planes. This difference is relevant to the question as to why only *p*-cresol is able to form an adduct, whereas phenol compounds having either an ethyl or propyl substituent are regular VAO substrates (5). A modelling experiment showed that, if the methyl group of *p*-cresol were replaced by an ethyl substituent (e.g. 4-ethylphenol), the additional methyl group would make an unfavourable contact (< 2.4 Å) with either the flavin or Asp170 atoms. The same argument can be extended to also explain why 2-nitro-*p*-cresol does not form a covalent adduct: in this case, if the inhibitor plane were in the orientation required for adduct formation, the nitro substituent would make a short contact with Val185 (Fig. 7). Thus, the steric restrictions imposed by the shape of the active-site cavity are a key factor for preventing enzyme inactivation through covalent adduct stabilisation.

10.3.9. Substrate burying: a recurrent theme in flavoenzyme catalysis

The VAO catalytic reaction takes place in the solvent-protected environment provided by the active-site cavity. This strategy fulfils different concurrent reaction goals: the cavity has a rather rigid architecture, limiting size and structure of the active-site ligands; a solvent-protected environment is suited for binding the poorly soluble and hydrophobic VAO substrates; the low dielectric constant of the catalytic medium strengthens the electrostatic and polar interactions, which activate the substrate through phenolate formation; and a solvent inaccessible catalytic site is thought to effect the hydride transfer step leading to substrate oxidation. In this regard, it is fascinating that the strategy of embedding substrates and catalytic groups inside a solvent-protected site has been developed by a number of

flavin-dependent oxidases and oxidoreductases such as cholesterol oxidase (23), D-amino acid oxidase (12), dihydroorotate dehydrogenase (24) and medium acyl-CoA dehydrogenase (25). All of these enzymes use this feature to catalyse substrate oxidation/reduction via an hydride transfer mechanism. In several of these enzymes (i.e. cholesterol oxidase, D-amino acid oxidase and dihydroorotate dehydrogenase) a loop changes conformation during the catalytic cycle, thus controlling the accessibility of the catalytic site. Analysis of the VAO structure, however, does not unambiguously reveal any structural element to act as an active-site gate. We shall address this problem by a combination of site directed mutagenesis and structural studies.

10.3.10. Biological implications

Flavoenzymes are involved in a variety of chemical processes, ranging from simple redox reactions to DNA repair and light emission. In spite of this broad spectrum of activity, flavoenzymes can be grouped into a small number of classes, the members of which share various biochemical properties.

The oxidase class is characterised by the ability of the reduced flavin to react very rapidly with oxygen; the aryl-alcohol oxidases are fungal enzymes involved in the oxidation of aromatic compounds derived from the degradation of lignin. These aryl alcohol oxidases typically display a broad substrate specificity, reflecting the highly heterogeneous composition of the lignin biopolymer. We report here the structure of vanillyl-alcohol oxidase (VAO), which is the first structure of a flavin-containing aryl-alcohol oxidase to be determined. VAO catalyses the oxidation of a vast array of phenolic compounds, ranging from various 4-alkylphenols to 4-hydroxybenzyl alcohols and 4-hydroxybenzylamines. VAO consists of eight identical subunits assembled into an oligomer having 42 symmetry. Each subunit consists of two domains, which bind the flavin isoalloxazine ring at their interface. The folding topology of VAO closely resembles that of the flavoenzyme *p*-cresol methylhydroxylase and is likely to be shared by the members of a recently discovered family of evolutionary related flavin-containing oxidoreductases.

In VAO, the flavin ring is covalently bound to His422; covalent attachment is not associated to any distortion of the flavin, which is planar. This observation is relevant for the design of semisynthetic enzymes, made highly stable by the covalent linkage of the cofactor. Such semisynthetic proteins would be particularly suitable for biotechnological applications.

The crystal structures of four VAO—ligand complexes reveal the remarkable architecture of the VAO active-site, which comprises a completely solvent inaccessible, elongated cavity. The binding mode of the ligands within this catalytic cavity is compatible with substrate oxidation occurring via direct hydride transfer from the substrate C α atom to

the flavin N5. Moreover, on the surface of the cavity, the sidechains of Tyr108, Tyr503 and Arg504 form an anion-binding site, that activates the substrate through the stabilisation of its phenolate form.

The burial of the substrate underneath the protein surface is an emerging theme, common to several flavin-dependent enzymes. The VAO structure reveals how this feature is instrumental to the control of the substrate specificity and effects the hydride transfer reaction leading to substrate oxidation.

Acknowledgements

We thank Prof. F.S. Mathews (Washington University, St. Louis) for providing us with the PCMH coordinates and Dr. J. Visser and Dr. J.A.E. Benen (Wageningen University) for the VAO amino acid sequence. We are indebted to all members of the Pavia protein crystallography group for a number of useful suggestions throughout the development of the project. The supervision of the EMBL/DESY staff during synchrotron data collection is gratefully acknowledged. This research was supported by a grant from the Consiglio Nazionale delle Ricerche (Contract n° 9502989CT14) to A.M.. We thank the European Union for support at the EMBL/DESY, through Human Capital Mobility Program to Large Scale Installations Project, Contract CHGE-CT93-0040.

9.4. References

1. Kirk T.K. & Farrell, R.L. (1987). Enzymatic "combustion": the microbial degradation of lignin. *Ann. Rev. Microbiol.* **41**, 465-505.
2. De Jong, E., Field, J.A. & de Bont, J.A.M. (1994). Aryl alcohols in the physiology of ligninolytic fungi. *FEMS Microbiol. rev.* **13**, 153-188.
3. De Jong, E., van Berkel, W.J.H., van der Zwan, R.P. & de Bont, J.A.M. (1992). Purification and characterization of flavin-dependent vanillyl-alcohol oxidase from *Penicillium simplicissimum*. *Eur. J. Biochem.* **208**, 651-657.
4. Fraaije, M.W., Veeger, C. & van Berkel, W.J.H. (1995). Substrate specificity of flavin-dependent vanillyl-alcohol oxidase from *Penicillium simplicissimum*. *Eur. J. Biochem.* **234**, 271-277.
5. Fraaije, M.W., Drijfhout, F., Meulenbeld, G.H., van Berkel, W.J.H. & Mattevi, A. (1997) Vanillyl-alcohol oxidase from *Penicillium simplicissimum*: Reactivity with *p*-cresol and preliminary structural analysis, in *Flavins and flavoproteins XII* (Stevenson, K., Massey, V., and Williams, C.H. jr, eds.), pp. 261-264, University Press, Calgary.
6. Fraaije, M.W., Pikkemaat, M. & van Berkel, W.J.H. (1997). Enigmatic gratuitous induction of the covalent flavoprotein vanillyl-alcohol oxidase in *Penicillium simplicissimum*. *Appl. Environ. Microbiol.* **63**, 435-439.
7. Mushegian, A.R. & Koonin, E.V. (1995). A putative FAD-binding domain in a distinct group of oxidases including a protein involved in plant development. *Protein Science* **4**, 1243-1244.
8. Murzin, A.G. (1996). Structural classification of proteins: new superfamilies. *Curr. Opin. Struct. Biol.* **6**, 386-394.
9. Xia, Z.X. & Mathews, F.S. (1990). Molecular structure of flavocytochrome *b*₂ at 2.4 Å resolution. *J. Mol. Biol.* **212**, 837-863.
10. Kim, J., Fuller, J.H., Kuusk, V., Cunane, L., Chen, Z., Mathews, F.S. & McIntire, W.S. (1995). The cytochrome subunit is necessary for covalent FAD attachment to the flavoprotein subunit of *p*-cresol methylhydroxylase. *J. Biol. Chem.* **270**, 31202-31209.
11. Stocker, A., Hecht, H.J., Buckmann, A.F. (1996). Synthesis, characterisation and preliminary crystallographic data of N⁶-(6-carboamylhexyl)-FAD D-amino acid oxidase: a semisynthetic oxidase. *Eur. J. Biochem.* **238**, 519-528.

12. Mattevi, A., Vanoni, M.A., Todone, F., Rizzi, M., Teplyakov, A., Coda, A., Bolognesi, M. & Curti, B. (1996). Crystal structure of D-amino acid oxidase: a case of active site mirror-image convergent evolution with flavocytochrome *b*₂. *Proc. Natl. Acad. Sci. USA* **93**, 7496-7501.
13. Entsch, B. & van Berkel, W.J.H. (1995). Structure and mechanism of *para*-hydroxybenzoate hydroxylase. *FASEB J.* **9**, 476-483.
14. van Berkel, W.J.H., Fraaije, M.W., De Jong, E. (1997). Process for producing 4-hydroxycinnamyl alcohols. European Patent application 0710289B1.
15. Benson, T.E., Filman, D.J., Walsh, C.T. & Hogle, J.M. (1995). An enzyme-substrate complex involved in bacterial cell wall biosynthesis. *Nat. Struct. Biol.* **2**, 644-653.
16. Fraaije, M.W., Mattevi, A. & van Berkel, W.J.H. (1997). Mercuration of vanillyl-alcohol oxidase from *Penicillium simplicissimum* generates inactive dimers. *FEBS Lett.* **402**, 33-35.
17. Ghisla, S. & Massey, V. (1989) Mechanisms of flavoprotein-catalyzed reactions. *Eur. J. Biochem.* **181**, 1-17.
18. Fox, K.M. & Karplus, P.A. (1994). Old yellow enzyme at 2 Å resolution: overall structure, ligand binding, and comparison with related flavoproteins. *Structure* **2**, 1089-1105.
19. Kleywegt, G.J. & Jones, T.A. (1994). Detection, delineation, measurement and display of cavities in macromolecular structures. *Acta Cryst. D* **50**, 178-185.
20. Mozzarelli, A. & Rossi, G.L. (1996). Protein function in the crystal. *Annu. Rev. Biophys. Biomol. Struct.* **25**, 343-365.
21. Ghisla, S., Massey, V. & Choong, Y.S. (1979). Covalent adducts of lactate oxidase. Photochemical formation and structure identification. *J. Biol. Chem.* **254**, 10662-10669.
22. Fraaije, M.W. & van Berkel, W.J.H. (1997). Catalytic mechanism of the oxidative demethylation of 4-(methoxymethyl)phenol by vanillyl-alcohol oxidase. *J. Biol. Chem.* **272**, 18111-18116.
23. Li, J., Vrieland, A., Brick, P. & Blow, D. (1993). Crystal structure of cholesterol oxidase complexed with a steroid substrate: implications for flavin adenine dinucleotide dependent alcohol oxidases. *Biochemistry* **32**, 11507-11515
24. Rowland, P., Nielsen, F.S., Jensen, K.F. & Larsen, S. (1997). The crystal structure of the flavin containing enzyme dihydroorotate dehydrogenase A from *Lactococcus lactis*. *Structure* **5**, 239-252.
25. Kim, J., Wang, M. & Paschke, R. (1993). Crystal structures of medium-chain acyl-CoA dehydrogenase from pig liver mitochondria with and without substrate. *Proc. Natl. Acad. Sci. USA* **90**, 7523-7527.
26. Mattevi, A., Fraaije, M.W., Coda, A. & van Berkel, W.J.H. (1997). Crystallization and preliminary X-ray analysis of the flavoenzyme vanillyl-alcohol oxidase from *Penicillium simplicissimum*. *Proteins* **27**, 601-603.
27. Collaborative Computational Project Number 4. (1994). The CCP4 suite: programs for protein crystallography. *Acta Cryst. D* **50**, 760-767.
28. Otwinoski, Z. & Minor, W. (1993). *DENZO: A film processing program for macromolecular crystallography*. Yale University, New Haven, CT.
29. Sheldrick, G.M. (1991). Heavy atom location using SHELXS-90. In *Isomorphous replacement and anomalous scattering: proceedings of the CCP4 study weekend 25-26 January 1991*. (Wolf, W., Evans, P.R. & Leslie, A.G.W. eds.), pp. 23-38, SERC Daresbury Laboratory, Warrington, UK.
30. Tong, L. & Rossmann, M.G. (1990). The locked rotation function. *Acta Cryst. A* **46**, 783-792.
31. Podjarny, A.D. & Rees, B. (1991). Density modification: theory and practice. In *Crystallographic computing 5: from chemistry to biology*. (Moras, D., Podjarny, A.D. & Thierry, J.C., eds.), pp. 361-372, Oxford University Press, Oxford, UK.
32. Cowtan, K.D. & Main, P. (1996). Phase combination and cross validation in iterated density-modification calculations. *Acta Cryst. D* **52**, 43-48.
33. Navaza, J. (1994). AMORE: an automated procedure for molecular replacement. *Acta Cryst. A* **50**, 157-163.
34. Read, R.J. & Schierbeek, A.J. (1988). A phased translation function. *J. Appl. Cryst.* **21**, 490-495.
35. Tronrud, D.E., Ten Eyck, L.F. & Matthews, B.W. (1987). An efficient general-purpose least-squares refinement program for macromolecular structures. *Acta Cryst. A* **43**, 489-501.
36. Rossmann, M.G. (1990). The molecular replacement method. *Acta Cryst. A* **46**, 73-82.
37. Jones, T.A., Zou, J.Y., Cowan, S.W. & Kjeldgaard, M. (1991). Improved methods for building models in electron density maps and the location of errors in these models. *Acta Cryst. A* **47**, 110-119.

38. Brünger, A.T. (1992). Free R value: a novel statistical quantity for assessing the accuracy of crystal structures. *Nature* **355**, 472-475.
39. Kleywegt, G.J. & Jones, T.A. (1996). Phi/Psi-chology: Ramachandran revisited. *Structure* **4**, 1395-1400.
40. Kraulis, P.J. (1991). MOLSCRIPT: a program to produce both detailed and schematic plots of protein structures. *J. Appl. Cryst.* **24**, 946-950.

11

A novel oxidoreductase family sharing a conserved FAD binding domain

**Sequence analysis revealed a novel flavoprotein family which includes several
oxidases containing a covalently bound FAD**

Marco W. Fraaije, Andrea Mattevi, Jacques A.E. Benen,
Jaap Visser and Willem J.H. van Berkel

Modified version submitted to *Trends in Biochemical Sciences*

Introduction

Most flavin dependent enzymes contain a dissociable FAD molecule which is tightly bound. A well-known dinucleotide binding domain observed in many FAD binding proteins is represented by the Rossmann fold¹. This fold contains a $\beta\alpha\beta$ -motif involved in binding the ADP moiety of the FAD molecule. However, also some other structural motifs capable of binding FAD have been identified². Furthermore, it has been found that in some cases the isoalloxazine ring of the flavin is covalently linked to an amino acid of the polypeptide chain. At present, 5 different types of covalent flavin binding have been observed³.

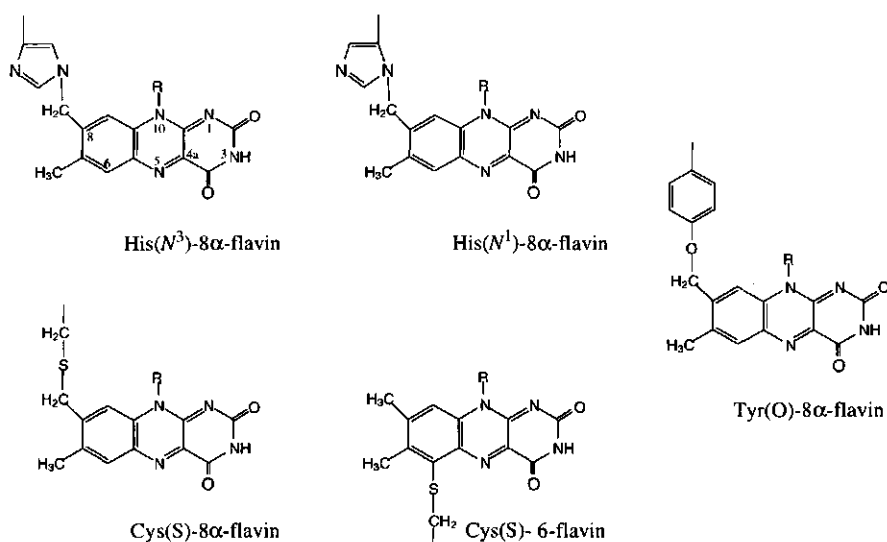


Figure 1. Aminoacyl-flavin bonds observed in flavoproteins. R : ribityl-5'-phosphate for FMN and ribityl-5'-diphosphoadenosine for FAD.

In all these cases a histidine, cysteine or a tyrosine is involved in the covalent attachment (Fig. 1). Linkage to a histidine is by far the most favored as of all covalent flavoproteins discovered (± 30) the majority contains a histidyl bound FAD⁴. Remarkably, covalent binding of FAD is not a prerequisite for activity as has been shown by mutagenesis studies⁵. Recently, it was shown that covalent flavinylation of apoenzyme is an autocatalytic process for which the exact mechanism is still obscure as is the rationale for covalent binding^{6,7,8}. By sequence homology analysis and inspection of the crystal structures of two covalent flavoproteins, we have identified a novel FAD binding domain which is shared by many covalent flavoproteins.

Sequence homology

Recently, we solved the first crystal structure of an 8α -(N^3 -histidyl)-FAD containing flavoprotein; vanillyl-alcohol oxidase (VAO)⁹. This octameric enzyme catalyzes the oxidation of a variety of phenolic compounds enabling the fungus *Penicillium simplicissimum* to grow on some lignin derived metabolites^{10,11}. With the recently solved primary structure of VAO (Benen et al., submitted), a computer-assisted sequence comparison analysis was performed using the BLASTP program¹². Sequence homology was found with *p*-cresol methylhydroxylase (PCMH) from *Pseudomonas putida*, D-lactate dehydrogenase (DLD) from yeast, L-gulonon- γ -lactone oxidase (GLO) from rat, glycolate oxidase subunit D (GLCD) from *Escherichia coli* and several unidentified gene products. Interestingly, the enzymes mentioned above are FAD-dependent enzymes and of similar length. Furthermore, it had already been noted that GLO shows sequence homology with some other flavoenzymes and uncharacterized open reading frame products^{13,14} including DLD from yeast (25% sequence identity)¹⁵ and alkyl-dihydroxyacetonephosphate synthase (ADPS) from human and guinea pig (15% sequence identity)¹⁶. The regions of these homologs with most conservation were used for a more extensive search. As a result, a group of 44 homologous protein sequences was found. In Figure 2, an alignment of the sequences of which the gene products have been identified is shown. All other related sequences represent enzyme analogs or unidentified gene products (legend Fig. 2). Except for a few N- or C-terminal extensions all sequences encode proteins containing about 500 amino acids. Regions with homology were found in the N-terminal halves and at the very end of the C-termini. The region without any significant overall homology separating the two conserved regions has a typical length of about 240 residues. Except for a few sequences, the length of the extensions at the termini relative to the two major conserved regions is restricted in size; 1-27 residues at the C-terminus and 20-70 residues at the N-terminus. For DLD from *Kluyveromyces lactis*, the relatively long N-terminal extension probably represents a presequence of about 90 residues which contains information to target the protein to the mitochondria¹⁵. The N-terminus of ADPS contains a cleavable presequence containing a peroxisomal targeting signal¹⁶.

Novel flavoprotein family

The sequence analysis has revealed a family of related flavoproteins, which are found in all life forms (animals, plants, fungi, archea, and eubacteria). Members of this family which have been so far characterised, contain FAD as cofactor and catalyze an oxidoreductase reaction, though they are involved in highly diverse metabolic pathways.

VAO and PCMH both are involved in the oxidation and hydroxylation of aromatic compounds^{11,17}. GLO is involved in the oxidation of L-gulonolactone by which most animals are able to generate ascorbic acid *de novo*¹⁸. Similarly, yeasts convert L-galactonolactone by action of D-arabino-1,4-lactone oxidase (DALO)¹⁹. 6-Hydroxy-D-nicotine oxidase (HDNO) activity is essential for microbial degradation of nicotinoids²⁰ and the plant enzyme berberine bridge enzyme (BBE) oxidizes S-reticuline and related alkaloids²¹. The *mcrA* gene from *Streptomyces lavendulae* has been proposed to represent an oxidase (MMCO) able to convert a reduced form of the antitumor antibiotic agent mitomycin C¹³. The FASC-gene product from *Rhodococcus fascians* is involved in fasciation of host plants²². Hexose oxidase (HOX) from the red alga *Chondrus crispus* oxidizes a range of aldose sugars^{23,24} and concomitantly forms hydrogen peroxide inhibiting growth of competing green alga. Mitochondrial DLD from *Kluyveromyces lactis* enables the yeast to utilise D-lactate as a carbon source¹⁵ and GLCD from *Escherichia coli*²⁵ is similarly involved in the metabolism of glycolate. The peroxisomal enzyme ADPS from guinea pig, which is involved in ether phospholipid synthesis, has recently been cloned and sequenced¹⁶. No cofactors have yet been identified in MMCO, FASC and ADPS. However, our results suggest that also these enzymes are flavin-dependent.

Conserved FAD binding domain

Compelling evidence that the homologous sequences represent a structurally related family comes from inspection of the three-dimensional structure of VAO and comparison with the crystal structures of the bacterial flavoenzymes, PCMH²⁶ and UDP-N-acetylenolpyruvylglucosamine reductase (MurB), a bacterial flavoenzyme involved in cell wall biosynthesis²⁷. The crystallographic analysis has revealed the composite nature of the VAO subunit, which consists of two domains forming the active site at their interface (Fig. 3). The FAD binding domain (residues 1-270 and 500-560) provides the cofactor binding site whereas the so-called cap domain (residues 271-499) covers the catalytic centre and forms the substrate binding site. A similar topology characterises the structure of the flavoprotein subunit of the flavocytochrome PCMH²⁶, which shares 31% sequence identity to VAO. From the inspection of the three-dimensional structures of the two related enzymes, it is evident that the regions conserved among the members of the oxidoreductase family represent a conservation of the FAD-binding domain (Fig. 3). When relating the sequence alignment to the three-dimensional structure of VAO it is apparent that several conserved residues are involved in binding the FAD cofactor (Fig. 2). In particular, a short stretch of small residues forms a loop interacting with the

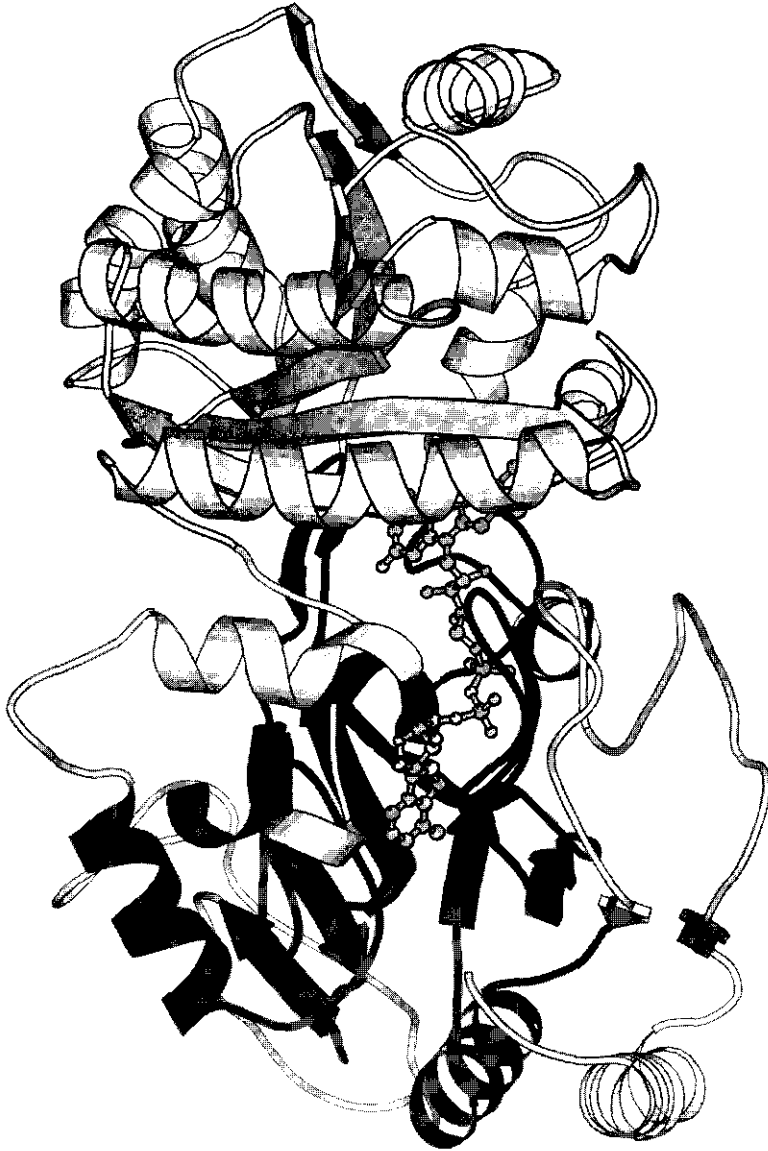


Figure 3. Ribbon diagram of the monomer of VAO from *Penicillium simplicissimum*. The covalently bound FAD is represented in ball-and-stick model. The conserved regions at the protein N- and C-termini are shown as full gray-coloured ribbons. The figure was rendered with MOLSCRIPT²⁹.

pyrophosphate portion of FAD⁹. Furthermore, several conserved glycines are involved in interactions with the ADP moiety or the isoalloxazine ring of the flavin cofactor. The intervening non-conserved region of about 240 residues exactly corresponds to the cap domain, which, therefore, may differ in topology among the members of the family. In keeping with this hypothesis is the structure of MurB²⁷. MurB has a FAD binding domain topologically identical to that of VAO, while its substrate binding domain is unrelated to the cap domain of VAO⁹. However, the sequence identity between the VAO and MurB flavin binding domains is only 16%, which explains why MurB was not identified to be related to VAO just by sequence comparison analysis.

Covalent flavin binding

Interestingly, several of the above described VAO related enzymes were shown to contain a covalently bound FAD. For HDNO and BBE, it is known to which residue the FAD is covalently bound^{20,21} (Fig. 2). Remarkably, a histidine in a position homologous to the flavinylated histidine of these two covalent flavoproteins is found in 15 (out of 44) members of the family, suggesting that they also are covalently flavinylated. Indeed, GLO, DALO and HOX are known to contain a covalently bound FAD cofactor^{18,19,24}. Furthermore, the position of the flavinylated histidine in HDNO is homologous to Arg₁₀₄ of VAO. Inspection of the three-dimensional structure of VAO reveals that Arg₁₀₄ is close to the 8 α -methyl group of the FAD isoalloxazine ring, which is compatible with covalent bond formation. This is in accordance with the hypothesis that the topology of these proteins shows resemblance. Interestingly, when all 15 sequences containing the conserved histidine truly represent covalent flavoproteins, the percentage of covalent flavoproteins within this new oxidoreductase family is relatively high considering that only 30 flavoproteins have been described to contain covalently linked flavin among several hundreds of flavoproteins⁴. Although PCMH and VAO do not contain the conserved histidine, they both contain a covalent flavin. In these enzymes, the FAD is linked to a residue which is located in the cap domain. These data altogether indicate that this newly discovered conserved FAD binding fold favours covalent binding of FAD. The conservation of this novel FAD binding fold may also represent a remnant of an ancestral covalent flavoprotein. In any case, the exact functional and/or structural meaning, if any, of covalent flavinylation remains to be elucidated.

References

1. Wierenga, R.K., Drenth, J. & Schulz, G.E. *J. Mol. Biol.* **167**, 725-739 (1983).
2. Mathews, F.S. *Curr. Opin. Struct. Biol.* **1**, 954-967 (1991).
3. Singer, T.P. & McIntire W.S. *Methods Enzymol.* **106**, 369-378 (1984).
4. Mewies, M., McIntire, W.S. & Scrutton, N.S. *Protein Sci.* **7**, 7-20 (1998).
5. Hiro, I., Tsugeno, Y., Hirashiki, I., Ogata, F. & Ito, A. *J. Biochem.* **120**, 759-765 (1996).
6. Kim, J., Fuller, J.H., Kuusk, V., Cunane, L., Chen, Z., Mathews, F.S. & McIntire, W.S. *J. Biol. Chem.* **270**, 31202-31209 (1995).
7. Brandsch, R. & Bichler, V. *J. Biol. Chem.* **266**, 19056-19062 (1991).
8. Mewies, M., Basran, J., Packman, L.C., Hille, R. & Scrutton, N.S. *Biochemistry* **36**, 7162-7168 (1997).
9. Mattevi, A., Fraaije, M.W., Mozzarelli, A., Olivi, L., Coda, A. & van Berkel, W.J.H. *Structure* **5**, 907-920 (1997).
10. Fraaije, M.W., Veeger, C. & van Berkel, W.J.H. *Eur. J. Biochem.* **234**, 271-277 (1995).
11. Fraaije, M.W., Pikkemaat, M. and van Berkel, W.J.H. *Appl. Environ. Microbiol.* **63**, 435-439 (1997).
12. Altschul, S.F., Gish, W., Miller, W., Myers, E.W. & Lipman, D.J. *J. Mol. Biol.* **215**, 403-10 (1990).
13. August, P.R., Flickinger, M.C. & Sherman, D.H. *J. Bacteriol* **176**, 4448-4454 (1994).
14. Mushegian, A.R. & Koonin E.V. *Protein Sci.* **4**, 1243-1244 (1995).
15. Lodi, T., O'Connor, D., Goffrini, P. & Ferrero, I. *Mol. Gen. Genet.* **244**, 622-629 (1994).
16. de Vet, E.C.J.M., Zomer, A.W.M., Lahaut, G.T.H.T.J. & van den Bosch, H. *J. Biol. Chem.* **272**, 798-803 (1997).
17. McIntire, W., Hopper, D.J. & Singer, T.P. *Biochem. J.* **228**, 325-335 (1985).
18. Kenney, W.C., Edmondson, D.E., Singer, T.P., Nakagawa, H., Asano, A. & Sato, R. *Biochem. Biophys. Res. Commun.* **71**, 1194-1200 (1976).
19. Kenney, W.C., Edmondson, D.E., Singer, T.P., Nishikimi, M., Nuguchi, E. & Yagi, K. *FEBS Lett.* **97**, 40-42 (1979).
20. Brandsch, R., Hinkkanen, A.E., Mauch, L., Nagursky, H. & Decker, K. *Eur. J. Biochem.* **167**, 315-320 (1987).
21. Kutchan, T.M. & Dittrich, H. *J. Biol. Chem.* **270**, 24475-24481 (1995).
22. Crespi, M., Vereecke, D., Temmerman, W., van Montagu, M., & Desomer, J. *J. Bacteriol.* **176**, 2492-2501 (1994).
23. Hansen, O.C. & Stougaard, P. *J. Biol. Chem.* **272**, 11581-11587 (1997).
24. Groen, B.W., de Vries, S. & Duine, J.A. *Eur. J. Biochem.* **244**, 858-861 (1997).
25. Pellicer, M.T., Badia, J., Aguilar, J. & Baldoma, L. *J. Bacteriol.* **178**, 2051-2059 (1996).
26. Mathews, F.S., Chen, Z. & Bellamy, H. *Biochem.* **30**, 238-247 (1991).
27. Benson, T.E., Filman, D.J., Walsh, C.T. & Hogle, J.M. *Nature Struct. Biol.* **2**, 644-653 (1995).
28. Thompson, J.D., Higgins, D.G. & Gibson, T.J. *Nucleic Acids Res.* **22**, 4673-4680 (1994).
29. Kraulis, P.J. *J. Appl. Crystallogr.* **24**, 946-950 (1991).

Abbreviations and nomenclature

A_x	absorbance at x nm
\AA	angstrom (0.1 nm)
ABTS	2,2'-azino-bis(3-ethylbenzothiazoline-6-sulfonic acid)
ADP	adenosine diphosphate
ATCC	American Type Culture Collection
CBS	Centraalbureau voor schimmelcultures
DNA	deoxyribonucleic acid
E	enzyme
ϵ_x	extinction coefficient at x nm
EPR	Electron Paramagnetic Resonance
g	g -factor
GC	gas chromatography
FAD	flavin adenine dinucleotide
FMN	flavin mononucleotide (riboflavin-5'-phosphate)
Hepes	4-(2-hydroxyethyl)-1-piperazineethane sulfonic acid
HPLC	high performance liquid chromatography
IgG	Immunoglobulin G
k	rate constant
K_d	dissociation constant
K_M	Michaelis constant
kDa	kilodalton
L	ligand
λ_{max}	position of absorption maximum
Mes	2-(<i>N</i> -morpholino)ethanesulphonic acid
MS	mass spectrometry
NADPH	nicotinamide adenine dinucleotide phosphate(reduced)
NMR	nuclear magnetic resonance
ox	oxidized
P	product
PAC	atypical catalase from <i>P. simplicissimum</i>
PAGE	polyacrylamide gel electrophoresis
PCP	catalase-peroxidase from <i>P. simplicissimum</i>
PCMH	<i>p</i> -cresol methylhydroxylase
PEG	poly(ethylene glycol)
PTS	peroxisomal targeting signal
Q	<i>p</i> -quinone methide

red	reduced
S	substrate; spin
$S_{20,w}$	sedimentation coefficient at 20°C in water
SDS	sodium dodecyl sulphate
SIR	single-isomorphous-replacement
TBAF	tetrabutylammoniumfluoride
TBDMSCl	<i>t</i> -butyldimethylsilylchloride
TMS	tetramethylsilane
TLC	thin layer chromatography
U	amount of enzyme converting 1 μmol substrate min^{-1}
VAO	vanillyl-alcohol oxidase
adrenalone	3',4'-dihydroxy-2-methylaminoacetophenone
4-allylanisole	4-methoxy-allylbenzene
anisyl alcohol	4-methoxybenzyl alcohol
caffeic acid	3,4-dimethoxycinnamic acid
chavicol	4-allylphenol
cinnamyl alcohol	3-phenyl-2-propene-1-ol
coniferyl alcohol	4-hydroxy-3-methoxycinnamyl alcohol
coumaryl alcohol	4-hydroxycinnamyl alcohol
epinephrine	3,4-dihydroxy- α -(methylaminomethyl)benzyl alcohol (adrenalin)
eugenol	4-allyl-2-methoxyphenol
ferulic acid	4-hydroxy-3-methoxycinnamic acid
homovanillyl alcohol	4-hydroxy-3-methoxyphenethyl alcohol
isoeugenol	2-methoxy-4-propenylphenol
isosafrole	1,2-(methylenedioxy)-4-propenylbenzene
metanephrine	4-hydroxy-3-methoxy- α -(methylaminomethyl)benzyl alcohol
norepinephrine	α -(aminomethyl)-3,4-dihydroxybenzyl alcohol (noradrenalin)
normetanephrine	α -(aminomethyl)-4-hydroxy-3-methoxybenzyl alcohol
octopamine	α -(aminomethyl)-4-hydroxybenzyl alcohol
<i>p</i> -cresol	4-methylphenol
safrole	4-allyl-1,2-(methylenedioxy)benzene
sinapyl alcohol	4-hydroxy-3,5-dimethoxycinnamyl alcohol
synephrine	4-hydroxy- α -(methylaminomethyl)benzyl alcohol
vanillyl alcohol	4-hydroxy-3-methoxybenzyl alcohol
vanillylamine	4-hydroxy-3-methoxybenzylamine
vanillin	4-hydroxy-3-methoxybenzaldehyde
veratryl alcohol	3,4-dimethoxybenzyl alcohol
4-vinylphenol	4-ethenylphenol

Summary

Lignin is a heterogeneous aromatic polymer formed by all higher plants. As the biopolymer lignin is a major constituent of wood, it is highly abundant. Lignin biodegradation, an essential process to complete the Earth's carbon cycle, is initiated by action of several oxidoreductases excreted by white-rot fungi. The resulting degradation products may subsequently be used by other microorganisms. The non-lignolytic fungus *Penicillium simplicissimum* can grow on various lignin metabolites. When this ascomycete is grown on veratryl alcohol, a major lignin metabolite, production of an intracellular aryl alcohol oxidase is induced. Purification and initial characterization revealed that this enzyme is able to oxidize vanillyl alcohol into vanillin and was therefore named: vanillyl-alcohol oxidase (VAO). Furthermore, it was found that VAO is a homooctamer of about 500 kDa with each subunit containing a covalently bound 8α -(N^3 -histidyl)-FAD redox group. As VAO showed some interesting catalytical and structural features, a PhD-project was started in 1993 with the aim of elucidating its reaction mechanism.

BIOLOGICAL FUNCTION

Induction of VAO

In the initial stage this PhD-project, it was found that VAO has a rather broad substrate specificity. However, it was unclear which substrates are of physiological relevance. In a recent study, evidence was obtained that 4-(methoxymethyl)phenol represents a physiological substrate (Chapter 2). When the fungus is grown on 4-(methoxymethyl)phenol, VAO is expressed in large amounts, while the phenolic compound is fully degraded. HPLC analysis showed that VAO catalyzes the first step in the degradation pathway of 4-(methoxymethyl)phenol (Fig. 1).

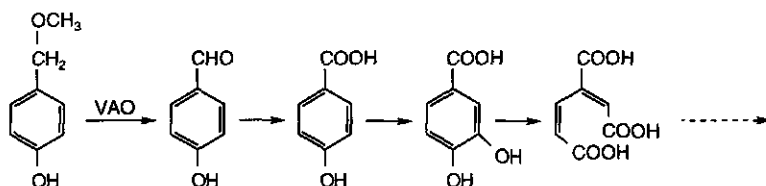


Figure 1. Degradation pathway of 4-(methoxymethyl)phenol in *Penicillium simplicissimum*.

This type of reaction (breakage of an ether bond) is new for flavoprotein oxidases. Furthermore, 4-(methoxymethyl)phenol has never been described in the literature as being present in nature. Yet, it can be envisaged that this phenolic compound is formed transiently during the biodegradation of lignin, a biopolymer of phenolic moieties with many ether bonds.

Catalase-peroxidase

Concomitant with the induction of VAO a relatively high level of catalase activity was observed. A further investigation revealed that *P. simplicissimum* contains at least two hydroperoxidases both exhibiting catalase activities: an atypical catalase and a catalase-peroxidase (Chapter 3). Purification of both enzymes showed that the periplasmic atypical catalase contains an uncommon chlorin-type heme as cofactor. The intracellular catalase-peroxidase represents the first purified dimeric eucaryotic catalase-peroxidase. So far, similar catalase-peroxidases have only been identified in bacteria. These procaryotic hydroperoxidases show some sequence homology with cytochrome *c* peroxidase from yeast which is in line with their peroxidase activity. EPR experiments revealed that the catalase-peroxidase from *P. simplicissimum* contains a histidine as proximal heme ligand and thereby can be regarded as a peroxidase-type enzyme resembling the characterized procaryotic catalase-peroxidases.

Immunolocalization

In Chapter 4, the subcellular localization of both VAO and catalase-peroxidase in *P. simplicissimum* was studied by immunocytochemical techniques. It was found that VAO and catalase-peroxidase are only partially compartmentalized. For both enzymes, most of the label was found in the cytosol and nuclei, while also some label was observed in the peroxisomes. The similar subcellular distribution of both oxidative enzymes suggests that catalase-peroxidase is involved in the removal of hydrogen peroxide formed by VAO. The VAO amino acid sequence revealed no clear peroxisomal targeting signal (PTS). However, the C-terminus consists of a tryptophan-lysine-leucine (WKL) sequence which resembles the well-known PTS1 which is characterized by a C-terminal serine-lysine-leucine (SKL) consensus sequence.

CATALYTIC MECHANISM

Substrate specificity

Soon after the start of the project, it was discovered that, aside from aromatic alcohols, VAO also converts a wide range of other phenolic compounds, including

aromatic amines, alkylphenols, allylphenols and aromatic methylethers (Chapter 5). Based on the substrate specificity (Fig. 2) and results from binding studies, it was suggested that VAO preferentially binds the phenolate form of the substrate. From this and the relatively high pH optimum for turnover, it was proposed that the vanillyl-alcohol oxidase catalyzed conversion of 4-allylphenols proceeds through a hydride transfer mechanism involving the formation of a *p*-quinone methide intermediate.

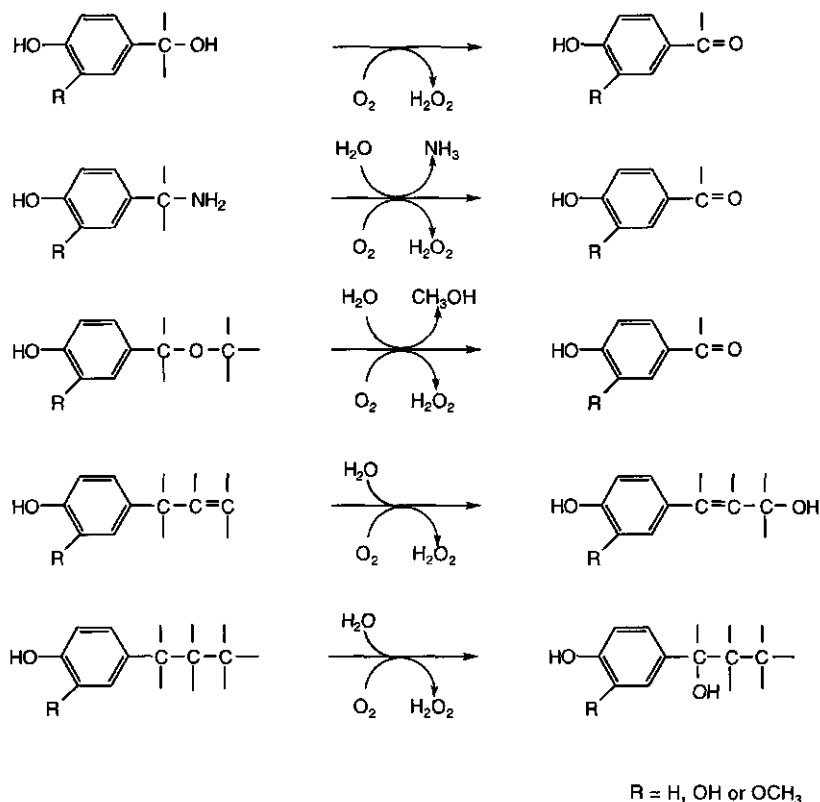


Figure 2. Reactions catalyzed by VAO.

Kinetic mechanism with 4-(methoxymethyl)phenol

In Chapter 6, the kinetic mechanism of the oxidative demethylation of 4-(methoxymethyl)phenol was studied in further detail using the stopped-flow technique. It was established that the rate-limiting step during catalysis is the reduction of the flavin cofactor by the aromatic substrate (Fig. 3). Furthermore, it was found that during this step a binary complex is formed between the reduced enzyme and a product intermediate. Spectral analysis revealed that the enzyme-bound intermediate is the *p*-quinone methide

form of 4-(methoxymethyl)phenol. Upon reaction of this complex with molecular oxygen, the final product is formed and released in a relatively fast process. Using H_2^{18}O , we could demonstrate that, upon flavin reoxidation, water attacks the electrophilic quinone methide intermediate to form the aromatic product 4-hydroxybenzaldehyde.

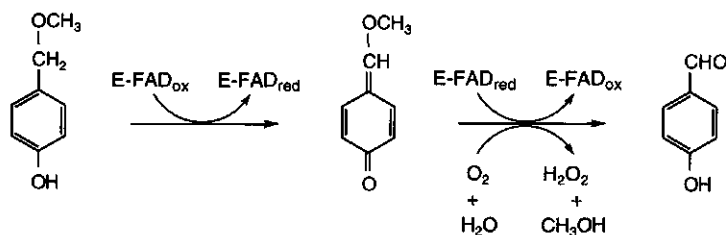


Figure 3. Reaction mechanism for the oxidative demethylation of 4-(methoxymethyl)phenol.

Enantioselectivity

In Chapter 7, the enantioselectivity of VAO was investigated. VAO catalyzes the enantioselective hydroxylation of 4-ethylphenol, 4-propylphenol and 2-methoxy-4-propylphenol with an *ee* of 94% for the R-enantiomer. Isotope labeling experiments confirmed that the oxygen atom incorporated into the alcoholic products is derived from water. During the VAO-mediated conversion of short-chain 4-alkylphenols, 4-alkenylic phenols are produced as well. The reaction of VAO with 4-alkylphenols also results in minor amounts of phenolic ketones which is indicative for a consecutive oxidation step.

Kinetic mechanism with 4-alkylphenols

Also the kinetic mechanism of VAO with 4-alkylphenols was studied (Chapter 8). For the determination of kinetic isotope effects, C_α -deuterated analogues were synthesized. Interestingly, conversion of 4-methylphenol appeared to be extremely slow, whereas 4-ethyl- and 4-propylphenol were rapidly converted. With these latter two substrates, relatively large kinetic deuterium isotope effects on the turnover rates were observed indicating that the rate of flavin reduction is rate-limiting. With all three 4-alkylphenols, the process of flavin reduction was reversible with the rate of reduction being in the same range as the rate of the reverse reaction. With 4-ethylphenol and 4-propylphenol, a transient intermediate is formed during the reductive half-reaction. From this and based on the studies with 4-(methoxymethyl)phenol, a kinetic mechanism was proposed which obeys an ordered sequential binding mechanism. With 4-ethylphenol and 4-propylphenol, the rate of flavin reduction determines the turnover rate, while with 4-methylphenol, a step involved in the reoxidation of the flavin seems to be rate limiting. The latter step might be involved in the decomposition of a flavin N5 adduct.

PROTEIN STRUCTURE

Mercuration of VAO

During crystallization experiments it was found that VAO crystals are highly sensitive towards mercury and other heavy atom derivatives. Therefore, the reactivity of VAO towards mercury in solution was studied (Chapter 9). Treatment of VAO with *p*-mercuribenzoate showed that one cysteine residue reacts rapidly without loss of enzyme activity. Subsequently, three sulphhydryl groups react leading to enzyme inactivation and dissociation of the octamer into dimers. From this, it was proposed that subunit dissociation accounts for the observed sensitivity of VAO crystals towards mercury compounds.

Crystal structure of VAO

Recently, the crystal structure of VAO was solved (Chapter 10). The VAO structure represents the first crystal structure of a flavoenzyme with a histidyl bound FAD. The VAO monomer comprises two domains (Fig. 4).

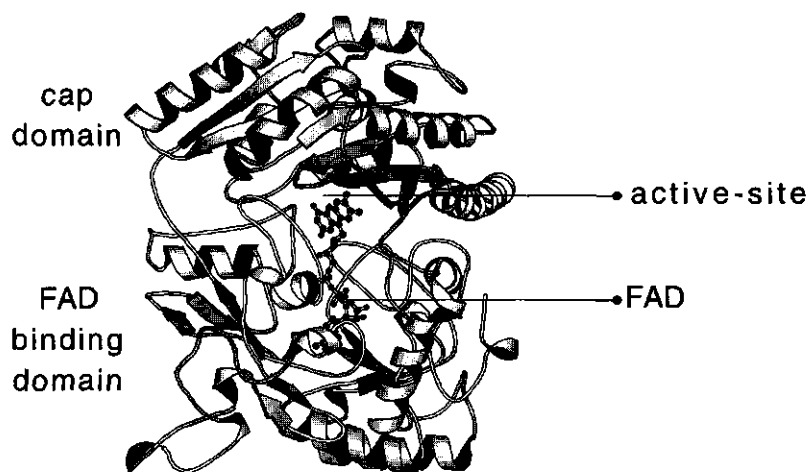


Figure 4. Crystal structure of VAO at 0.25 nm resolution.

The larger domain forms a FAD-binding module while the other domain, the cap domain, covers the reactive part of the FAD cofactor. By solving the binding mode of several inhibitors, the active site of VAO could be defined. This has clarified several aspects of the catalytic mechanism of this novel flavoprotein. Three residues, Tyr108, Tyr503 and Arg504, are involved in substrate activation by stabilizing the phenolate form of the

substrate. This is in line with the proposed formation and stabilisation of the *p*-quinone methide intermediate and the substrate specificity of VAO. The structure of the enzyme 4-heptenylphenol complex revealed that the shape of the active-site cavity controls substrate specificity by providing a 'size exclusion mechanism'. Furthermore, the active site cavity has a rigid architecture and is solvent-inaccessible. A major role in FAD binding is played by residues 99-110, which form the so-called 'PP loop'. This loop contributes to the binding of the adenine portion of FAD and compensates for the negative charge of the pyrophosphate moiety of the cofactor. The crystal structure also established that the C8-methyl group of the isoalloxazine ring is linked to the Nε2 atom of His422. Intriguingly, this residue is located in the cap domain.

A novel flavoprotein family sharing a conserved FAD binding fold

From the crystallographic data and sequence alignments, we have found that VAO belongs to a new family of structurally related flavin-dependent oxidoreductases (Chapter 11). In this study, 43 sequences were found, which show moderate homology with the VAO sequence. As sequence homology was mainly found in the C-terminal and N-terminal parts of the proteins, it could be concluded that the homology is indicative for the conservation of a novel FAD-binding domain as was found in the crystal structure of VAO (Fig. 5). This structurally related protein family includes flavin-dependent oxidoreductases isolated from (archae) bacteria, fungi, plants, animals and humans, indicating that this family is widespread. Furthermore, the sequence analysis predicts that many members of this family are covalent flavoproteins containing a histidyl bound FAD.

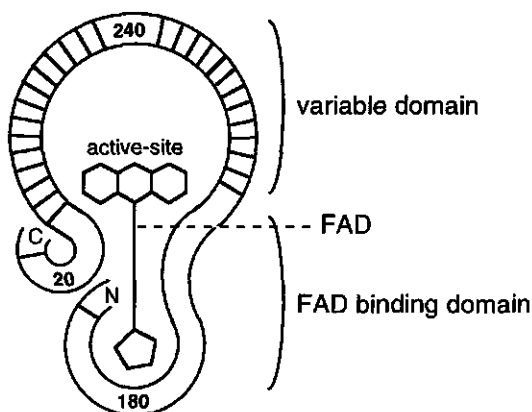


Figure 5. Schematic drawing of the structural fold of the newly discovered flavoprotein family.

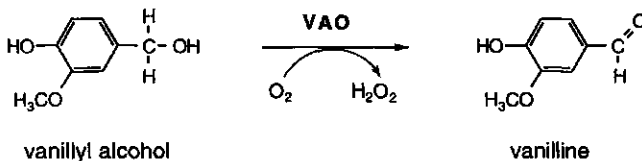
BIOTECHNOLOGICAL APPLICATIONS

Some of the VAO-mediated reactions are of relevance for the flavour and fragrance industry. For example, reactions of VAO with vanillyl alcohol, vanillylamine or creosol all result in the formation of vanillin, the major constituent of the well-known vanilla flavour. Furthermore, as shown in Chapter 7, VAO is able to enantioselectively hydroxylate phenolic compounds resulting in the production of interesting synthons for the fine-chemical industry. Because of its versatile catalytic potential and as VAO does not need external cofactors, but only uses molecular oxygen as a cheap and mild oxidant, VAO may develop as a valuable tool for the biotechnological industry. Furthermore, the recent cloning of the VAO gene and the available crystal structure will allow protein engineering to redesign the catalytic performance of VAO, which is of main interest for biotechnological applications. Therefore, like glucose oxidase and D-amino acid oxidase, VAO can be placed among an emerging group of flavoprotein oxidases, that catalyze transformations of industrial relevance.

Samenvatting

Biochemie is de wetenschap die zich bezighoudt met het bestuderen van biologische processen. Binnen dit vakgebied wordt veel onderzoek gedaan aan eiwitten. Een eiwit is opgebouwd uit een keten van relatief eenvoudige bouwstenen, aminozuren, waarvan er 20 verschillende soorten bestaan. Met deze 20 aminozuren is in een lange keten een oneindig aantal variaties te maken. In het DNA van ieder organisme ligt de erfelijke informatie besloten die ervoor zorgt dat er specifieke volgordes en lengtes van aminozuurketens, d.w.z. specifieke eiwitten, worden gemaakt.

Eiwitten die bepaalde chemische reacties kunnen katalyseren, worden enzymen genoemd. Enzymen zorgen ervoor dat reacties die onder normale omstandigheden niet of nauwelijks plaatsvinden, zeer snel, efficiënt en gecontroleerd verlopen. In het algemeen ligt de kracht van enzymen in hun vermogen de omgeving van substraten zodanig te veranderen dat deze substraten relatief makkelijk om te zetten zijn. Hiervoor is er in ieder enzym een actief centrum waar de reactie plaatsvindt. Vaak hebben enzymen een hulpstof (cofactor) nodig voor activiteit. Deze cofactoren bevatten veelal metalen (bv. ijzer) of vitamines zoals vitamine B₂ (= riboflavine). Enzymen die laatstgenoemde cofactor bevatten worden ook wel flavo-enzymen genoemd. Flavo-enzymen gebruiken de flavinecofactor veelal om tijdelijk van het substraat één of twee elektronen op te nemen en deze vervolgens aan een andere verbinding af te staan. Het enzym vanillyl-alcohol oxidase (VAO) is ook een flavine-bevattend enzym. Aanvankelijk was gevonden dat VAO alleen de oxidatie van vanillyl alcohol kon katalyseren. Het gevormde product bij deze reactie is vanilline: de belangrijkste geur- en smaakstof van het vanille aroma. Gedurende deze reactie worden twee elektronen van het substraat, vanillyl alcohol, via het flavine overgedragen aan zuurstof, hetgeen hierdoor gereduceerd wordt tot waterstofperoxide:



Omzetting van vanillyl alcohol gekatalyseerd door VAO.

In het onderzoek dat beschreven staat in dit proefschrift zijn de katalytische en structurele eigenschappen van VAO bestudeerd. Verder is ook aandacht besteed aan de opheldering van de biologische functie van dit veelzijdige enzym.

Functie

In de eerste hoofdstukken (2-4) is het onderzoek beschreven dat tot doel had de biologische functie van VAO op te helderen. Hoewel uit ander onderzoek (Hoofdstuk 5) bleek dat VAO in staat is om een breed scala aan fenol-achtige verbindingen te oxideren, was het onduidelijk welke specifieke reactie VAO in de schimmel *Penicillium simplicissimum* katalyseert. Om te bepalen welke verbinding het fysiologisch substraat van VAO is, werd *P. simplicissimum* gekweekt op verschillende groeisubstraten. Het blijkt dat VAO alleen geproduceerd wordt als de schimmel op drie specifieke aromaten groeit (Hoofdstuk 2). Van deze drie zogenaamde 'inducers' is alleen 4-(methoxymethyl)fenol ook een substraat voor VAO.

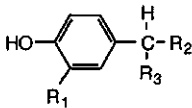
Als bijproduct produceert VAO waterstofperoxide. *P. simplicissimum* blijkt twee enzymen te bevatten die deze giftige verbinding onschadelijk kunnen maken: een katalase en een katalase-peroxidase. In Hoofdstuk 3 is de zuivering en karakterisering van deze twee enzymen beschreven. Het katalase heeft ongeveer dezelfde eigenschappen als katalases die ook in allerlei andere organismen voorkomen. Een verschil is dat de ijzer bevattende heem cofactor een iets afwijkende structuur heeft. Katalase-peroxidases waren tot voor kort alleen bekend van bacteriën. Karakterisering van het katalase-peroxidase uit *P. simplicissimum* is dan ook de eerste uitgebreide studie aan een eukaryotisch katalase-peroxidase. Uit EPR-metingen (waarbij het gedrag van een vrij elektron m.b.v. een magneetveld wordt bepaald) blijkt dat het ijzer atoom van de heem cofactor eenzelfde omgeving heeft als die in de bacteriële katalase-peroxidases en andere peroxidases.

Hoofdstuk 4 beschrijft de studie waarbij met behulp van specifieke antilichamen (eiwitten die binden aan een specifiek antigeen, b.v. een eiwit) de intracellulaire locatie van VAO en het katalase-peroxidase is bepaald. Het bleek dat beide enzymen in dezelfde gedeeltes van de cel zijn gelocaliseerd: in de celkernen, de peroxisomen en het cytosol. Daarnaast blijkt dat er een verhoogde productie van het katalase-peroxidase is als de aanmaak van VAO wordt geïnduceerd. Deze resultaten duiden erop dat het katalase-peroxidase verantwoordelijk is voor de afbraak van het waterstofperoxide dat door VAO geproduceerd wordt.

Mechanisme

In Hoofdstuk 5 is onderzocht welke verbindingen door VAO kunnen worden omgezet en welke producten er worden gevormd. Het enzym blijkt in staat om behalve vanillyl alcohol een groot scala aan aromaten te kunnen oxideren, variërend van complexe verbindingen zoals adrenaline tot relatief eenvoudige fenolen. Alle substraten hebben gemeen dat ze een bepaalde basisstructuur moeten bevatten. Dit onderzoek heeft verder

aangetoond dat VAO de substraten eerst deprotoneert alvorens het flavine het substraat oxideert. Uitgaande van deze resultaten is er een reactiemechanisme voorgesteld voor de omzetting van 4-allylphenolen, waarbij na deprotonering van het substraat en reactie met de cofactor een tussenproduct ontstaat dat met water tot het uiteindelijk product reageert.



R₁ : H, OH, OCH₃

R₂ : H, OH, OCH₃, NH₂, alkyl, alkenyl

R₃ : variabel

Basis structuurformule waaraan alle VAO-substraten voldoen.

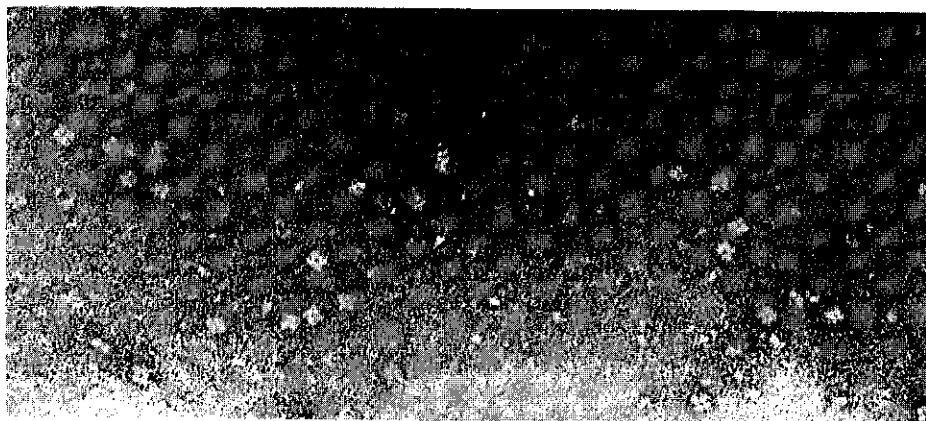
Omdat gevonden was dat 4-(methoxymethyl)fenol een fysiologisch substraat van VAO is, werd deze verbinding als model substraat gebruikt voor een kinetisch studie (Hoofdstuk 6). Met behulp van de zogenaamde 'stopped-flow' techniek werden de verschillende deelreacties, die tijdens de omzetting van het substraat plaatsvinden, gevolgd op korte tijdschaal. De reactie van het substraat met het flavine, waarbij de elektronen worden overgedragen naar de cofactor, blijkt de langzaamste stap tijdens de katalyse te zijn. De vervolgreactie met zuurstof en het loslaten van het product zijn relatief snelle processen. Verder kon, gebruikmakend van gelabeld water, aangetoond worden dat er gedurende de omzetting een watermolecuul reageert met het substraat. De combinatie van de verkregen gegevens levert een nauwkeurig beeld op van het kinetisch mechanisme van VAO. Hierdoor is nu bekend welk soort deelreacties er plaatsvinden en met welke snelheden de verschillende stappen gekatalyseerd worden. Een belangrijke conclusie van dit onderzoek is dat voor de vorming van het uiteindelijk product eerst een tussenproduct (een *p*-quinon methide) gevormd wordt dat vervolgens met water reageert tot het eindproduct. Vorming van dit tussenproduct is in overeenstemming met het in Hoofdstuk 5 voorgestelde reactiemechanisme.

Hoofdstukken 7 en 8 behandelen het katalytisch en kinetisch mechanisme van de omzetting van 4-alkylphenolen. Door een nauwkeurige analyse van de gevormde producten is aangetoond dat VAO in staat is om 4-alkylphenolen enantioselectief te hydroxyleren. Met andere woorden: VAO laat water specifiek met het substraat reageren, zodat bij vorming van een asymmetrisch product slechts één enantiomeer (spiegelbeeldisomeer) gevormd wordt. Met enkele 4-alkylphenolen is een kinetische studie verricht. Hieruit blijkt dat ook voor 4-ethylfenol en 4-propylfenol geldt dat de reactie van het substraat met het flavine reactiesnelheidsbepalend is. Tevens is voor deze reacties ook weer de vorming van een *p*-quinon methide tussenproduct aangetoond. Deze resultaten sluiten aan bij de resultaten die verkregen zijn met het fysiologisch substraat. De omzettingssnelheid van 4-methylfenol is uitzonderlijk langzaam. Dit kan verklaard worden door de vorming van een stabiel

complex van het substraat met de cofactor, welke slechts zeer langzaam verval. Andere aanwijzingen voor een dergelijk afwijkend reactiemechanisme zijn te vinden in Hoofdstuk 10.

Structuur

Het onderzoek dat beschreven staat in de laatste hoofdstukken (9-11) van dit proefschrift heeft betrekking op de structurele eigenschappen van VAO. Een enkel VAO molecuul (een VAO monomeer) bestaat uit 560 aminozuren en een covalent gebonden flavine. In oplossing blijken VAO monomeren te associëren tot octameren met een diameter van ongeveer 10 nm. Als VAO echter wordt behandeld met kwik-verbindingen, die reageren met specifieke aminozuren (cysteïnes), dissociëren de octameren tot inactieve dimeren (Hoofdstuk 9). Als de kwik-aminozuur bindingen vervolgens verbroken worden, associëren de dimeren weer tot actieve octameren; het proces is dus reversibel. Uit ontvouwingsstudies was al eerder gebleken dat VAO kan dissociëren tot actieve dimeren. Actieve monomeren zijn nog nooit aangetoond. Hieruit is af te leiden dat een VAO octameer is opgebouwd uit een tetrameer van dimeren.



Elektronenmicroscopische foto van VAO (50.000x vergroot).

In Hoofdstuk 10 staat de kristalstructuur van VAO op atomaire schaal beschreven. Met behulp van röntgendiffractietechnieken is de eiwitstructuur tot op 0,25 nm nauwkeurig bepaald. De structuur van een VAO monomeer is in te delen in twee gedeeltes (domeinen) waarvan de één de cofactor bindt en de ander het actieve centrum overkoepelt. Verder bevestigt de structuur dat de flavine cofactor via een ongebruikelijke binding aan het eiwit is gekoppeld. Van de honderden bekende flavine-afhankelijke enzymen is deze specifieke flavinebinding slechts bij ongeveer 25 andere flavo-enzymen aangetroffen. De

VAO structuur is de eerste opgehelderde kristalstructuur die een dergelijke flavinebinding bevat. Uit de structuurbepaling is ook gebleken dat twee VAO monomeren uitgebreide onderlinge interactie vertonen en zodoende dimeren vormen. De interactie tussen de verschillende dimeren is minder intensief, hetgeen verklaart dat de octameren relatief makkelijk uiteen kunnen vallen tot dimeren (zie Hoofdstuk 9). Doordat er ook VAO structuren zijn bepaald waarbij een substraatanaloog gebonden is, kon ook het actieve centrum van VAO gelocaliseerd worden. Het actieve centrum is gelegen tussen de twee verschillende domeinen. De substraatanaloga worden door enkele specifieke aminozuren zodanig gebonden dat ze dichtbij het reactieve deel van het flavine worden gebracht. Hierdoor kan de cofactor relatief makkelijk elektronen van het substraat ontvangen en hiermee de oxidatiereactie katalyseren. De ruimte die aanwezig is in het actieve centrum blijkt overeen te stemmen met de grootte van de verschillende substraten die gevonden zijn. Dit duidt erop dat de vorm van deze ruimte bepalend is voor de substraatspecificiteit van VAO.

Uit een vergelijking van de VAO aminozuurvolgorde (eiwitsequentie) met alle bekende eiwitsequenties is gebleken dat gedeeltes van de VAO sequentie ook in andere sequenties voorkomen (Hoofdstuk 11). Een uitgebreide sequentievergelijking leverde 43 andere eiwitsequenties op die een dergelijke homologie met elkaar vertoonden. Van deze nieuwe eiwitfamilie zijn tot nog toe slechts enkele enzymen goed bestudeerd. Al deze enzymen bevatten een flavine als enige cofactor en katalyseren een oxidatieve reactie. Hieruit kunnen we afleiden dat deze nieuwe eiwitfamilie waarschijnlijk bestaat uit flavine afhankelijke oxidatieve enzymen.

De resultaten van het in dit proefschrift beschreven onderzoek hebben geleid tot een beter inzicht in de manier waarop VAO specifieke reacties katalyseert. Hiermee is ook een bijdrage geleverd aan het verbreden van de kennis omtrent enzymreacties die door flavo-enzymen worden gekatalyseerd. Verschillende door VAO gekatalyseerde reacties zijn in potentie ook van industrieel belang. Zo is het mogelijk om vanuit vier verschillende substraten de belangrijkste component van het vanille aroma te synthetiseren. Een andere interessante omzetting, die inmiddels is gepatenteerd, is de oxidatie van eugenol (belangrijkste bestanddeel van kruidnagelen) tot coniferyl alcohol. Door de brede substraatspecificiteit en de relatief eenvoudige condities waaronder VAO-katalyse kan plaatsvinden, kan dit enzym in de toekomst een belangrijke biokatalysator worden voor de fijn-chemicaliënindustrie. De opheldering van de kristalstructuur en de recente clonering van het VAO-gen biedt een uitstekend perspectief om verschillende aspecten van dit veelzijdige enzym nader te bestuderen. Zo kan met behulp van "proteïn engineering" de functionaliteit van de ongebruikelijke FAD-histidyl binding worden opgehelderd of kunnen de katalytische eigenschappen veranderd worden.

Curriculum vitae

Marco Wilhelmus Fraaije werd op 7 december 1968 geboren te 's-Hertogenbosch. In 1987 behaalde hij het VWO diploma aan het Jacob Roelands Lyceum te Boxtel. Vervolgens werd begonnen met de studie Moleculaire Wetenschappen aan de Landbouwwuniversiteit te Wageningen. Tijdens de doctoraalfase werden afstudeervakken gevolgd bij de vakgroepen Levensmiddelentechnologie (sectie Industriële Microbiologie, Prof. J.A.M. de Bont), Biochemie (Prof. C. Veeger) en Plantencytologie en -morfologie (Dr. J.H.N. Schel). Tevens werd er een stage uitgevoerd bij Pharmaceutical R&D, sectie Non-Solids van Organon International (Oss), AKZO (Dr. A. Skrabanja). In augustus 1993 behaalde hij het doctoraal diploma en ontving tevens de Unilever Research prijs voor het werk verricht op de vakgroep Biochemie.

Van september 1993 tot september 1997 is hij als assistent in opleiding (AIO) verbonden geweest aan de vakgroep Biochemie van de Landbouwwuniversiteit te Wageningen. Hier werd het onderzoek, zoals beschreven in dit proefschrift, uitgevoerd onder supervisie van Dr. W.J.H. van Berkel en Prof. N.C.M. Laane. Vanaf april 1998 zal hij als post-doctoral EMBO-fellow werkzaam zijn aan de Universiteit van Pavia.

List of publications

- van Berkel, W.J.H., Fraaije, M.W., de Jong, E. and de Bont, J.A.M. (1994) Vanillyl-alcohol oxidase from *Penicillium simplicissimum*: a novel flavoprotein containing 8 α -(N³-histidyl)-FAD, in *Flavins and flavoproteins XI* (K. Yagi ed.) pp 799-802, De Gruyter, Berlin, New-York.
- Fraaije, M.W., Veeger, C. and van Berkel, W.J.H. (1995) Substrate specificity of flavin-dependent vanillyl-alcohol oxidase from *Penicillium simplicissimum*. *Eur. J. Biochem.* **234**, 271-277.
- Fraaije, M.W. and Fraaije, R.H.B. (1995) Miocene bracket fungi (Basidiomycetes, Aphyllophorales) from The Netherlands. *Contr. Tert. Quatern. Geol.* **32**, 27-33.
- Fraaije, M.W., Roubroeks, H.P., Hagen, W.R. and van Berkel, W.J.H. (1996) Purification and characterization of an intracellular catalase-peroxidase from *Penicillium simplicissimum*. *Eur. J. Biochem.* **235**, 192-198.
- Fraaije, M.W., Drijfhout, F., Meulenbeld, G.H. and van Berkel, W.J.H. (1996) Conversion of *p*-alkylphenols by vanillyl-alcohol oxidase, Abstr. 6th Netherlands Biotechnology Congress, PH1, Amsterdam.
- van Berkel, W.J.H., Fraaije, M.W. and de Jong, E. (1997) Process for producing 4-hydroxycinnamyl alcohols. European Patent application 0710289B1.
- Fraaije, M.W., Pikkemaat, M. and van Berkel, W.J.H. (1997) Enigmatic gratuitous induction of the covalent flavoprotein vanillyl-alcohol oxidase in *Penicillium simplicissimum*. *Appl. Environ. Microbiol.* **63**, 435-439.
- Fraaije, M.W., Mattevi, A. and van Berkel, W.J.H. (1997) Mercuration of vanillyl-alcohol oxidase from *Penicillium simplicissimum* generates inactive dimers. *FEBS Lett.* **402**, 33-35.
- Mattevi, A., Fraaije, M.W., Coda, A. and van Berkel, W.J.H. (1997) Crystallization and preliminary X-ray analysis of the flavoenzyme vanillyl-alcohol oxidase from *Penicillium simplicissimum*. *Proteins: Structure, Function and Genetics* **27**, 601-603.
- Fraaije, M.W., van Berkel, W.J.H., Benen, J.A.E., Visser, J. and Mattevi, A. (1997) Structure and mechanism of vanillyl-alcohol oxidase from *Penicillium simplicissimum*, Abstr. The Protein Society 2nd European Symposium, Cambridge, *Protein Sci.* **6** suppl. 1, 305.

- Fraaije, M.W.** and van Berkel, W.J.H. (1997) Catalytic mechanism of the oxidative demethylation of 4-(methoxymethyl)phenol by vanillyl-alcohol oxidase. *J. Biol. Chem.* **272**, 18111-18116.
- Mattevi, A., **Fraaije, M.W.**, Mozzarelli, A., Olivi, L., Coda, A. and van Berkel, W.J.H. (1997) Crystal structure and inhibitor binding in the octameric flavoenzyme vanillyl-alcohol oxidase. *Structure* **5**, 907-920.
- Fraaije, M.W.**, Drijfhout, F., Meulenbeld, G.H., van Berkel, W.J.H. and Mattevi, A. (1997) Vanillyl-alcohol oxidase from *Penicillium simplicissimum*: reactivity with *p*-cresol and preliminary structural analysis, in *Flavins and flavoproteins XII* (Stevenson, K., Massey, V., and Williams, C., eds.) pp 261-264, University Press, Calgary.
- Fraaije, M.W.**, Mattevi, A. and van Berkel, W.J.H. (1997) Crystal structure of vanillyl-alcohol oxidase: a flavoenzyme containing a histidyl bound flavin, Abstr. 17th Int. Congress of Bioch. and Mol. Biol., San Francisco, *FASEB J.* **11**, 173.
- Drijfhout, F.P., **Fraaije, M.W.**, Jongejan, H., van Berkel, W.J.H. and Franssen, M.C.R. (1998) Enantioselective hydroxylation of 4-alkylphenols by vanillyl-alcohol oxidase. *Biotech. Bioeng.*, in press.
- Fraaije, M.W.**, Sjollem, K.A. Veenhuis, M. and van Berkel, W.J.H. (1998) Immunolocalisation of vanillyl-alcohol oxidase, *FEBS Lett.* **422**, 65-68.
- Benen, J.A.E., Sánchez-Torres, P., Wagemaker, M.J.M., **Fraaije, M.W.**, van Berkel, W.J.H. and Visser, J. (1998) Molecular cloning, sequencing and heterologous expression of the *vaoA* gene from *Penicillium simplicissimum* CBS 170.90 encoding vanillyl-alcohol oxidase, *J. Biol. Chem.*, in press.
- Fraaije, M.W.**, Mattevi, A., Benen, J.A.E., Visser, J. and van Berkel, W.J.H. (1998) A novel oxidoreductase family sharing a conserved FAD binding domain, submitted to *Trends in Biochemical Sciences*.
- Fraaije, M.W.**, van den Heuvel, R.H.H., Roelofs, J.C.A.A. and van Berkel, W.J.H. (1998) Kinetic mechanism of vanillyl-alcohol oxidase with short-chain 4-alkylphenols, submitted to *Eur. J. Biochem.*
- van den Heuvel, R.H.H., **Fraaije, M.W.** and van Berkel, W.J.H. (1998) Reactivity of vanillyl-alcohol oxidase with 4-alkylphenols, in preparation.

Dankwoord

Dit proefschrift is het resultaat van een lange periode van plezierige arbeid en verschillende interessante en leerzame samenwerkingsverbanden. Hierbij was de samenwerking en/of vriendschap met verschillende personen (copromotor, promotor, collega's, studenten, vrienden en familie) onmisbaar. Hieronder zal ik enkele personen in het bijzonder bedanken, daarbij beseffend dat ik wellicht verschillende mensen tekort doe.

Allereerst wil ik mijn copromotor Willem van Berkel bedanken. Willem, jij was in dit onderzoek de belangrijkste (co)factor: onmisbaar en inspirerend. Jouw enthousiasme voor het 'gele' onderzoek is besmettelijk gebleken. De nuttige discussies en de vrijheid die je me tijdens het onderzoek gegeven hebt, heb ik als zeer prettig ervaren. Vooral je kritische blik en je oog voor details hebben een belangrijke bijdrage geleverd aan het totstandkomen van de verschillende publicaties.

Mijn promotor Colja Laane wil ik bedanken voor zijn betrokkenheid en de ondersteuning van mijn onderzoek. Cees Veeger ben ik dank verschuldigd voor de mogelijkheid die hij mij geboden heeft om op de vakgroep als AIO te mogen starten.

Fred Hagen ben ik erkentelijk voor de ondersteuning bij de EPR-metingen die beschreven staan in Hoofdstuk 3.

Na een eerste eigen poging VAO te localiseren bleek hiervoor de expertise van Klaas Sjollema en Marten Veenhuis echter onmisbaar. Klaas, bedankt voor het uitvoeren van de verschillende localisatie experimenten. Marten, bedankt voor de vruchtbare samenwerking.

Maurice Franssen en Hugo Jongejan, jullie hulp bij het synthetiseren van de verschillende aromaten was van essentieel belang voor het werk dat beschreven staat in hoofdstukken 7 en 8: bedankt voor de zeer prettige samenwerking.

Zonder de sequentie van het VAO-gen waren de laatste twee hoofdstukken er nooit van gekomen. Hiervoor ben ik Jacques Benen en Jaap Visser veel dank verschuldigd.

Voor het assisteren bij het kweken van de honderden liters schimmel wil ik Fred van den End bedanken. De opschaling van literkweek naar de 300 liter fermentor was van groot belang voor het onderzoek.

Het onderzoek kreeg een belangrijke impuls door de samenwerking met Andrea Mattevi. *Andrea, your enthusiasm and collaboration has been a very pleasant experience and was highly appreciated. I hope that our future plans will be as rewarding.*

De afstudeervakkers Hanno Roubroeks, Mariël Pikkemaat, Falko Drijfhout, Gerwin Meulenbeld, Jules Roelofs en Matthé Wagemakers wil ik allen bedanken voor hun waardevolle bijdrages aan dit proefschrift. Het doet mij genoegen dat jullie allemaal mede-auteur van één van de publicaties zijn geworden. Jullie inzet heeft ervoor gezorgd dat de verschillende deelonderzoeken succesvol zijn geweest. Succes met jullie eigen promotie-onderzoek.

Zonder de aanwezigheid van Frank, Michel en Robert waren de tijden doorgebracht op lab 5 (en daarbuiten) lang niet zo plezierig geweest. Frank, het was een leuke en waardevolle tijd. Jongens, het is me gelukt, nu zijn jullie aan de beurt.

Elles, de gezelligheid en collegialiteit op ons kamertje zal me altijd bijblijven. Hopelijk krijg je in Zweden niet te veel buikpijn van het praktische werk. We moeten in de toekomst maar regelmatig bij elkaar op de stoel komen.

Marjon, de kletspraatjes waren een welkome afwisseling tijdens het 'echte' werk. Laura, bedankt voor alle regedingetjes. Alle andere vakgroep/laboratorium medewerkers, bedankt voor jullie hulp en gezelligheid.

Verder wil ik mijn familie, vrienden en kennissen bedanken voor hun steun en de nodige ontspanning. Bart, Annette en André, doordat we allemaal in een zelfde soort schuitje zaten, waren jullie prettige gesprekspartners voor het uiten van onderzoek-gerelateerde frustraties (en soms ook vreugden).

Pap, bedankt voor de steun en getoonde interesse. Mam, jammer dat je het niet hebt mogen meemaken.

Marleen, het is ons allebei gelukt! De afgelopen jaren zijn een boeiende periode geweest waarbij jou liefde, steun en betrokkenheid van onschatbare waarde waren.